Kodaikanal Obs. Bull. (1993) 12, 15-91

Stellar Winds in O and B Type Stars: Hydrogen Atmosphere

A.Peraiah and B.A.Varghese

Received 7th May 1993 , accepted 17th May 1993

Abstract

We present the results of calculations of radiation driven stellar winds in O-B stars. The equations of conservation of mass and momentum are solved self consistently with the equation of line transfer. The influence of radiation pressure in the line on the outward momentum of the outer layers of the O and B type stars is investigated assuming an isothermal Hydrogen atmosphere. Lines in Lyman, Balmer Paschen, Brackett series are used to calculate the line radiation pressure assuming 10 levels of H. We have considered realistic stars by using their observational data. In addition to the radiation pressure in the lines we have taken into account the electron scattering and the continuum radiation is neglected. We employed Saha equation for estimating the ionized H atoms and Boltzmann equation for calculating the occupation numbers in different stages of excitation. We have applied a non-LTE two level-atom approximation to solve the line transfer for the purpose of calculating the radiation pressure in the line. The effects of radial velocity gradients, transverse velocity gradients, aberration and advection have been taken into account in the calculation of radiation pressure in the lines. We have applied this theory to several stars making use of their observationally derived temperatures, masses, radii and mass loss rates. We have derived the ionized fraction of the hydrogen atoms, electron density, the population density in different states of excitation, thermalization parameters, radial optical depths, the line radiation pressure due to combined effect of Lyman, Balmer, Paschen and Brackett lines upto 10 levels.

The system of equations converge in 4 to 5 iterations. The convergence to the desired terminal velocity depends on the initial conditions of the iteration, particularly the velocity in the first iteration. The computed terminal velocities are compared with the observed terminal velocities. Using the mass loss rates and the newly derived velocity, new density distribution in the wind is obtained.

Key words: stellar winds-hydrogen-radiative transfer-radiation pressure-mass loss

1. Introduction

Mass loss in early type and late type stars is a well known phenomenon. This has a profound effect on the evolution of stars. P Cygni profiles (Beals, 1929) are indications of the material being lost to the star. Morton (1967) observed several lines in ultraviolet part of the spectrum which indicated the loss of mass in the outer layers of the stars. Infrared and radio observations also reveal mass loss (Barlow and Cohen 1977; Abbott et al. 1980; Abbott et al. 1984; Lamers and Waters, 1984; Bertout et al., 1985). In early type stars, the mass loss rates vary between 10^{-5} to $10^{-7} M_{\odot}$/year (Garmany 1988). The stellar wind problem is a highly complicated phenomenon. It is influenced by the type of energy generated,

radiation field, magnetic field, rotation, pulsation, turbulence in the outer layers where the wind becomes prominent, corona, tidal effects due to the presence of the companion in a close binary system, scattering of radiation (diffuse, back scattered radiation etc). Furthermore, the fundamental parameters such as mass, radius, temperature and composition would effect the wind generation profoundly. The ionization pattern throughout the outerlayers (where the wind forms) plays an important role in furthering the wind velocities.

Lucy and Solomon (1970) showed that in O stars radiation force in a line is more powerful than the force due to gravity. Castor et al. (1975), henceforth called CAK in a fundamental paper showed that radiation force is indeed a very powerful force in producing stellar wind. Further important results have been worked out by Abbott (1982), Pauldrach et al. (1986), Pauldrach (1987), Pauldrach et al. (1990), Blomme (1990a,b) Blomme, Vanbeveren and Van Rensbergen (1990), Blomme, Van Rensbergen (1988) and others. In CAK, the line force was calculated by CIII lines only while Abbott (1982) has included several lines. However several discrepancies remained unresolved between theory and observations. Sobolev approximation and radial streaming approximation are to be replaced by correct estimations of radiation field (Weber 1981, Leroy and Lafon 1982, Abbott 1986). Many other points are discussed in Pauldrach et al. (1986) and Blomme (1990a).

The effects of diffuse radiation is not considered in a consistent way. In the extended region of the outer layer, the high velocities produce effects such as radial, transverse velocity gradients, aberration and advection. These will change the radiation field considerably (Peraiah 1991). As it was shown that line radiation plays the most critical part in the stellar winds of O and B stars, it is necessary to calculate the line radiation correctly.

We have solved the equations of conservation of mass and momentum self consistently with that of the equation of radiative transfer. We have assumed an isothermal, spherically symmetric, hydrogen medium. The population densities are calculated using Saha-Boltzmann formulation. The primary aim of this paper is to derive the terminal velocities of the winds in O and B stars.

2. Procedure and Results

The equation of momentum in a steady state and spherically symmetric medium is given by (Pauldrach et al., 1986)

$$v(r)\frac{dv(r)}{dr} = -\frac{1}{\rho(r)}\frac{dp(r)}{dr} - \frac{GM}{r^2} + g_{rad} \tag{1}$$

the equation of mass is given by

$$\dot{M} = 4\pi r^2 \rho(r) v(r) \tag{2}$$

and the radiative transfer equation is given by (Peraiah, 1991)

$$(\mu_0+\gamma)\frac{\partial U(r,\mu_0,x)}{\partial r} + \frac{1-\mu_0^2}{r}\left[1+\mu_0\gamma\left(1-\frac{r}{\gamma}\frac{d\gamma}{dr}\right)\right]\frac{\partial U(r,\mu_0,x)}{\partial \mu_0} + \left\{3\left[\frac{\gamma}{r}(1-\mu_0^2)+\mu_0^2\frac{d\gamma}{dr}\right]\right.$$

$$\left.-\frac{2(\mu_0+\gamma)}{r}\right\}U(r,\mu_0,x) = \left[\frac{v'}{r}(1-\mu_0^2)+\mu_0^2\frac{dv'}{dr}\right]\frac{\partial U(r,\mu_0,x)}{\partial x} + K_L(r)\left[S(r,x)-U(r,\mu_0,x)\right] \tag{3}$$

Various symbols in the above equations are explained below:

r = radius of the star (cm)

ρ = density (gr cm^{-3})

v = bulk velocity of the medium (cm s^{-1})

$\dot{M}$ = mass of the star (gr)

$\dot{M} = \frac{dM}{dt}$ = rate of mass loss ($M_\odot$/yr or gr s^{-1})

G = Gravitational constant (cm^3 gr^{-1} s^{-2})

P = pressure (gr cm^{-1} s^{-2})

$$U = 4\pi r^2 I(r, \mu_0, x) \tag{4}$$

$I(r, \mu_0, x)$ = specific intensity (ergs cm^{-2} s^{-1} st^{-1} hz^{-1})

$\gamma = v/c$

c = velocity of light (cm s^{-1})

$v' = v/v_{th}$

v_{th} = thermal velocity (cm s^{-1})

$$v_{th} = \left(\frac{2kT}{m_i}\right)^{1/2}$$

where k is the Boltzmann constant, T is the temperature and m_i is the mass of the ion.

$$\mu_0 = \frac{\mu - \gamma}{1 - \mu\gamma} \tag{5}$$

μ = cosine of the angle made by the ray with the radius vector (spherically symmetric geometry is assumed)

$$x = \frac{\nu - \nu_0}{\Delta\nu_D} \tag{6}$$

$\Delta\nu_D$ = Doppler width (hz)

$\Delta\nu_D = \nu_0(v_{th}/c)$

ν = frequency point in the line (hz)

ν_0 = central frequency point (hz)

$K_L(r)$= absorption coefficient (cm^{-1})

$S(r, x)$ = source function given by (ergs cm^{-2} s^{-1} hz^{-1} ster^{-1})

$$S(x, \mu_0, r) = \frac{\phi(x, \mu_0, r) S_L(r) + \beta' S_c(r)}{\beta' + \phi(x, \mu_0, r)} \tag{7}$$

$\phi(x, \mu_0, r)$ = profile function.

β' = ratio of absorption coefficient in the continuum to that in the centre of the line.

S_L = the line source function given as

$$S_L = \frac{1-\epsilon}{2}\int_{-1}^{+\infty}\int_{-1}^{+1} I(x,\mu',r)\phi(x')dx'd\mu' + \epsilon B_\nu(T(r)) \tag{8}$$

S_c = the continuum source function, (ergs cm^{-2} S^{-1} Hz^{-1} Ster^{-1}) given as

$$S_c = \rho' B_\nu(T(r)) \tag{8a}$$

$$B_\nu(T(r)) = \text{Planck function} \tag{9}$$

ρ' = the suitable factor such as dilution factor.

ϵ = the probability of a photon being destroyed (thermalised) per scatter by collisional de-excitation.

g_{rad} = radiation force term (cm s^{-2})

$$g_{rad} = \frac{1}{c\rho(r)}\left[N_e(r)\sigma_{Th}\sigma_B T_{eff}^4(r) + 4\pi\int_0^\infty \chi_\nu^C(r)F_\nu^C(r)d\nu + +4\pi\sum_{\text{all lines}}\int_{-\infty}^{\infty}\chi_\nu^L(r)F_\nu^L(r)d\nu\right] \tag{10}$$

$\sigma_{Th}(r)$ = Thompson scattering coefficient (cm^2)

$N_e(r)$ = electron density (cm^{-3})

σ_B = Stefan-Boltzmann constant (erg cm$^2 s^{-1} deg^{-4}$)

T_{eff} = effective temperature of the star (deg, K)

χ_ν^C = continuum absorption coefficient (cm^{-1})

χ_ν^L = line absorption coefficient (cm^{-1})

F_ν^C = continuum flux (ergs cm$^{-2} s^{-1} hz^{-1}$)

F_ν^L = Eddington line flux (ergs cm$^{-2} s^{-1} hz^{-1}$)

$F_\nu = \frac{1}{2}\int_{-1}^{+1} I(\mu)\mu d\mu$

We have derived the difference equation corresponding to the equations of mass and momentum. The transfer equation is solved using the method described in Peraiah (1980, 1991).

We shall choose the radial mesh with $\{r_i\}\{i = 1,2,\ldots N; r_{i+1} > r_i\}$ with r_1 equal to the radius of the star. Similarly we represent ρ, v on this mesh. The quantities $\Delta r, r, \Delta\rho, \rho, \Delta v, v$ are represented by,

$$\Delta r = r_i - r_{i-1}$$

$$\Delta\rho = \rho_i - \rho_{i-1}$$

$$\Delta v = v_i - v_{i-1}$$

$$\Delta T = T_i - T_{i-1}$$

$$r = (r_{i-1} + r_i)/2$$

$$\rho = (\rho_{i-1} + \rho_i/2$$

$$v = (v_{i-1} + v_i)/2$$

$$T = (T_{i-1} + T_i)/2. \tag{11}$$

We shall write

$$P(r) = N(r)kT(r) \tag{12}$$

where N is the particle density and k is the Boltzmann constant. Therefore

$$\frac{dP(r)}{dr} = k\{T(r)\frac{dN(r)}{dr} + N(r)\frac{dT(r)}{dr}\} \tag{13}$$

or

$$dP(r) = k\{T(r)dN(r) + N(r)dT(r)\}. \tag{14}$$

Equation (13) can be written in the difference form

$$P_i - P_{i-1} = k\{(\frac{T_{i-1} + T_i}{2})(N_i - N_{i-1}) + (\frac{N_{i-1} + N_i}{2})(T_i - T_{i-1})\}$$

which simplifies to

$$P_i - P_{i-1} = k(T_iN_i - T_{i-1}N_{i-1}). \tag{15}$$

Let us write

$$R = 4\pi \int_{-\infty}^{+\infty} \chi_\nu^L F_\nu^L d\nu \tag{16}$$

then

$$R_i = (R_{i-1} + R_i)/2. \tag{17}$$

We can rewrite the equation momentum in its difference equivalent as,

$$(\frac{v_i + v_{i-1}}{2})(\frac{v_i - v_{i-1}}{r_i - r_{i-1}}) = -\frac{2k}{(\rho_i + \rho_{i-1})}\frac{(N_iT_i - N_{i-1}T_{i-1})}{(r_i - r_{i-1})} - \frac{4GM}{(r_i - r_{i-1})^2}$$

$$+\frac{2}{c(\rho_i + \rho_{i-1})}[(\frac{N_i^e + N_{i-1}^e}{2})\sigma_{Th}\sigma_B(\frac{T_i + T_{i-1}}{2})^4 + \frac{R_i + R_{i-1}}{2}] \tag{18}$$

which reduces to

$$v_i^2 = v_{i-1}^2 - \frac{4k}{(\rho_{i-1} + \rho_i)}(N_iT_i - N_{i-1}T_{i-1}) - \frac{8GM}{(r_{i-1} + r_i)^2}(r_i - r_{i-1})$$

$$+\frac{(r_i - r_{i-1})}{c(\rho_{i-1} + \rho_i)}[\frac{1}{8}\sigma_{Th}\sigma_B(N_{i-1}^e + N_i^e)(T_{i-1} + T_i)^4 + 2(R_{i-1} + R_i)]. \tag{19}$$

We have considered an hydrogen atmosphere. We need to find the ionized and neutral hydrogen atoms. For this purpose we use Saha equation of ionization given by (see Aller 1963)

$$log\frac{N_1}{N_0}P_e = -\frac{5040}{T}I + 2.5logT - 0.48 + log\frac{2U_1(T)}{U_0(T)}, \tag{20}$$

where N_1 is the number of ionised atoms, N_0 is the number of neutral atoms, P_e is the electron pressure, and $U_1(T)$ is the partition function of the ionized atoms and $U_0(T)$ is the partition function of the neutral atoms, I is the ionization potential in eV. The calculation of the partition function is somewhat difficult. The partition function $U_1 = 1$ in the ionized hydrogen atom and U_0 can be taken equal to 2 at cooler

temperatures as the number of atoms in the higher states of excitation are very few compared to those in the ground state (see Bohm-Vitense 1989). The simplest approach is to use the formula (Aller 1963)

$$U_i(T) = g_{i,1} + g_{i,2}e^{-\chi_{i,2}/kT} + \ldots = \sum_r g_{i,r}e^{-\chi_{i,r}/kT} \tag{21}$$

where g is the statistical weights, χ_r is the excitation potential of the r^{th} state of excitation.

However, this neglects the collisions among particles. The distance between the particles fluctuate randomly so that the orbits perturb and eject the electron before an actual interlocking of the orbits occur. We shall use the method of calculating the partition function as described in Aller (1963). The expression for the partition function is

$$U = \sum_j p_j g_j e^{-\chi_j/kT} \tag{22}$$

where p_j is the probability that the j^{th} level is occupied at the density under consideration. Further,

$$P_j = e^{-C(z)}P_e n^6 \theta \tag{23}$$

where $\theta = 5040/T, C(z) = 1.927 \times 10^{-10}$ for Z = 1 for neutral atoms. In equations (20) and (23), the quantity P_e is common. Unless we know P_e we cannot calculate the Saha equation and the partition functions U_0. For hydrogen, the ionized atoms consists of equal number of protons N_p and electrons N_e. Therefore,

$N_e = N_p = N_1$ = Number of ionized atoms. From Saha equation (20), we can write,

$$log\frac{N_p^2}{N_0} = -logkT - \frac{5040}{T}I + 2.5logT - 0.48 + log\frac{2U_1(T)}{U_0(T)}, \tag{24}$$

where we have put $P_e = N_e kT$.

Equation (24) reduces to

$$log\frac{N_p}{N_0} = 7.69 - \frac{2520}{T}I + 0.75logT + \frac{1}{2}log\frac{2U_1(T)}{U_0(T)}. \tag{25}$$

We solve the equation (24) without the last term on the R.H.S. Let

$$N_p = N_e. \tag{26}$$

The density ρ is given by

$$\rho = N_p m_p + N_0 m_p + N_0 m_e + N_e m_e$$

$$= m_p(N_0 + N_p) + m_e(N_0 + N_e)$$

or

$$\rho = (N_0 + N_p)(m_p + m_e) \tag{27}$$

where m_p and m_e are masses of proton and electron respectively.

But $m_p >> m_e$, therefore,

$$\rho \approx (N_0 + N_p)m_p$$

or

$$N_0 + N_p = \frac{\rho}{m_p}. \tag{28}$$

The ratio $\frac{N_p}{N_0}$ is obtained from Saha equation (24).

Let

$$N_0 + N_p = a \tag{29}$$

and

$$\frac{N_p}{N_0} = b \tag{30}$$

from which we obtain

$$N_0 = \frac{a}{1+b} \tag{31}$$

$$N_p = \frac{ab}{1+b}. \tag{32}$$

Using equations (26) and (32) we compute the electron pressure and this is used to compute the partition function in equation (22). Using this result, we go back to Saha equation (24) to calculate the quantity $\frac{N_p}{N_0}$ this time including the last term on the R.H.S of equation (24) which contains the partition functions. New electron density is obtained and this is used to calculate new partition functions. The calculation converges in 3 to 4 iteration to an accuracy of 1%. We have given a sample calculation $U_o(T)$ in Table 1.

Next step is to calculate the population densities in different stages of excitation. For this, we use Boltzmann equation (see Aller, 1963)

$$log\frac{N_r}{N_1} = -\theta\chi_r + log\frac{g_r}{g_1} \tag{33}$$

where N_r, χ_r and g_r are the number of atoms, excitation potential and statistical weight of the r^{th} state of excitation respectively. N_1 and g_1 are the number of atoms and statistical weight of the ground state respectively.

We need to find N_1, N_2 etc. Let

$$N_0 = N_1 + N_2 + N_3 + \ldots \tag{34}$$

where N_0 is the total number of neutral atoms and N_1, N_2 etc are the number of atoms in 1st, 2nd states of excitation. Let

$$a_1 = \frac{N_2}{N_1}, \quad a_2 = \frac{N_3}{N_1}, \quad a_3 = \frac{N_4}{N_1} \quad etc. \tag{35}$$

Then

$$N_0 = N_1 + \frac{N_2}{N_1}N_1 + \frac{N_3}{N_1}N_1 + \ldots \tag{36}$$

$$= N_1(1 + a_1 + a_2 + a_3 + \ldots)$$

or

$$N_0 = N_1 A \tag{37}$$

where we have written

$$A = 1 + a_1 + a_2 + a_3 + \ldots \tag{38}$$

Then from (37) and (35), we obtain

$$N_1 = \frac{N_0}{A}$$

$$N_2 = N_1 a_1$$

$$N_3 = N_1 a_2, \qquad \text{etc.} \tag{39}$$

Table 1. Computed values of $U_0(T)$ for a density of $\rho = 10^{13}(grcm^{-3})$

Temperature (K)	U_0	$N_e(=N_p)(cm^{-3})$	$N_0(cm^{-3})$
10,000	0.0023	$\approx 10^{13}$	1.878×10^4
15,000	0.44	$\approx 10^{13}$	1.362×10^4
25,000	29.16	$\approx 10^{13}$	9.211×10^3
30,000	83.24	$\approx 10^{13}$	8.021×10^3
40,000	308.93	$\approx 10^{13}$	6.451×10^3
50,000	678.59	$\approx 10^{13}$	5.151×10^3

We require to calculate the radiation pressure in the lines. As we assumed that the atmosphere consists of only hydrogen, the calculation of occupation numbers become easy and the radial optical depths can be calculated immediately for the purpose of solving the radiative transfer equation. The steps we take are as follows:

(1) Given the radius, mass, mass loss rate, temperature (these are obtained from observations), calculate the density by using the thermal velocity (v_{th}) throughout the medium, from the relation (see equation (2))

$$\rho(r) = \dot{M}/4\pi r^2 v_{th} \tag{40}$$

(we are using gram-centimeter-second system throughout, M in gr sec^{-1}, r in cm, v in cm sec^{-1} or in km sec^{-1}, ρ in gr cm^{-3}). There is good amount of uncertainty in choosing $v = v_{th}$ in the equation (40) for starting the iteration. If this does not give expected v_∞ (= terminal velocity) we change $v_{initial}$, so that we reach v_∞.

(2) As the atmosphere consists of only hydrogen atoms, we get the total number of H atoms per cm^{-3} by dividing ρ by $m_p(= 1.602 \times 10^{-24} gr)$. Therefore we obtain,

$$N_H = \rho/1.602 \times 10^{-24} cm^{-3}. \tag{41}$$

We need to calculate the densities of neutral atoms and ionized H toms, that is, N_p, N_e, N_0. These are calculated following the procedure described in equations (20) to (39) using Saha equation. Further we need to calculate the N_r the number of atoms in the r^{th} state of excitation so that

$$N_0 = \sum N_r. \tag{42}$$

These quantities are calculated by following the procedure given in equations (34) to (39) in which Boltzmann equation is used.

(3) From the quantities $N_1, N_2 \ldots$ calculated above, we need to estimate the absorption coefficient in the lines. We choose ten levels of the H atom and the lines are calculated in the Lyman, Balmer, Paschen and Brackett series. The line centre absorption coefficient is calculated using the formula

$$\chi^L_{\nu_{ij}} = \frac{\pi e^2}{m_e c} \frac{g_i f_{ij}}{\Delta\nu_D \sqrt{\pi}} n_i \left(1 - \frac{n_j}{n_i}\frac{g_i}{g_j}\right) \tag{43}$$

where e and m_e are the electronic charge and mass respectively, c is the velocity of light, g the statistical weights, n the occupation numbers and f_{ij} is the f-value of the transition from i^{th} level to j^{th} level. $\Delta\nu_D$ is the Doppler width.

(4) We need to solve the equation of transfer in (3). We use a Doppler profile function given by

$$\phi(x) = \frac{1}{\sqrt{\pi}} e^{-x^2}. \tag{44}$$

The equation (3) is solved in the comoving frame (Peraiah 1980, 1991). As we are not considering the continuum, we set $\beta' = 0$. The quantity ϵ, the thermalization parameter is calculated by the expression,

$$\epsilon_{ji} = \frac{C_{ji}}{C_{ji} + A_{ji}\left[1 - exp(-\frac{h\nu_{ji}}{kT})\right]^{-1}} \tag{45}$$

where C_{ji} is the collisional transition rate from level j to i. A_{ji} is the Einstein coefficient of spontaneous emission. The quantity C_{ji} is given by

$$C_{ji} = 2.7 \times 10^{-10} \alpha_0^{-1.68} T^{-3/2} A_{ji} \left(\frac{I_H}{\chi_{ij}}\right)^2 N_e \tag{46}$$

(see Jefferies 1968, Mihalas 1978),

where I_H is the ionization potential of hydrogen, χ_{ij} is the excitation potential from level j to i and

$$\alpha_0 = \chi_0 / kT. \tag{47}$$

The quantities f_{ij}, A_{ji} are taken from Wiese et al. (1966). By solving the equation of transfer we obtain the specific intensities $I(r, \mu, x)$ which are used to calculate the Eddington flux, F_ν by using the formula,

$$F_\nu(r) = \frac{1}{2} \int_{-1}^{+1} I_\nu(r, \mu) \mu d\mu. \tag{48}$$

We calculate the fluxes in all the lines and compute the last term

$$\frac{4\pi}{c\rho(r)} \sum_{\text{all lines}} \int_0^\infty \chi^L_\nu(r) F^L_\nu(r) d\nu$$

on R.H.S in equation (10).

(5) next step is to calculate the first term, the term due to electron scattering, on the R.H.S. of equation (10). The electron density is obtained from the calculations described in step (2). It is assumed that this

term is changing as $1/r^2$ although the temperature remains constant. Thus we complete the calculation of the radiation term g_{rad}.

(6) The calculation of the pressure and the gravity terms is fairly simple. The pressure is by the equation (12). The number of particles is taken to be the sum of the number of protons, electrons and neutral atoms.

(7) In the first iteration of solving equation (19), we assume a constant velocity for v_{i-1} in the first term. This quantity is uncertain and it appears that the rate of convergence (number of iterations) and the converged terminal velocity are critically dependent on this initial velocity. We always choose the v_{th} as the starting velocity and if we do not obtain the expected v_∞, we change the initial velocity and start another iteration. This process is continued until we obtain the desired v_∞.

We have considered several OB stars whose observational data of masses, radii, mass loss rates, v_∞ are known. We have drawn the data from three sources Blomme (1990a), Abbott (1978) and Pauldrach et al. (1986). There appears to be a large variation in the data of temperatures, masses, radii, v_∞, mass loss rates etc. Abbott (1978) gives v_{edge} and not v_∞ while Pauldrach does not give mass directly and we calculate the masses from the given data of log g and radius. Blomme (1990a) gives the data on temperatures, masses, radii in the Table II.1.1 on page 42, v_∞ in the Table II.1.4 on page 53 and mass loss rates in the Table II.1.6 on page 62. He gives highest and lowest mass loss rates. He collected the data (according to his references) from Underhill et al. (1979), Mendoza (1958), Conti and Leep (1974), Hiltner et al. (1969), Johnson and Morgan (1953). We have generally adopted the data given by Blomme (1990a). We have quoted the data from the above three references whenever possible just to show variations in the data. Regarding the mass loss rates we have taken the average of maximum and minimum values given in Blomme (1990a). We have applied the theory to the following systems:

HD 10516 (ϕPer)
HD 24534 (X Per)
HD 30614 (α Cam)
HD 38666 (μCol)
HD 46150
HD 47129
HD 48099
HD 57061 (τCMa)
HD 144217 (βSco)
HD 147165 (σSco)
HD 149438 (τSco)
HD 149757 (ζ Oph)
HD 152234
HD 152236 (ζ Sco)
HD 152249
HD 157857
HD 164794 (9 Sgr)
HD 167263 (16 Sgr)
HD 175876
HD 210839 (λ Cep)
HD 37742 (ζOri)
HD 37128 (ϵ Ori)
HD 193237 (P Cyg)
HD 42088

We have chosen the geometrical extent of the wind medium to be equal to 10 times the stellar radii. We have calculated a large amount of information. These results would be interesting to see but lack

of space restricts the presentation of all of them. Consequently, we can not show all the details of the calculations. We are showing the following results for each star, in figures (a), (b), (c), (d), (e), (f), (g) and (h) which are explained below:

(a) Number of atoms excited in different stages of excitation at $R/R_0 = 1.36$, 5.41 and 9.91 where R_0 is the stellar radius. We have chosen 10 levels and $R/R_0 = 10$ for all the stars (see equation (39)).

(b) Neutral atom density is given from $R = R_0$ to $R = 10\ R_0$ (see equation (31)).

(c) Electron density of the medium is plotted from $R = R_0$ to $R = 10\ R_0$ (see equation (32)).

(d) The ϵ parameter defined in equation (45) is plotted across the medium $R = 10\ R_0$. These ϵ's correspond to Lyman α, Balmer α, Paschen α and Brackett α.

(e) We plot the total radial optical depth corresponding to Lyman α, Balmer α, Paschen α and Brackett α. The line absorption coefficient is calculated by using equation (43).

(f) For comparison sake, we plotted the three competing forces - radiation force, gravity force and gas pressure force across the medium from $R = R_0$ to $R = 10\ R_0$ (see equation (19)).

(g) The velocity profile calculated according to equation (19) is plotted. The dotted line represents the observed or the expected v_∞.

The velocity law given in Blomme (1990a) is taken for comparison. This is given by

$$v(r) = v_0 + (v_\infty - v_0)(1 - \frac{r_0}{r})^\beta \tag{49}$$

where v_0 is the initial velocity, v_∞ is the terminal velocity, r_0 is the reference distance from the centre of the star (here we shall take this as the radius of the star), $v(r)$ is the velocity at the radius r . β is the steepness parameter.

If we set $v_0 = 0$ then equation (49) becomes

$$v(r) = v_\infty\big(1 - \frac{r_0}{r}\big)^\beta \tag{50}$$

or

$$\frac{v(r)}{v_\infty} = \big(1 - \frac{r_0}{r}\big)^\beta. \tag{51}$$

This relation is graphically described in Figure 1.

(h) The variation of density across $R = 10R_0$ is plotted which is derived from $\rho(r) = \dot{M}/4\pi r^2 v(r)$ where ρ is the quantity given in Figure (g).

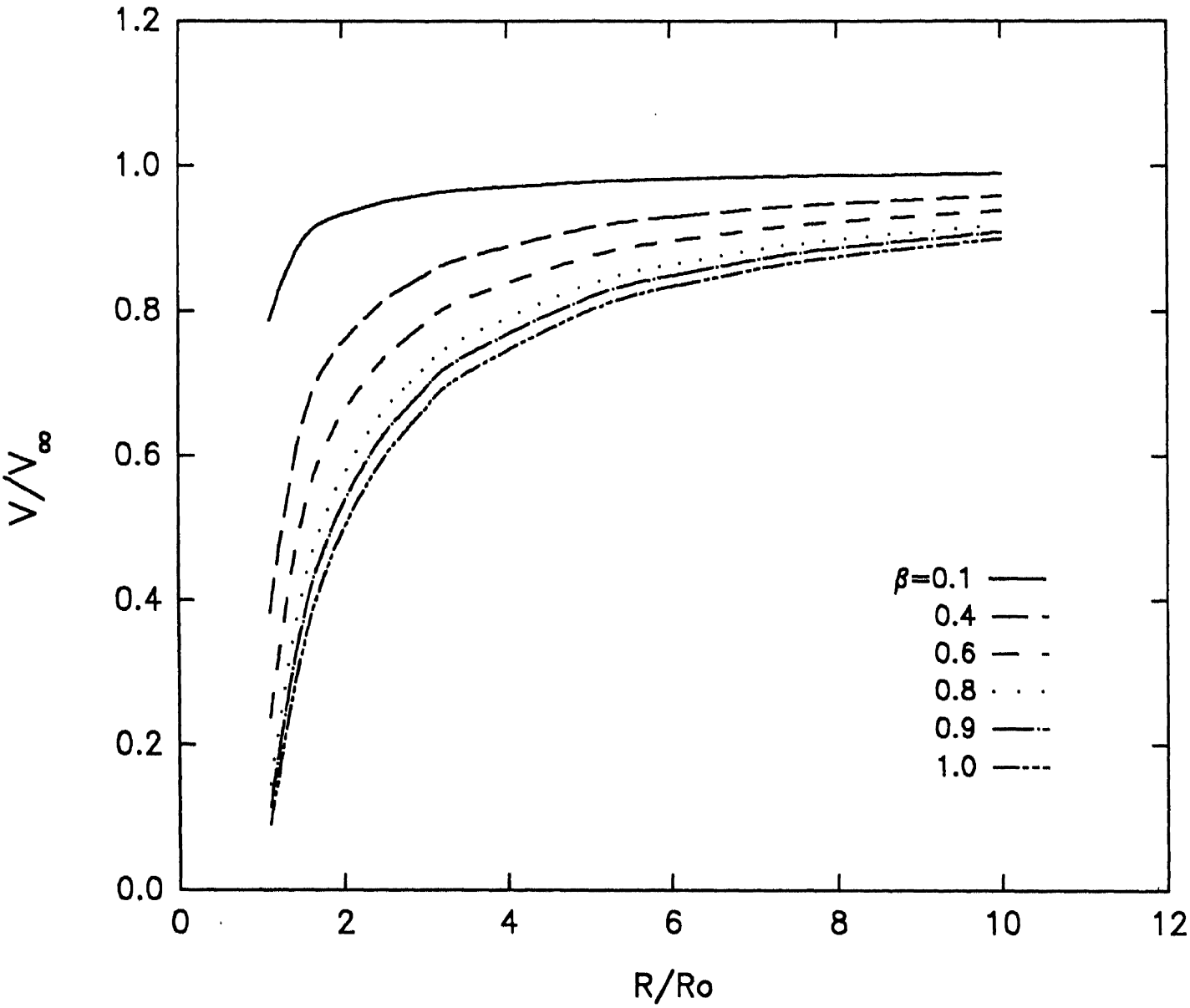

Figure 1 See equation (51)

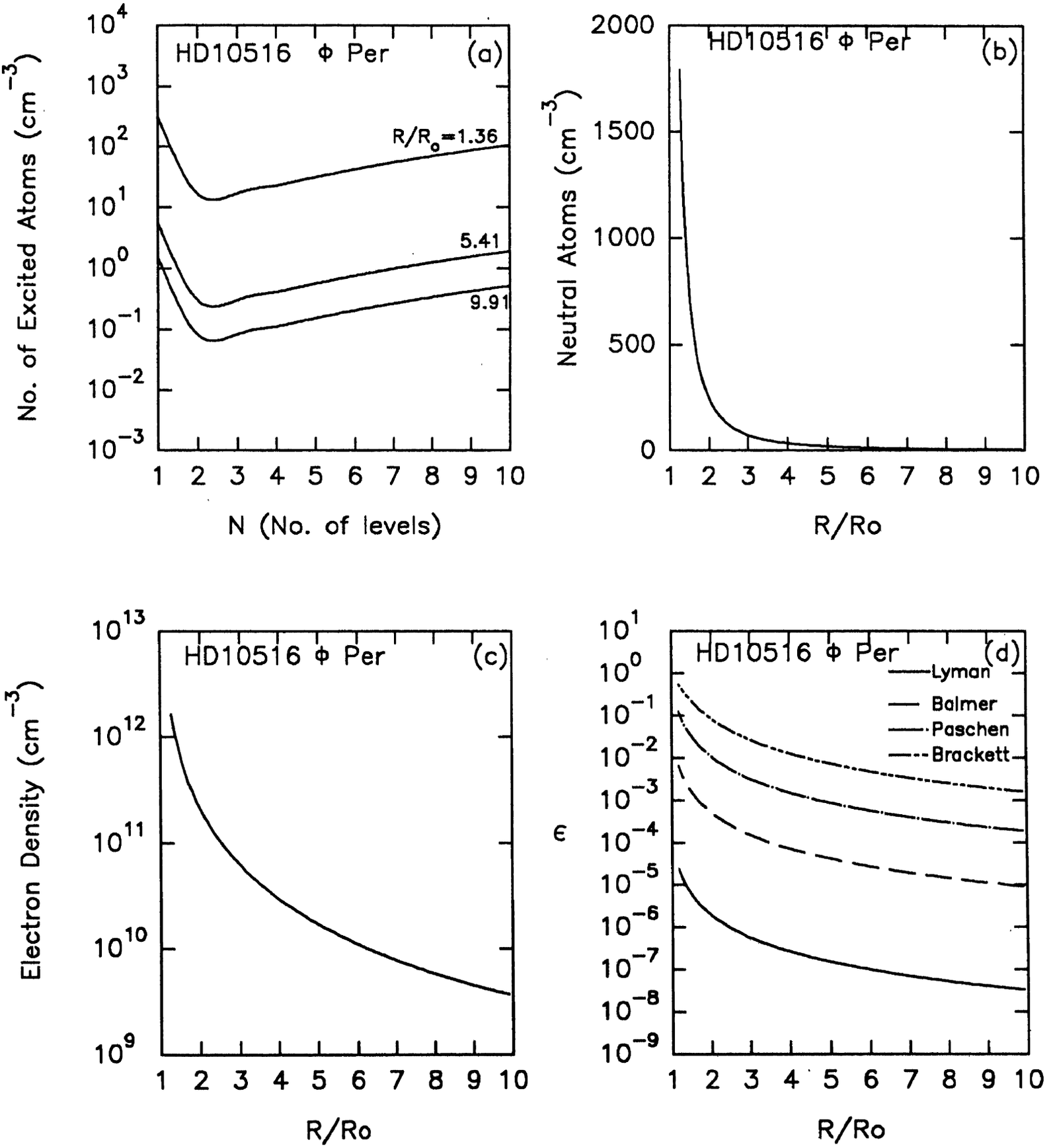

Figure 2 (a,b,c,d)

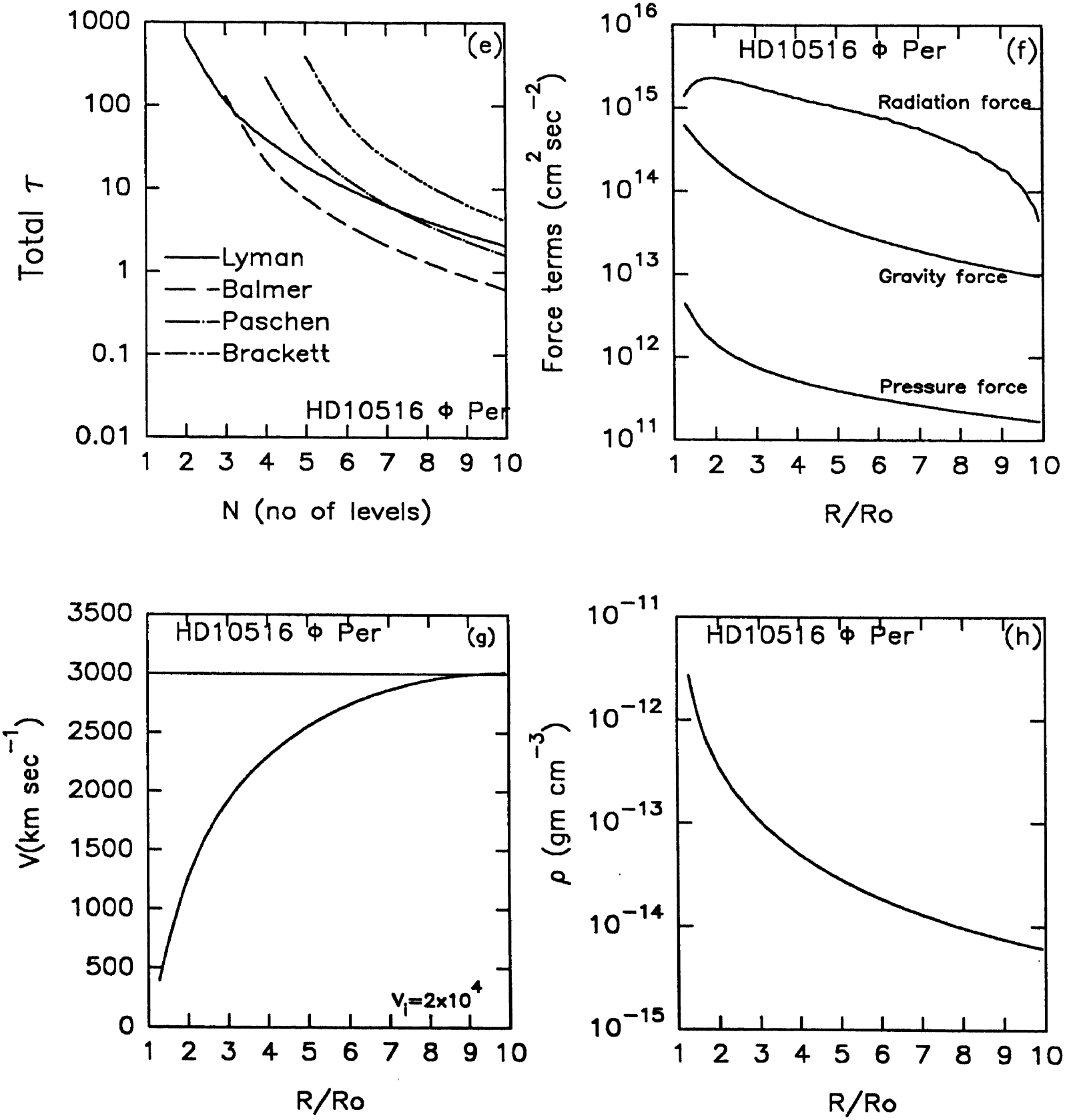

Figure 2 (e,f,g,h)

Figure 2.
HD 10516 (ϕ PER) B1 1Ve. Blomme (1990a)

*T_{eff} = 27542 K/24547 K

$M = 2.6 \times 10^{34}$ gr or 2.06×10^{34} gr

$R = 3.36 \times 10^{11}$ cm or 3.01×10^{11} cm

$V_esc = 1004$ km s^{-1} or 948 km s^{-1}

$V_\infty = 3000$ km s^{-1}

$\dot{M} = 3.847 \times 10^{-6} M_\odot$/yr.

*The spectral class and subclass are uncertain.

(a) The number of atoms N_r in different states of excitation are drawn against the quantum number n at $R/R_0 = 1.36$ (nearer to the stellar surface), at R/R_0=5.41 (at about half way in the medium) at R/R_0 = 9.91 (almost at the surface of the wind medium. At every point there is a drop in these numbers (N_r) in the second level and from r = 2 to 10, there is a gradual increase in the numbers. The reason for this is that the number of states at higher levels increase while the excitation energy does not increase at the same rate (see equation (33)). As the temperature is high, it is expected that higher levels become more populated than at lower temperatures.

(b) The variation of the total number of neutral atoms are shown against R/R_0. They vary from a few times 10^3 (cm^{-3}) at the surface of the star ($R/R_0 = 1$) to less than 10(cm^{-3}) at $R/R_0 = 10$. It is steeper than $1/r^2$ variation.

(c) The electron density variation is given at $R/R_0 = 1$ it is few times 10^{12} (cm^{-3}) to less than 10^{10} (cm^{-3}) at $R/R_0 = 10$. The density falls steeper than $1/r^2$.

(d) The variation of the non-LTE parameter ϵ is plotted for Lyman α, Balmer α, Paschen α and Brackett α, from $R/R_0 = 1$ to $R/R_0 = 10$ (see equation (45)). The variations of these four ϵ's are very similar except that the magnitudes increase from Lyman α to Brackett α. Near the surface of the star ($R/R_0 = 1$), there is less scattering of photons than at $R/R_0 = 10$. Further, there is more scattering (and more non-LTE effects) in Lyman α than in the Brackett α. The line source functions (see equations (8)) will have major contribution from scattering part in the Lyman α line and Brackett α will have from thermal emission. Brackett α is almost in LTE near $R/R_0 = 1$, while mildly in non-LTE at $R/R_0 = 10$. There is very little contribution from thermal emission to Lyman α and more contribution from scattering process. Therefore Lyman lines contribute more to the line pressure.

(e) Total radial optical depths (from $R/R_0 = 1$ to $R/R_0 = 10$) are shown from the four continua. Lyman α has largest depth while Balmer 10 has the smallest depth.

τ (Balmer α) < τ (Paschen α)

τ (Paschen α) < τ (Brackett α)

τ (Lyman α) < τ (Paschen α)

τ (Lyman α) $< \tau$ (Brackett α)

τ (Lyman α) $< \tau$ (Balmer α)

But

τ (Brackett 6) $> \tau$ (Lyman 9)

τ (Brackett 6) $> \tau$ (Balmer 8)

τ (Brackett 6) $> \tau$ (Paschen 7)

(f) The three competing forces (i.e) radiation, gravity and pressure are plotted for comparison. Gravity and the gas pressure forces vary as $1/r^2$ while the radiation force changes differently. Initially it raises for a short distance, then it starts falling. The radiation force g_{rad} is calculated using the relation given in equation (10). This consists of the first term $N_e(r)\sigma_{th}\sigma_B T_{eff}^4/c\rho(r)$ which represents the electron scattering and the third term

$$4\pi \sum_{\text{all lines}} \int_{-\infty}^{+\infty} \chi_\nu^L F_\nu^L(r) d\nu$$

due to line radiation pressure. We have considered 9 lines in Lyman, 8 in Balmer, 7 in Paschen and 6 in Brackett series of lines. The radiation force reduces slowly from $R/R_0 = 2$ to $R/R_0 = 8$. From this point it starts falling rapidly. We can see that the radiation force is predominant compared to gravity force. Pressure force is several order of magnitude less than both radiative force and gravity force.

(g) We plotted the converged velocity profile across the wind medium from $R/R_0 = 1$ to $R/R_0 = 10$. We started the iteration with v_{therm} which is derived from the relation $\rho(r) = \dot{M}/4\pi r^2 v_{therm}$. As the temperature remains constant, v_{th} = constant. The system converged in 5 iteration but reached too high v_∞. Therefore we changed the initial velocity until we obtain convergence to the observed v_∞ which is 3000 km sec^{-1} in this case. The initial velocity which gave convergence to v_∞ = 3000 km sec^{-1} is $v_i = 2 \times 10^4$cm sec^{-1}. $\beta \approx 0.85$.

(h) we plotted the density $\rho(r)$ corresponding to the velocity given in (g). The density is derived from $\rho(r) = \dot{M}/4\pi r^2 v(r)$.

Figure 3

HD 24534(X PER) BO eP Blomme (1990a)

$T_{eff}^* = 30200$ K.

M $= 3.2 \times 10^{34}$ gr

$R = 3.71 \times 10^{11}$ cm

$V_{esc} = 1054$ km s^{-1}

$V_\infty = 3150$ km s^{-1}

$\dot{M} = 1.3845 \times 10^{-5} M_\odot$/yr.

* The spectral class and subclass are uncertain.

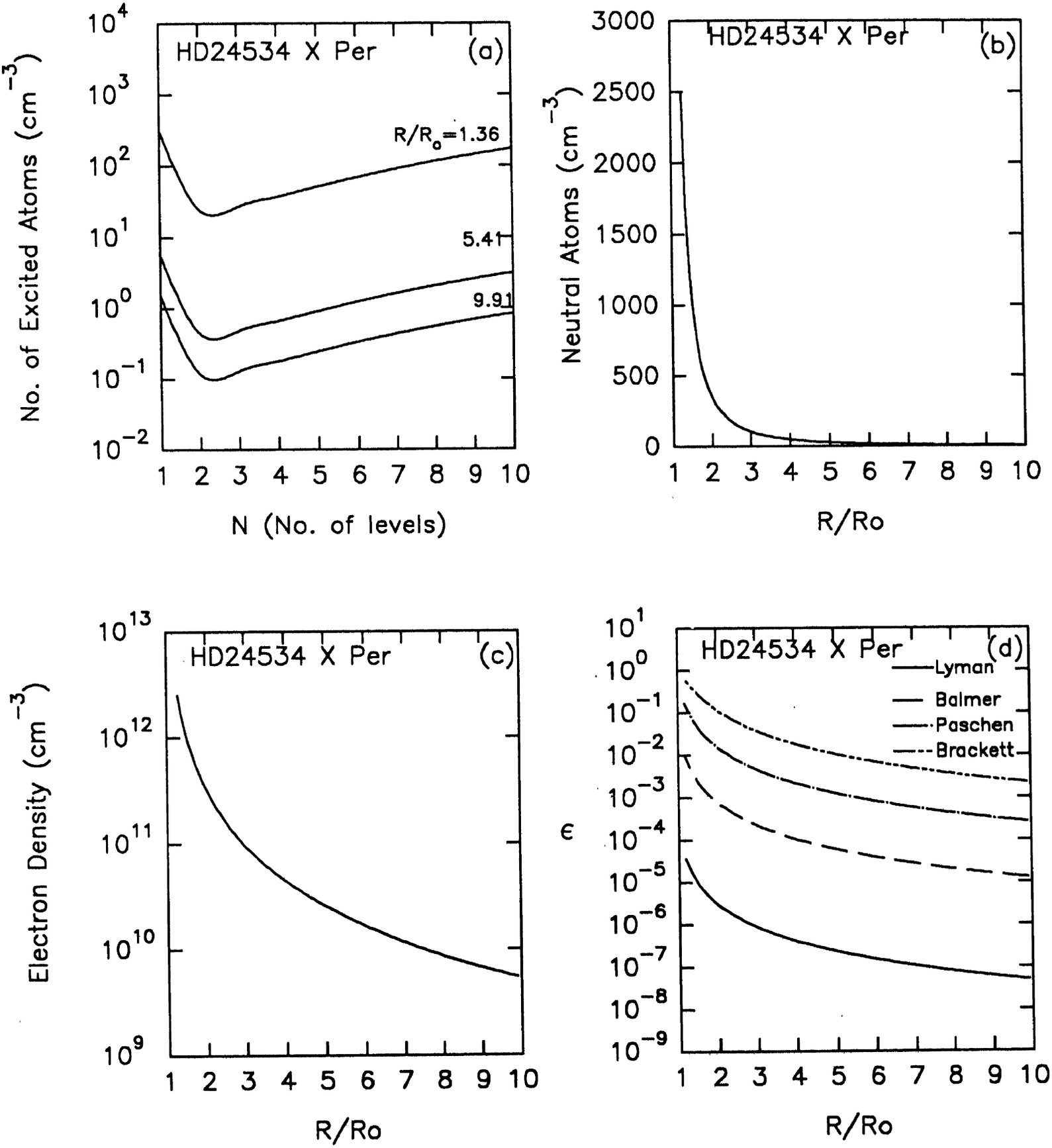

Figure 3 (a,b,c,d)

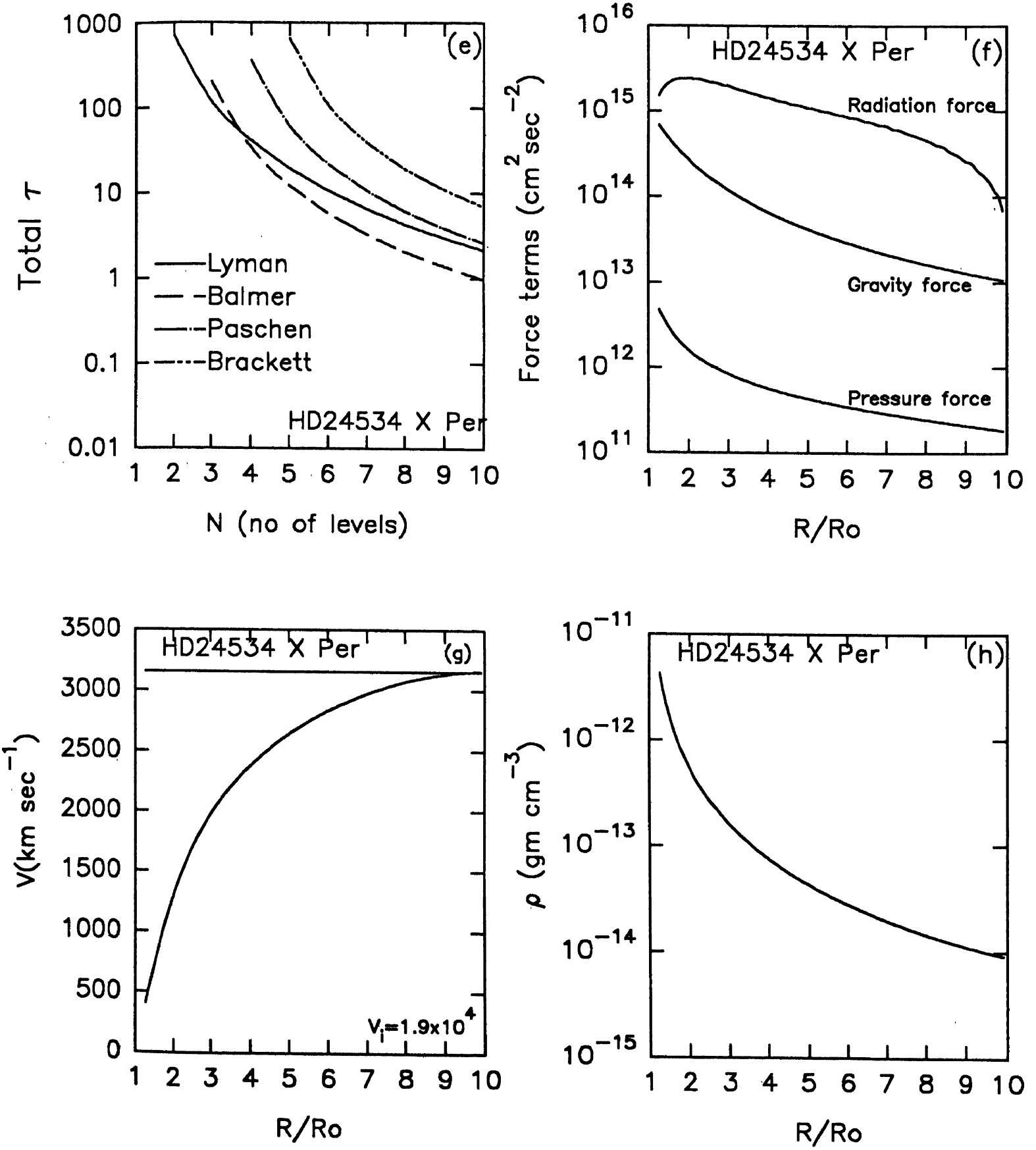

Figure 3 (e,f,g,h)

(a) The distribution of atoms in the excited states is very similar to that of HD 10516 (ϕ PER) although the temperature is slightly higher.

(b) The neutral atom density changes between few times 10^3 cm^{-3} at $R/R_0 = 1$ to less than 10 (cm^{-3})at $R/R_0 = 10$.

(c) The variation of the electron density is similar to that in HD 10516. The electron density is almost equal to the density $\rho(r)$.

(d) The values of ϵ are slightly higher than what are obtained in the case of HD 10516 (ϕ PER).

(e) The Lyman α and Brackett α attain optical depths of nearly 10^3 while τ (Lyman 9) is larger than τ (Balmer 9), it is less than Paschen 7 and Brackett 6.

(f) The radiation force exceeds the gravity force by several times but falls sharply at $R/R_0 = 10$.

(g) The velocity attains v_{max} at about $R/R_0 = 9$. It sharply rises from $R/R_0 = 1$. $\beta \approx 0.85$.

(h) The density is given according to the velocity given in (g).

Figure 4

HD 30614 (α CAM) 09.5 Ia

	Abbott (1978)	Blomme (1990a)
T_{eff}	28840 K	25119 K
M	9×10^{34} gr	6.12×10^{34} gr
R	2.24×10^{12} cm	2.436×10^{12} cm
V_{esc}	590 km s^{-1}	458 km s^{-1}
V_∞	1890 km s^{-1}	2450 km s^{-1}
$\dot{M}$		$7.0725 \times 10^{-5} M_\odot$/yr

(a) The number of excited atoms is quite small compared to those in previous cases i.e. HD 10516 and HD 24534. The main reason for this is the lower temperature of 25119 K.

(b) Neutral atom density is small for the same reason as mentioned above.

(c) Electron density changes from few times 10^{11} cm^{-3} to about 10^9 (cm^{-3}).

(d) The factors ϵ are much smaller than those in the previous cases and therefore the lines are more in non LTE.

(e) The total radial optical depths τ between few times 10^2 to less than 1.

(f) The radiation force falls more rapidly than gravity particularly from $R/R_\odot = 5$.

(g) The velocity converges at just above 2000 km s^{-1} while the observed $v_\infty = 2450$ km s^{-1} in Blomme (1990a) and 1890 km s^{-1} in Abbott (1978). The initial velocity for starting the iteration is $v_i = 2.5$ km s^{-1}. $\beta \approx 0.9$.

(h) Density changes between 10^{-12} gr cm^{-3} to 10^{-15} gr cm^{-3}.

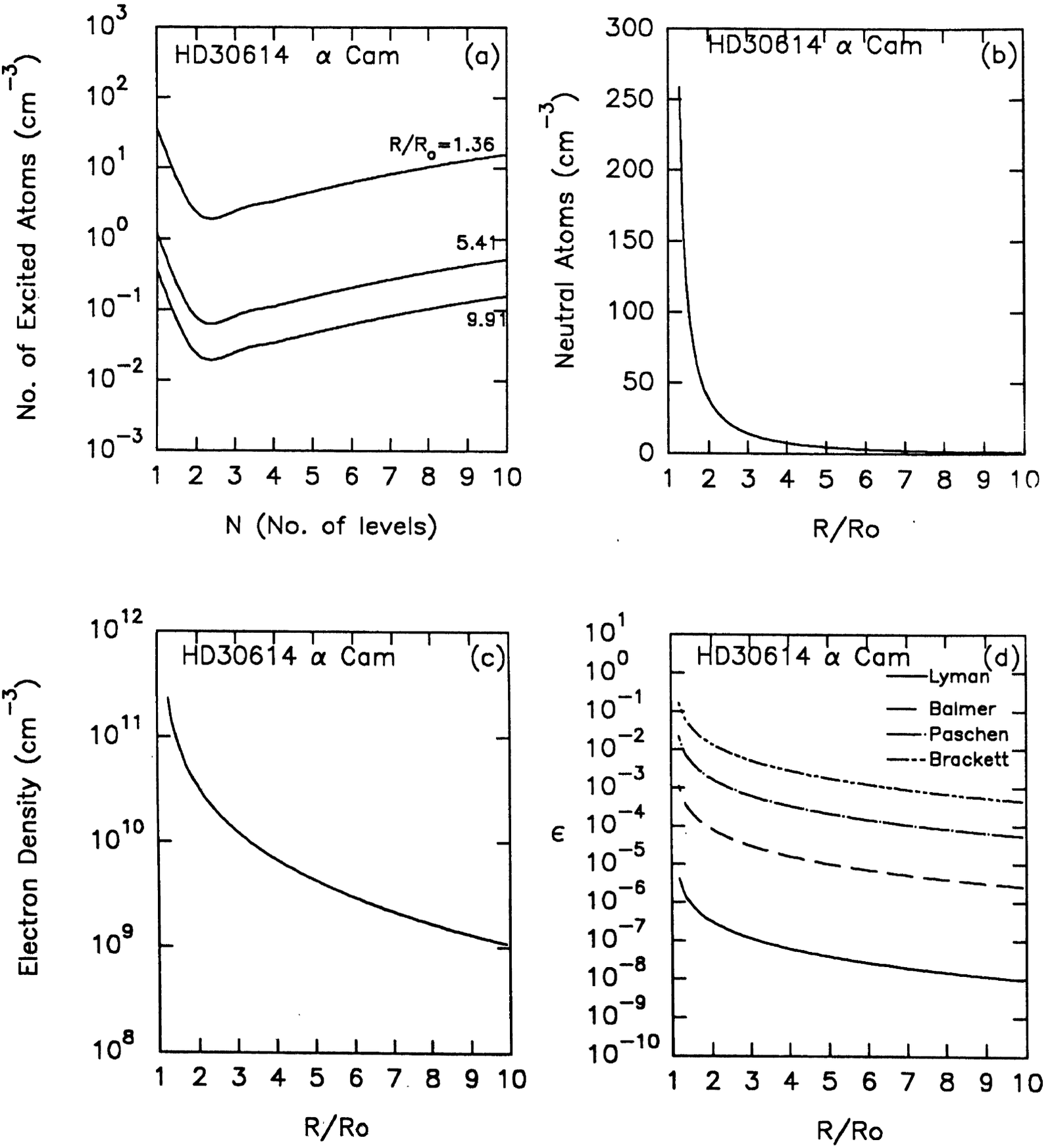

Figure 4 (a,b,c,d)

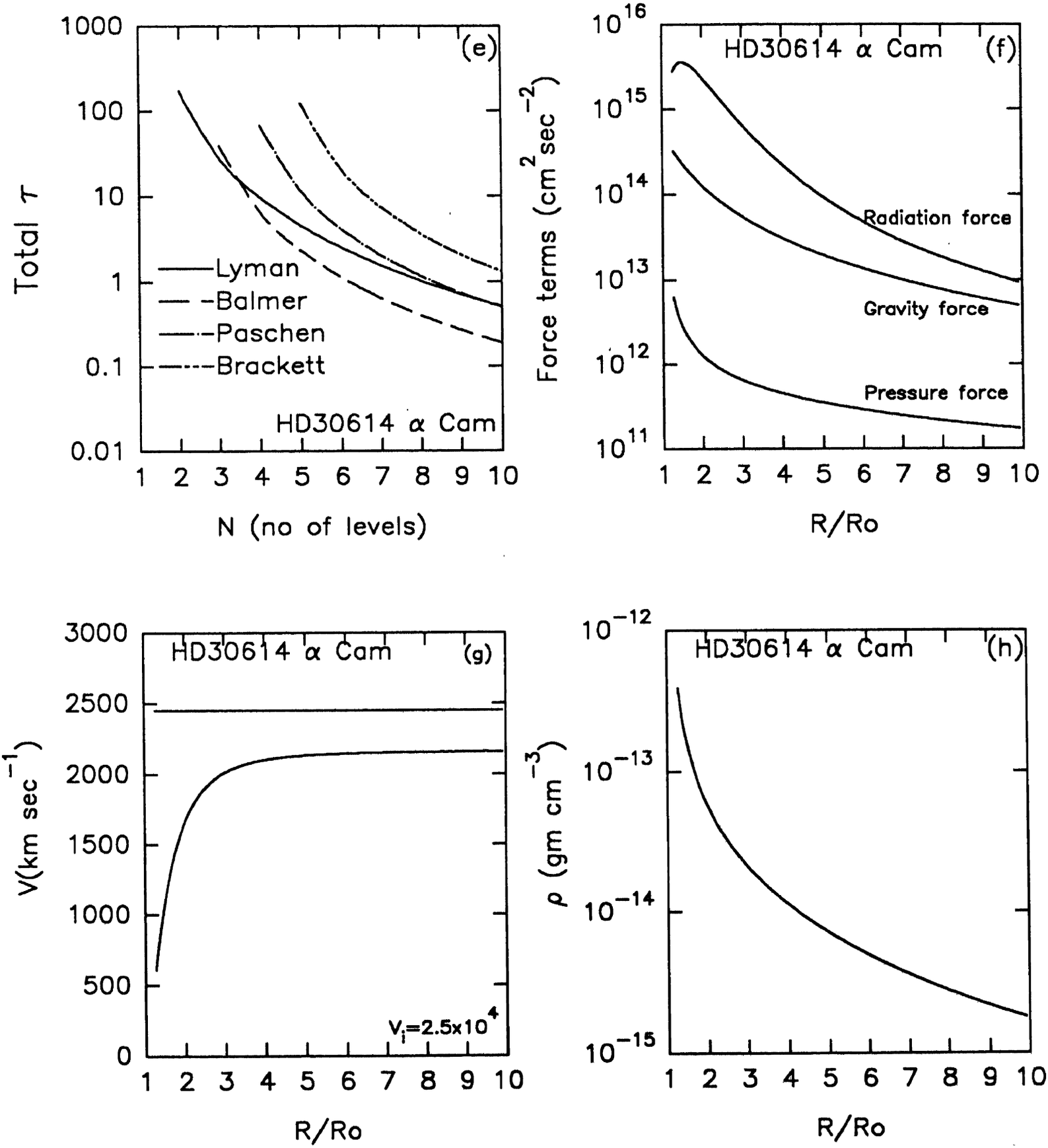

Figure 4 (e,f,g,h)

Figure 5

HD 38666 (μ Col) 09 V

	Abbott (1978)	Blomme (1990a)
T_{eff}	33884 K	33884 K
M	4.2×10^{34} gr	4.3×10^{34} gr
R	4.2×10^{11} cm	3.92×10^{11} cm
V_{esc}	1080 km s^{-1}	1182 km s^{-1}
V_∞	670 km s^{-1}	3550 km s^{-1}
$\dot{M}$		$7.8 \times 10^{-6} M_\odot$/yr

(a) and (b) The number of neutral atoms is much smaller as the temperature is fairly large and the velocity of expansion is large at $v_\infty = 3550$ km s^{-1}. Consequently the density is reduced and at higher temperatures most of the atoms are ionized. This will further reduce the density of neutral atoms.

(c) The electron density varies between $\approx 5 \times 10^{10}$ cm^{-3} at $R/R_0 = 1$ to $\approx 2 \times 10^8$ cm^{-3} at $R/R_0 = 10$.

(d) The quantity ϵ for Lyman α line changes from $\approx 10^{-6}$ to $\approx 10^{-9}$ between $R/R_0 = 1$ to R/R$_0$ = 10, while the ϵ for Brackett α changes from $\approx 10^{-2}$ to $\approx 10^{-4}$ ϵ (Balmer α) and ϵ (Paschen α) lie in between those of ϵ (Lyman α) and ϵ (Brackett α).

(e) The total radial optical depth varies in a similar way as in the previous cases.

(f) The radiation force falls faster than the gravity force and the latter overtakes the former at about $r/R_0 = 8.5$. However the change in velocity is so small it is not reflected in the velocity profile given (g) (see below).

(g) The initial velocity is $v_i = 10^4$ cm s^{-1}, and with $v_i = v_{therm}$, we obtain $v_\infty > 5000$ km s^{-1}. The solution converges at about $v_\infty \approx 3100$ km s^{-1}. While the observed $v_\infty \approx 3550$ km s^{-1}.

(h) The density varies between $\approx 10^{-13}$ gr cm $^{-3}$ to $\approx 5 \times 10^{-16}$ gr cm^{-3}.

Figure 6

HD 46150 05.5(f) Blomme (1990a)

$T_{eff} = 38019$ K

M $= 7.28 \times 10^{34}$ gr

R $= 9.59 \times 10^{11}$ cm

$V_{esc} = 874$ km s^{-1}

$V_\infty = 3400$ km s^{-1}

$\dot{M} = 2.685 \times 10^{-6} M_\odot$/yr

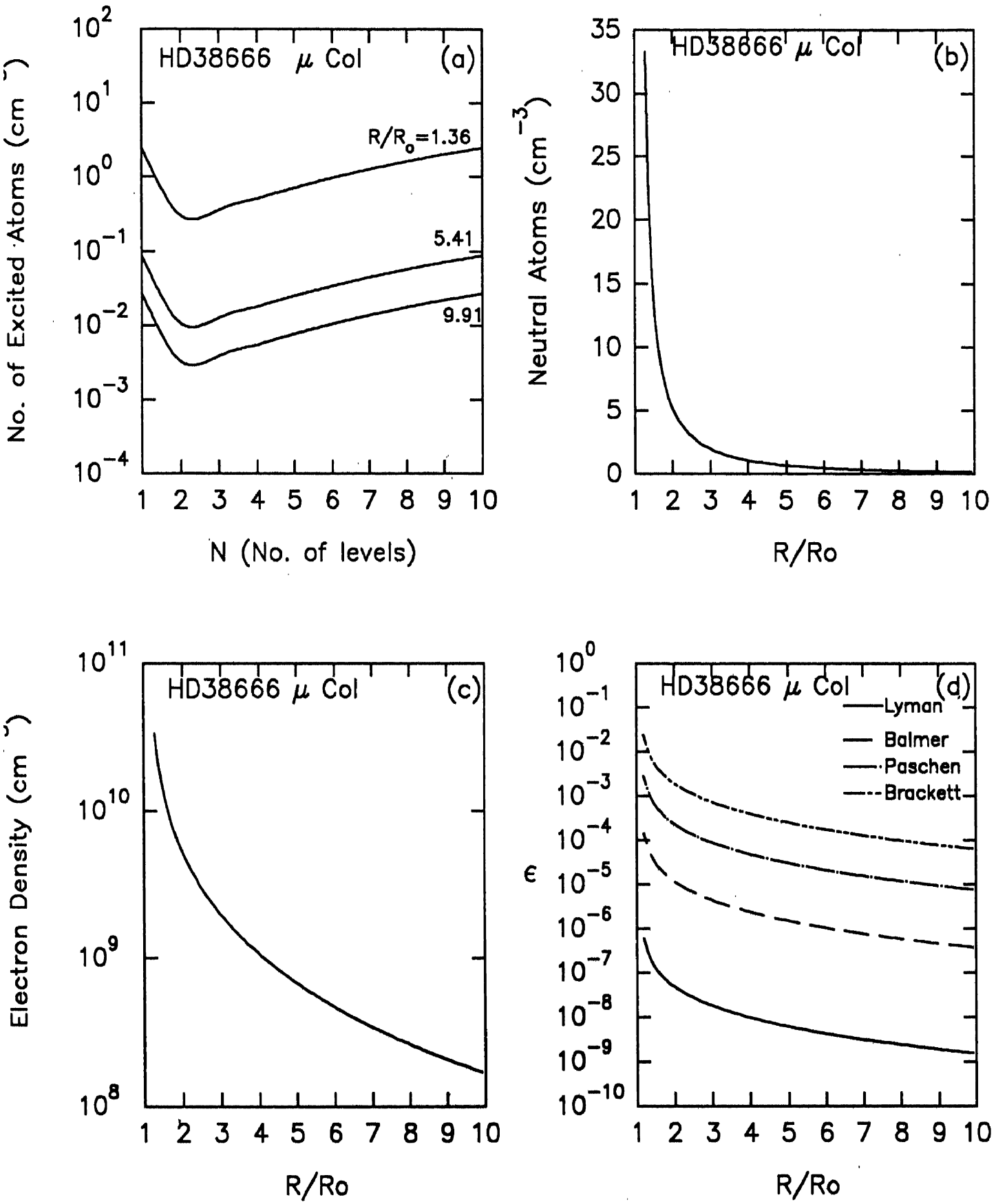

Figure 5 (a,b,c,d)

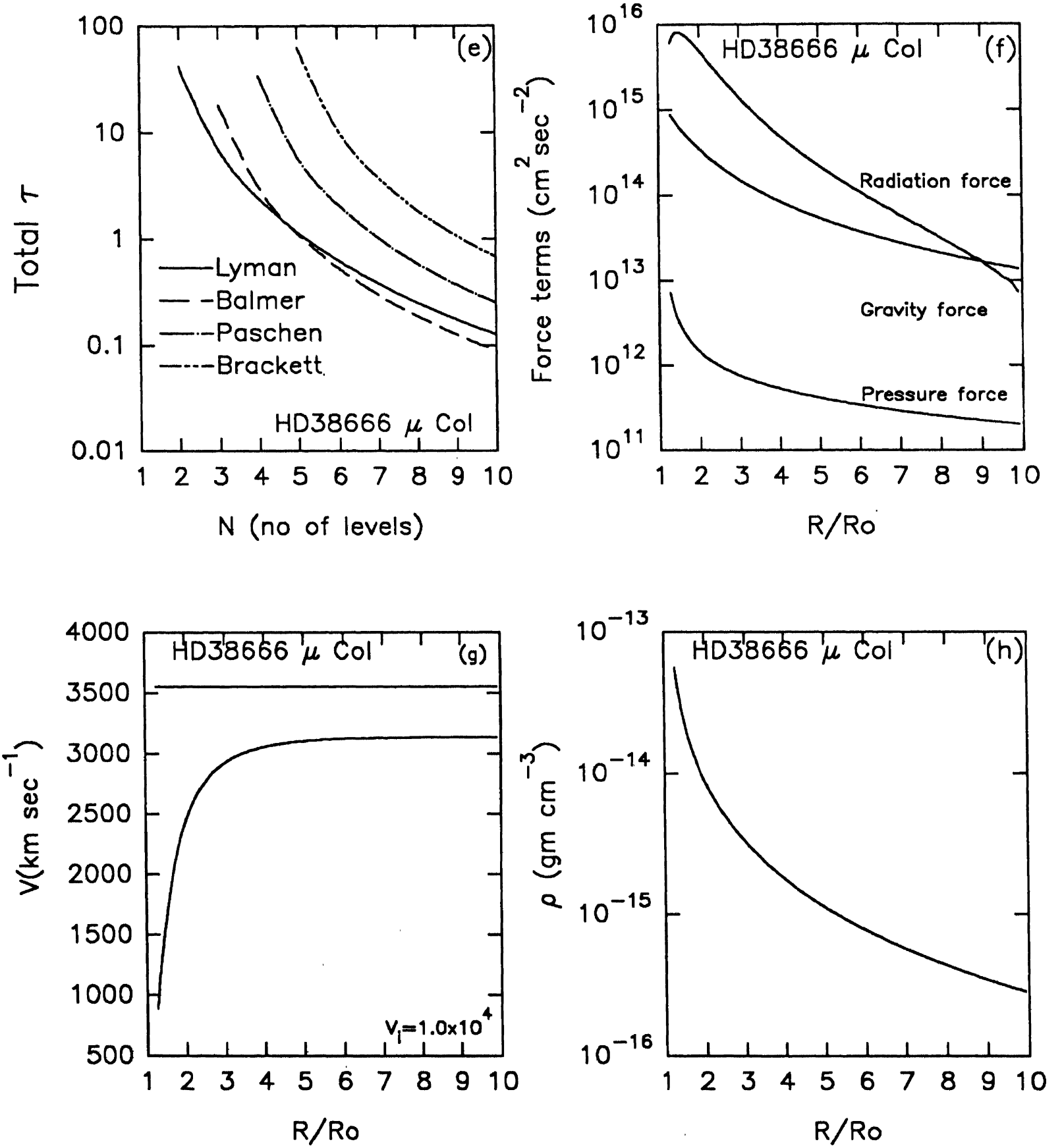

Figure 5 (e,f,g,h)

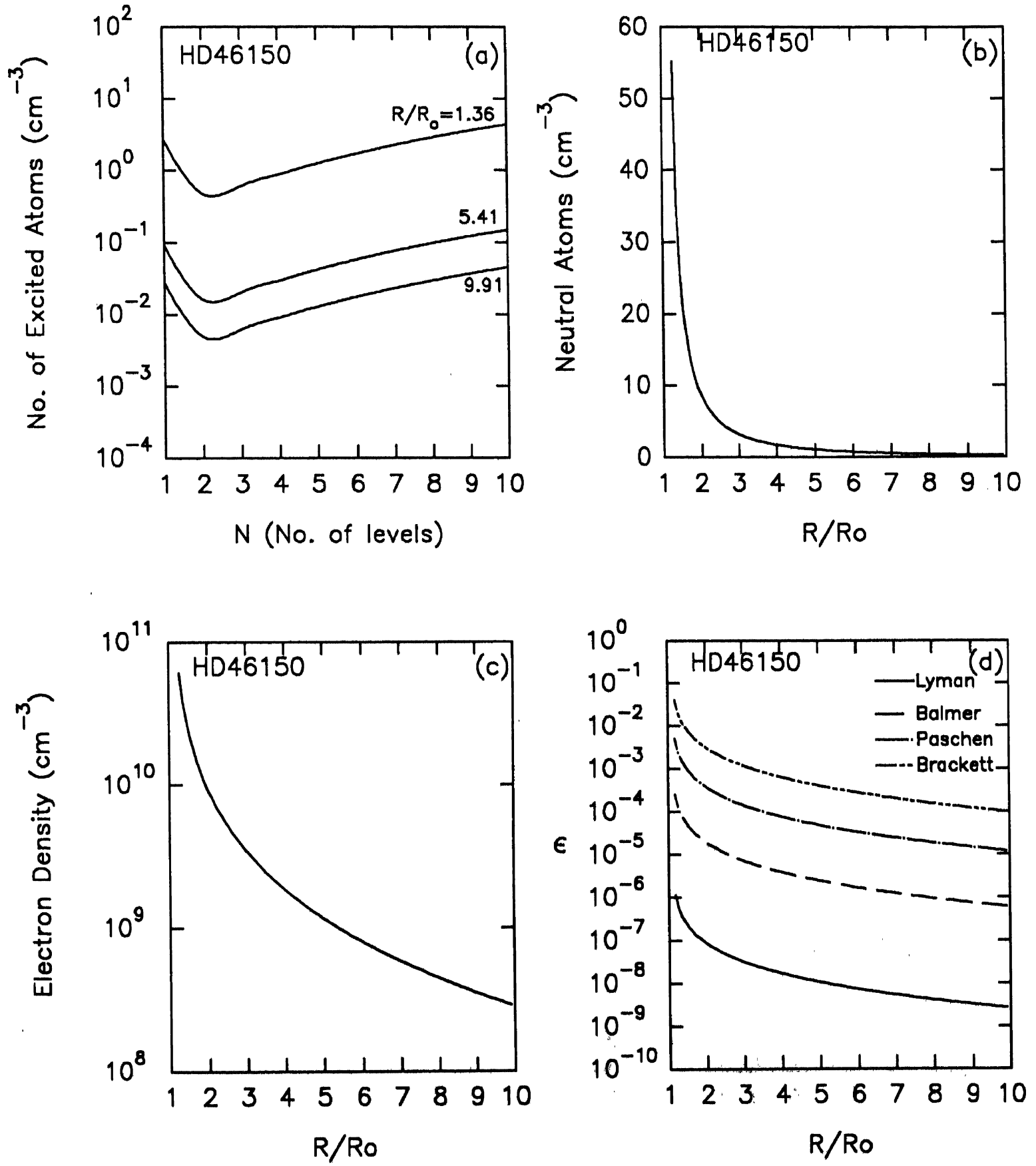

Figure 6 (a,b,c,d)

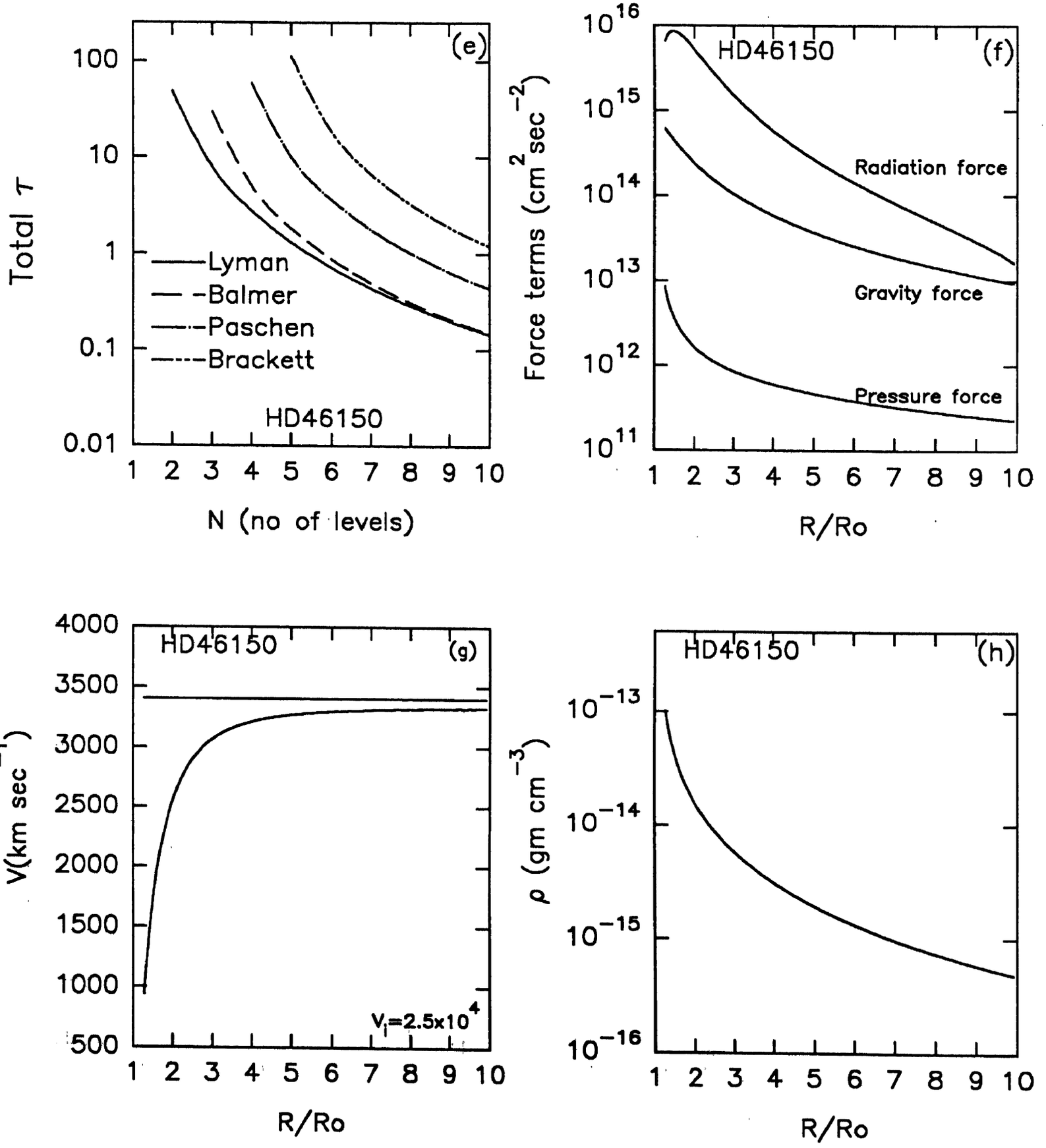

Figure 6 (e,f,g,h)

(a) and (b) As the velocity is high the density is correspondingly reduced. Therefore the number of H atoms is small and at higher temperatures a large fraction of them are ionized. Consequently we get small number of neutral atoms and excited atoms.

(c) Electron density is nearly equal to the density of H atoms as the neutral atoms are very few.

(d) The parameter ϵ for all the four lines Lyman α, Balmer α, Paschen α and Brackett α vary as in the other cases.

(e) τ (Brackett α) $>$ τ (Lyman α)

τ (Brackett α) $>$ τ (Balmer α)

τ (Brackett α) $>$ τ (Paschen α)

τ (Brackett 6) $>$ τ (Lyman 9)

τ (Brackett 6) $>$ τ (Paschen 7)

τ (Brackett 6) $>$ τ (Balmer 8)

(f) The radiation force is falling faster than that due to gravity. After $R/R_0 > 10$ it may be less than gravity but at this point the velocity of expansion reaches such large values, that the v_∞ will not change considerably and the expansion will continue with slightly reduced velocities.

(g) The expected $v_\infty \sim 3400$ km s^{-1}, with $v_i = v_{th}$ we get $v_\infty \sim 9000$ km s^{-1}, with $v_i = 2.5 \times 10^4$ cm s^{-1} we obtain $v_\infty \sim 3400$ km s^{-1}. $\beta \approx 0.9$.

(h) The density changes between 10^{13} gr cm^{-3} and $\approx 7 \times 10^{-16}$ gr cm^{-3}.

Figure 7

HD 47129 07.5 III (f)

	Abbott (1978)	Blomme (1990a)
T_{eff}	35481 K	36308 K
M	6.8×10^{34} gr	7.54×10^{34} gr
R	9.1×10^{11} cm	1.043×10^{12} cm
V_{esc}	900 km s^{-1}	854 km s^{-1}
V_∞ or V_{edge}	$V_{edge} = 3100$ km s^{-1}	2600 km s^{-1}
$\dot{M}$		$5.115 \times 10^{-6} M_\odot$/yr

(a) and (b) As the temperature is very high, the neutral atoms are few and the number of excited atoms in the higher levels (n $\approx$ 10) are slightly more than at lower levels at (n$\approx$ 1 or 2). There is a sudden drop in the number of neutral atoms at R/R_0 = 2.

(c) The electron density is same as the density of the medium.

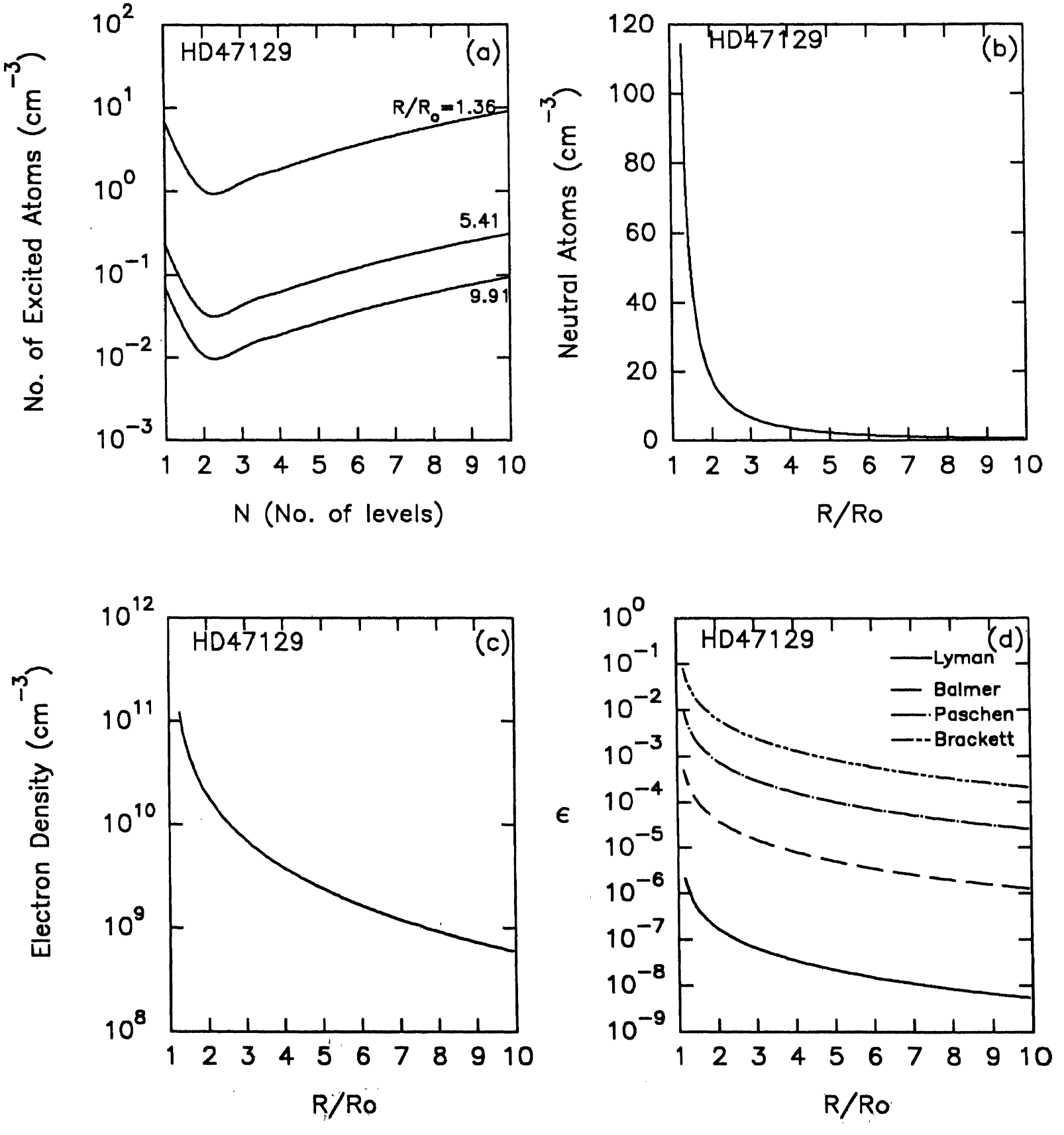

Figure 7 (a,b,c,d)

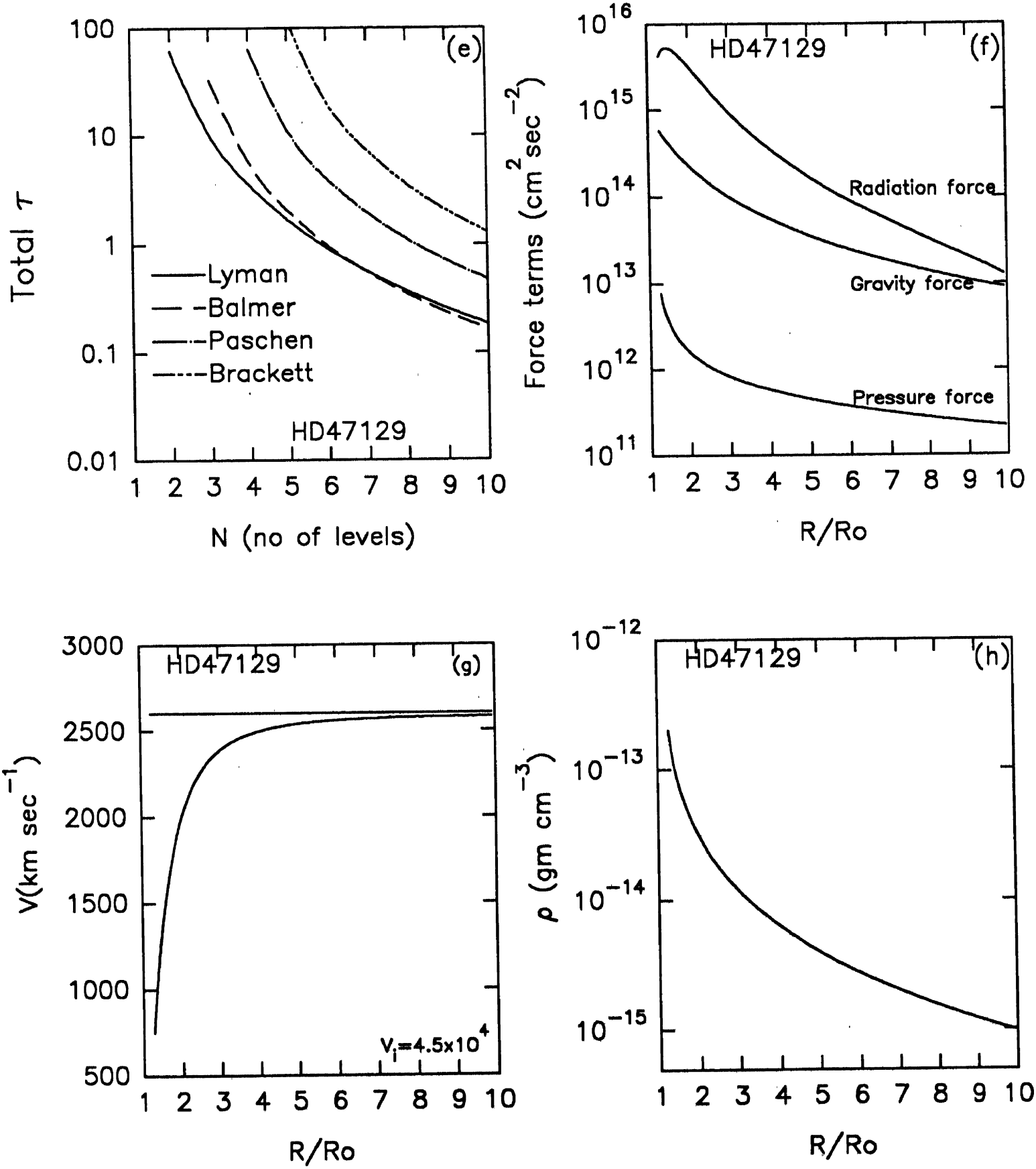

Figure 7 (e,f,g,h)

(d) The parameter ϵ (Lyman α) is very small therefore it will be dominated by scattering process, where as ϵ (Brackett α) is much larger particularly at R(R_0 = 1 to 2), thermal emission contributes considerably at $R/R_0 = 1$ and at $R/R_0 \sim 10$ it is dominated by scattering process.

τ(Brackett)> τ (Lyman, Balmer and Paschen).

(f) The radiation force falls more rapidly after $R/R_0 \approx 3$.

(g) The expected terminal velocity v_∞ is $\sim$ 1600 km s^{-1} we obtain a converged v_∞ about 2500 km s^{-1} at $R/R_0 \approx 10$. The β appears to be between 0.8 and 0.9 (see Figure 1).

(h) The density changes from $\approx 10^{-13}$ gr cm^{-3} to $\approx 10^{-15}$ gr cm^{-3}

Figure 8

HD 48099 06.5 V

	Pauldrauch et al. (1986)	Abbott (1978)	Blomme (1990a)
T_{eff}	3900 K	40740 K	37153 K
M	8.889 $\times$ 10^{34}* gr	6.6 $\times$ 10^{34} gr	7.34 $\times$ 10^{34} gr
R	7.7 $\times$ 10^{11} cm	7 $\times$ 10^{11} cm	8.26 $\times$ 10^{11} cm
V_{esc}		1060 km s^{-1}	994 km s^{-1}
V_∞	3500 km s^{-1}	V_{edge} = 3010 km s^{-1}	3300 km s^{-1}
$\dot{M}$	0.63 $\times$ 10$^{-6}M_\odot$ /yr		1.68 $\times$ 10$^{-5}M_\odot$/yr

*derived from log g and R, given in the Table 5.

(a) and (b) The densities of neutral atoms and excited atoms are very similar to those in HD 47129.

(c) Electron density varies from $\approx 4 \times 10^{10}$ cm^{-3} at $R/R_0 = 1$ to $\approx 10^8$ cm^{-3} at $R/R_0 = 10$.

(d) ϵ (Lyman α) < ϵ (Balmer α) < ϵ (Paschen) < ϵ (Brackett α).

τ (Brackett 6) > τ (Lyman 9)

τ (Brackett 6) > τ (Balmer 8)

τ (Brackett 6) > τ (Paschen 7)

(f) The radiation force is falling more rapidly than gravity force because of the fall in electron density and the assumption that total blackbody radiation is changing as $1/r^2$. The two forces are almost equal at $R/R_0 = 10$.

(g) With $v_i = 1.1 \times 10^4$cm s^{-1} we obtain the expected $v_\infty \approx$ 3300 km s^{-1}. The β factor could be about 0.9.

(h) The density $\rho(r)$ changes from 5 $\times$ 10^{14} gr cm^{-3} at $R/R_0 = 1$ to 8 $\times$ 10^{-16} gr cm^{-3}.

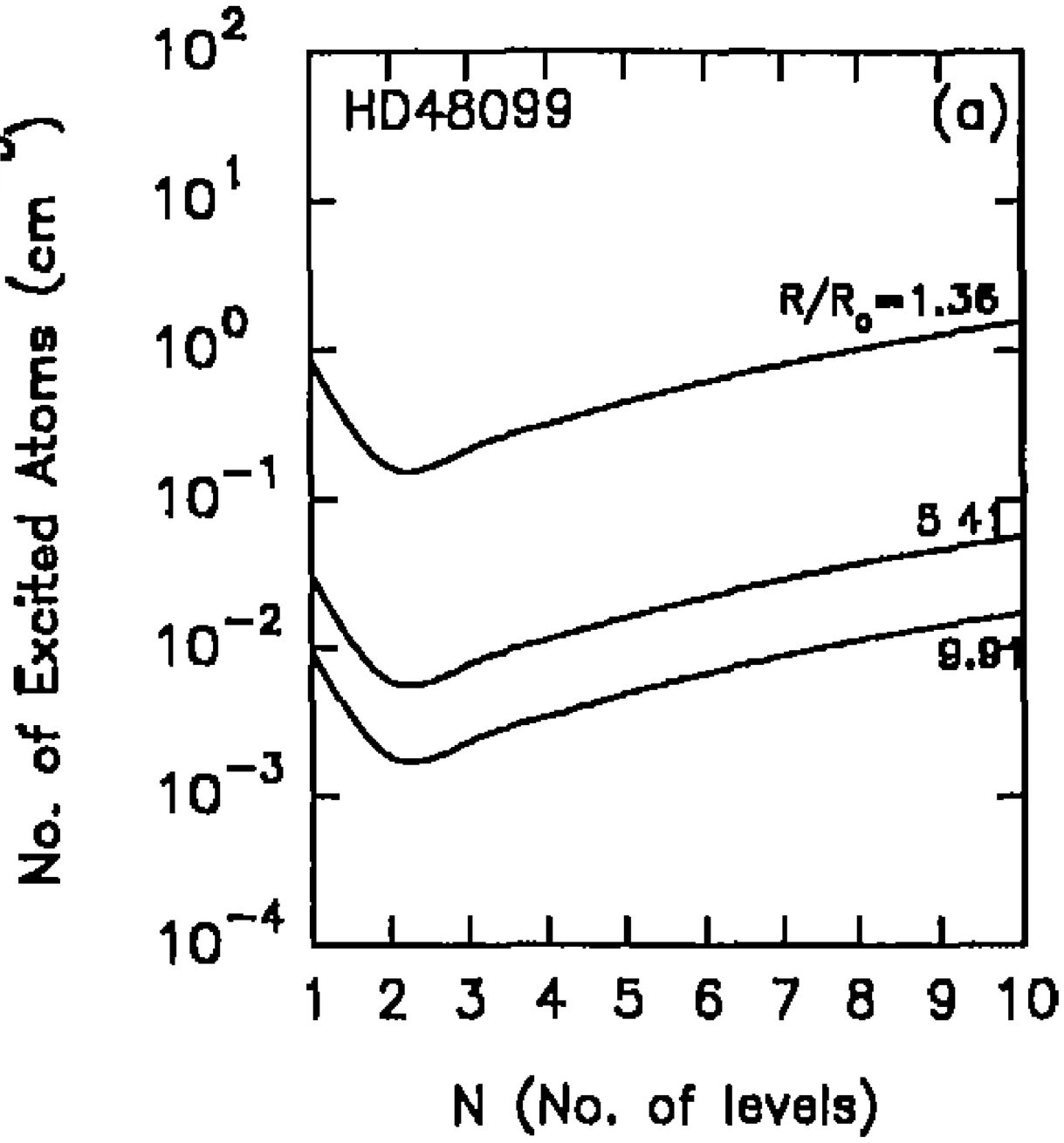

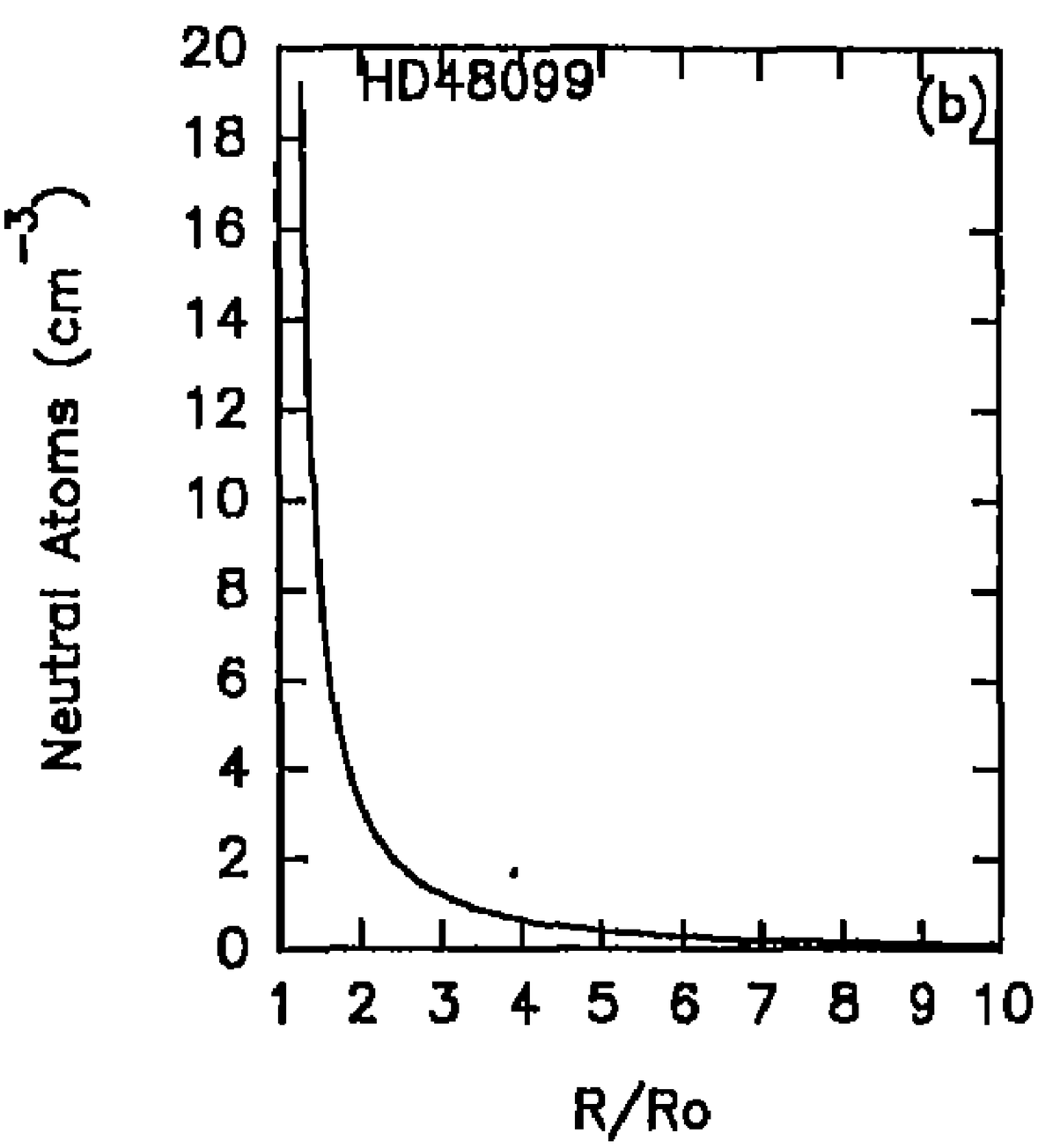

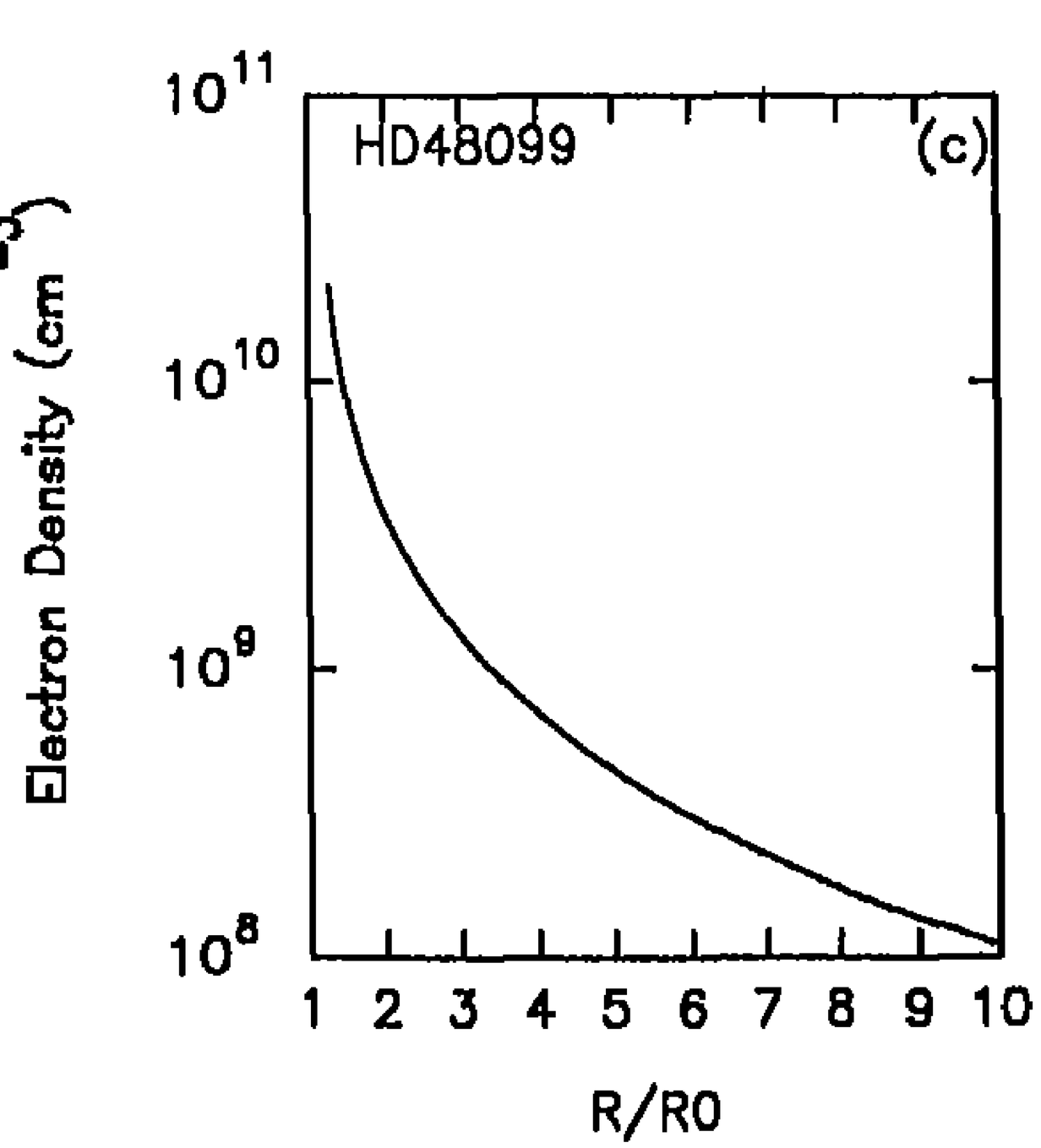

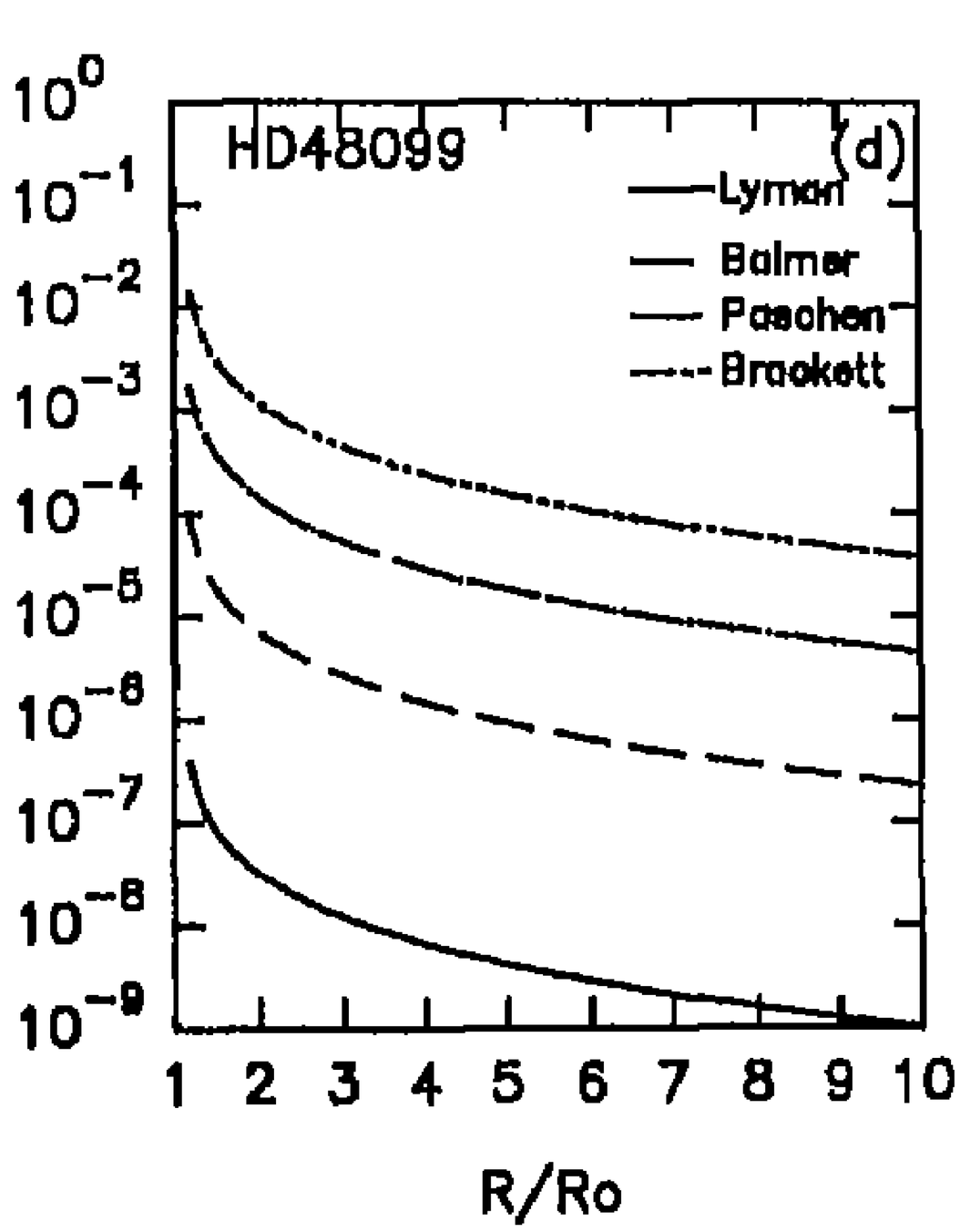

Figure 8 (a,b,c,d)

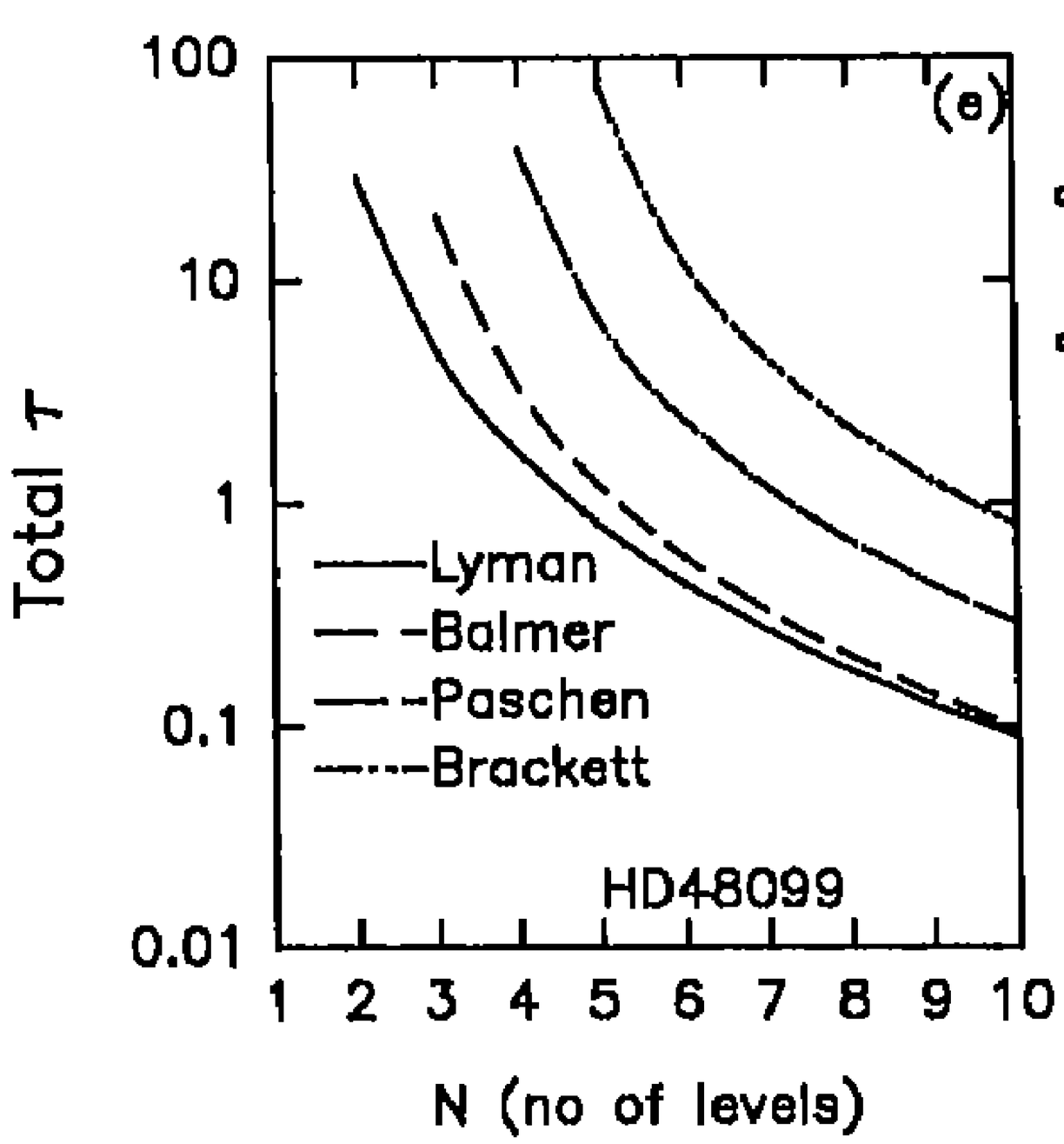

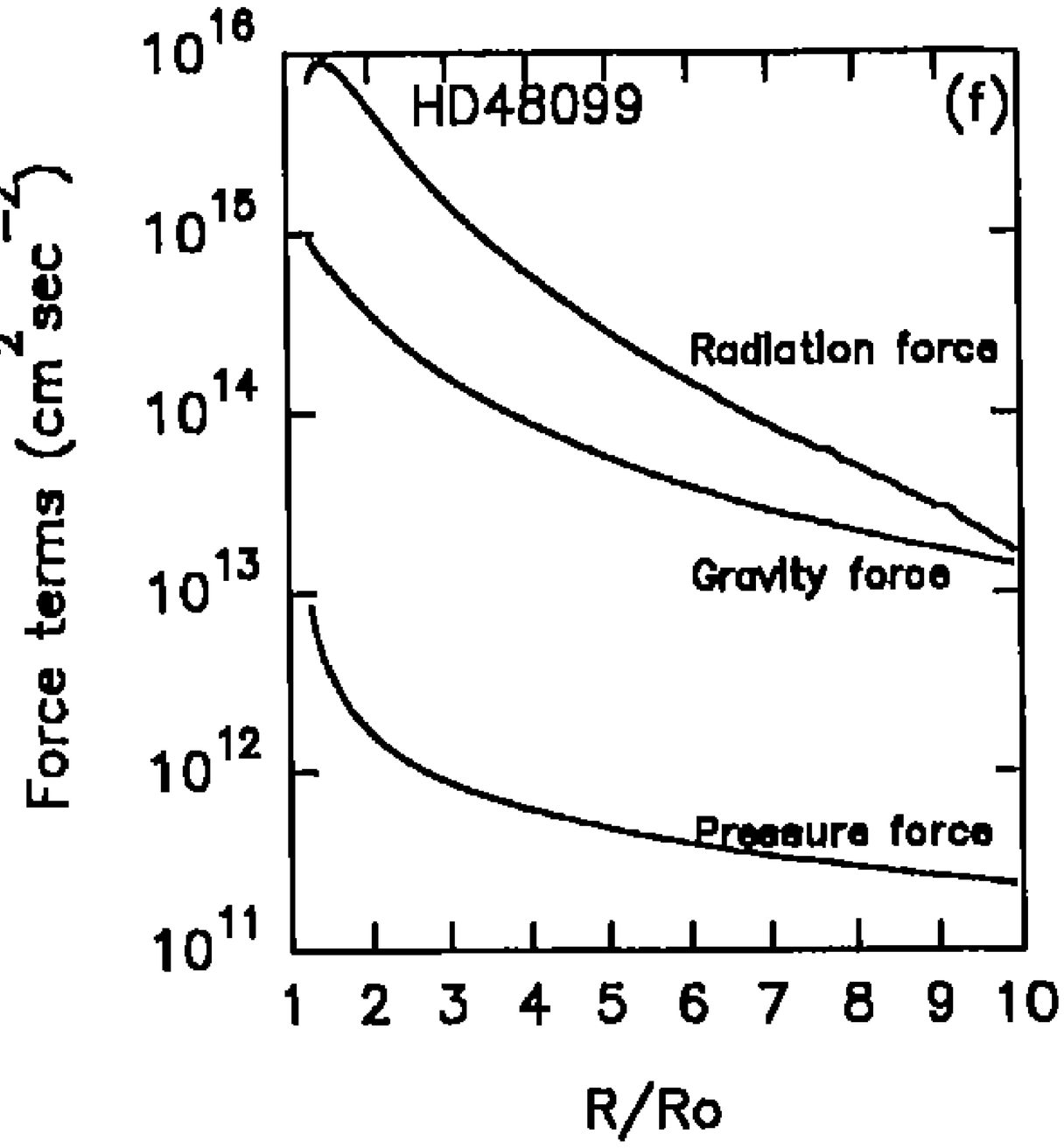

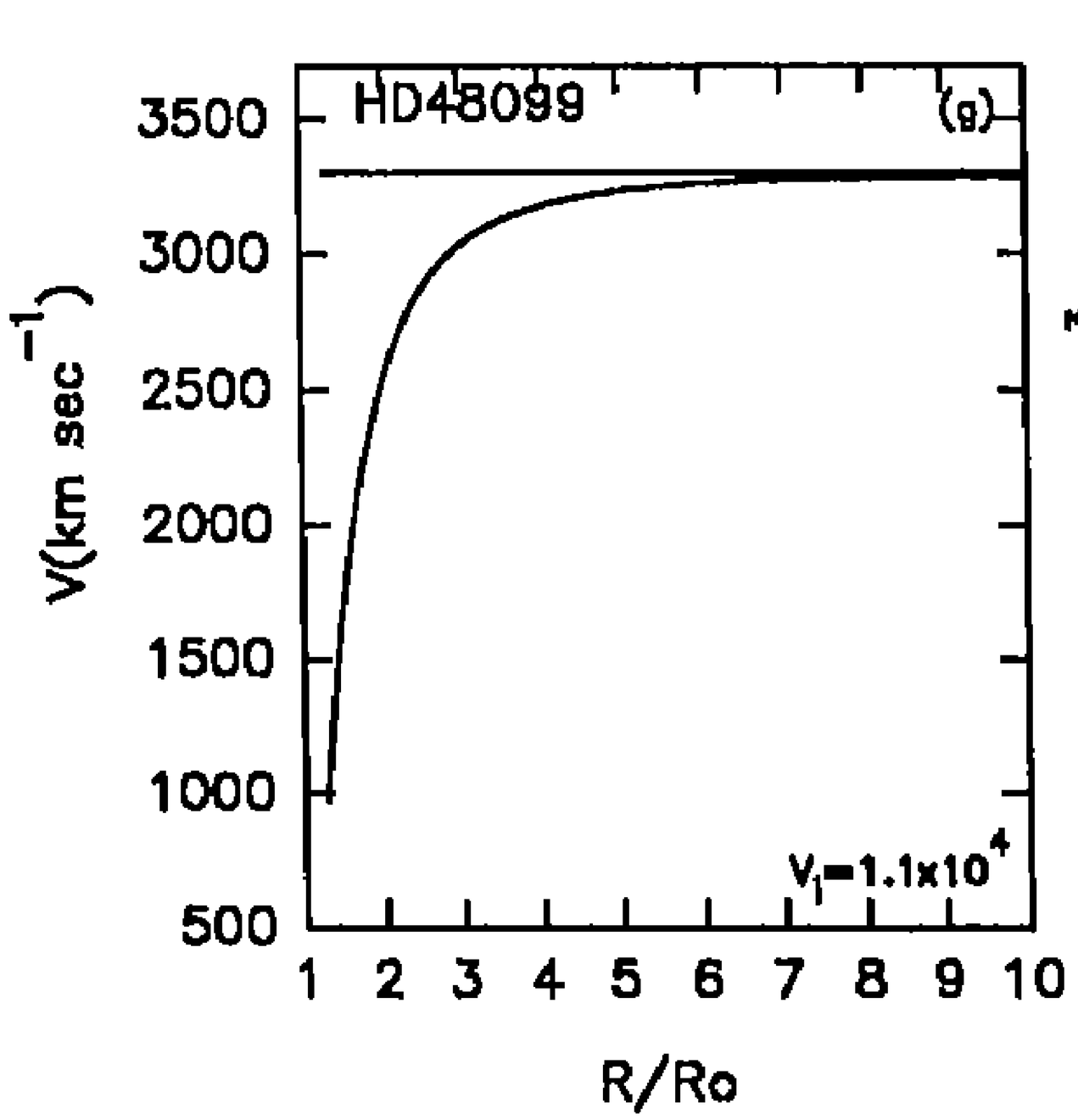

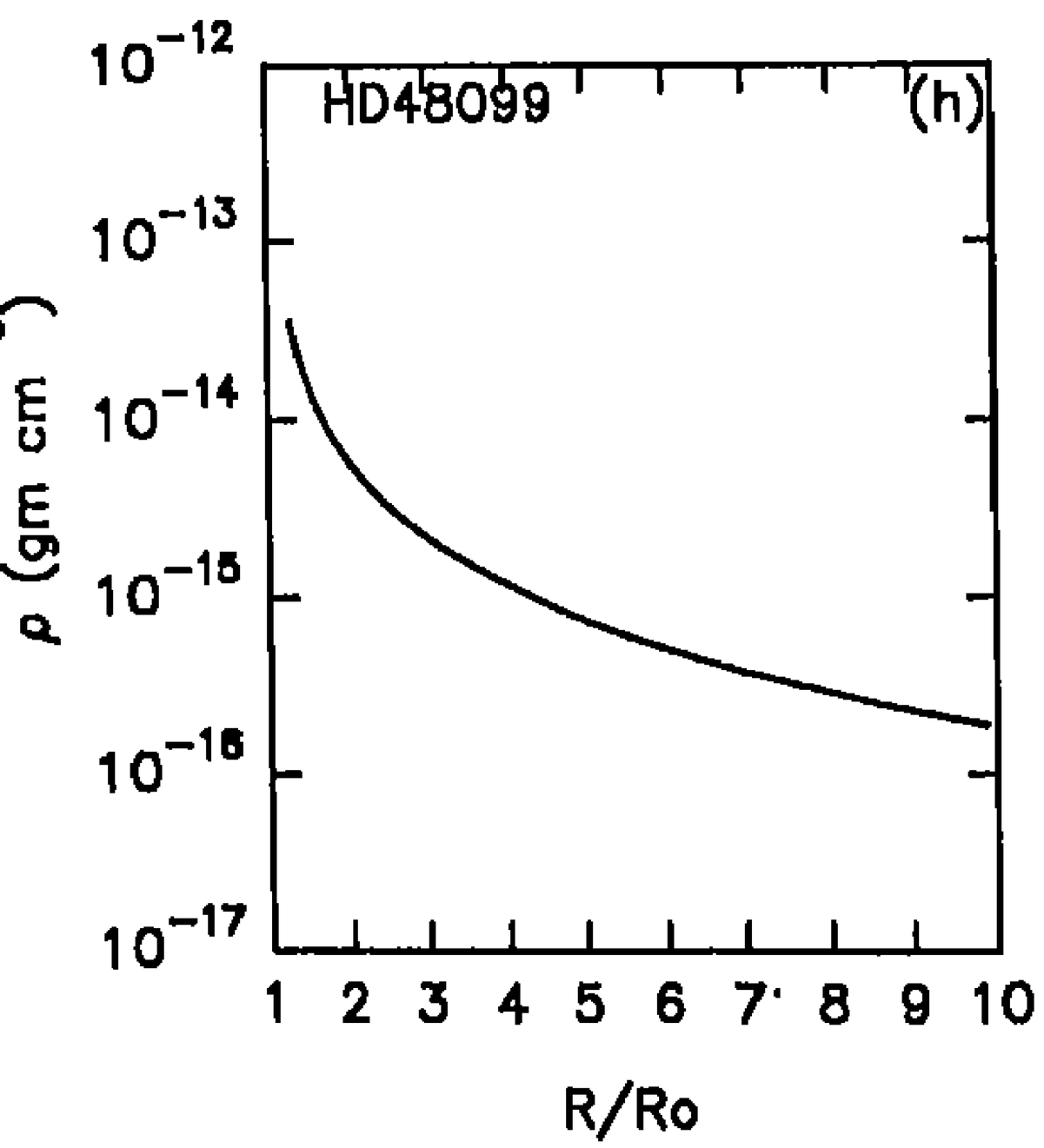

Figure 8 (e,f,g,h)

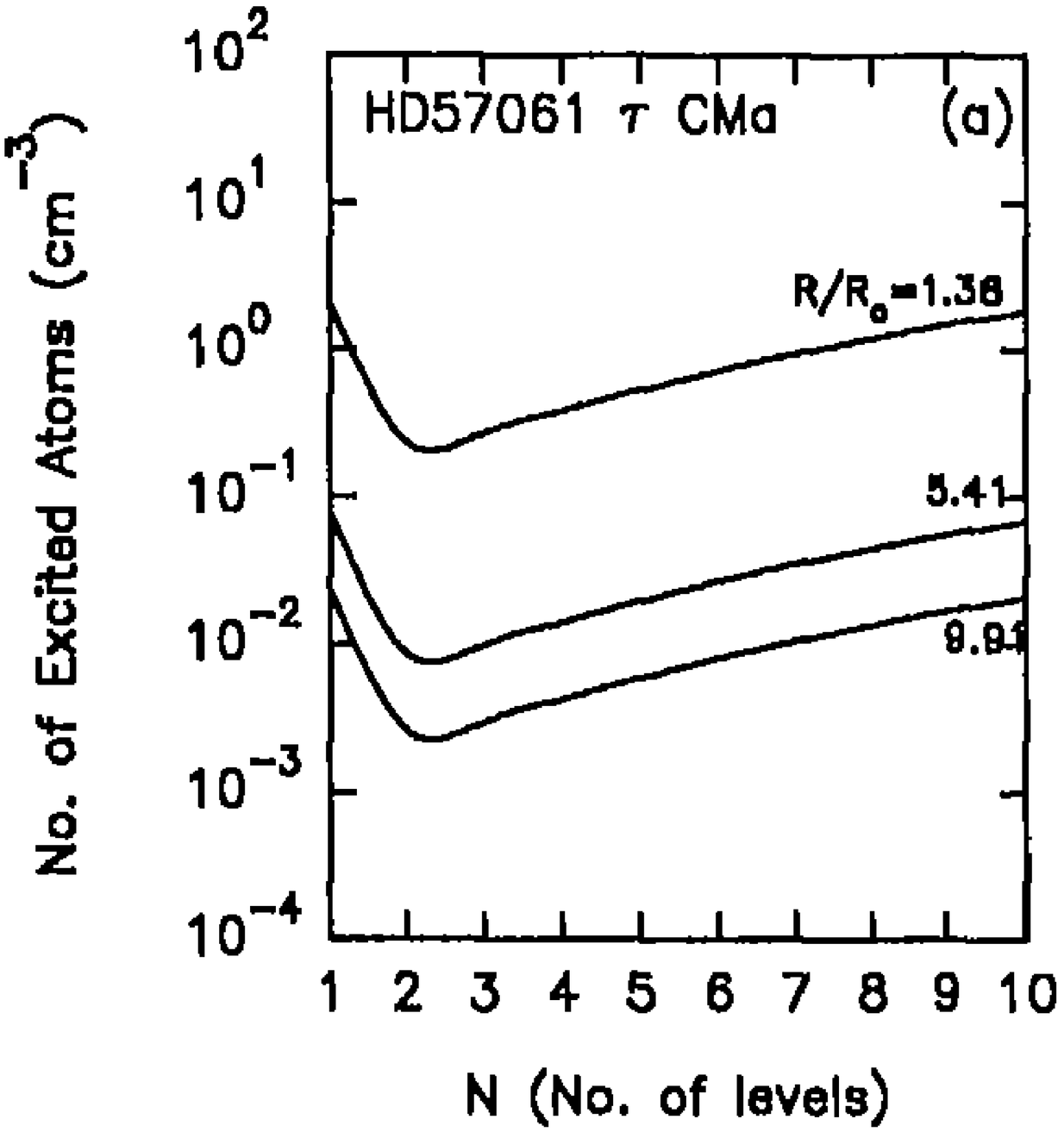

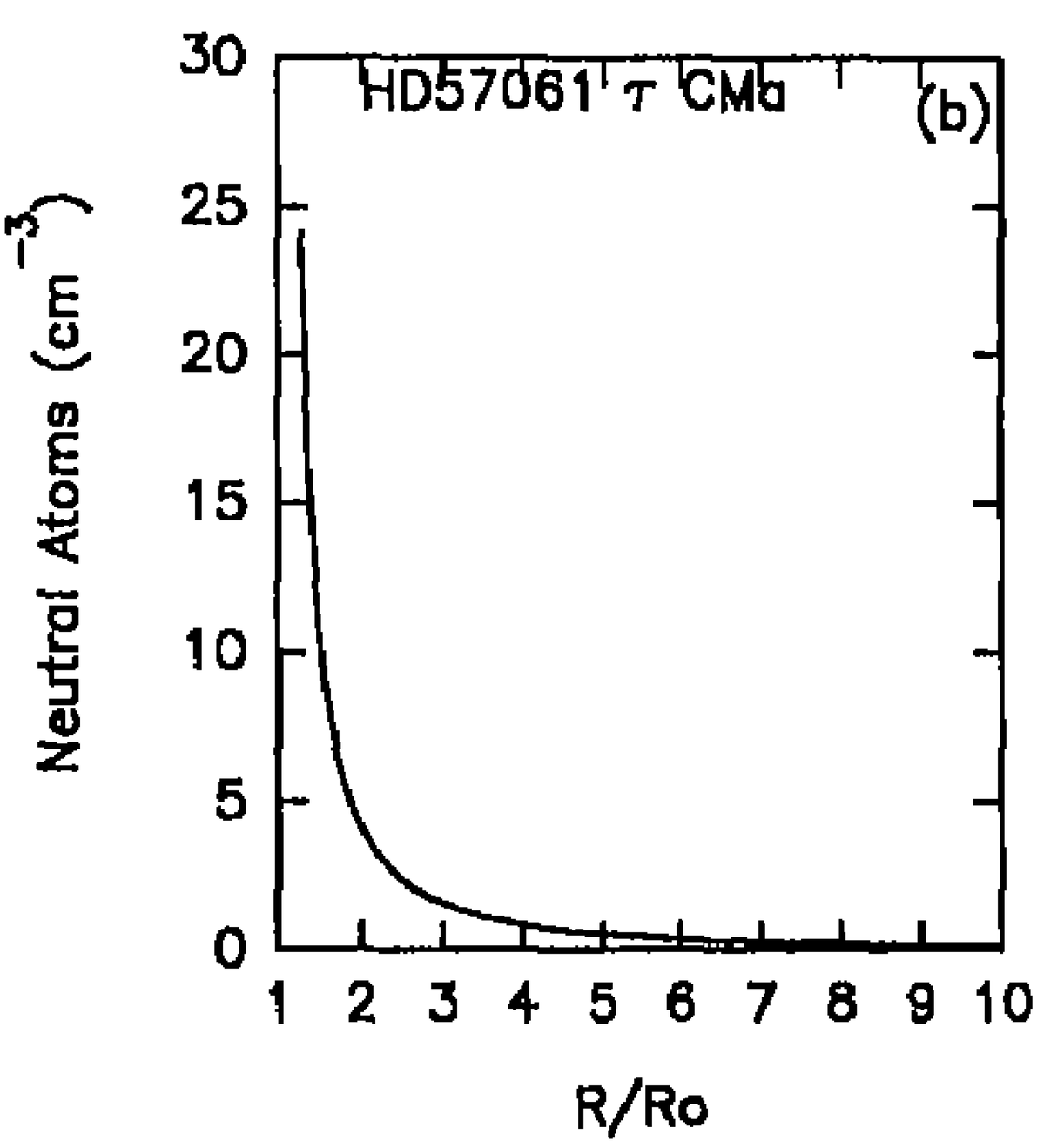

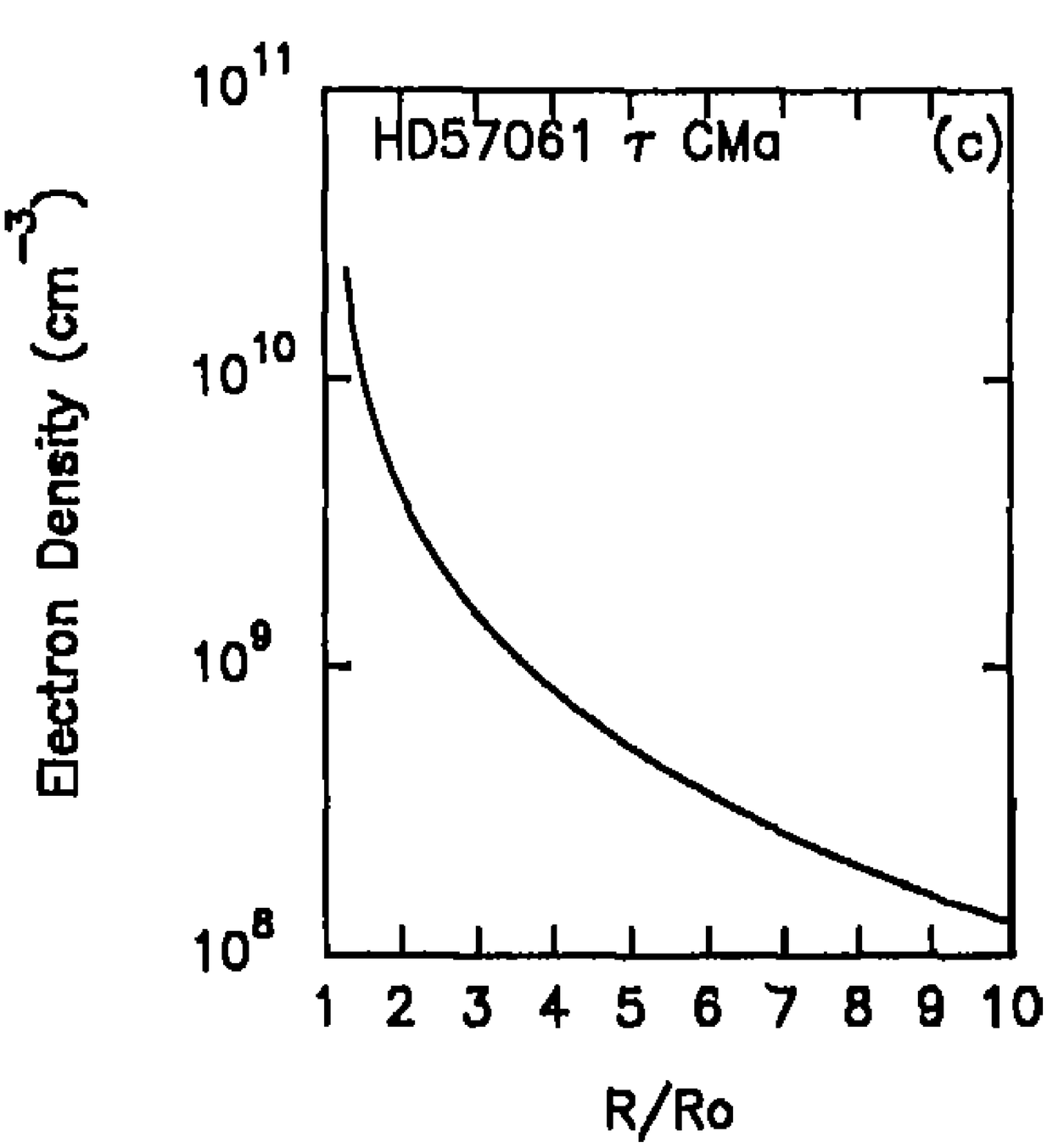

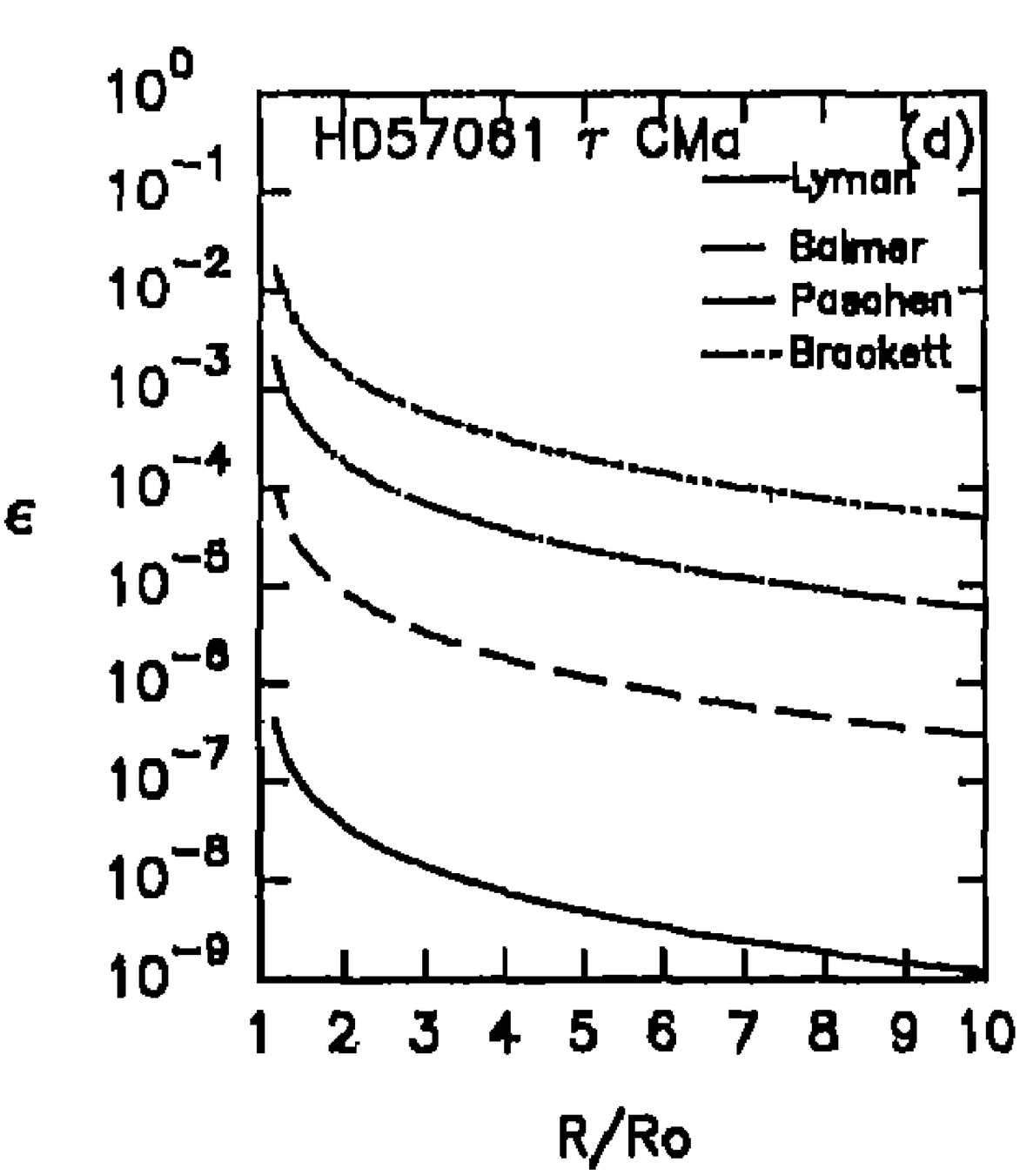

Figure 9 (a,b,c,d)

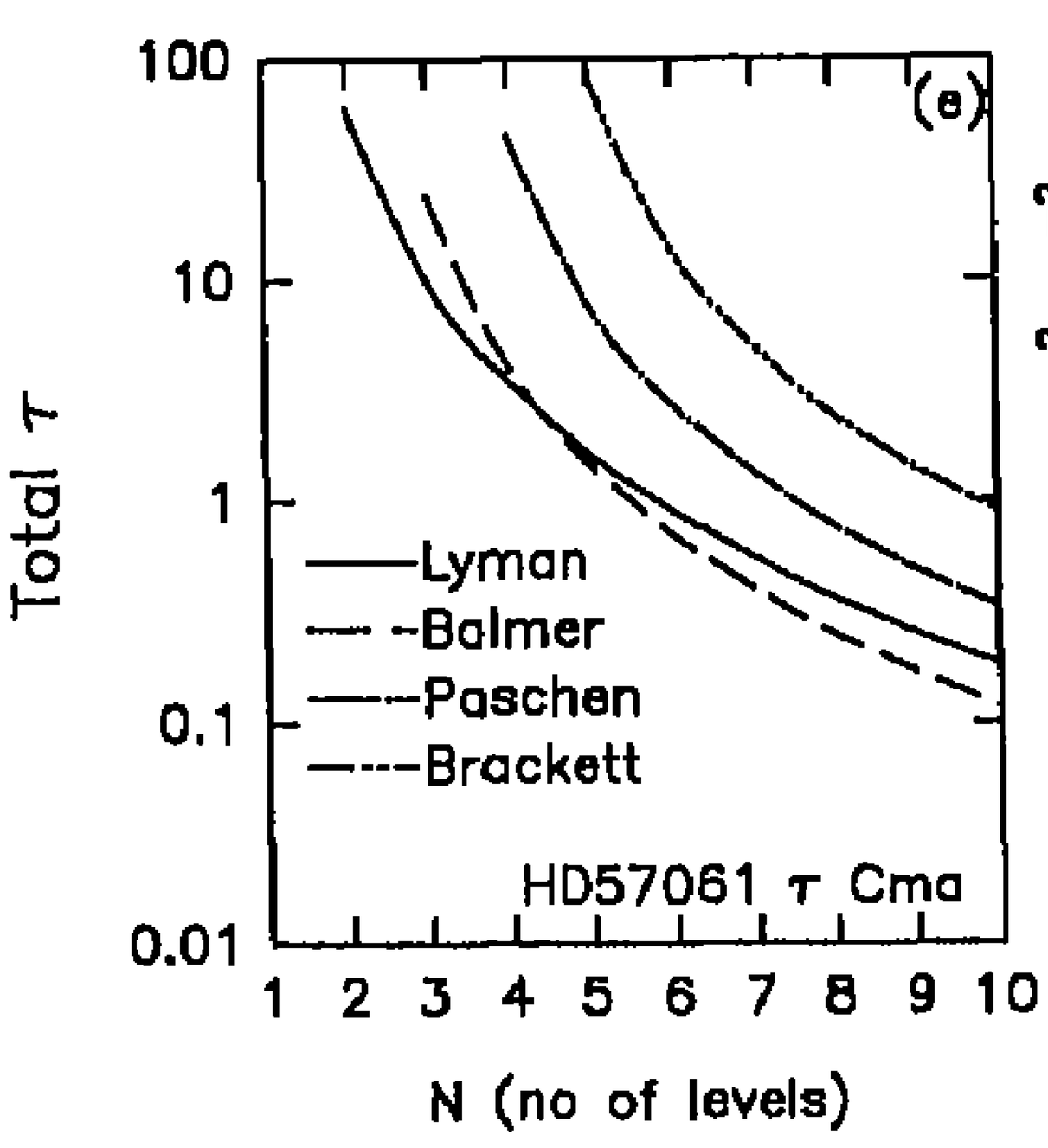

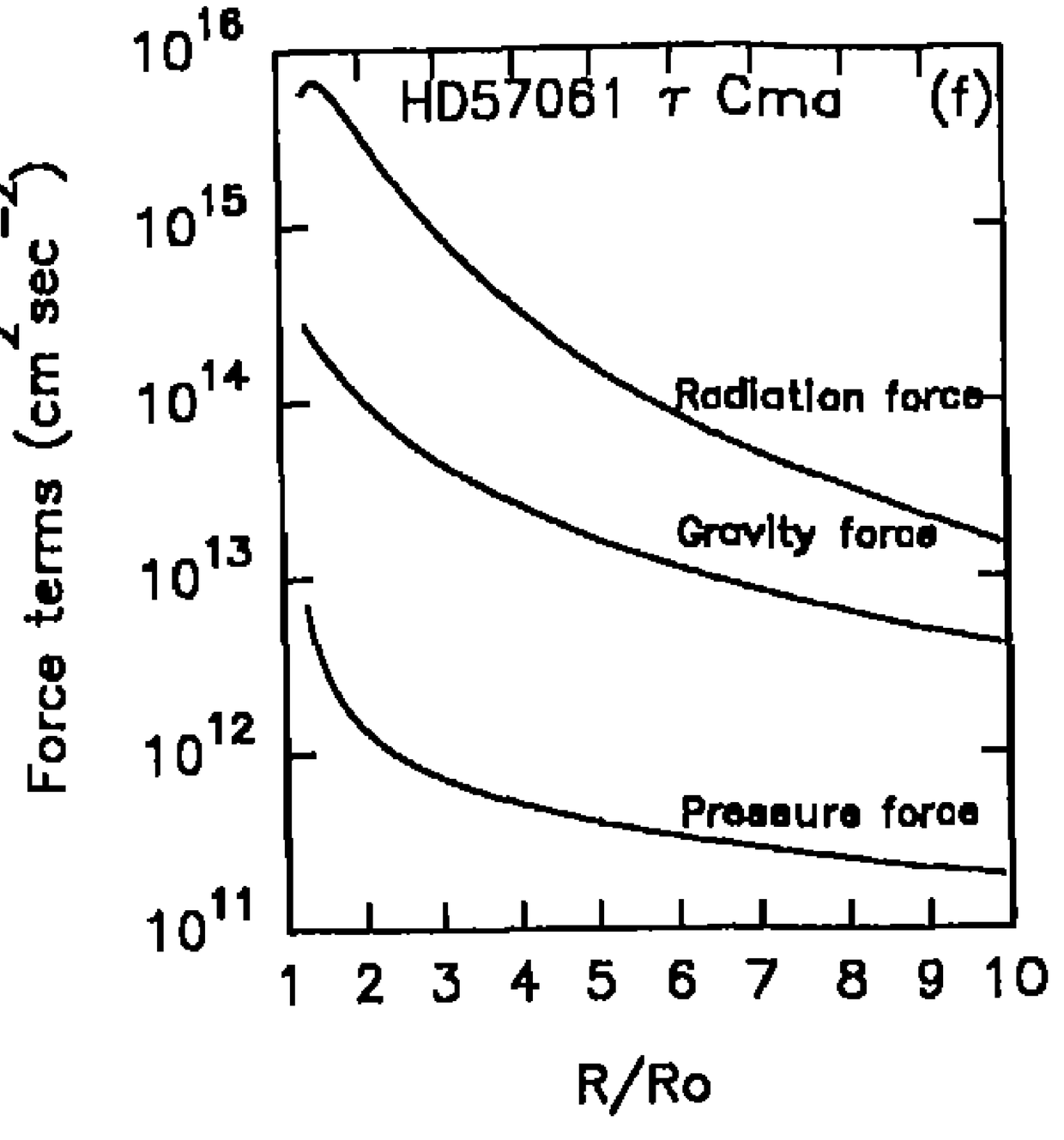

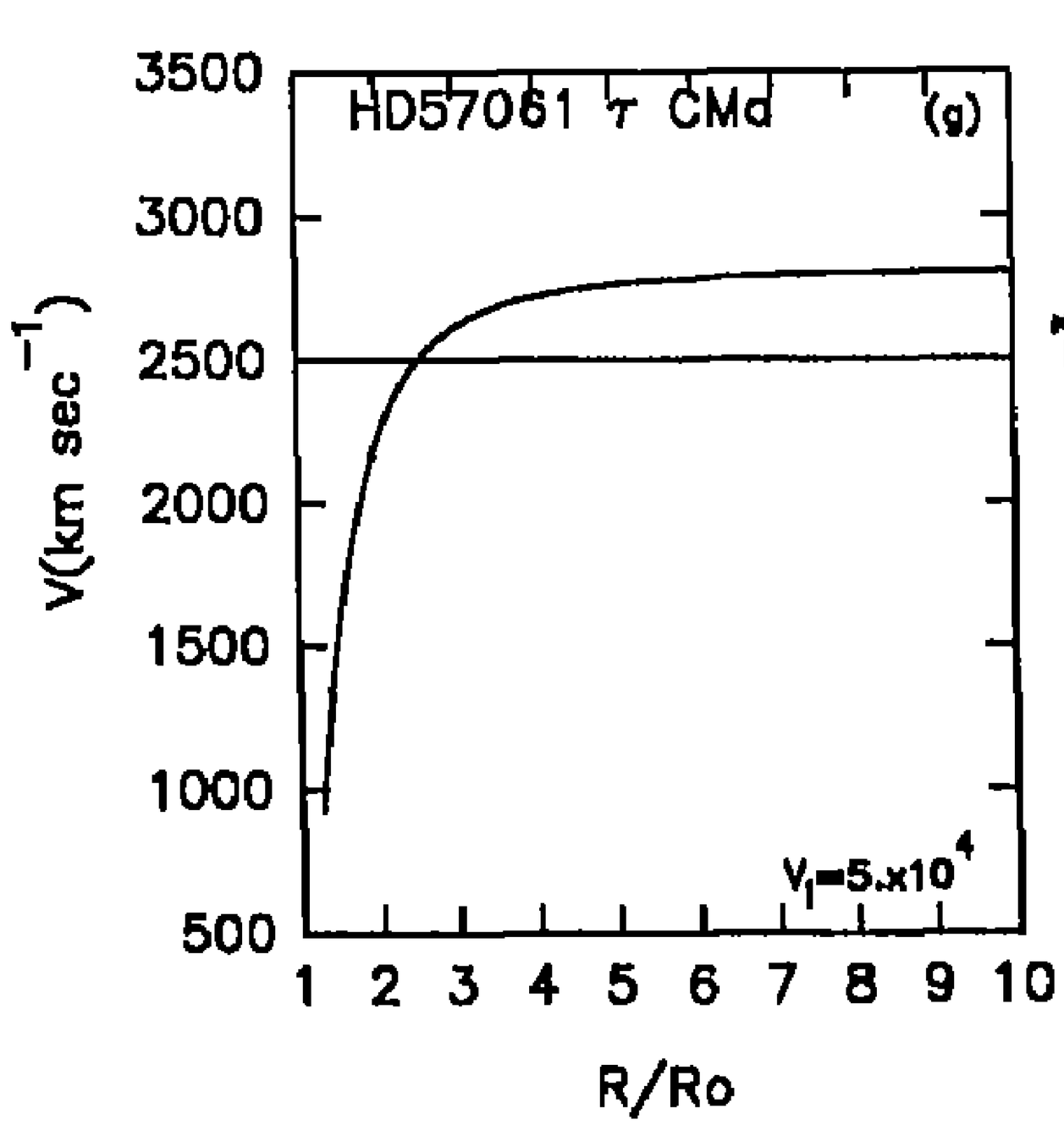

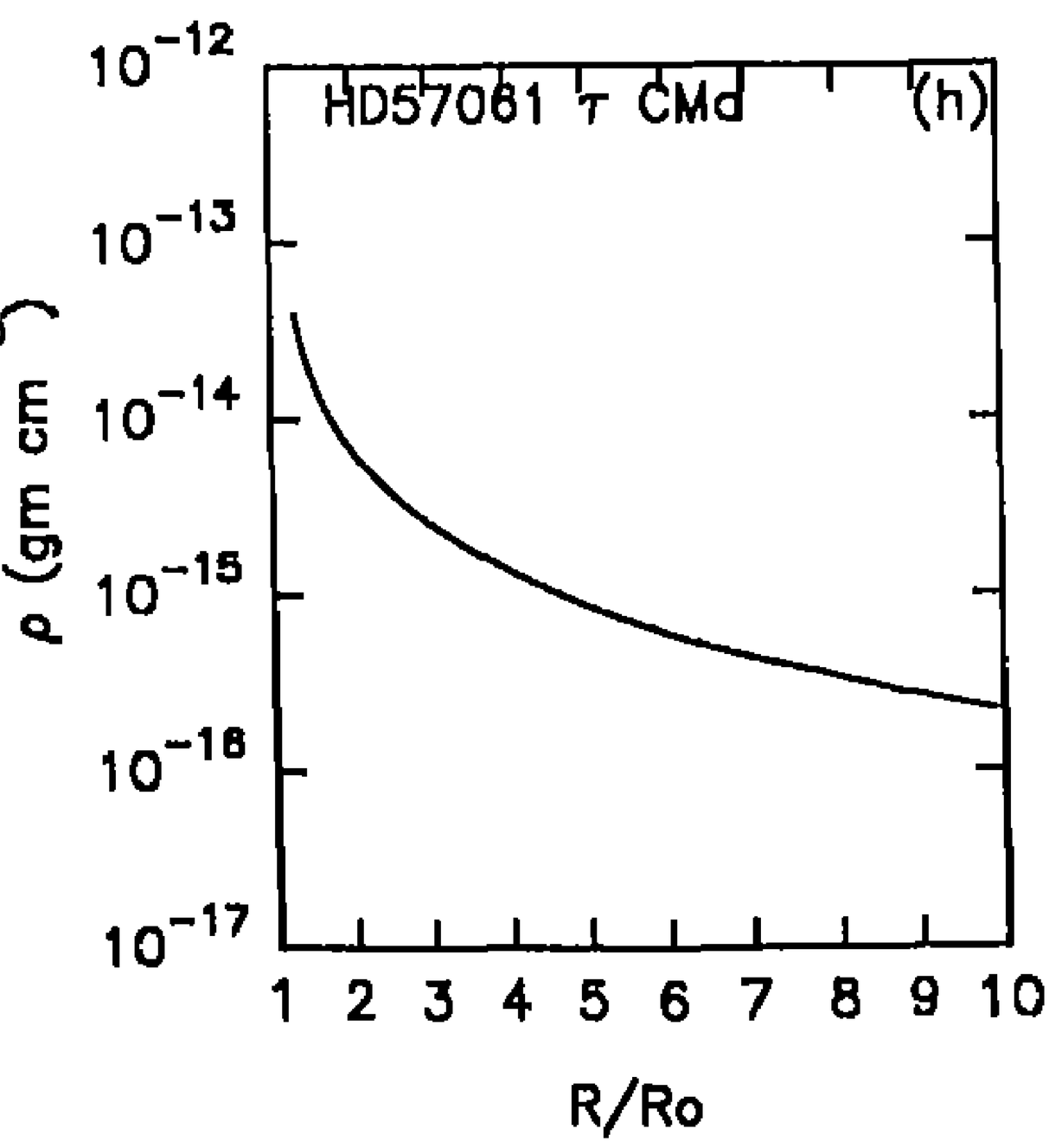

Figure 9 (c,f,g,h)

Figure 9

HD 57061 (τCMa) O9 Ib

	Abbott (1978)	Blomme (1990a)
T_{eff}	28840 K	33113 K
M	8.6×10^{34} gr	6.8×10^{34} gr
R	2.17×10^{12} cm	2.03×10^{12} cm
V_{esc}	600 km s^{-1}	364 km s^{-1}
V_∞	$V_{edge} = 2200$ km s^{-1}	2500 km s^{-1}
$\dot{M}$		$8.12 \times 10^{-6} M_\odot$/yr

The results in (a), (b), (c), (d) are similar as in the case of HD 48099.

(e) Here τ (Lyman α) > τ(Balmer α, Paschen α)

τ (Lyman α) $\approx$ τ (Brackett α)

τ (Lyman 9) > τ (Balmer 8)

τ (Lyman 9) < τ (Paschen 7, Brackett 6)

(f) Radiation force is much larger than the gravity force even at $R/R_0 = 10$.

(g) As the radiation is more powerful than the gravity we obtain a large terminal velocity exceeding the expected $v_\infty \approx 2500$ km s^{-1}. In this case $0.8 < \beta < 0.9$.

(h) The electron density changes from 6×10^{-14} gr cm^{-3} to 4×10^{-16} gr cm^{-3}.

Figure 10

HD 144217 (βSco).B O.5 V

	Abbott (1978)	Blomme (1990a)
T_{eff}	32359 K	29512 K
M	3.8×10^{34} gr	3.3×10^{34} gr
R	4.2×10^{11} cm	6.02×10^{11} cm
V_{esc}	1030 km s^{-1}	824 km s^{-1}
V_∞	$V_{edge} = 2000$ km s^{-1}	2450 km s^{-1}
$\dot{M}$		$7.16 \times 10^{-6} M_\odot$/yr

The results in (a), (b), (c), (d) and (e) are similar to those given in earlier cases.

(f) The radiation force falls very rapidly and the gravity dominates at about $R/R_0 \sim 9$.

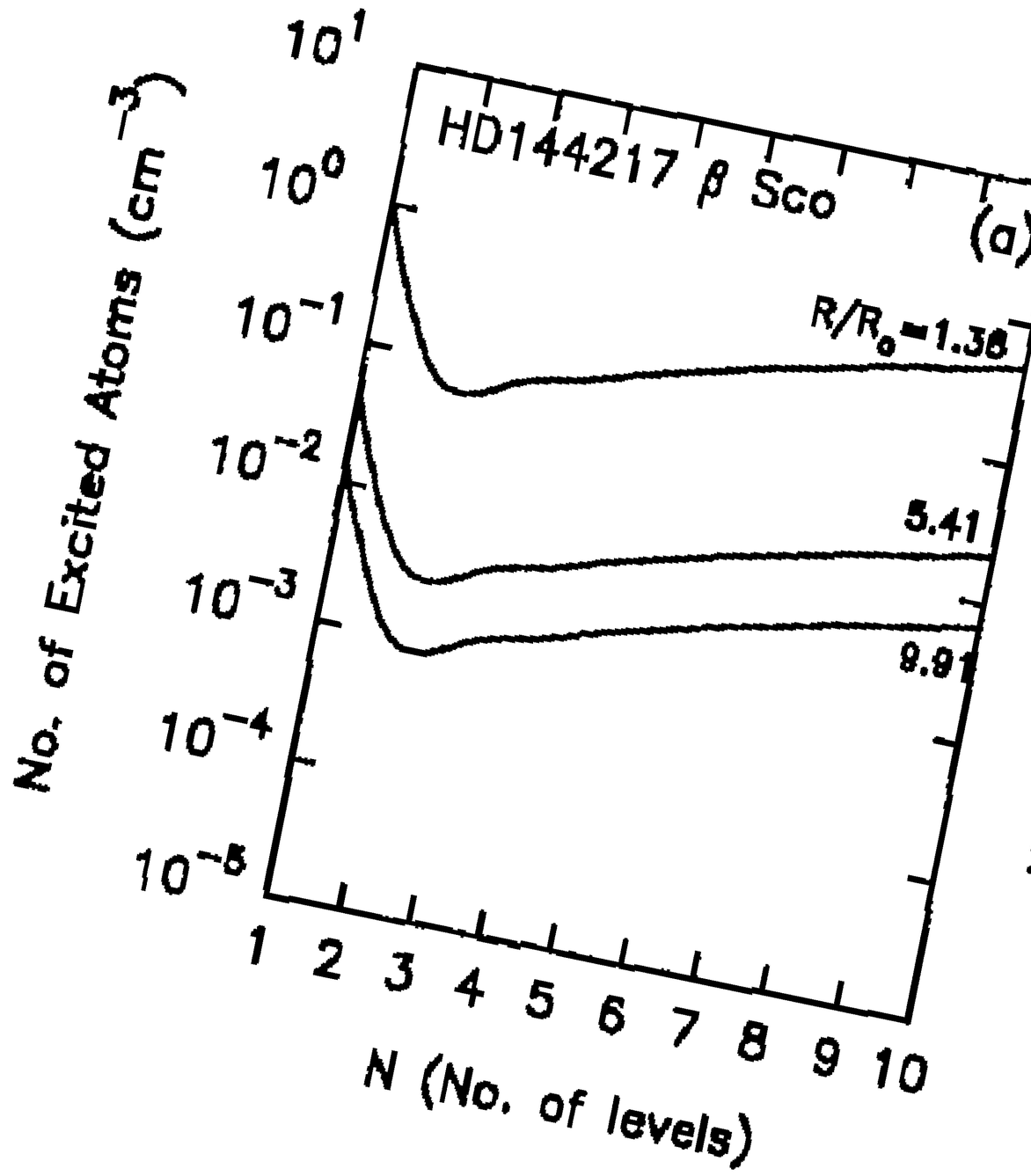

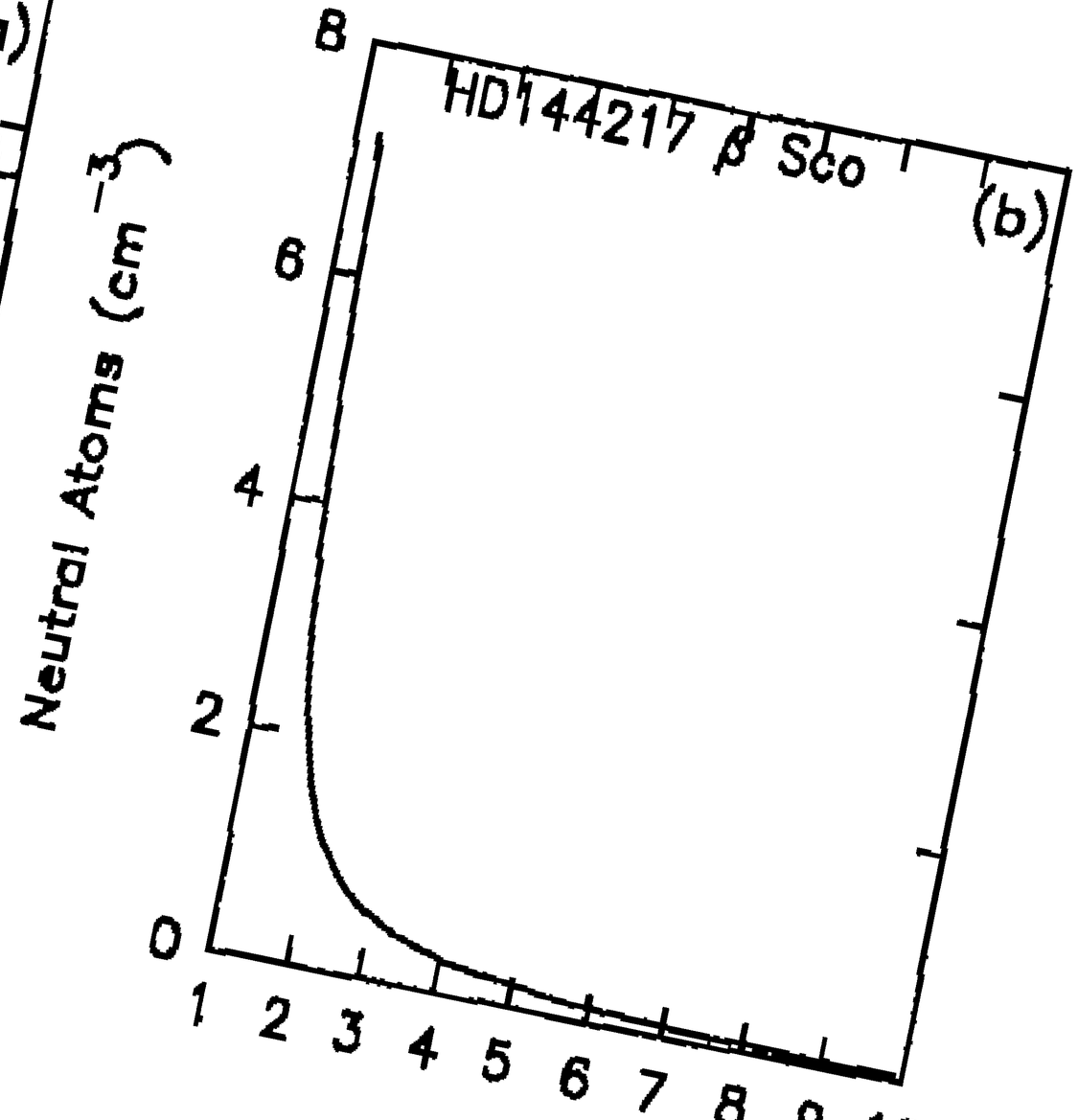

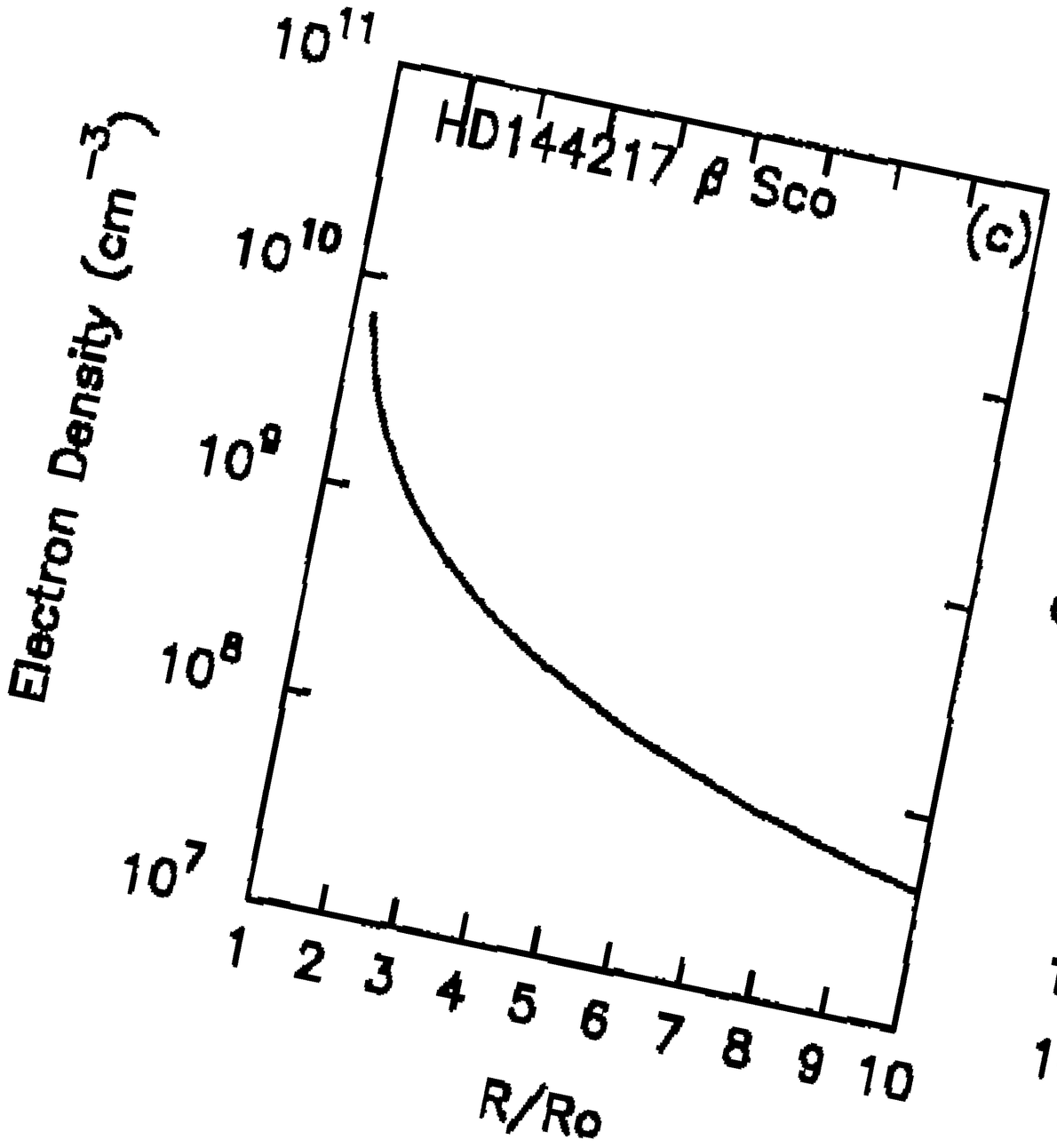

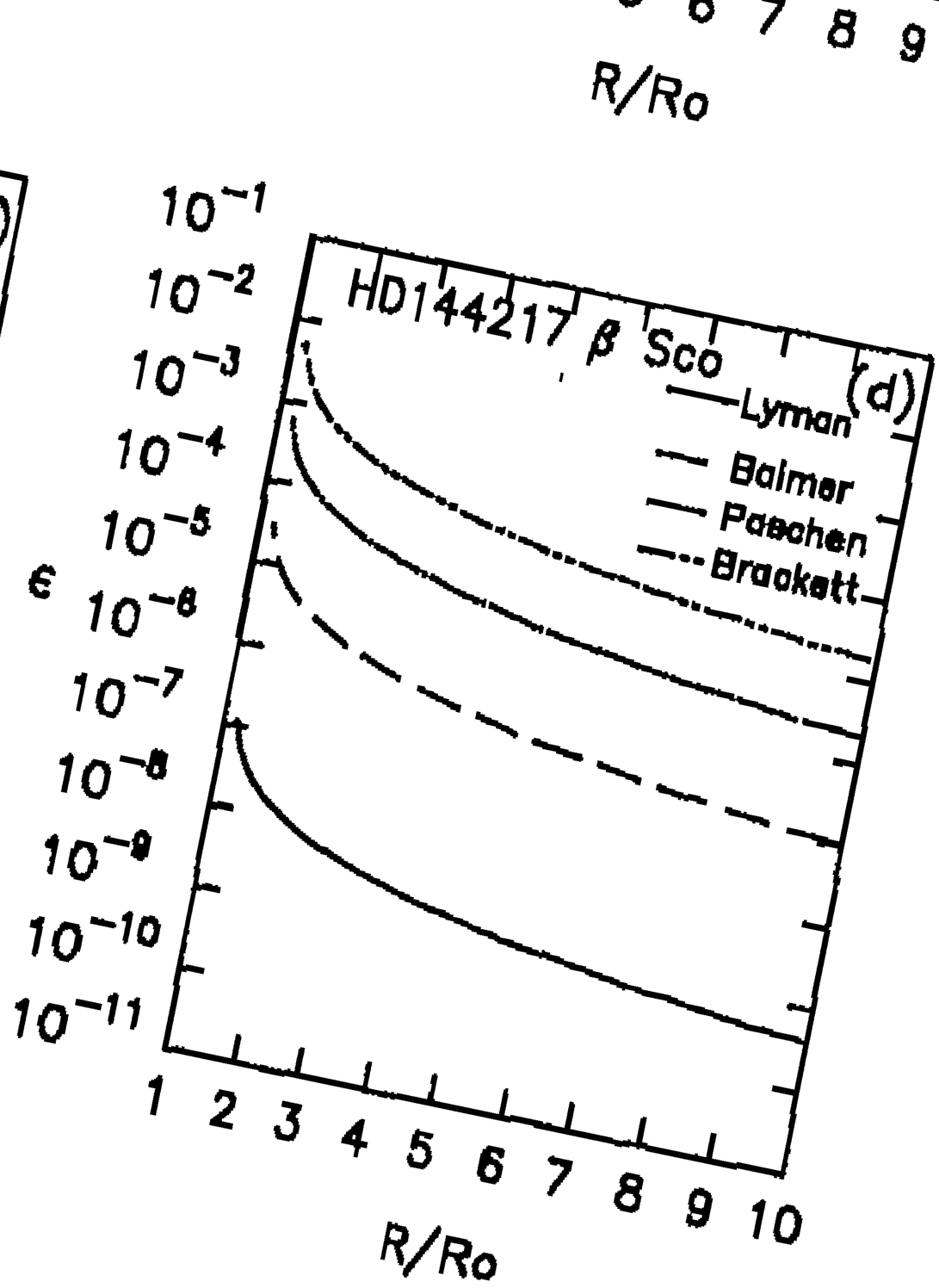

Figure 10 (a,b,c,d)

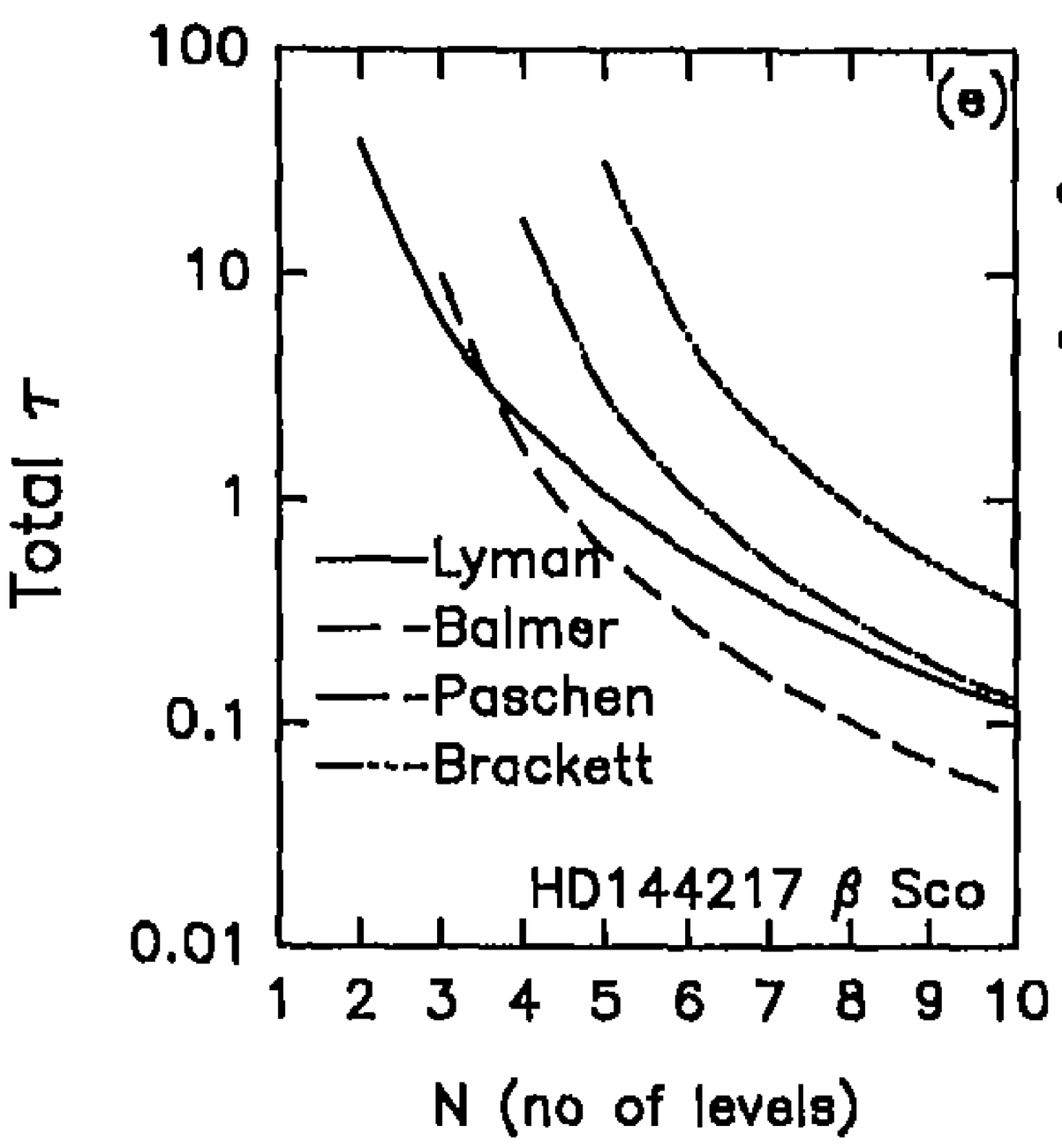

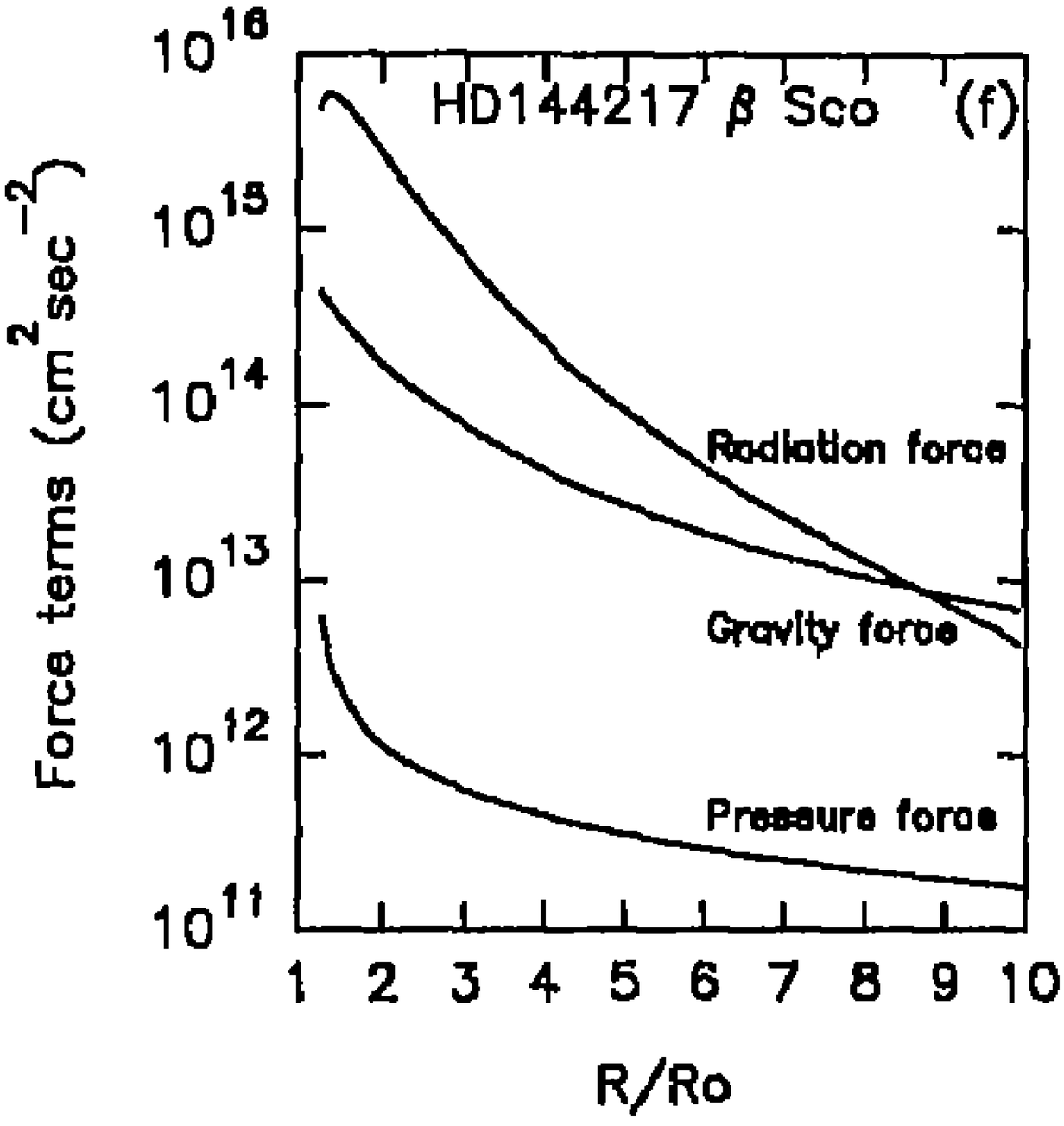

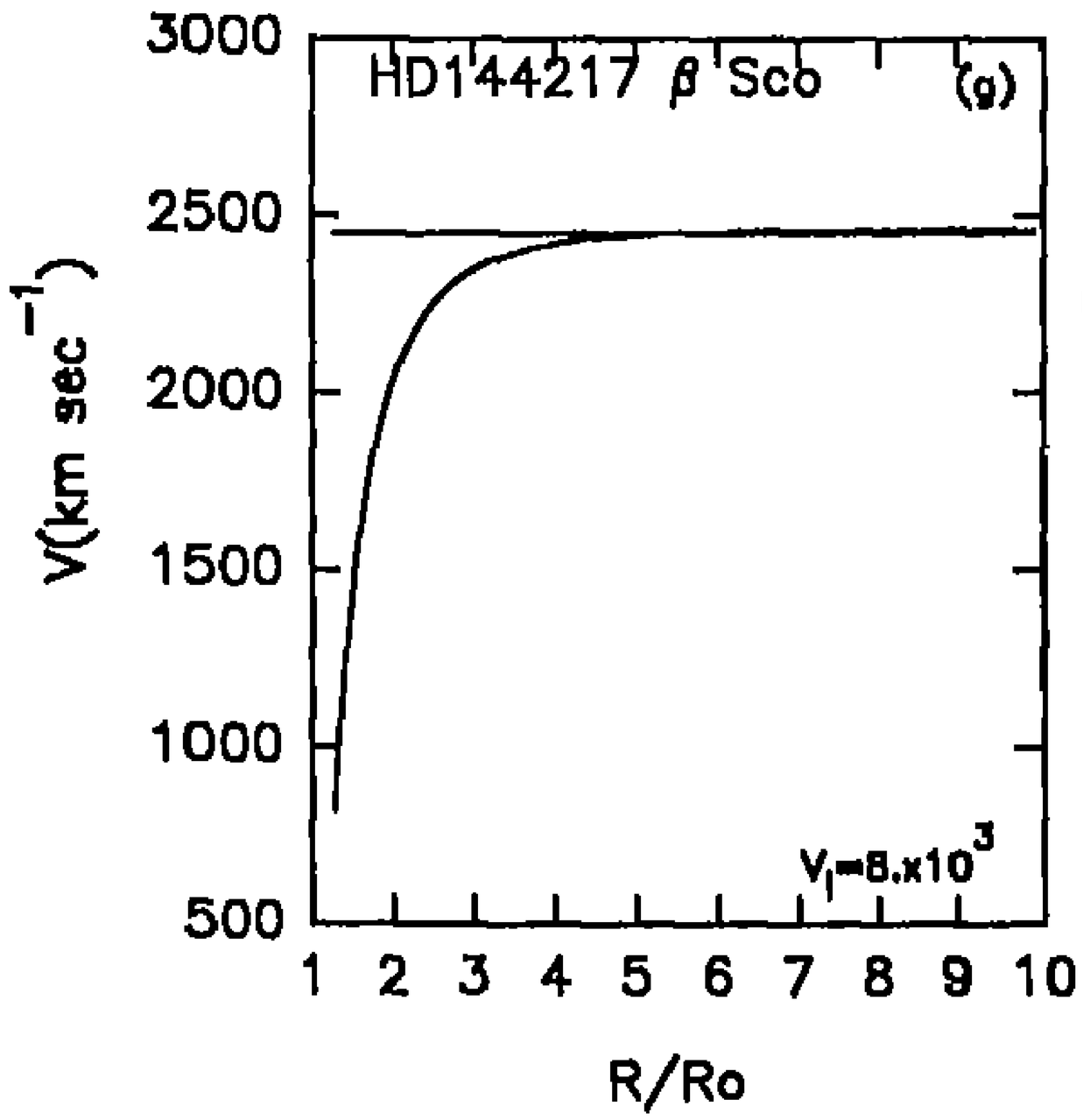

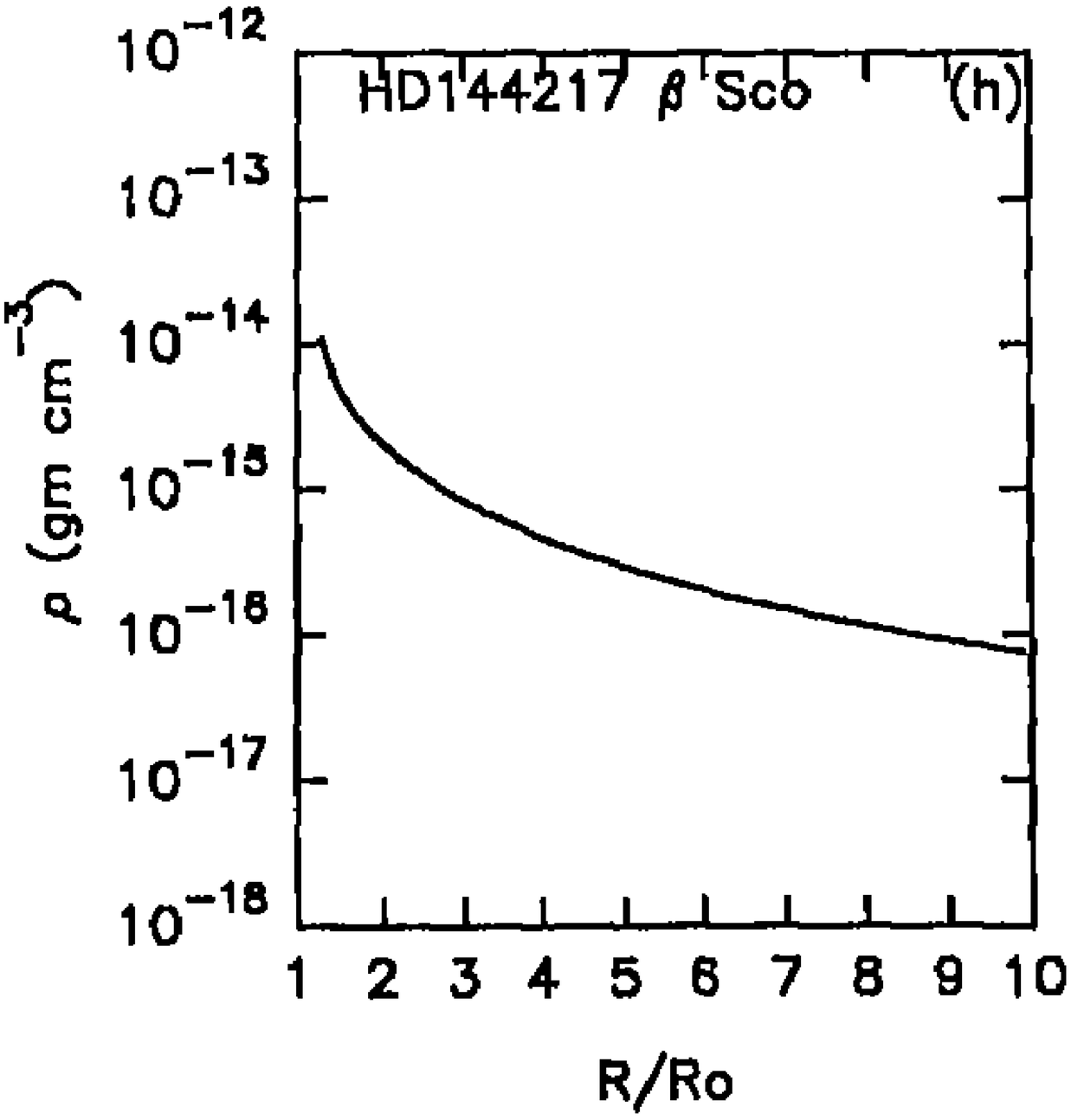

Figure 10 (e,f,g,h)

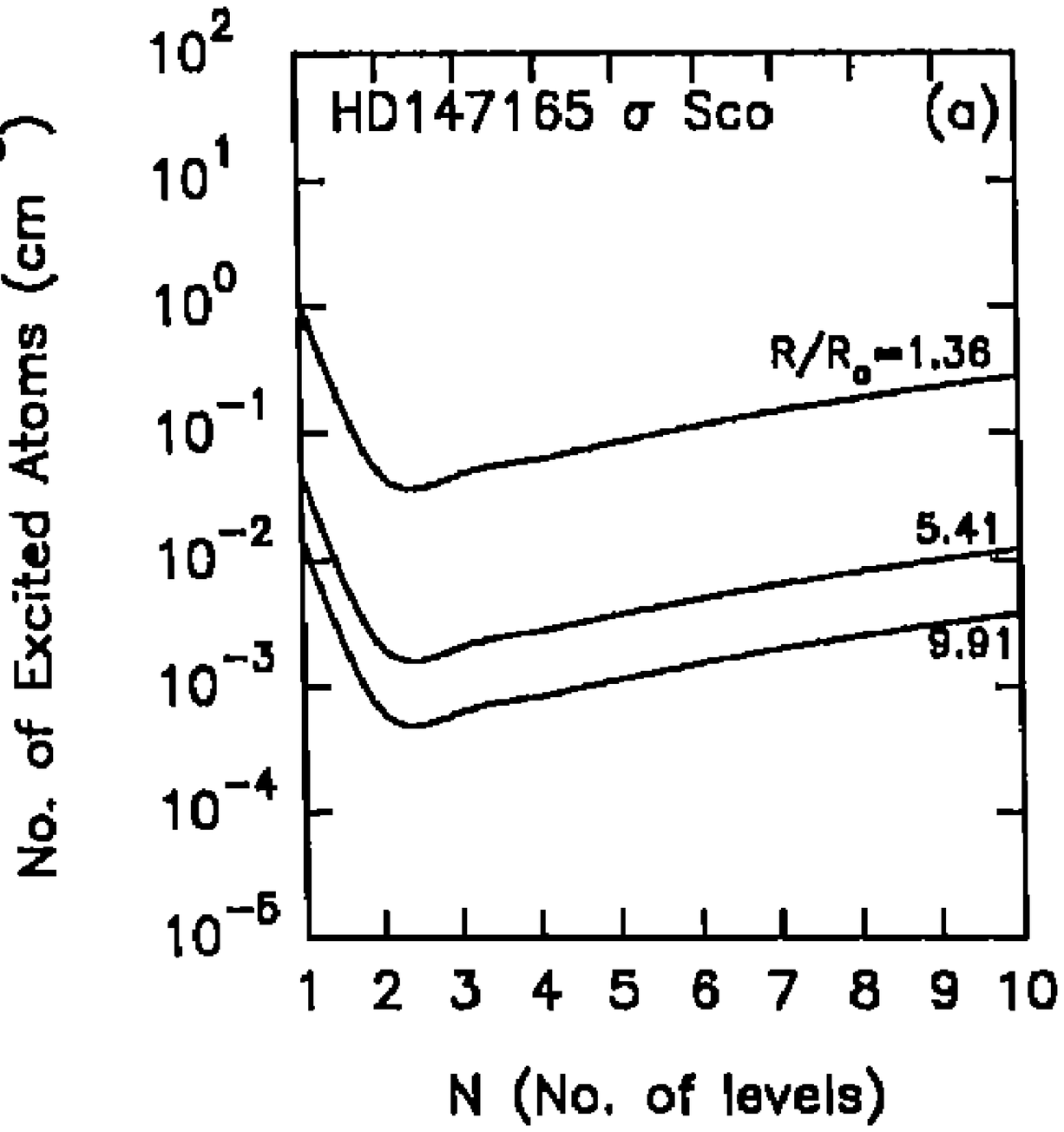

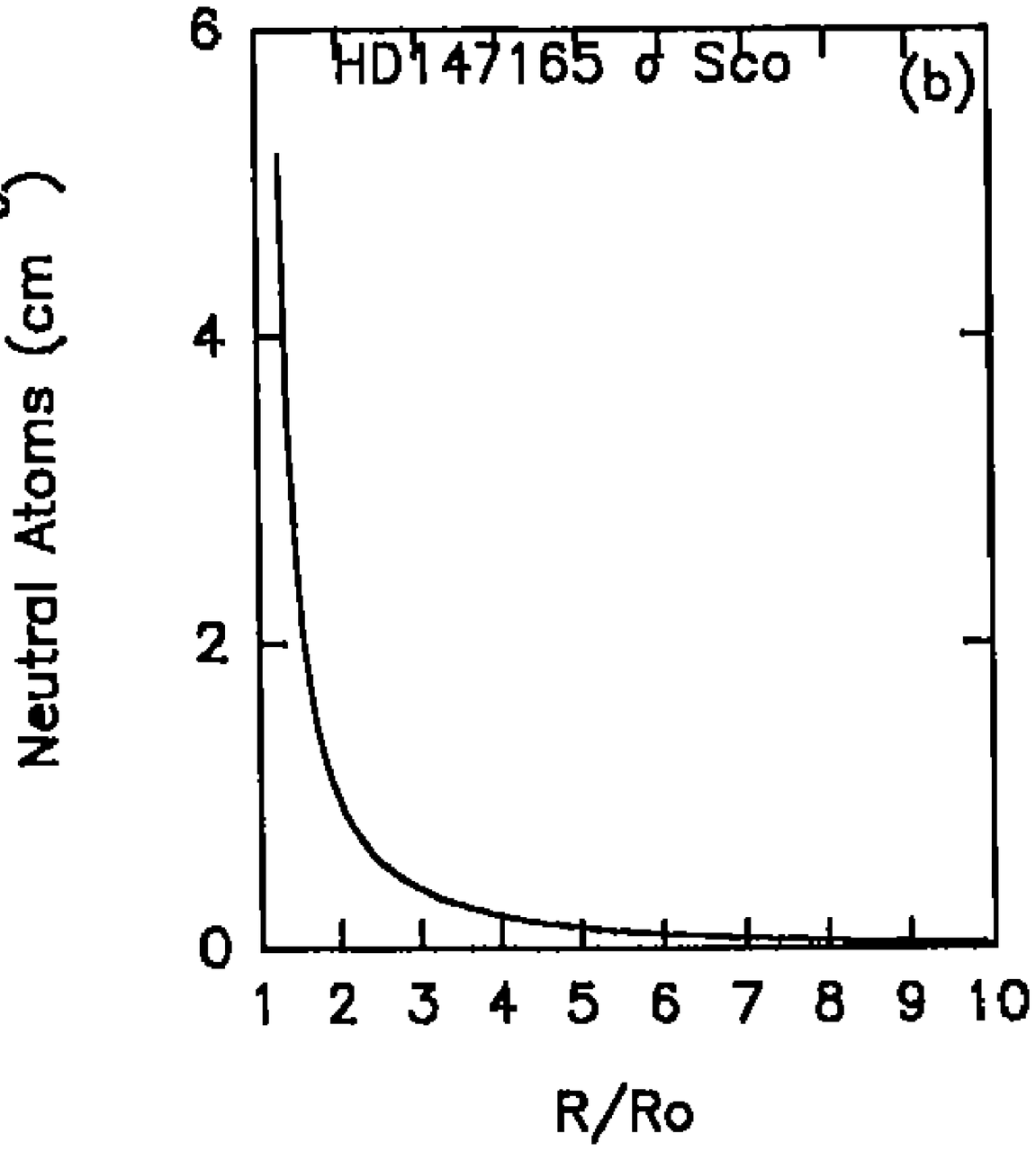

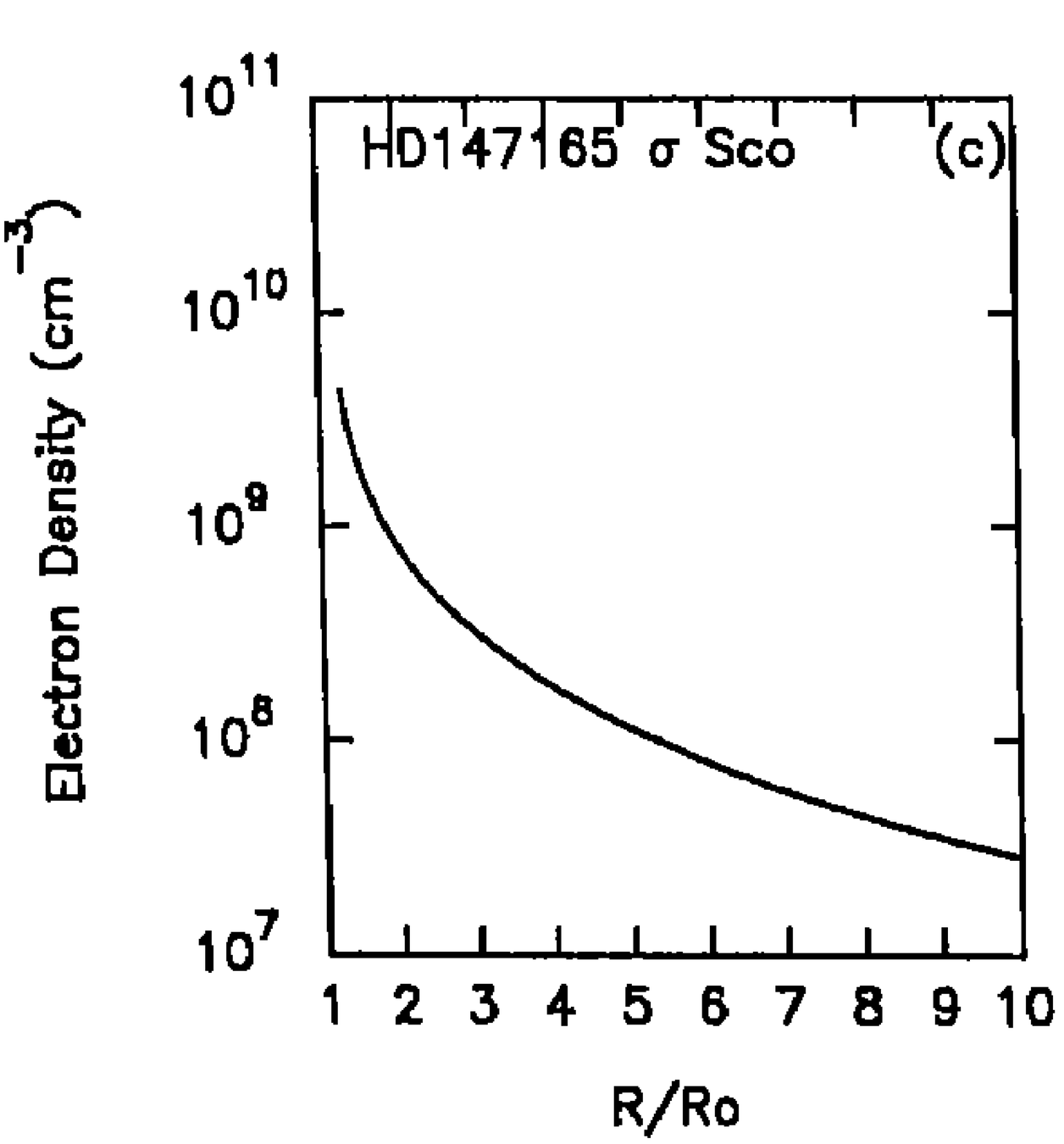

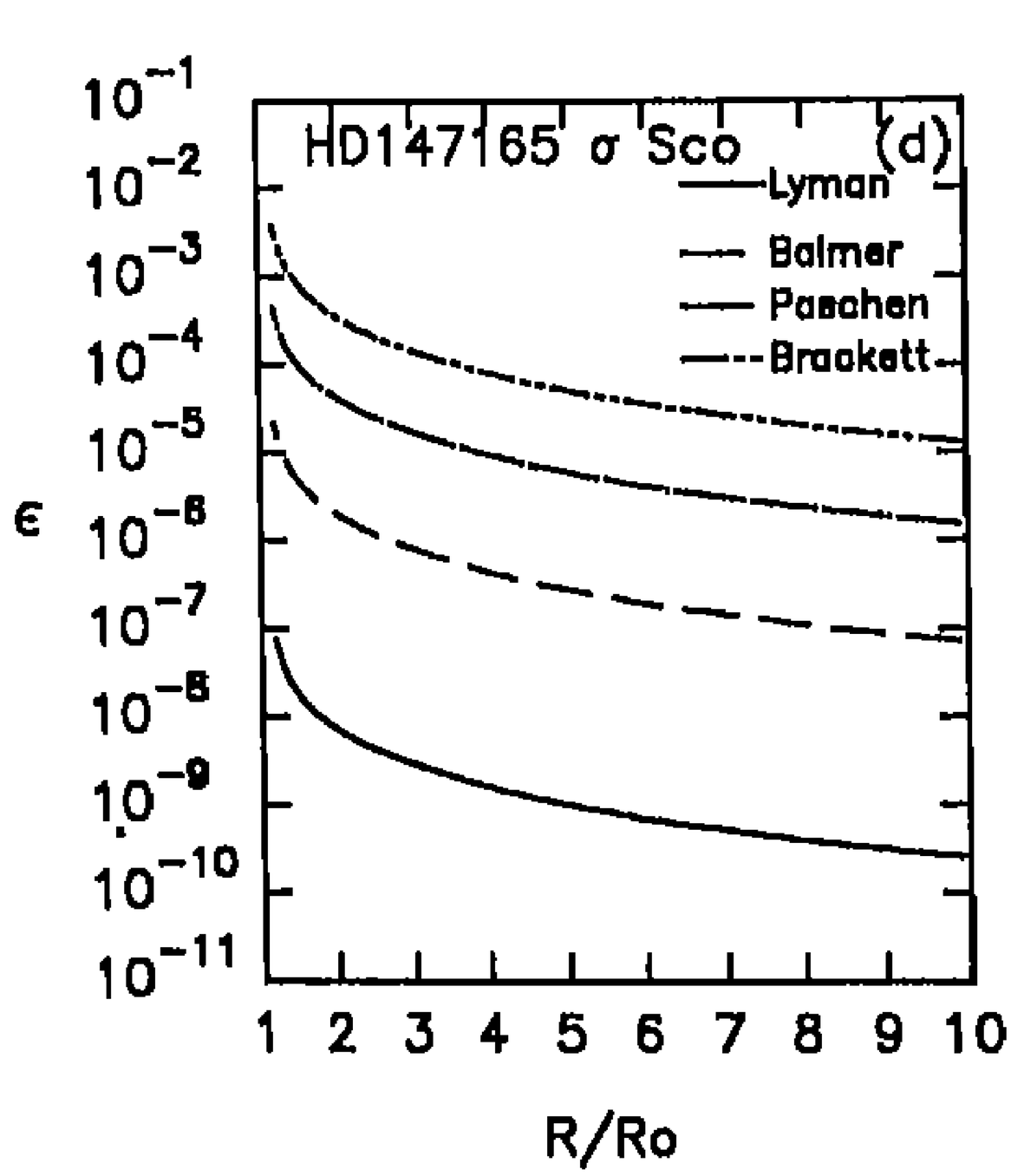

Figure 11 (a,b.c.d)

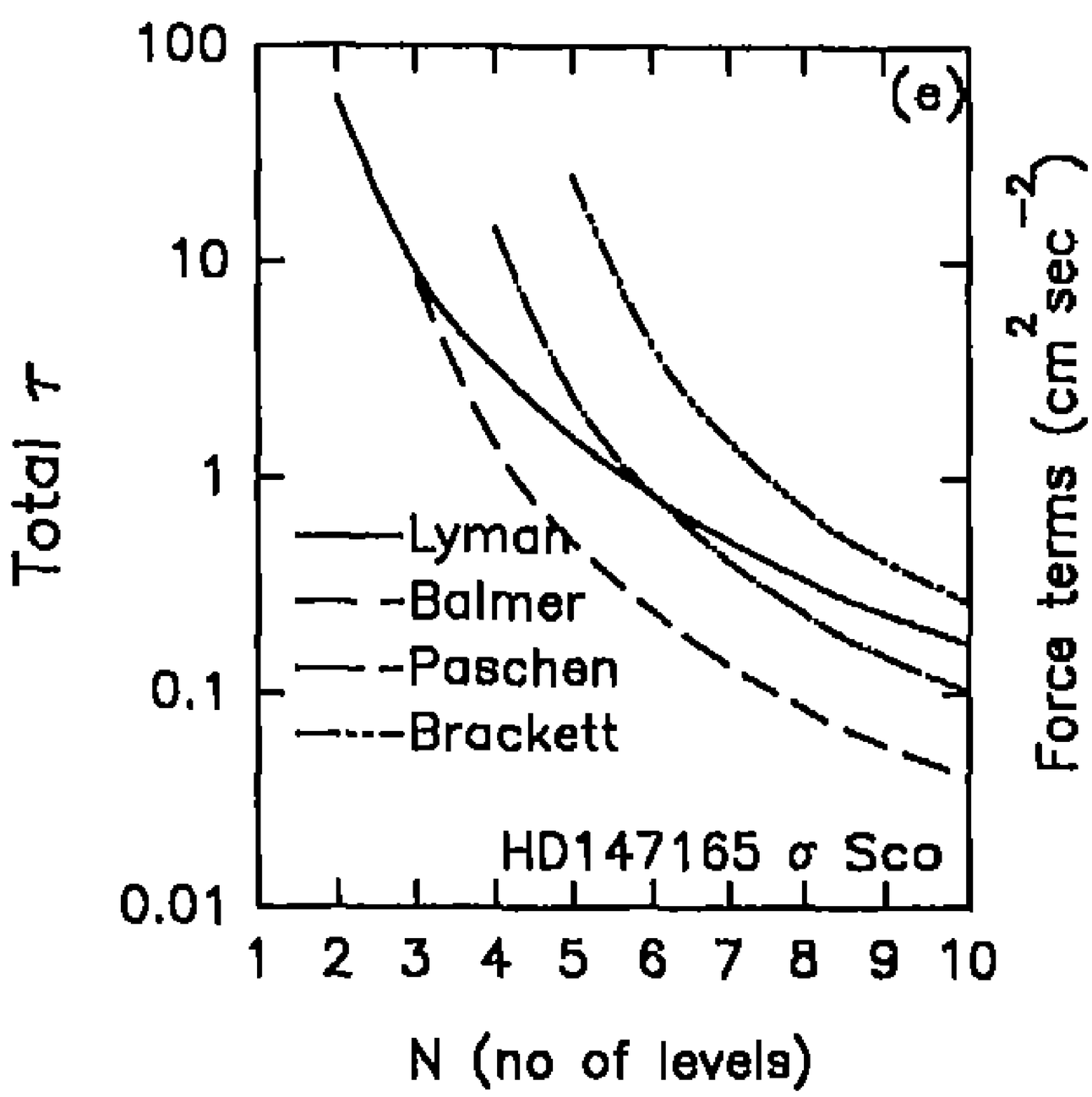

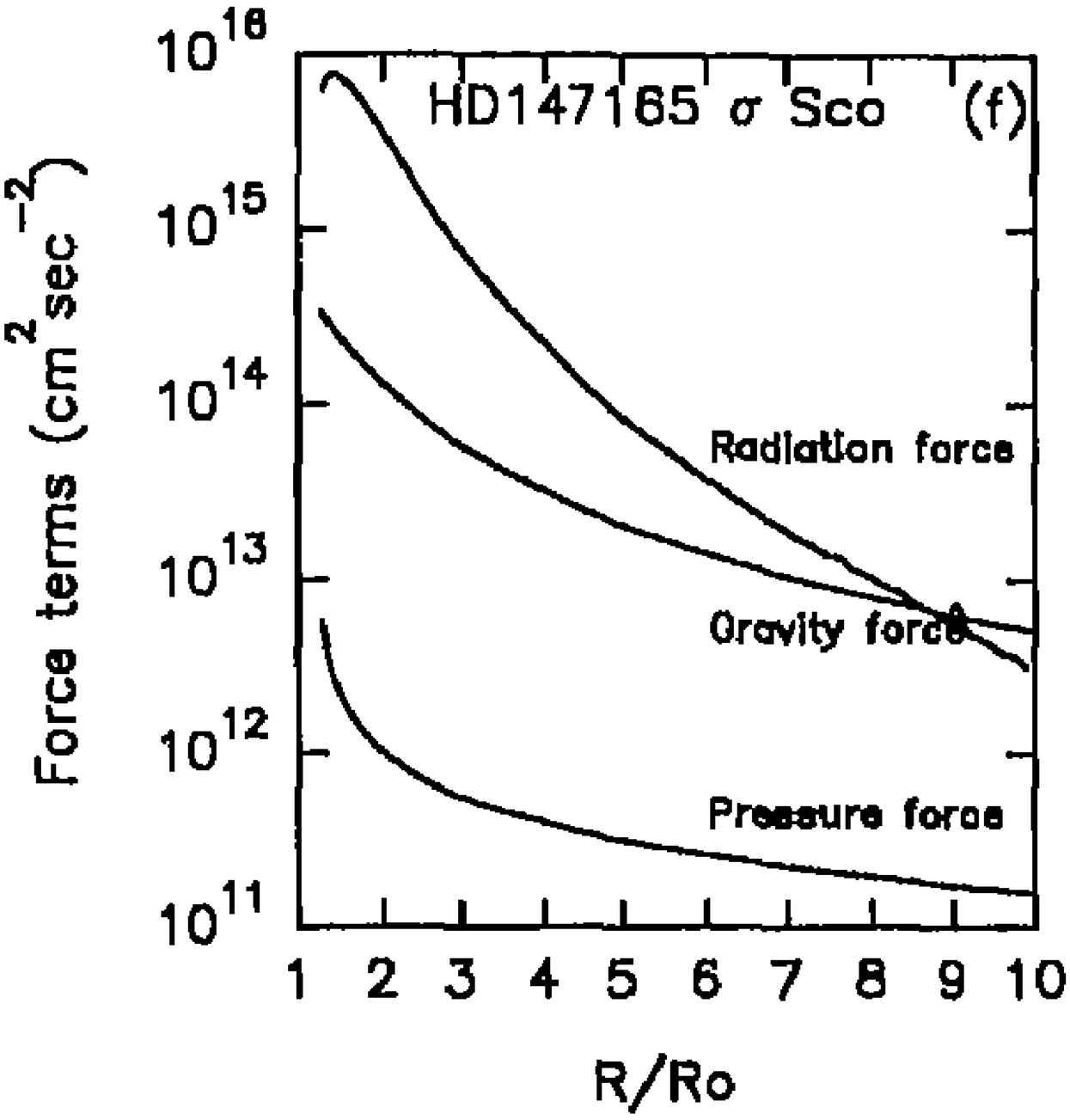

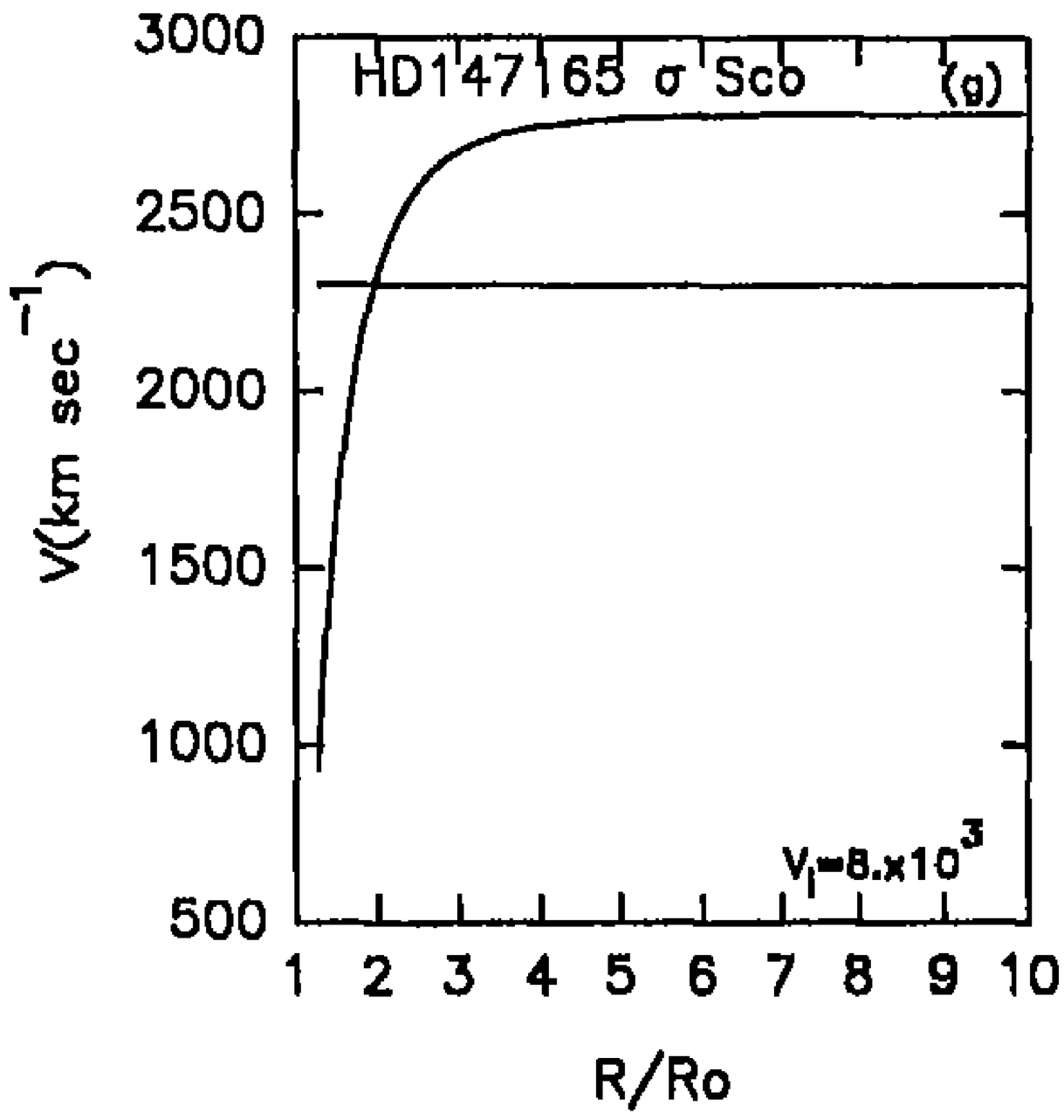

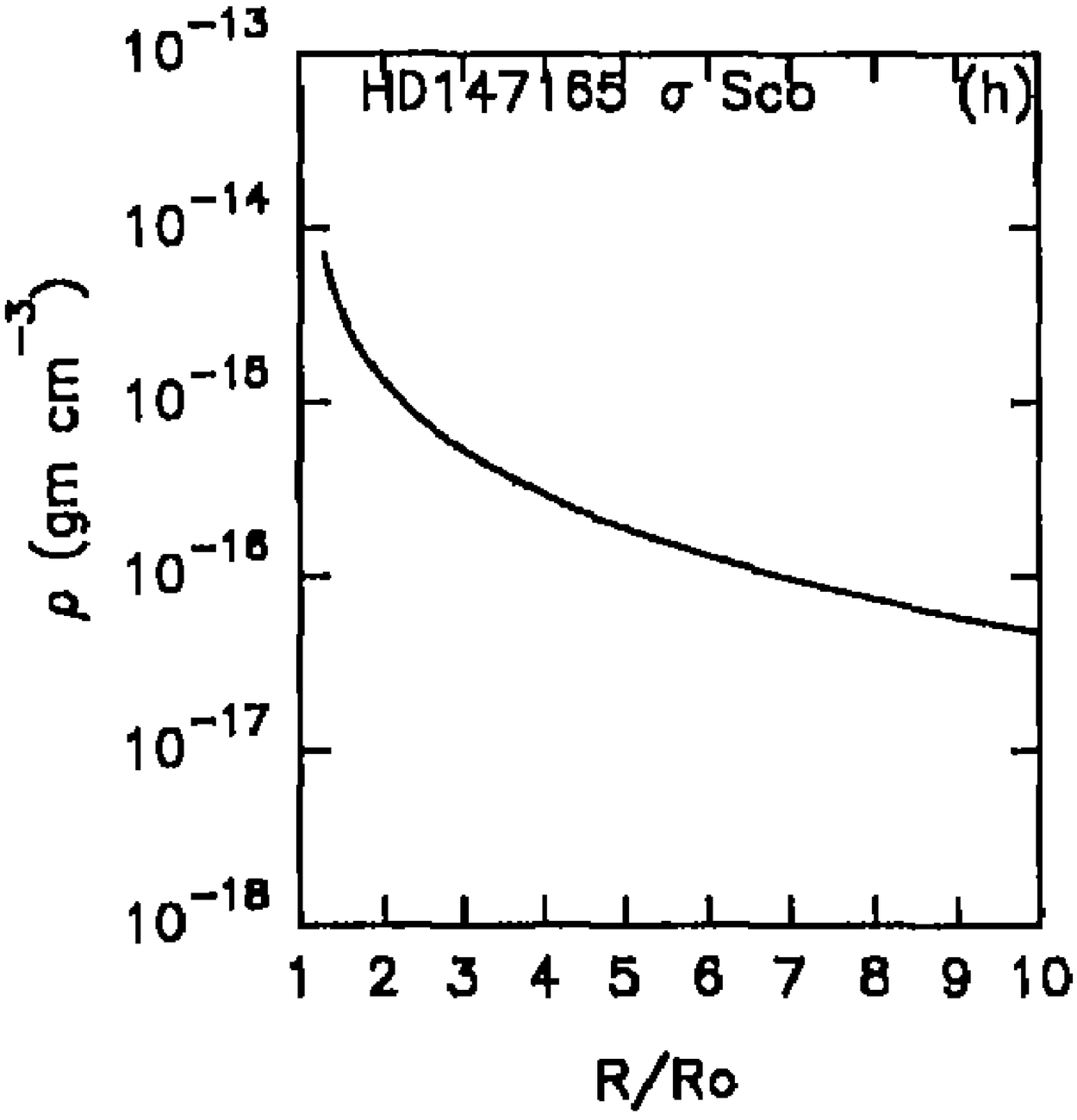

Figure 11 (e,f,g,h)

(g) The v_∞($\approx$ 2450 km s^{-1}) has reached at about $R/R_0 \sim 5$. Even though radiation has become less powerful than gravity (see (f)) the reduction in v_∞ is not substantial. The factor $\beta \approx 0.9$.

(f) The density changes between $\rho \sim 10^{-14}$ gr cm^{-3} to 10^{-16} gr cm^{-3}.

Figure 11

HD 147165 (σ Sco) B1 III (Blomme 1990a)

T_{eff} = 26302 K

M =2.9 $\times$ 10^{34} gr

R =6.93 $\times$ 10^{11} cm

V_{esc} = 718 km s^{-1}

V_∞ = 2300 km s^{-1}

M =1.326 $\times$ $10^{-5} M_\odot$/yr.

The results in (a), (b), (c), (d) are quite similar to those presented earlier.

(e) τ (Lyman α) > τ (Balmer α) Paschen α

τ (Lyman α) > τ (Paschen α)

τ (Lyman α) > τ (Brackett α)

τ (Lyman 9) > τ (Balmer 8)

τ (Lyman 9) > τ (Paschen 7)

τ (Lyman 9) > τ (Brackett 7)

(f) The gravity force exceeds the radiation force at about $R/R_0 \approx 9$.

(g) The calculated v_∞ > expected $v_\infty \approx$ 2300 km s^{-1} although the gravity force exceeds the radiation after $R/R_0 = 9$. Here $0.9 < \beta < 1.0$.

(h) The density changes from 10^{-14} gr cm^{-3} to 8×10^{-17} gr cm^{-3}.

Figure 12

HD 149438 (τSco) BO V

	Abbott (1978)	Blomme (1990a)
T_{eff}	32359 K	30902 K
M	3.8 $\times$ 10^{34} gr	3.38 $\times$ 10^{34} gr
R	4 .16 $\times$ 10^{11} cm	4.13 $\times$ 10^{11} cm
V_{esc}	1030 km s^{-1}	1021 km s^{-1}
V_∞	V_{edge} = 2000 km s^{-1}	3050 km s^{-1}
$\dot{M}$		5.82 $\times$ $10^{-6} M_\odot$/yr

These results are similar to those of HD 14165 (σ Sco).

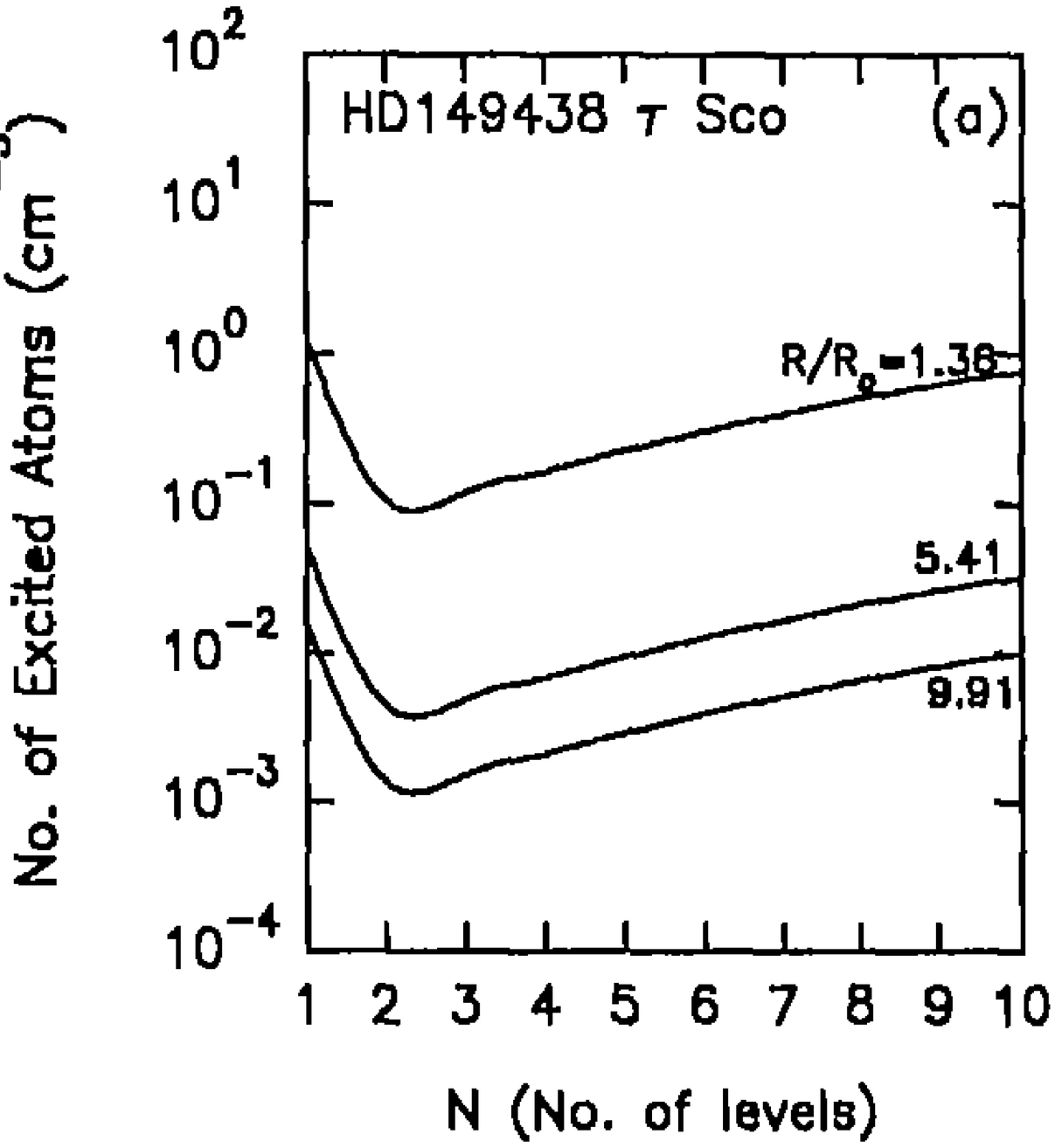

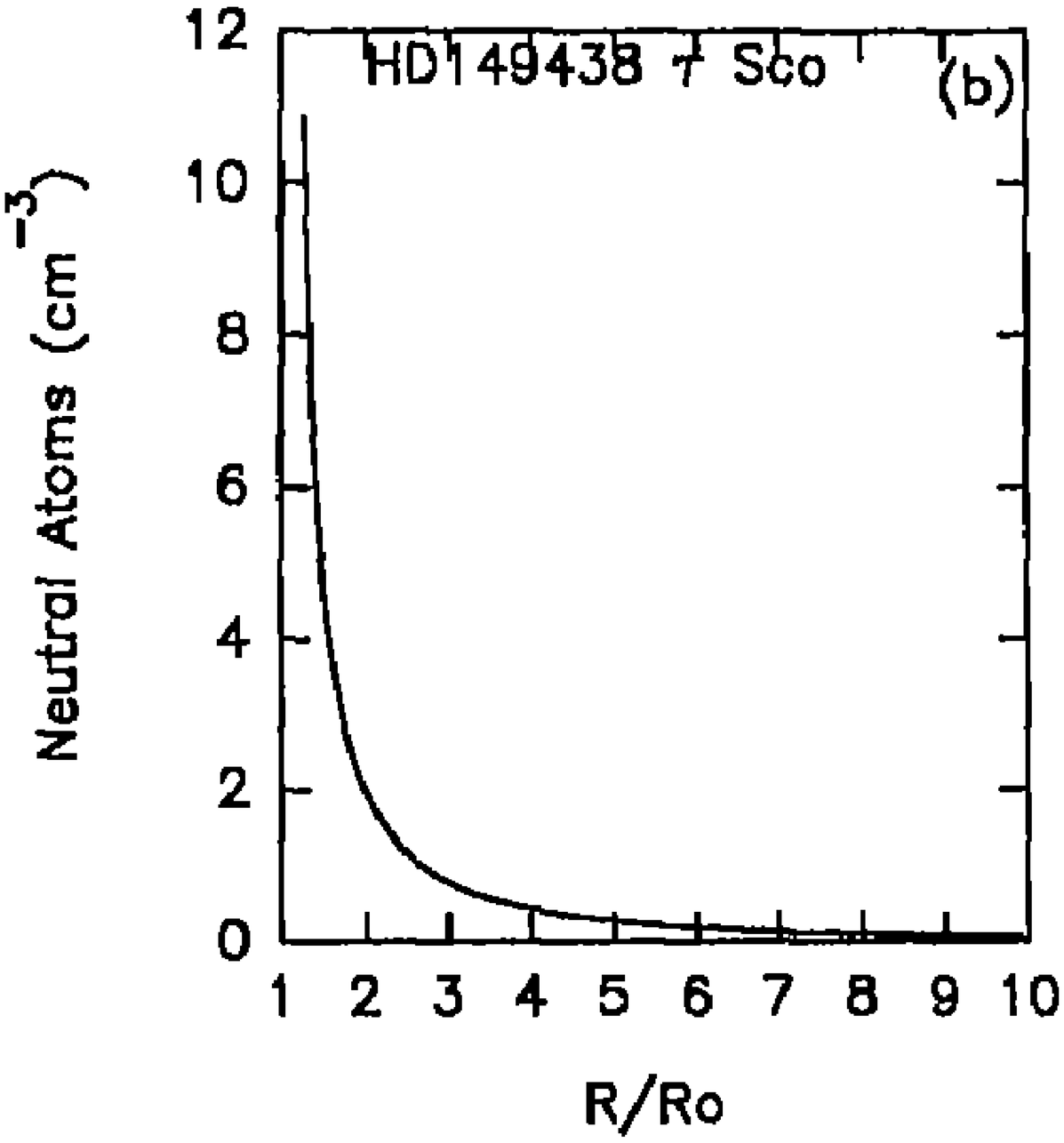

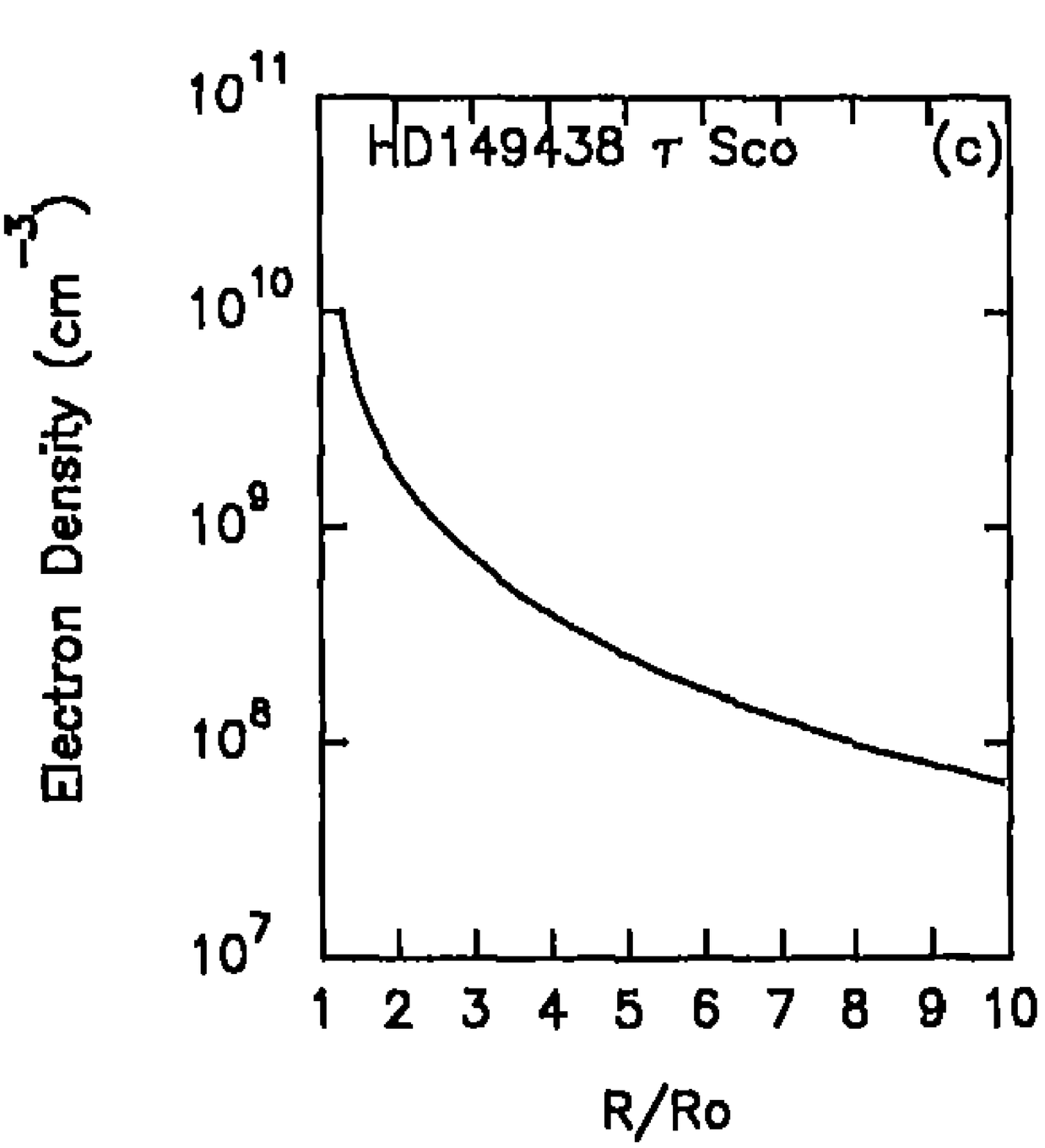

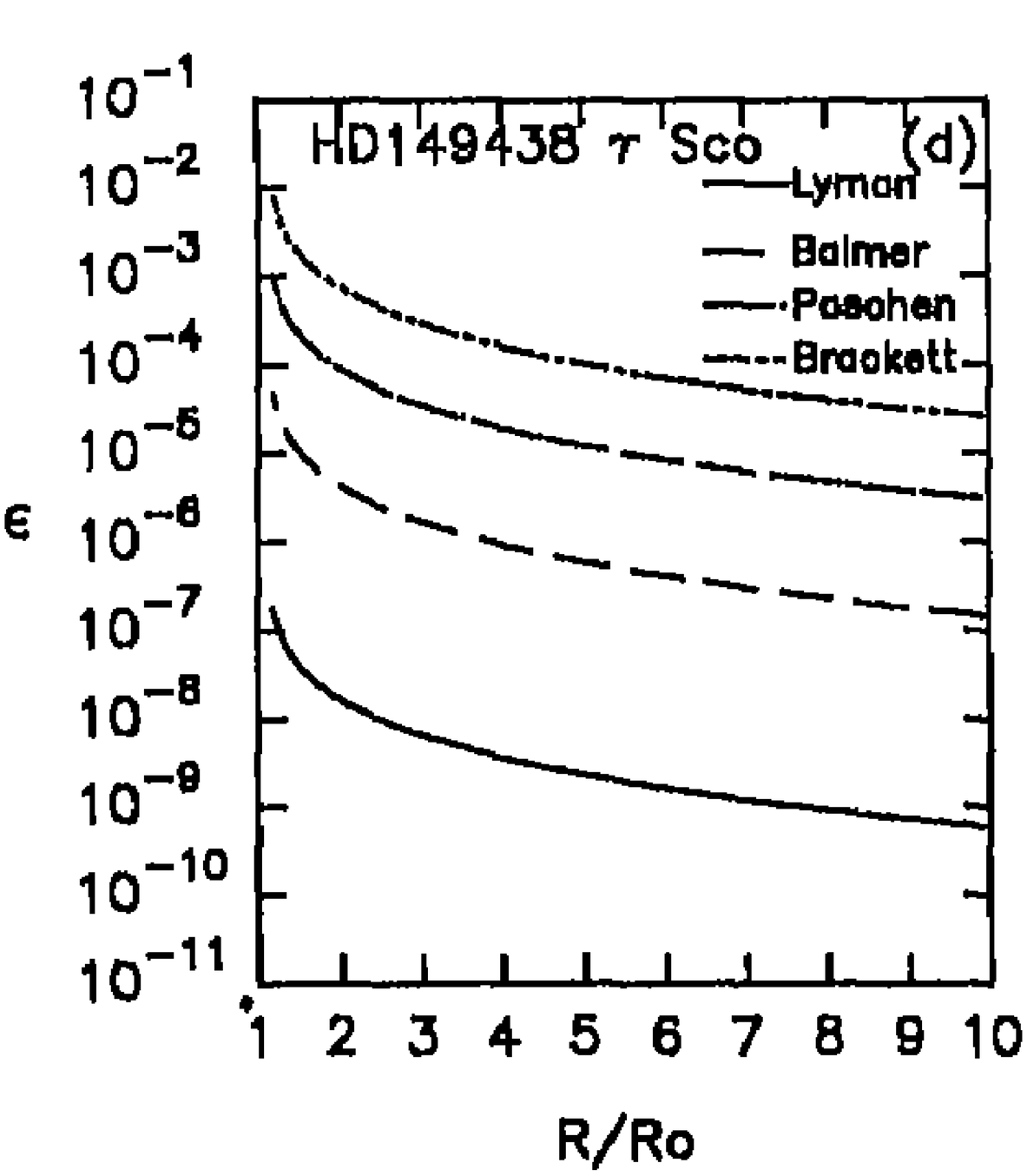

Figure 12 (a,b,c,d)

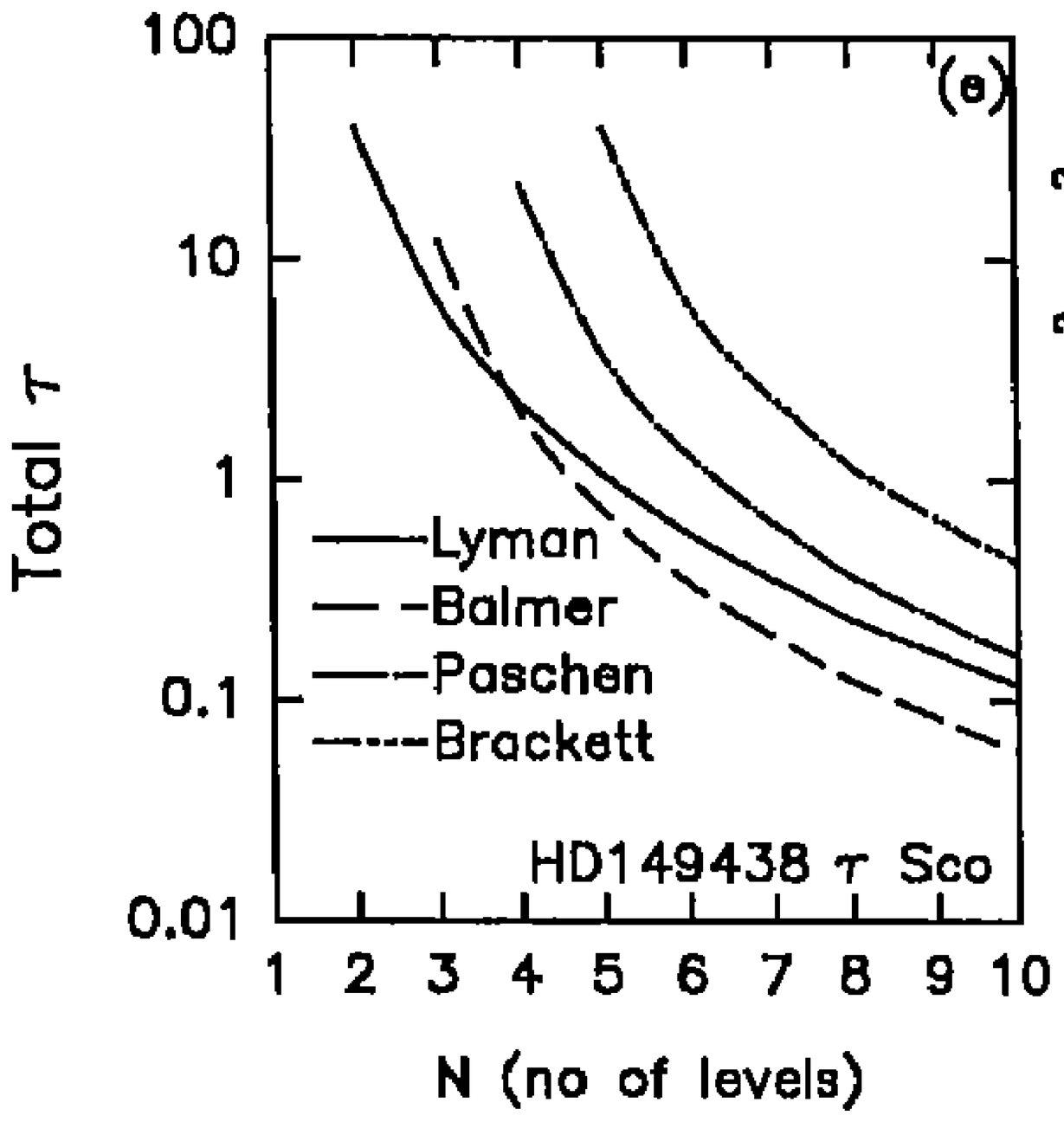

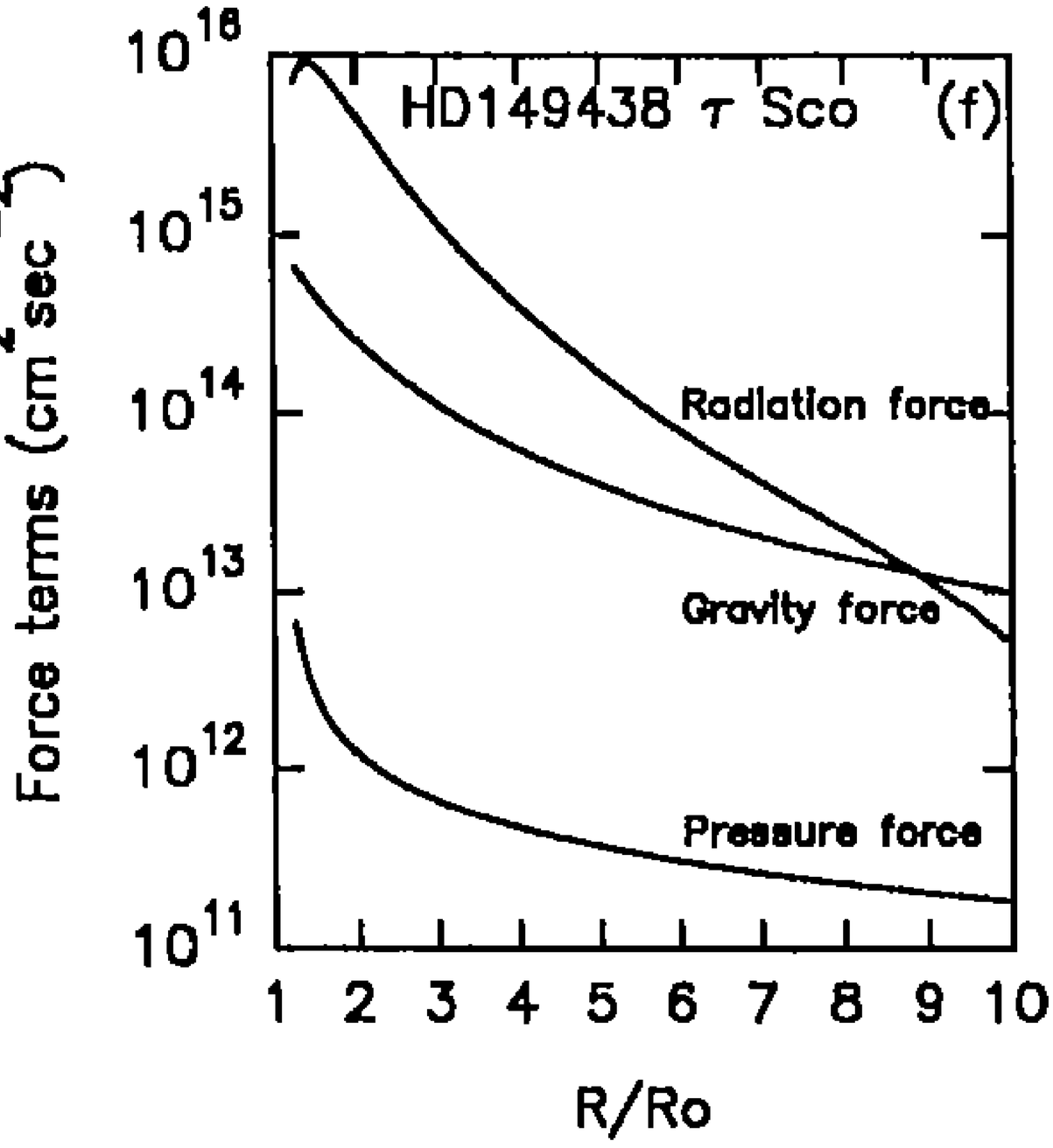

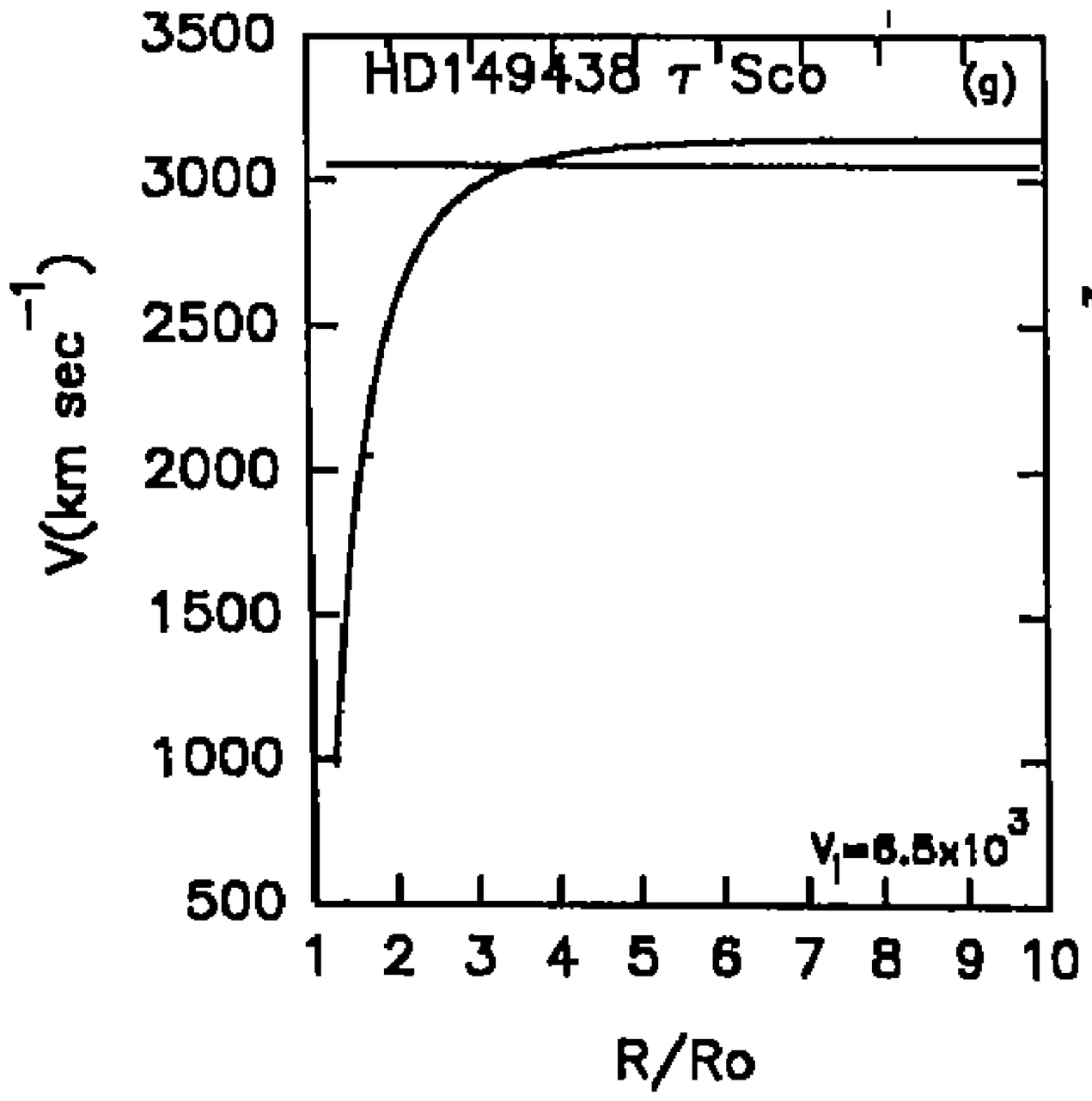

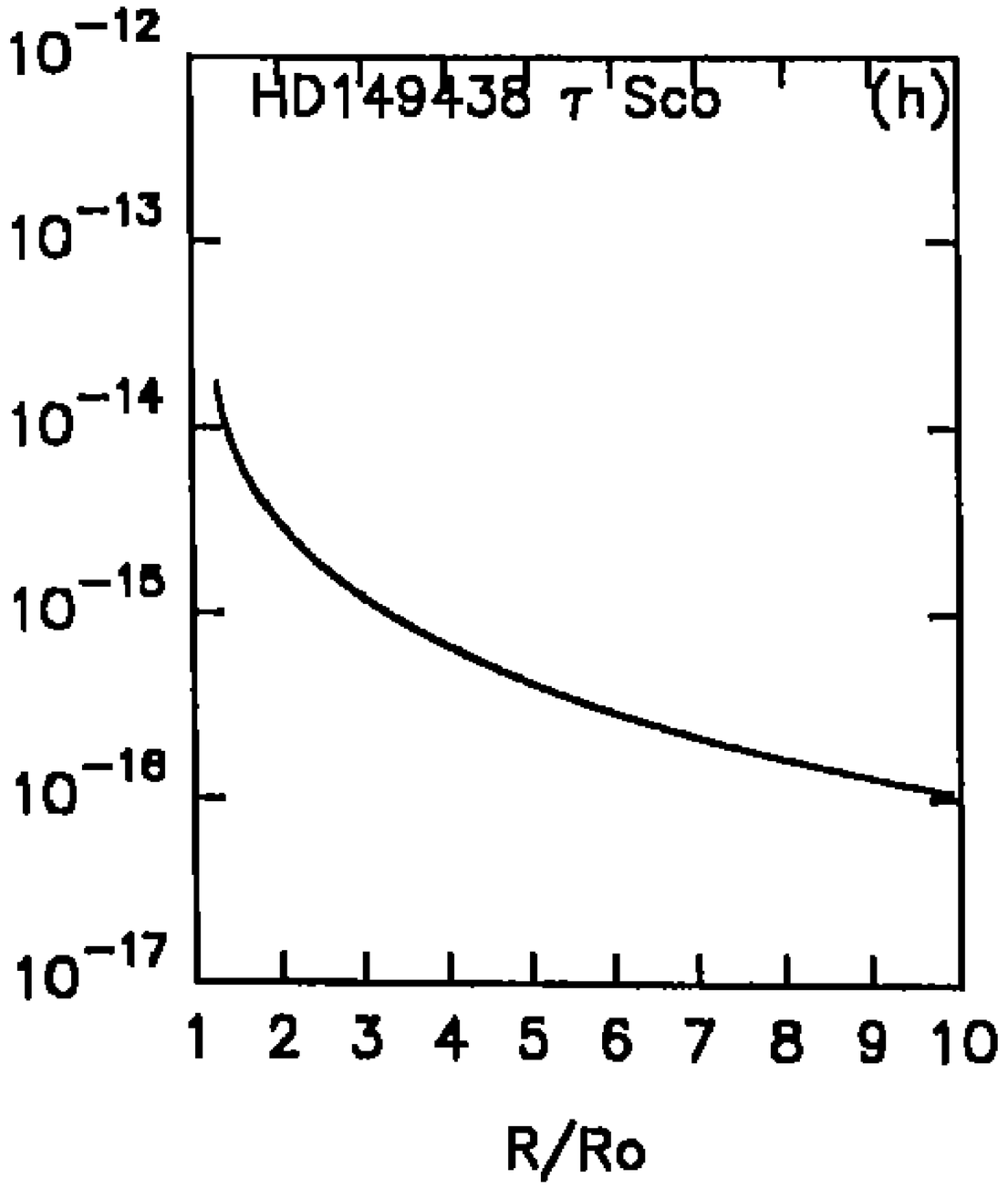

Figure 12 (e,f,g,h)

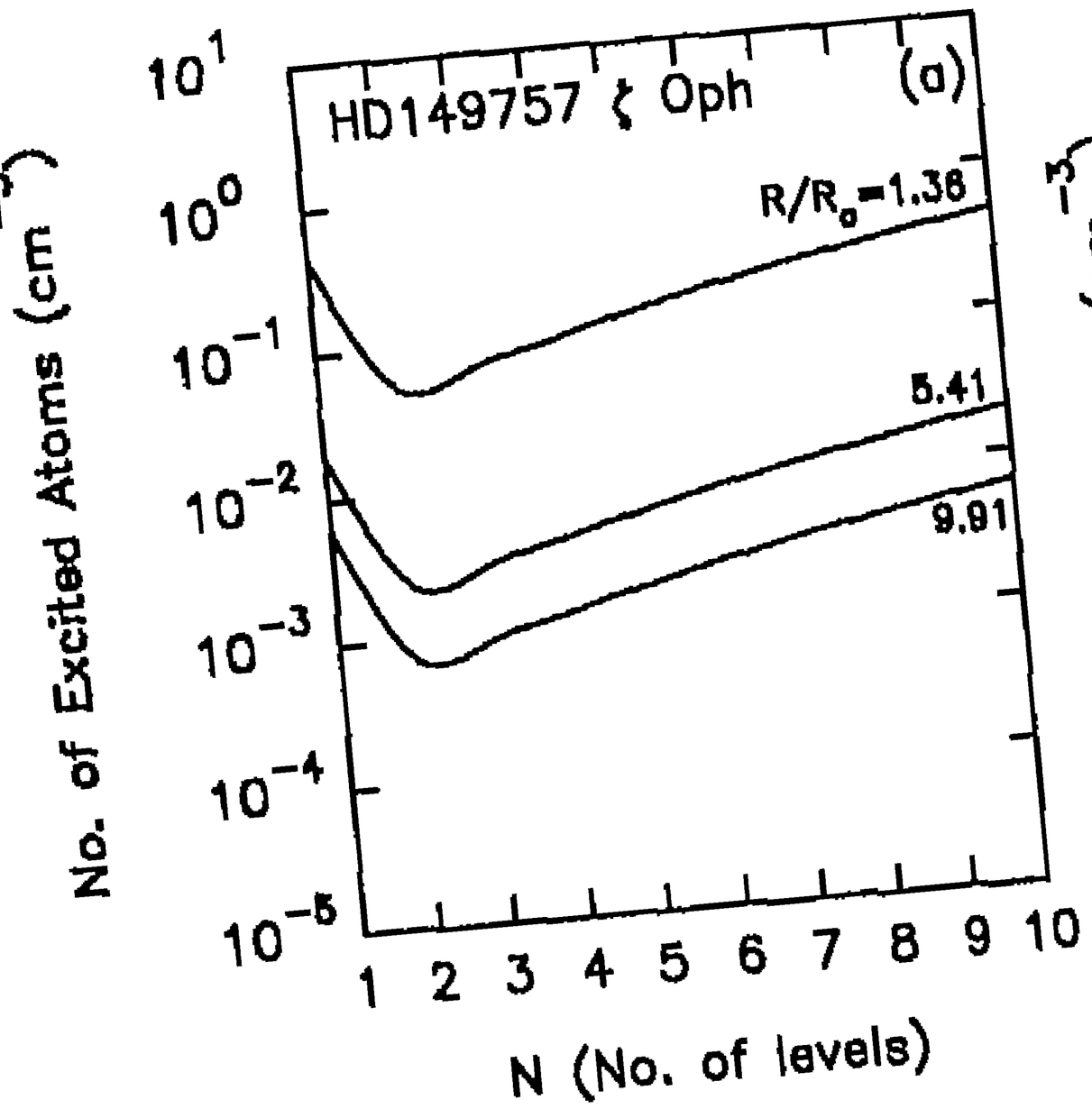

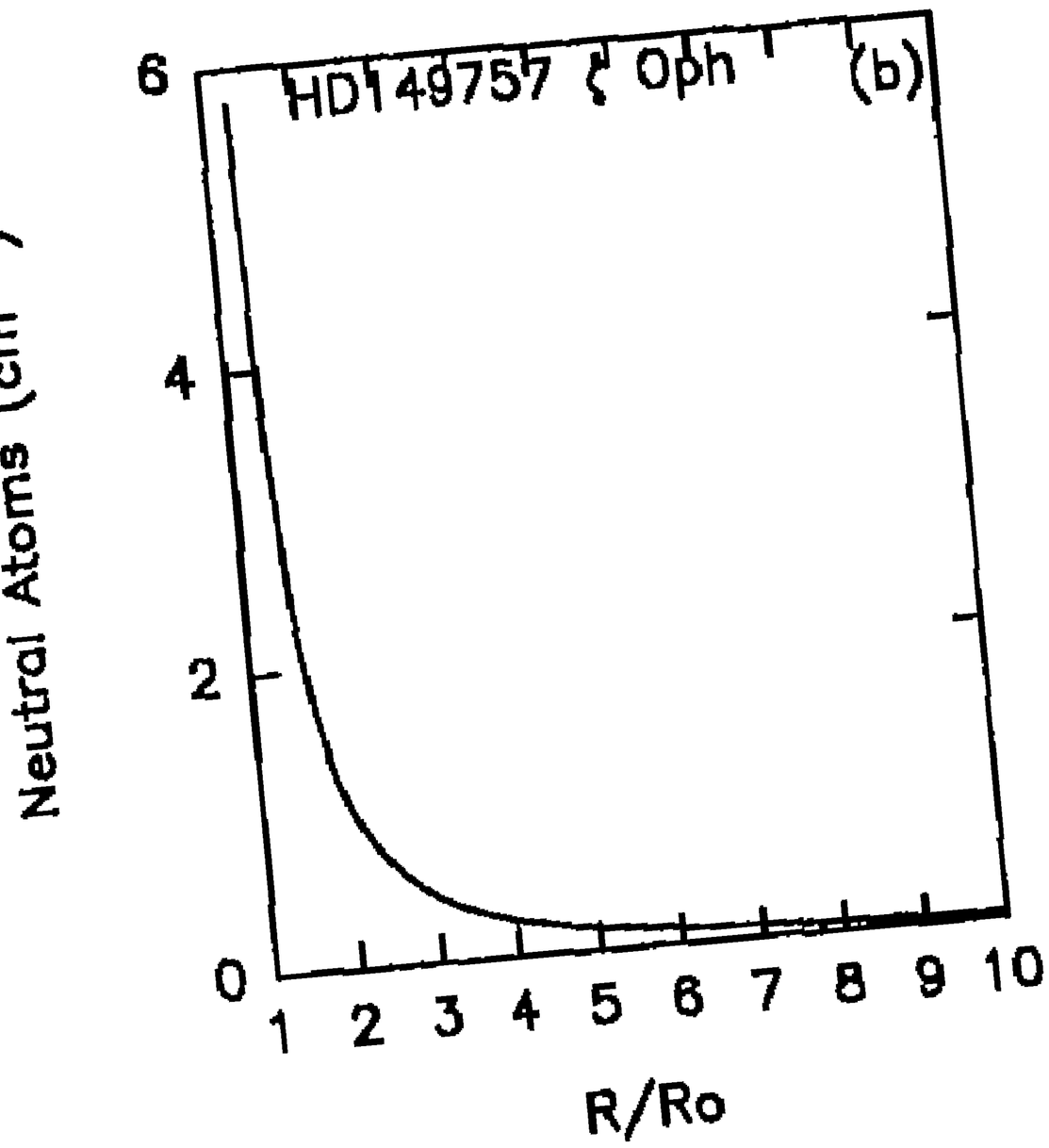

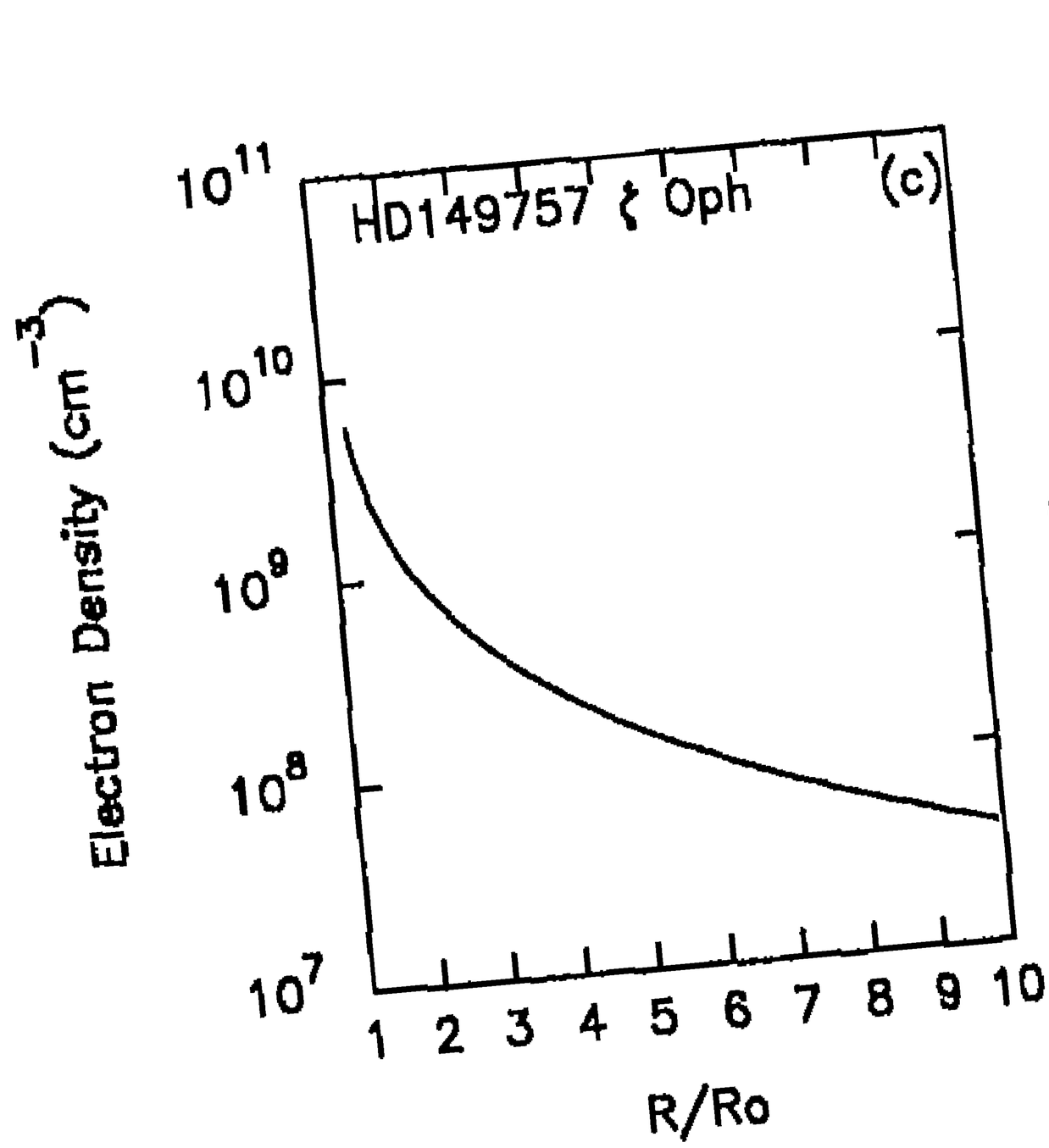

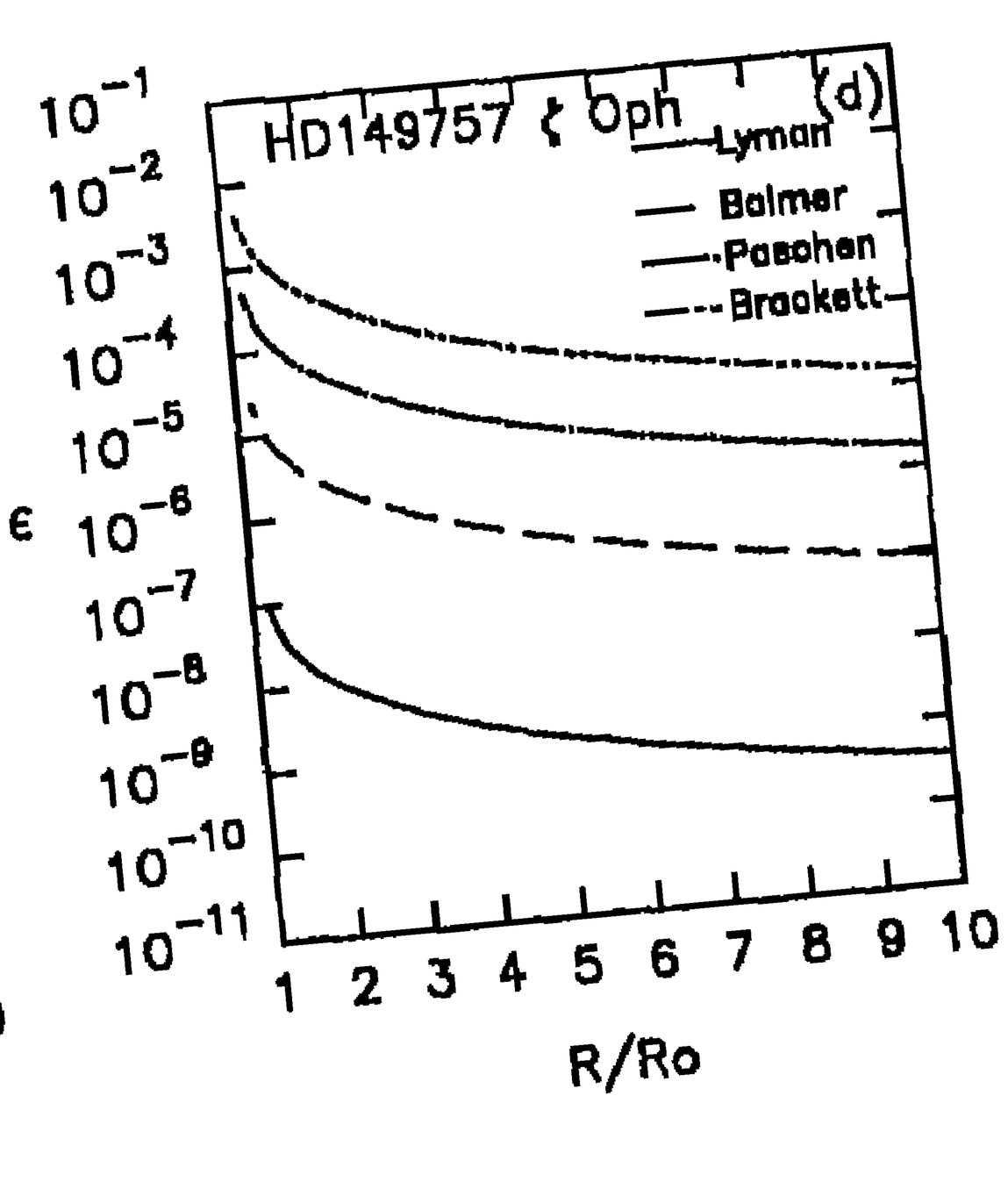

Figure 13 (a,b,c,d)

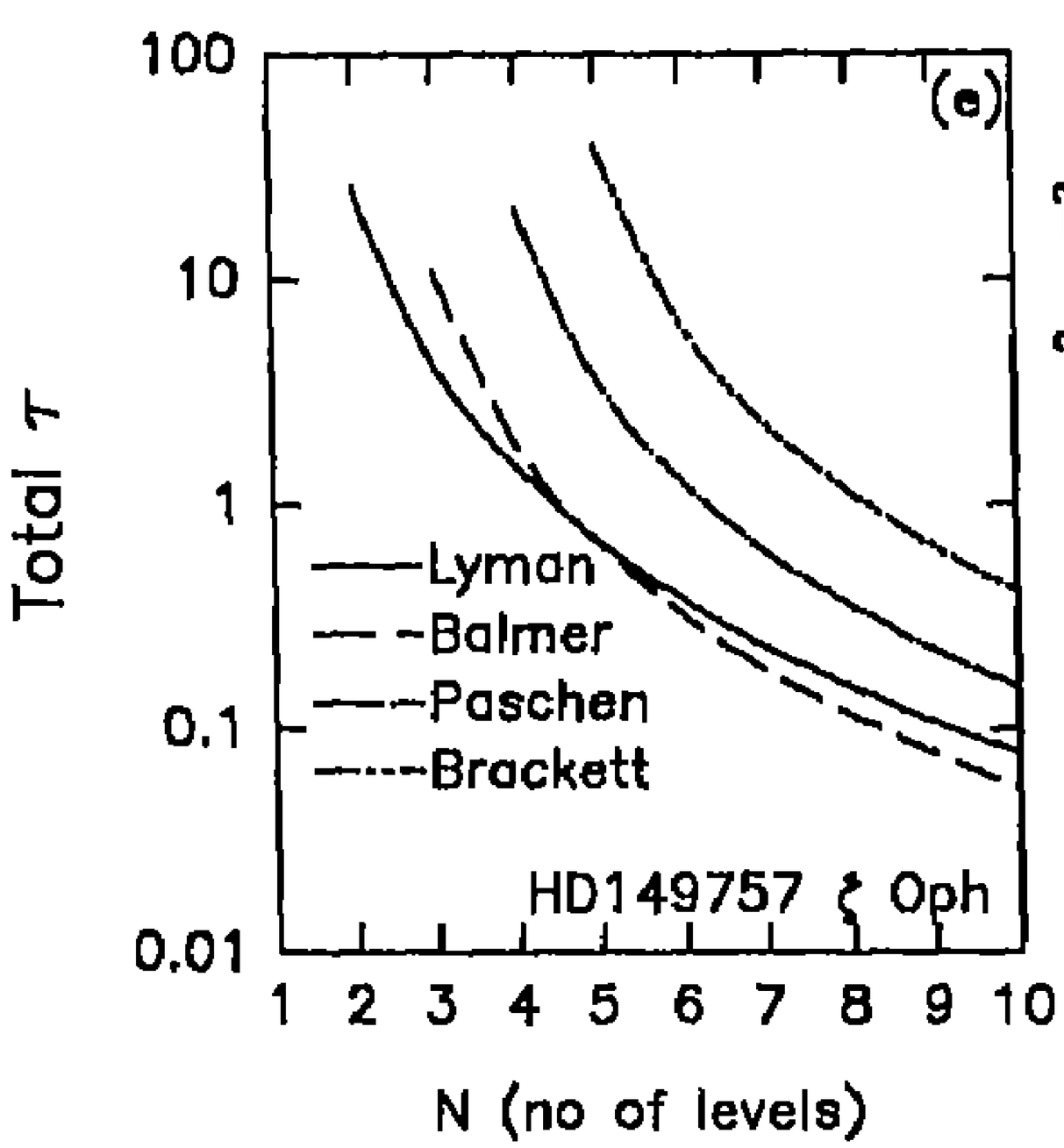

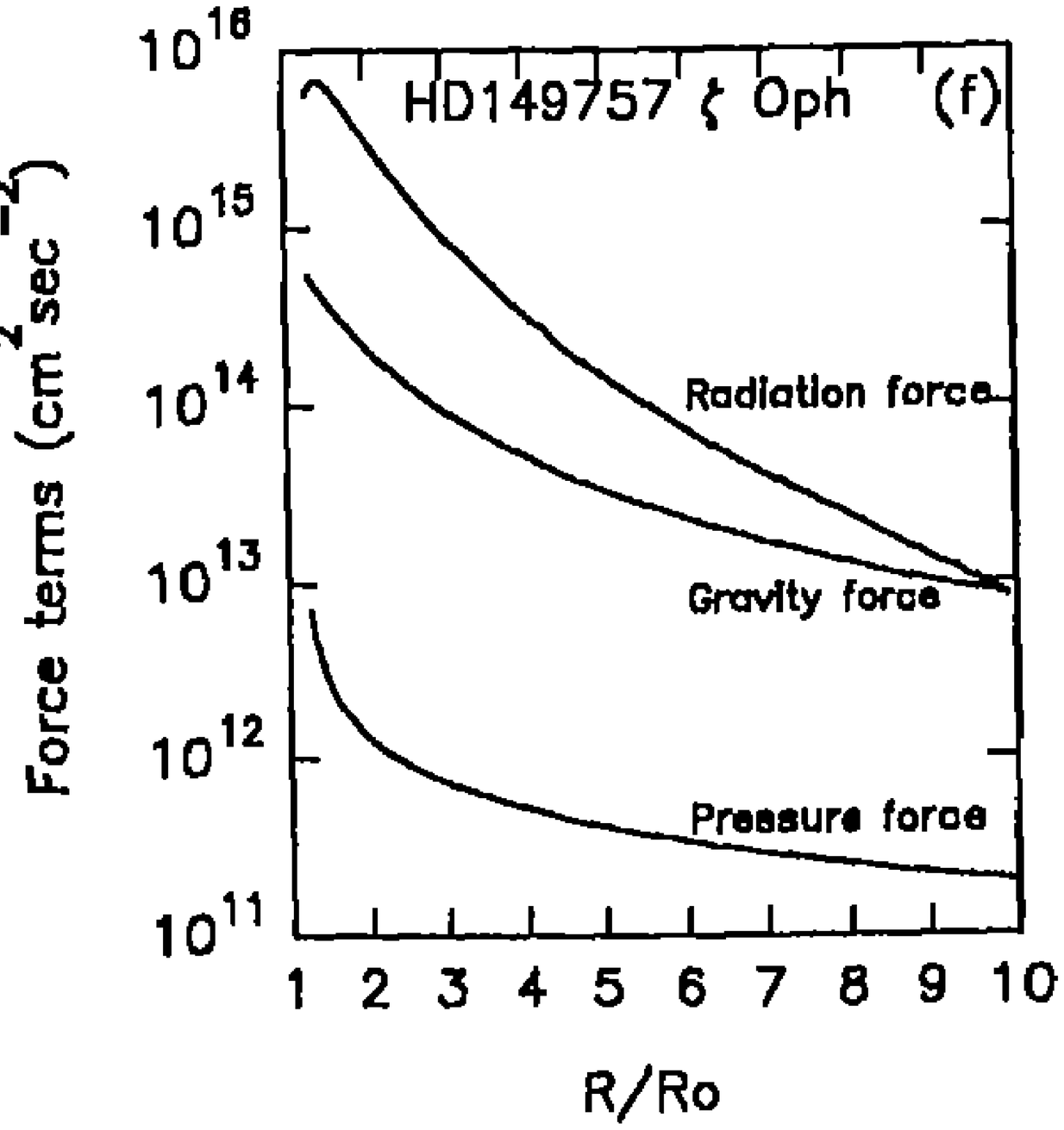

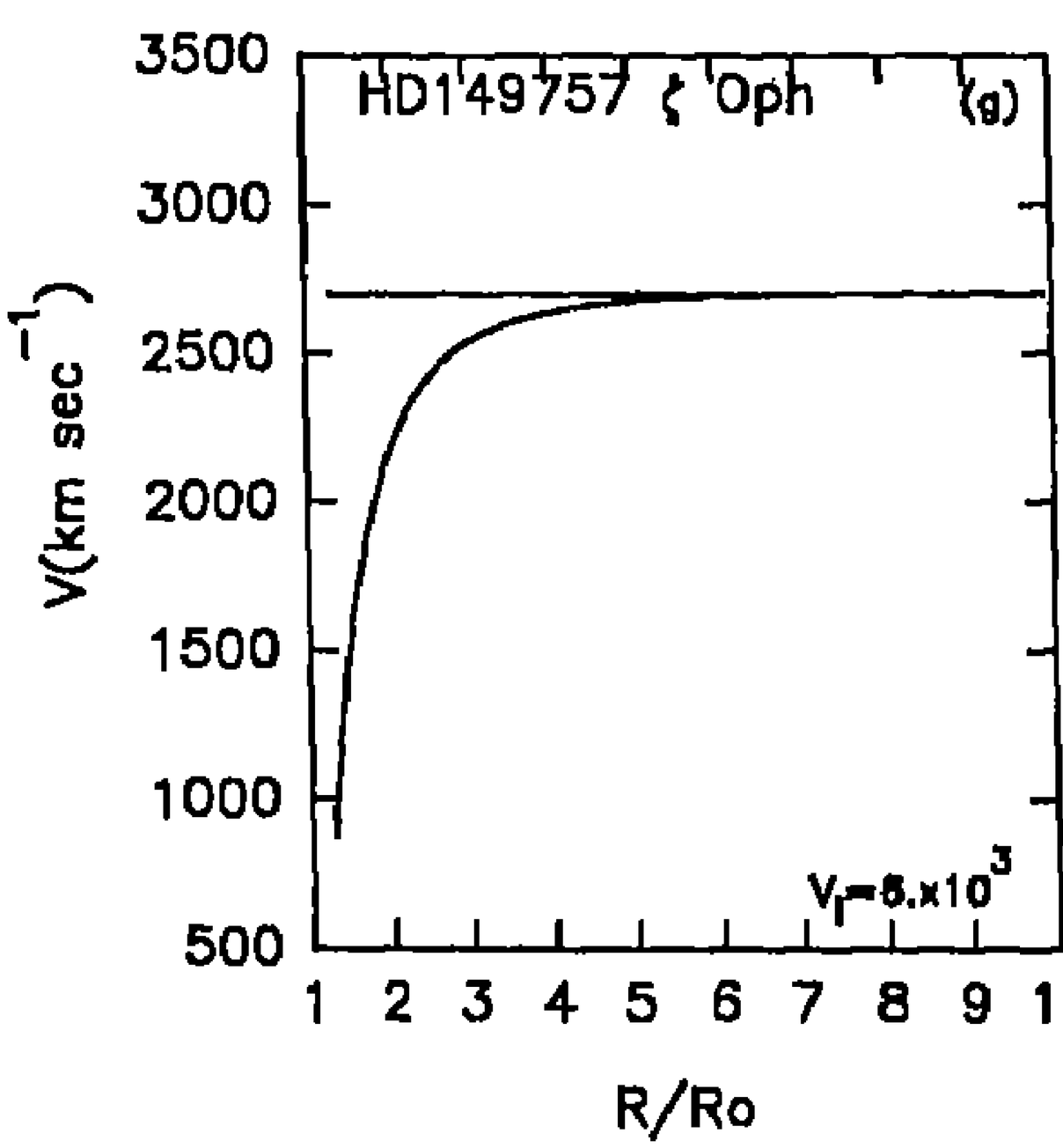

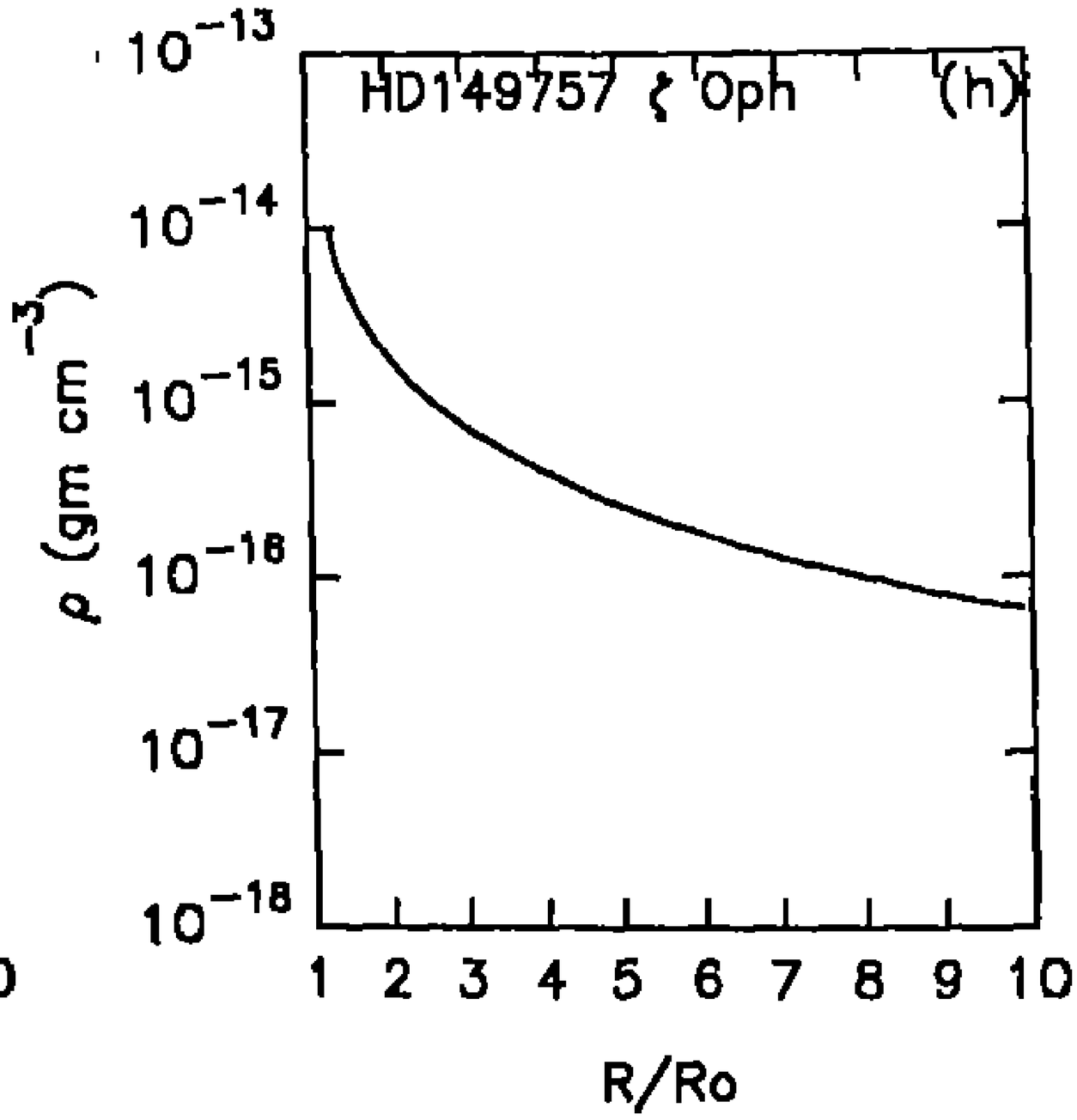

Figure 13 (e,f,g,h)

Figure 13

HD 149757 (ζOph) O9 V(o)

	Abbott (1978)	Blomme (1990a)
T_{eff}	32300 K	33884 K
M	5×10^{34} gr	4.18×10^{34} gr
R	7×10^{11} cm	6.58×10^{11} cm
V_{esc}	910 km s^{-1}	893 km s^{-1}
V_∞	$V_{eclips} = 1580$ km s^{-1}	2700 km s^{-1}
$\dot{M}$		$7.5 \times 10^{-6} M_\odot$/yr

The results presented in (a), (b), (c), (d) and (e) are similar to those of earlier systems.

(f) The radiation force becomes exactly equal to gravity force at $R/R_0 \simeq 10$. The matter moves with the previously acquired momentum.

(g) The expected v_∞ (= 2700 km s^{-1}) is obtained with $v_i = 6 \times 10^3$ cm s^{-1}. Here $\beta \sim 0.9$.

The density $\rho(r)$ varies from 10^{-14} gr cm^{-3} to $< 10^{-16}$ gr cm^{-3}.

Figure 14

HD 152234, BO.5, Ia (Blomme 1990a)

(We have taken the first set of data)

T_{eff} = 22908 K

M =5.5 $\times 10^{34}$ gr

R =2.709 $\times 10^{12}$ cm

V_{esc} = 418 km s^{-1}

V_∞ = 2650 km s^{-1}

$\dot{M}$ = 2.99 $\times 10^{-6} M_\odot$/yr

(a), (b), (c): As the mass loss rate is small the density is correspondingly small. Therefore low densities of excited atom and neutral atoms. Because of the low temperature the lower levels are more populated than the upper levels.

(d) The ϵ (Lyman α) at R/R$_0$ = 10 $\approx$ 0 for all practical purposes. Lyman α is almost in the scattering medium.

(e) τ (Lyman α, 9) > τ (Balmer α,8)

τ (Lyman α, 9) > τ (Paschen α, 7)

τ (Lyman α, 9) > τ (Brackett α, 6)

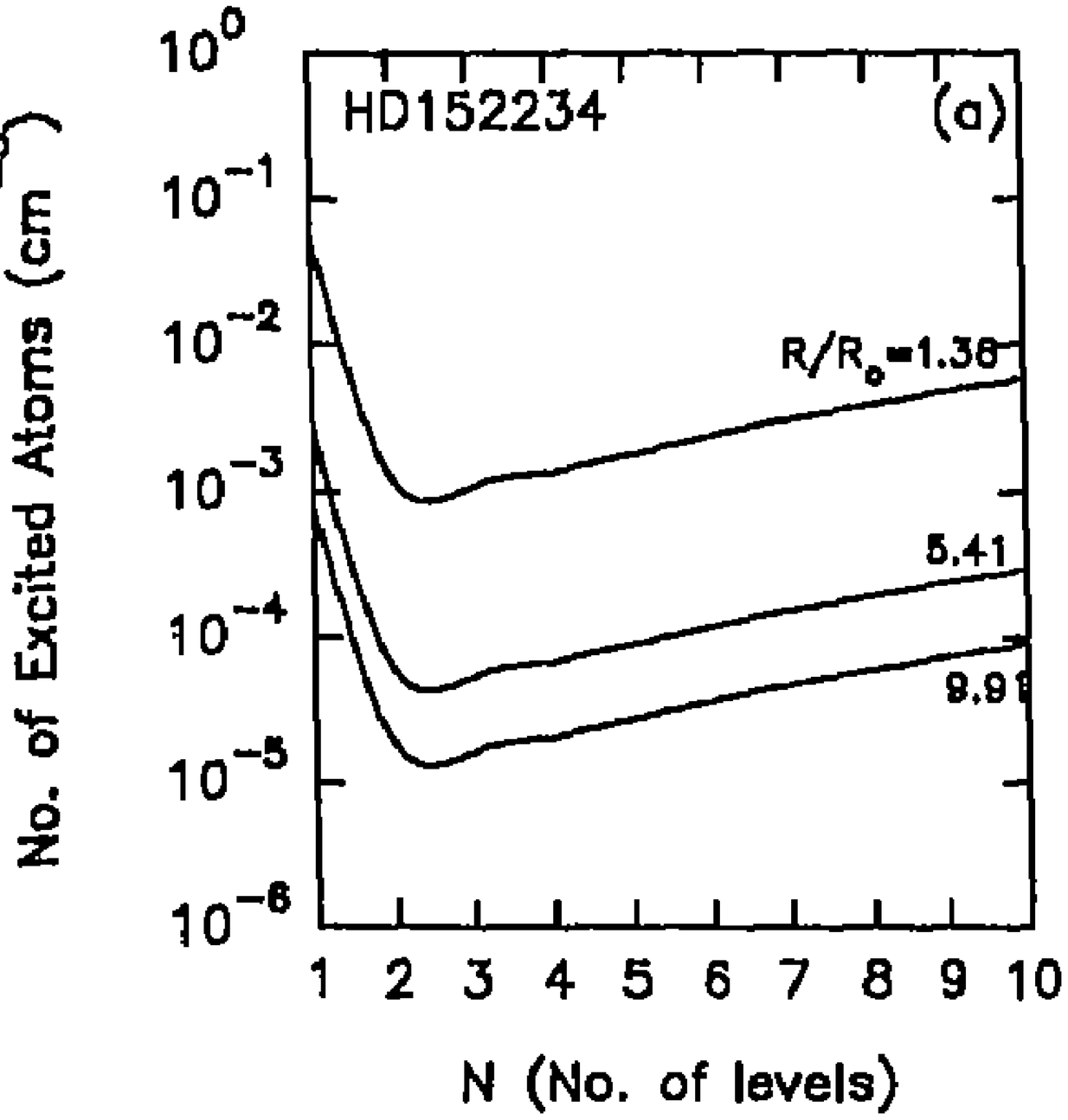

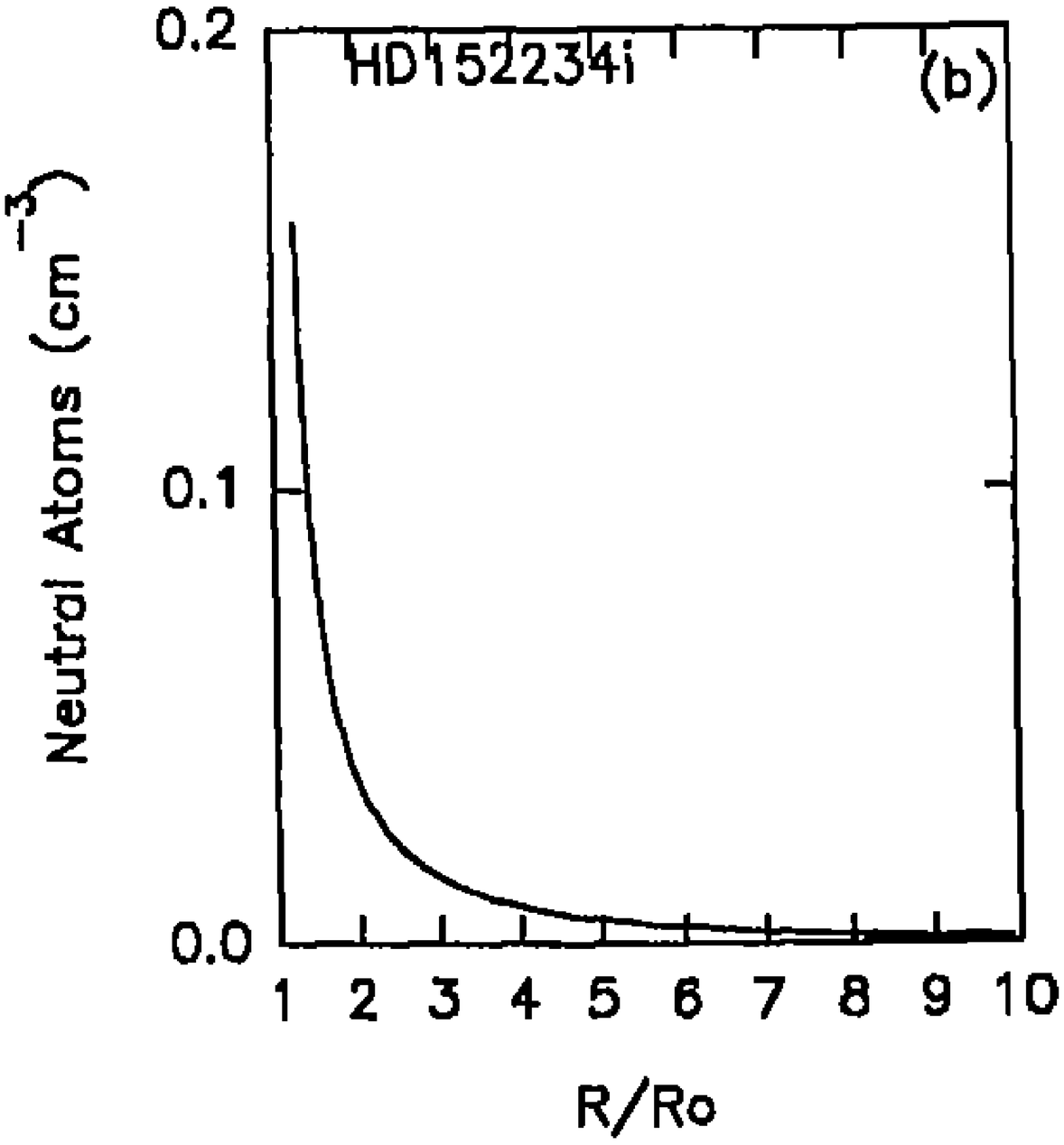

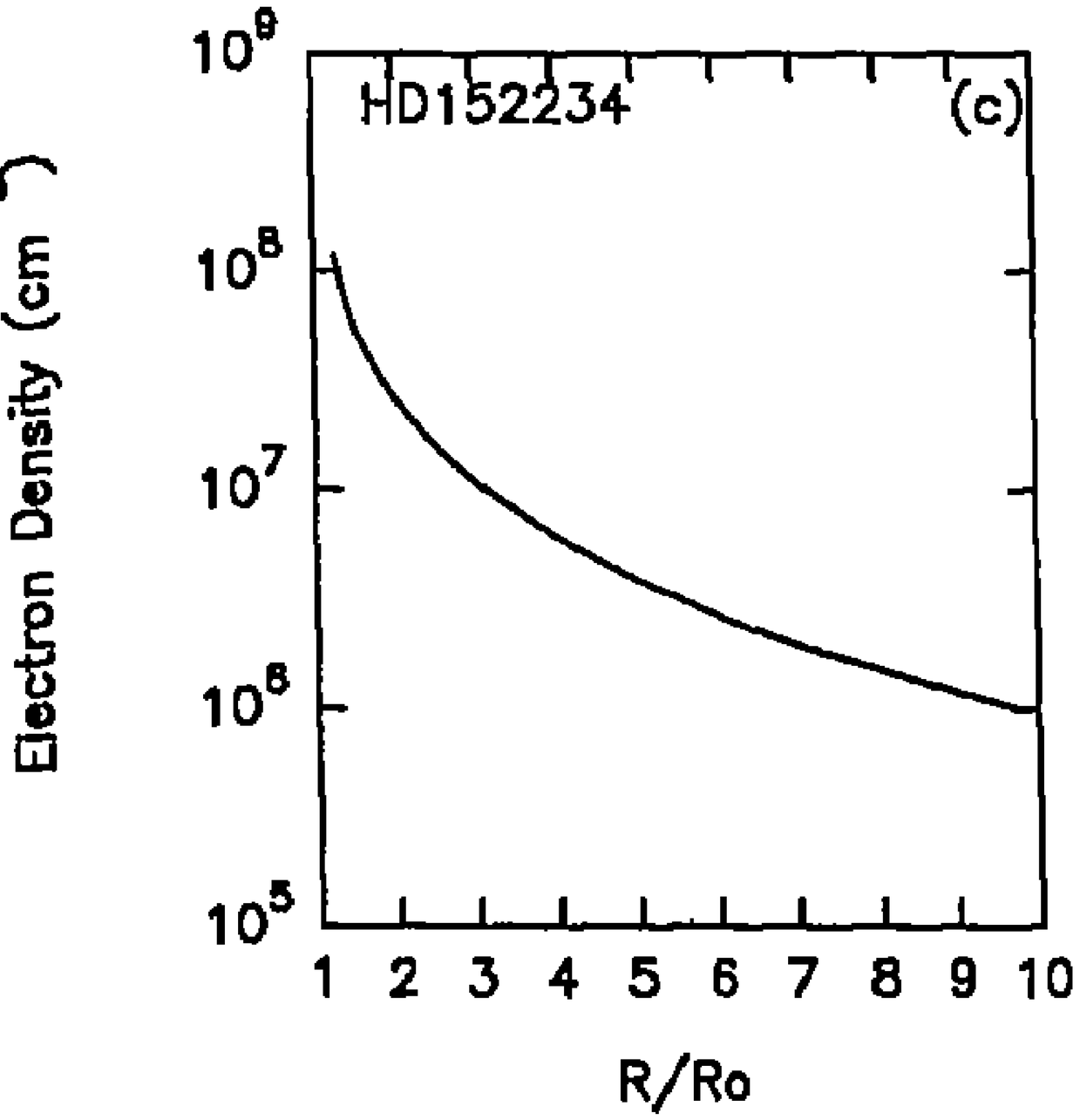

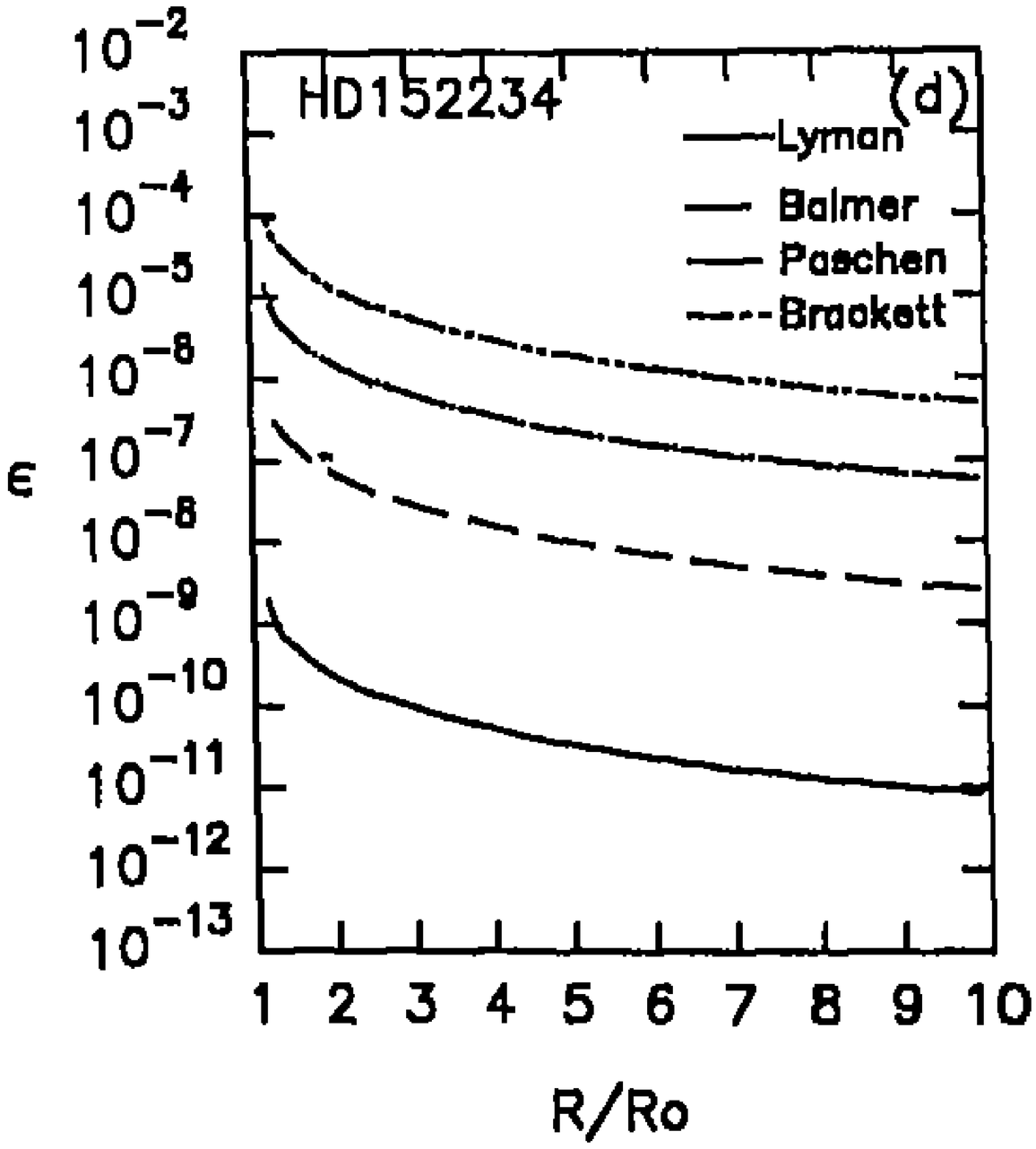

Figure 14 (a,b,c,d)

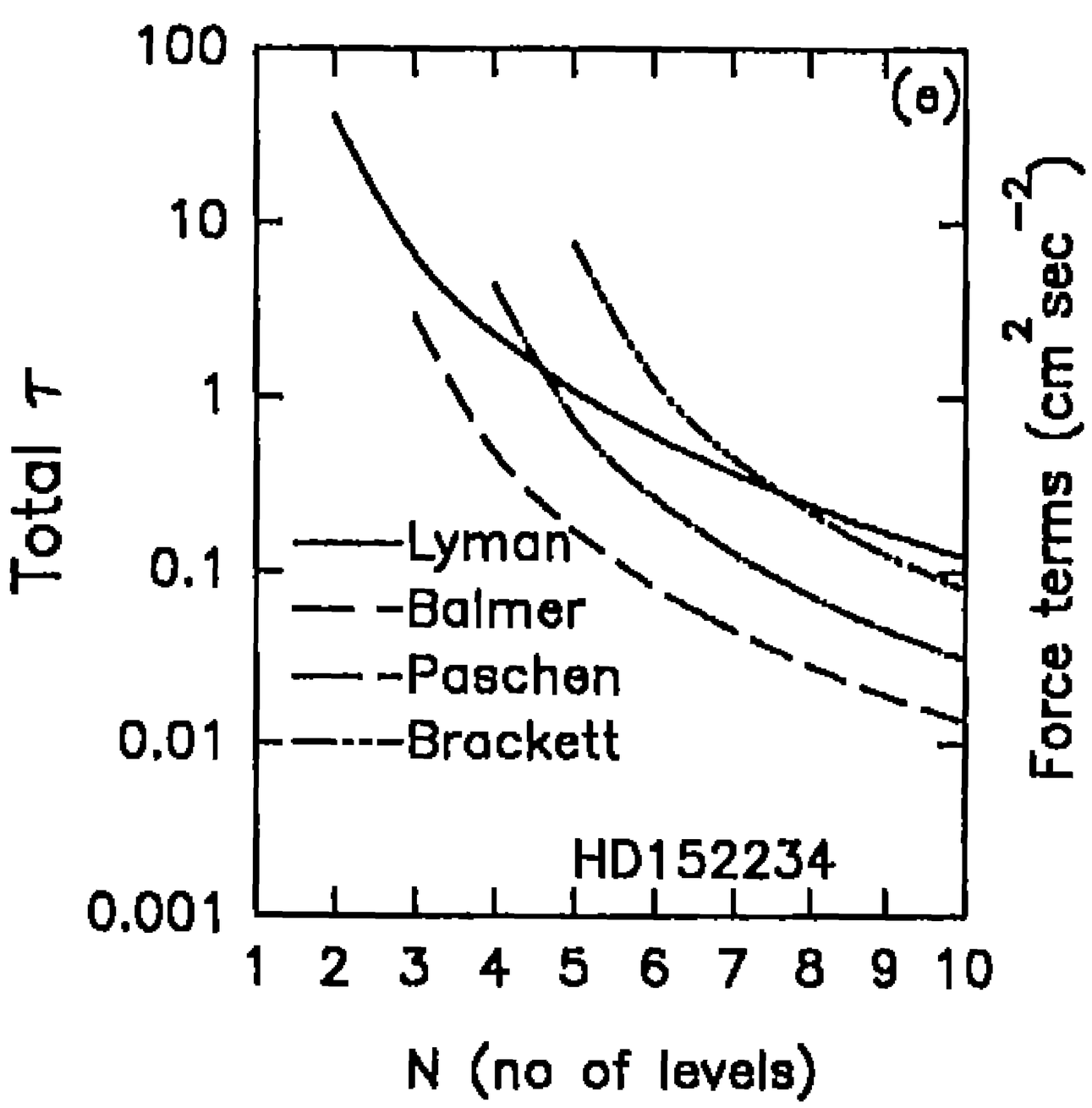

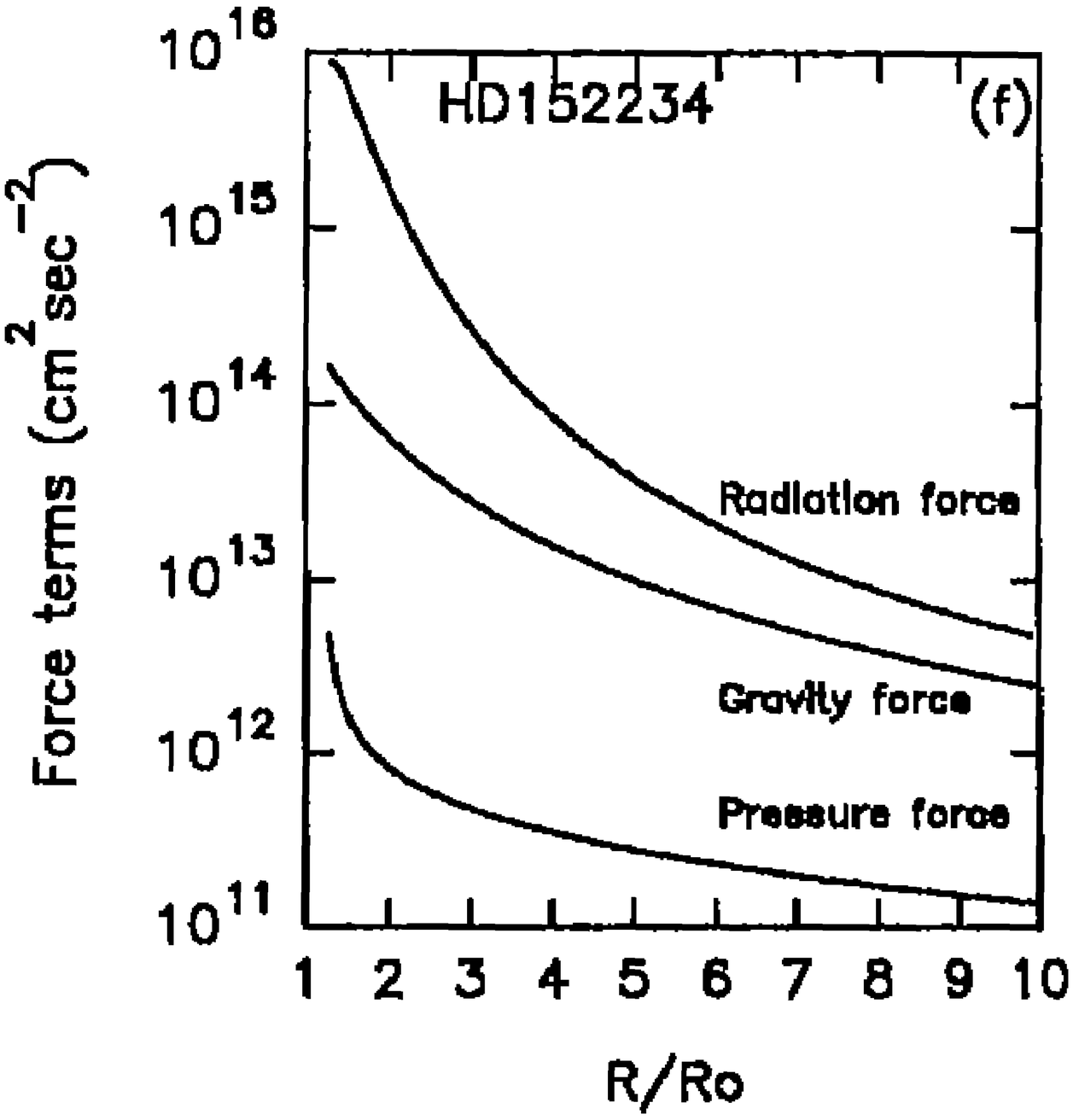

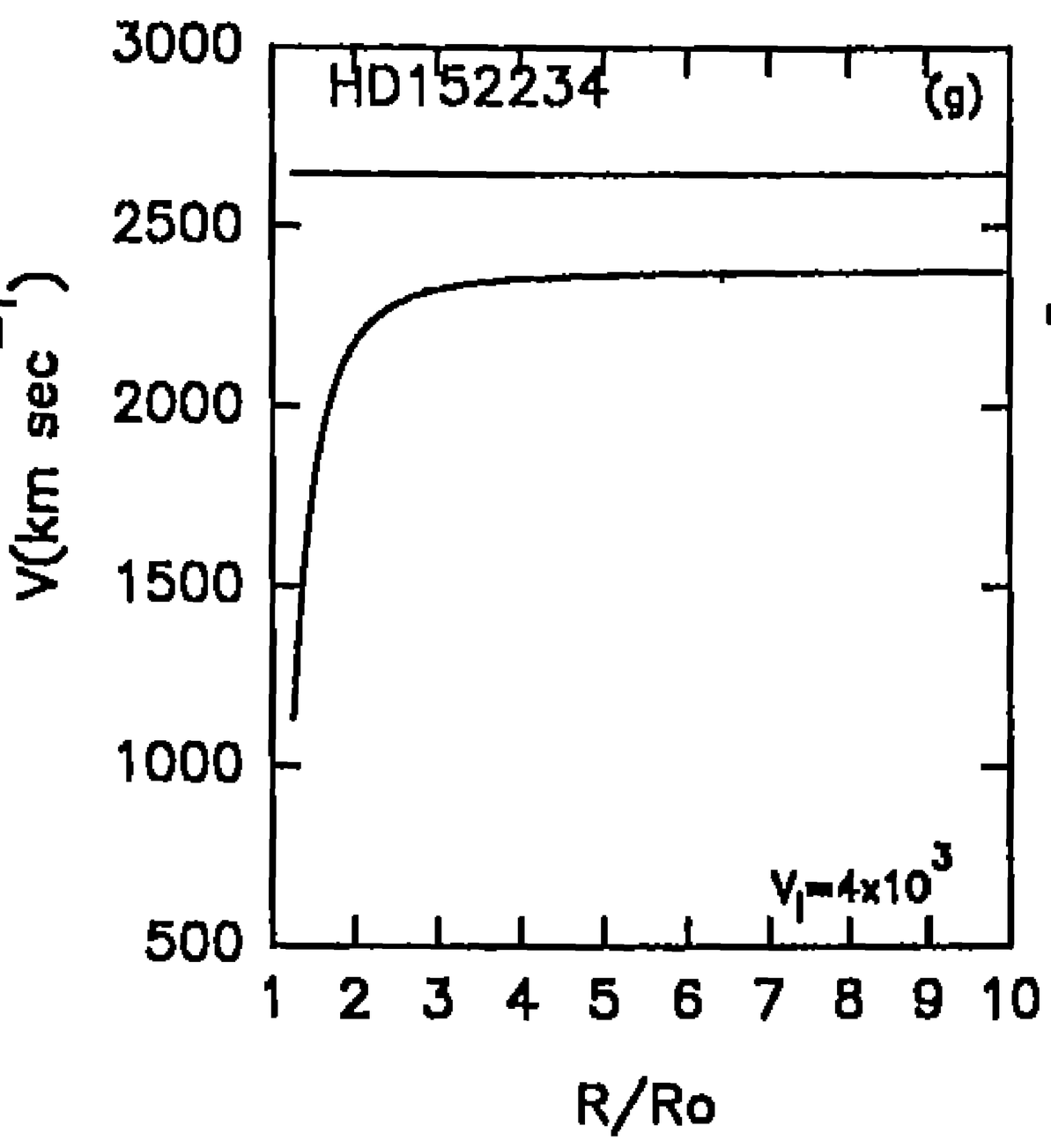

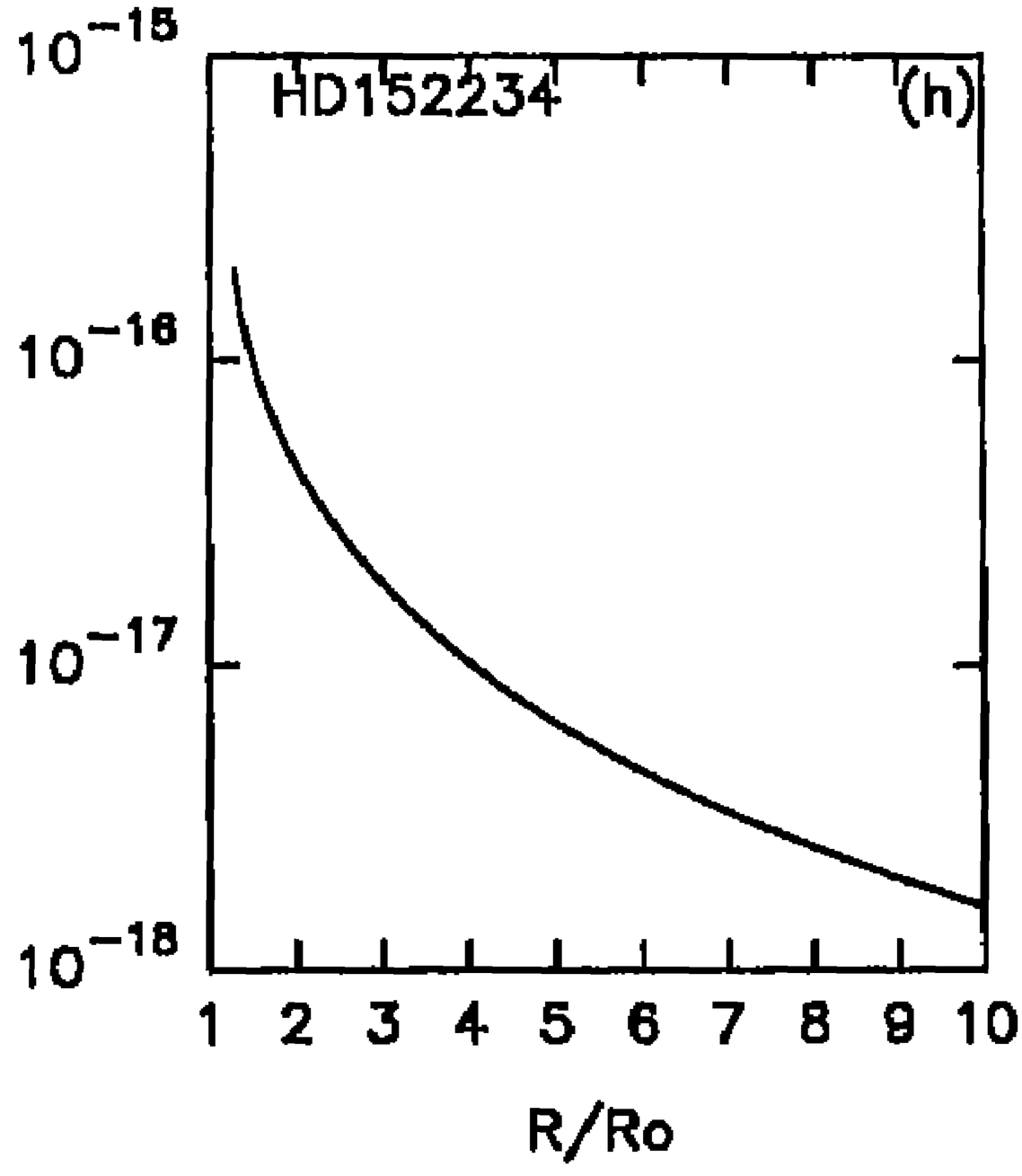

Figure 14 (e,f,g,h)

(f) The radiation force falls more rapidly than gravity force.

(g) We obtain v_∞ larger than 2650 km s^{-1} which is the expected value. $0.8 < \beta < 0.9$.

(h) density varies between few times 10^{-16} gr cm^{-3} to $\approx 10^{-18}$ gr cm^{-3}.

Figure 15

HD 152236 (ζ Sco) B1.5 Ia$^+$P. (Blomme 1990a)

T_{eff} = 18620 K

M =6.4 $\times$ 10^{34} gr

R =6.265 $\times$ 10^{12} cm

V_{esc} = 197 km s^{-1}

V_∞ = 1700 km s^{-1}

$\dot{M}$ =2.98 $\times$ $10^{-4} M_\odot$/yr.

(a), (b), (c), (d) are all similar to those in HD 152234.

(e) τ (Lyman) > τ (Balmer)

τ (Lyman) > τ (Paschen)

τ (Lyman) > τ (Brackett)

(f) Radiation force varies almost like $1/r^2$ at $R/R_0 = 10$.

(g) We obtain slightly larger than the expected $v_\infty \approx 1700$ km s^{-1}. $\beta \approx 0.9$.

(h) The density varies between 10^{-14} gr cm^{-3} and 10^{-17} gr cm^{-3}.

Figure 16

HD 152249, O9 Ib (Blomme 1990a)

(We have taken the first set of data)

T_{eff} = 32360 K

M =7.32 $\times$ 10^{34} gr

R =1.47 $\times$ 10^{12} cm

V_{esc} = 676 km s^{-1}

V_∞ = 2600 km s^{-1}

$\dot{M}$ =4.02 $\times$ $10^{-5} M_\odot$/yr.

(a), (b), (c), (d) are similar to those of HD 152236.

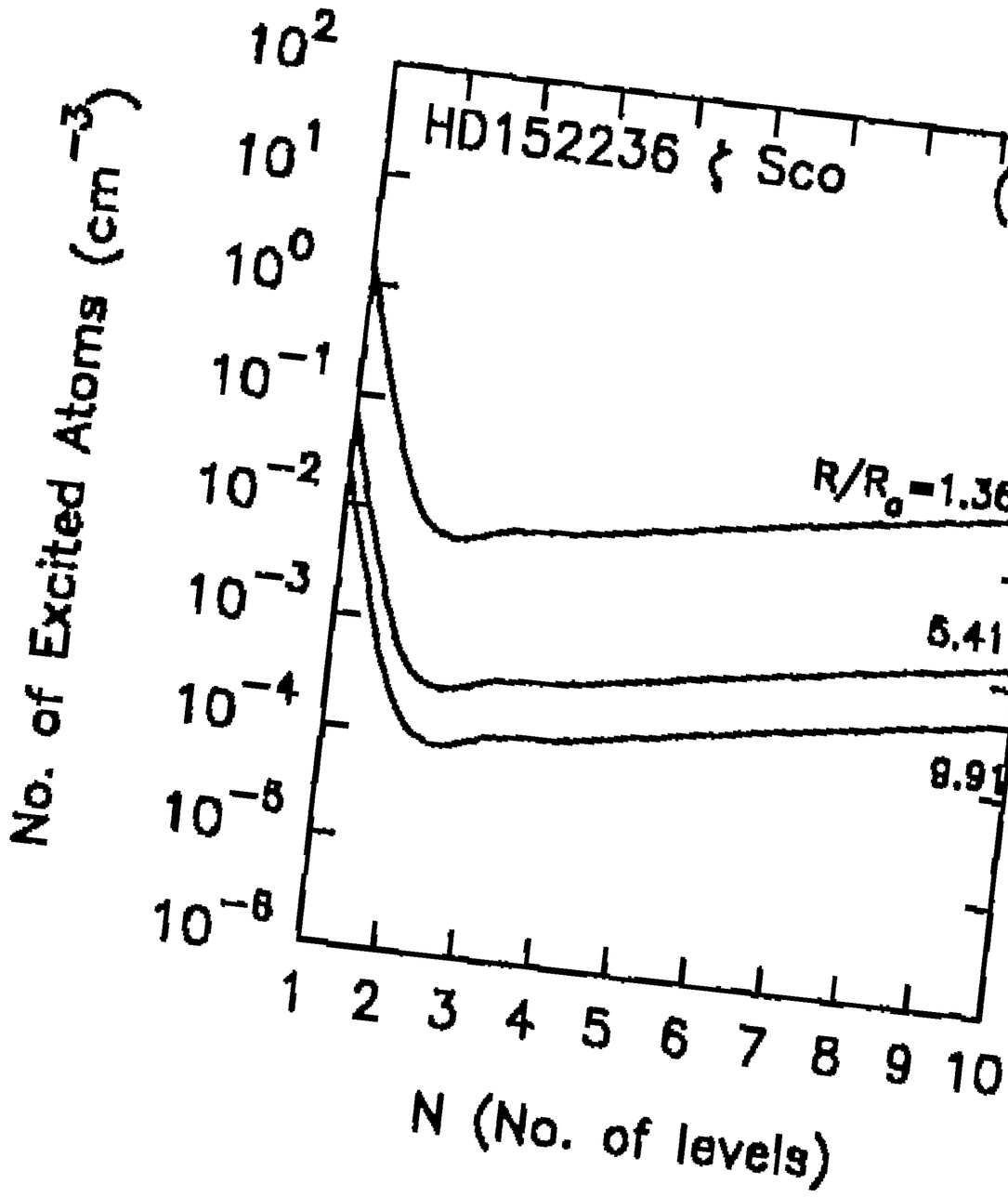

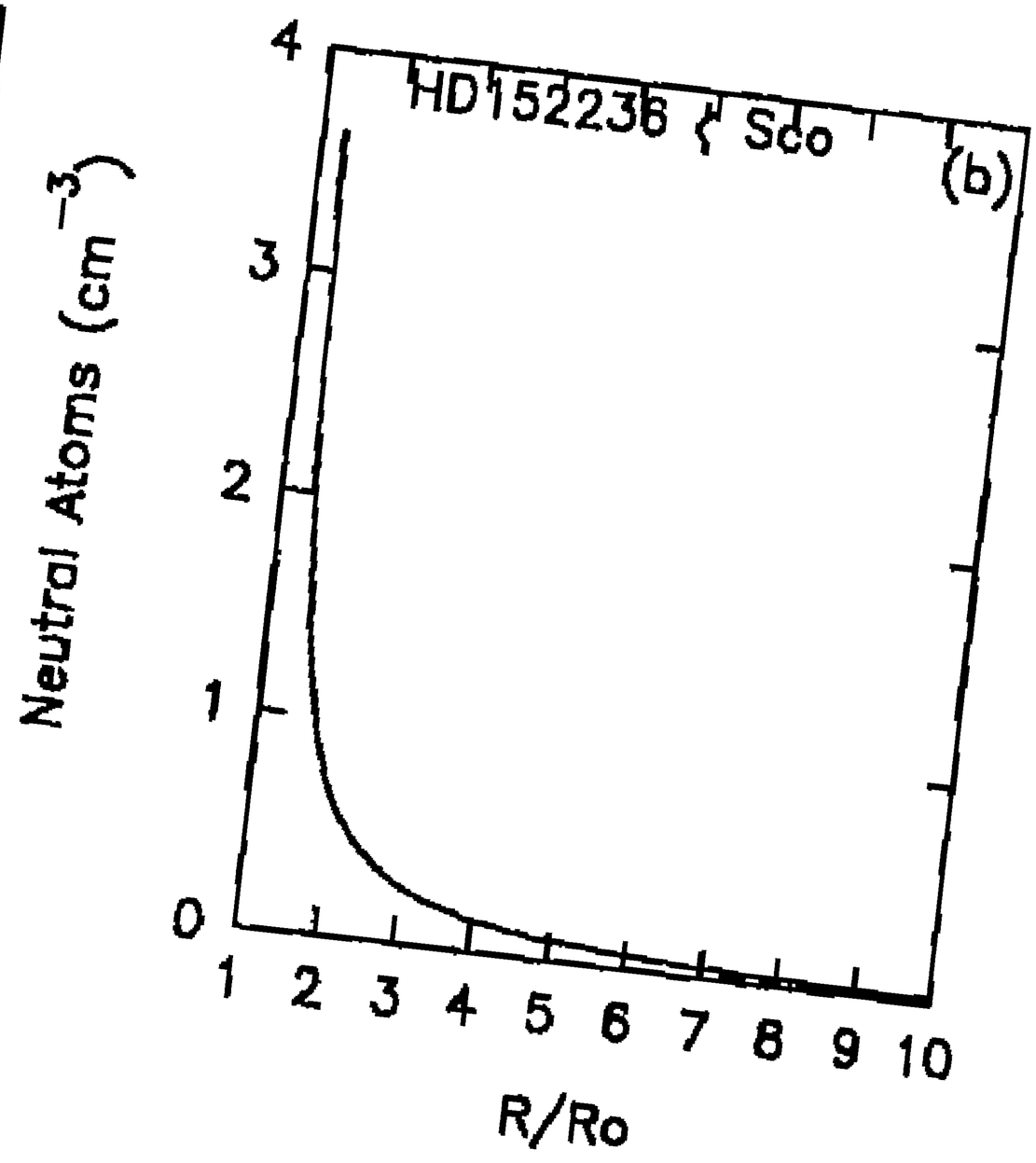

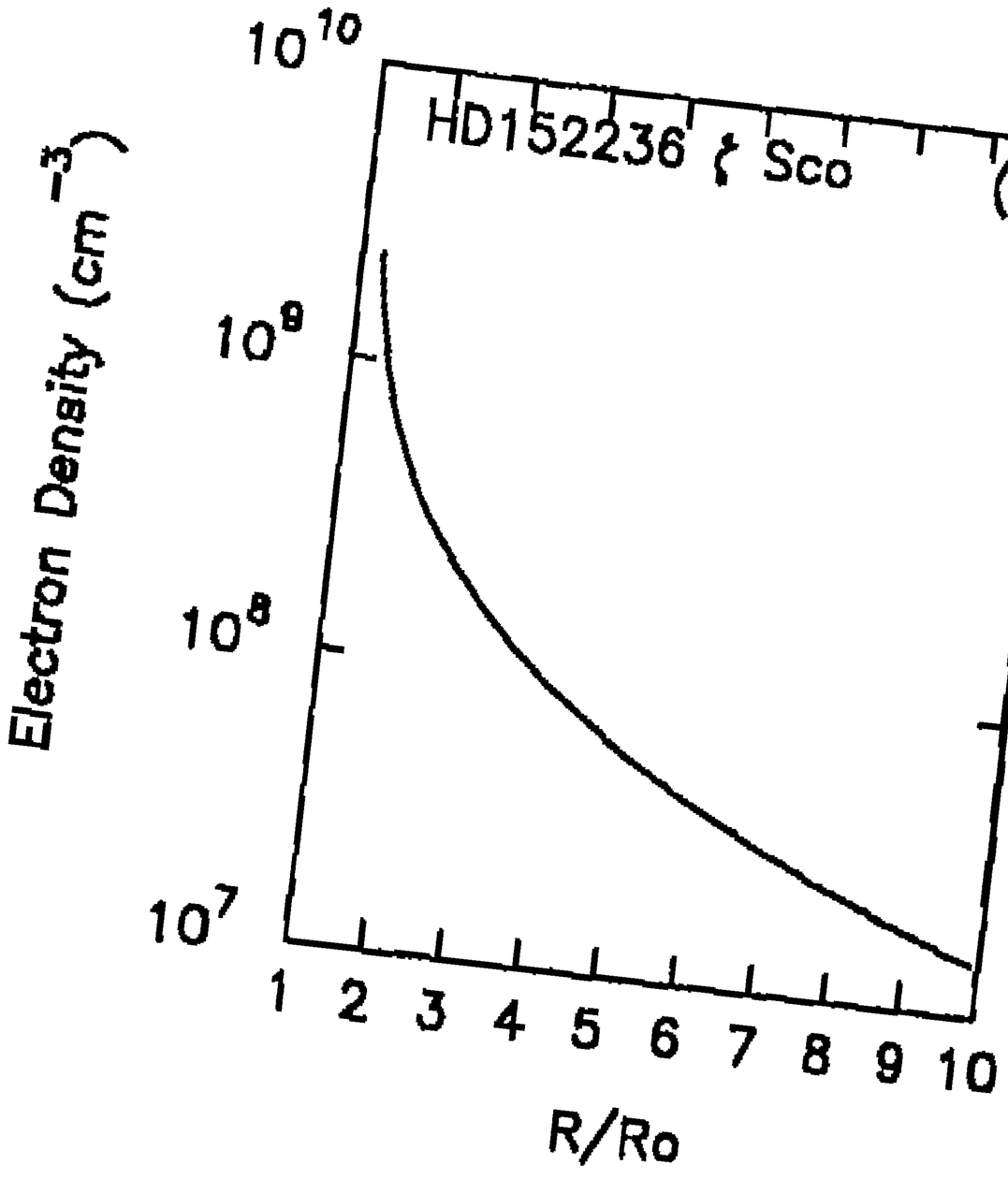

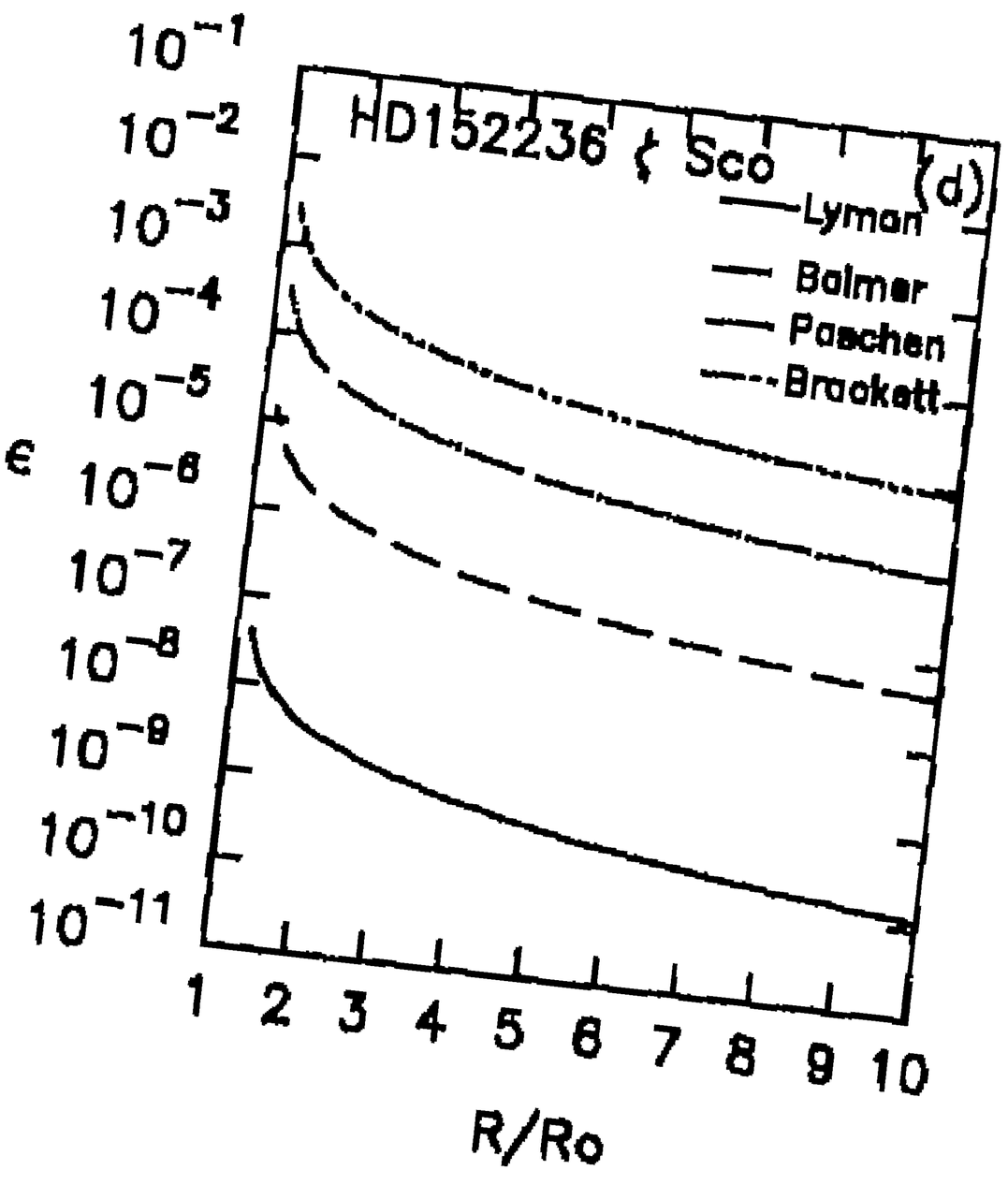

Figure 15 (a,b,c,d)

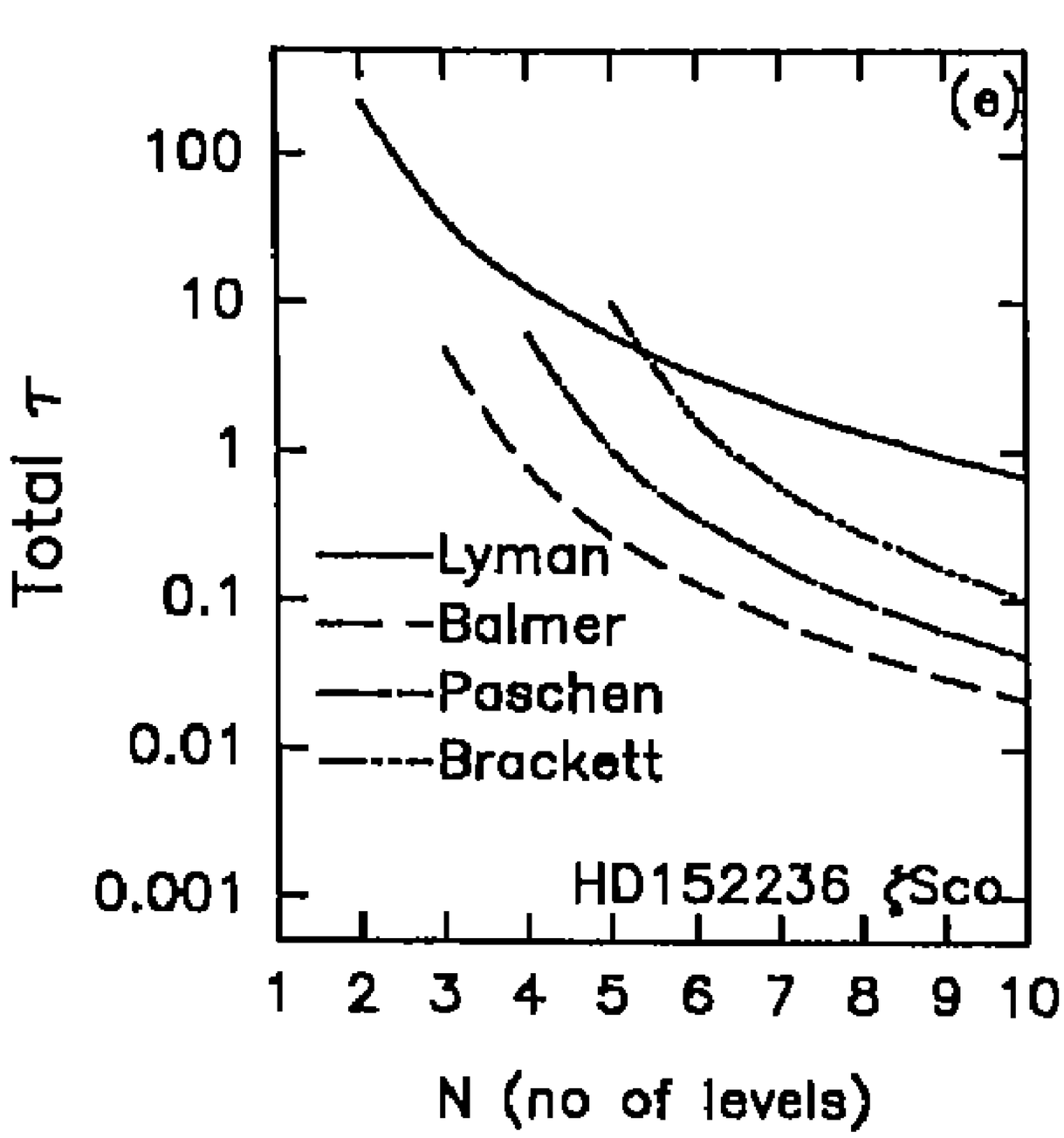

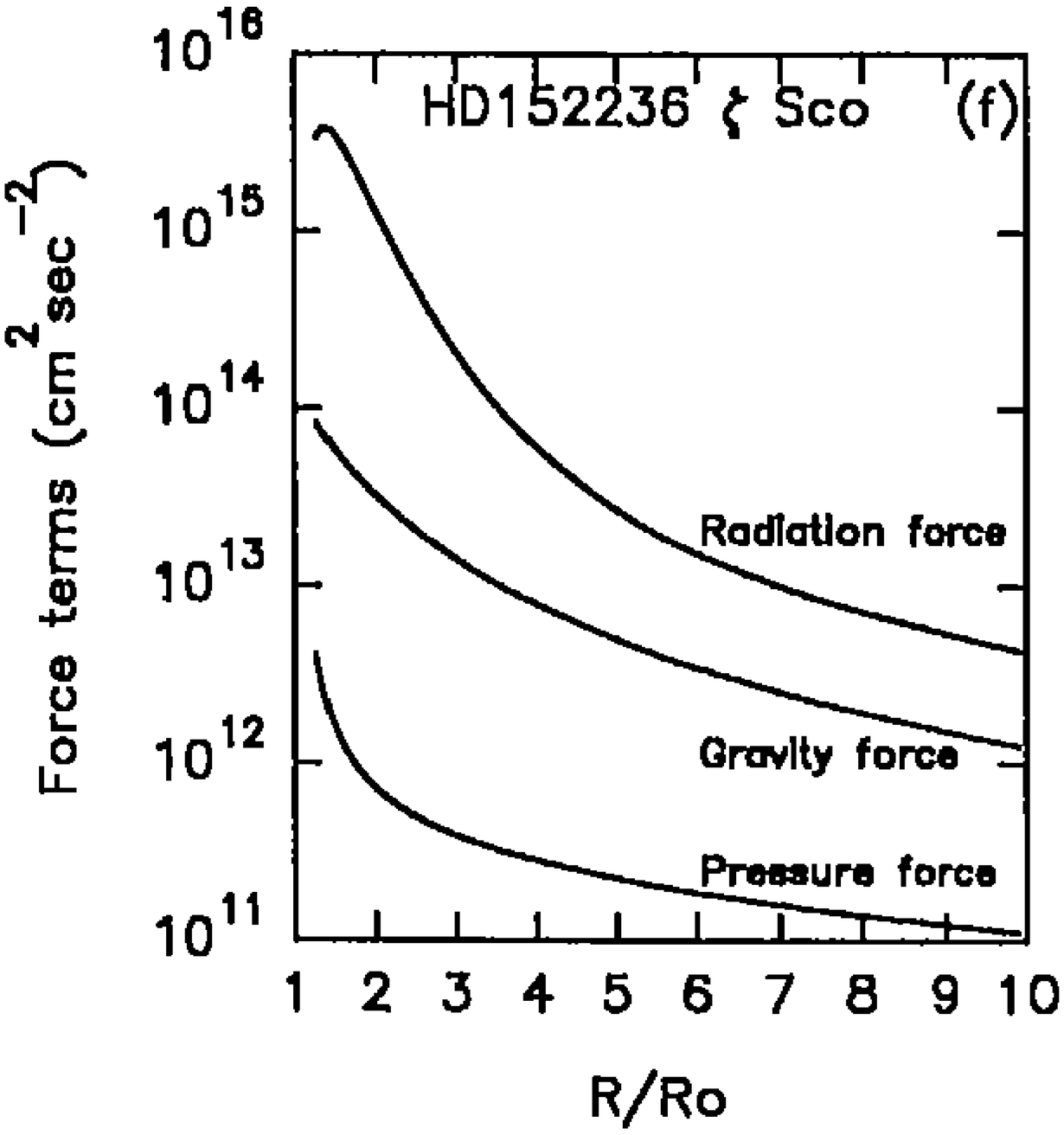

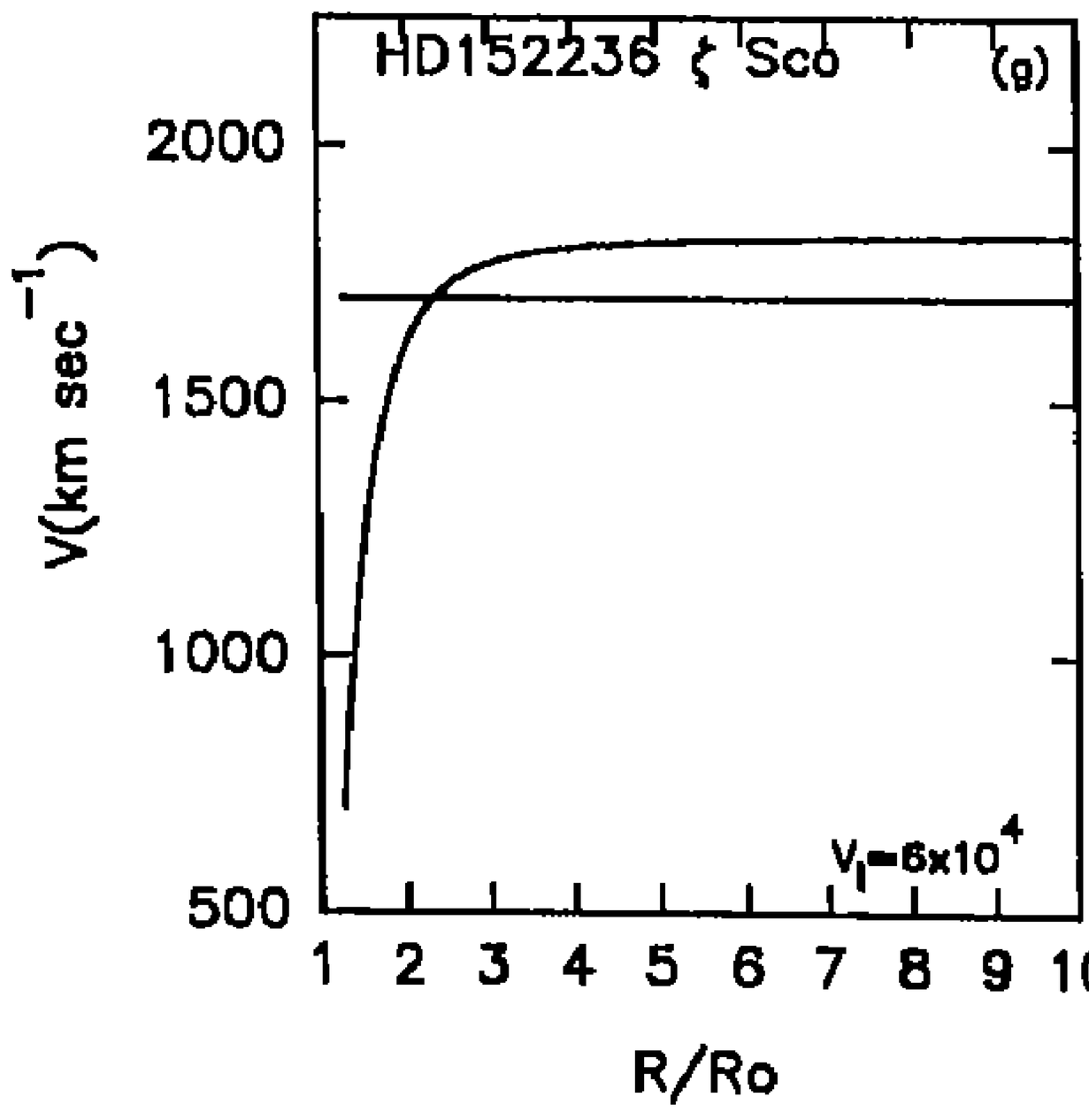

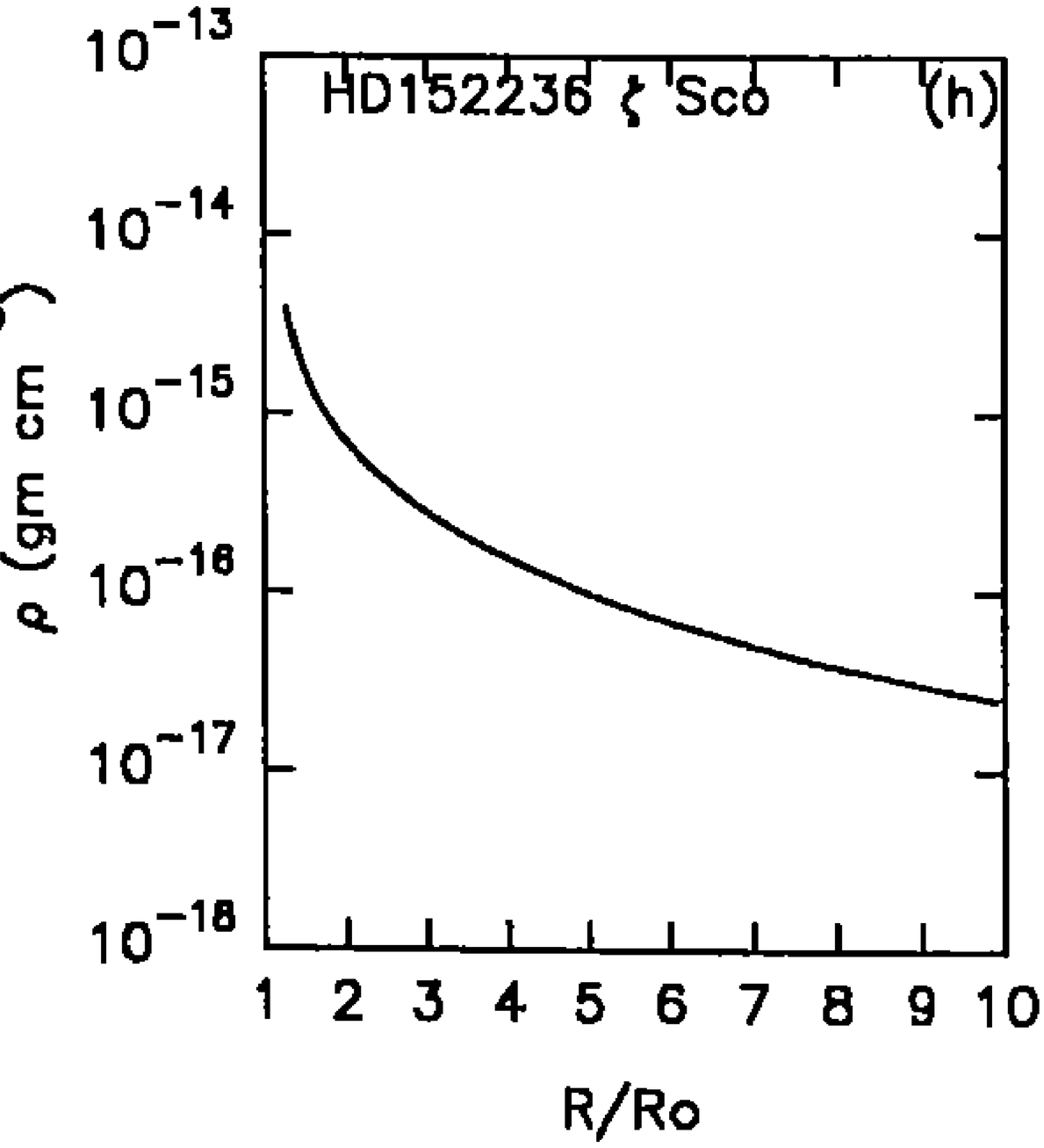

Figure 15 (e,f,g,h)

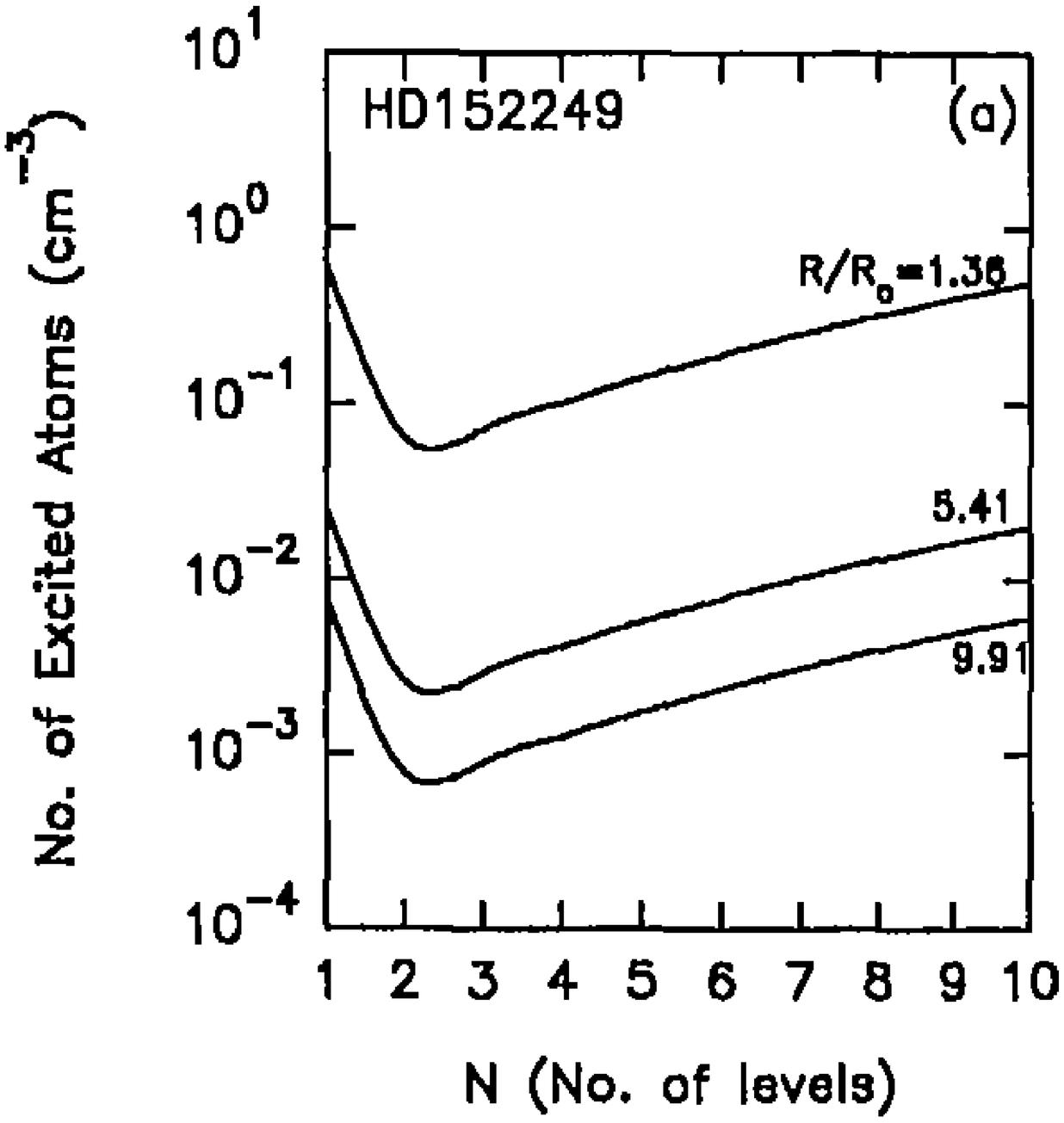

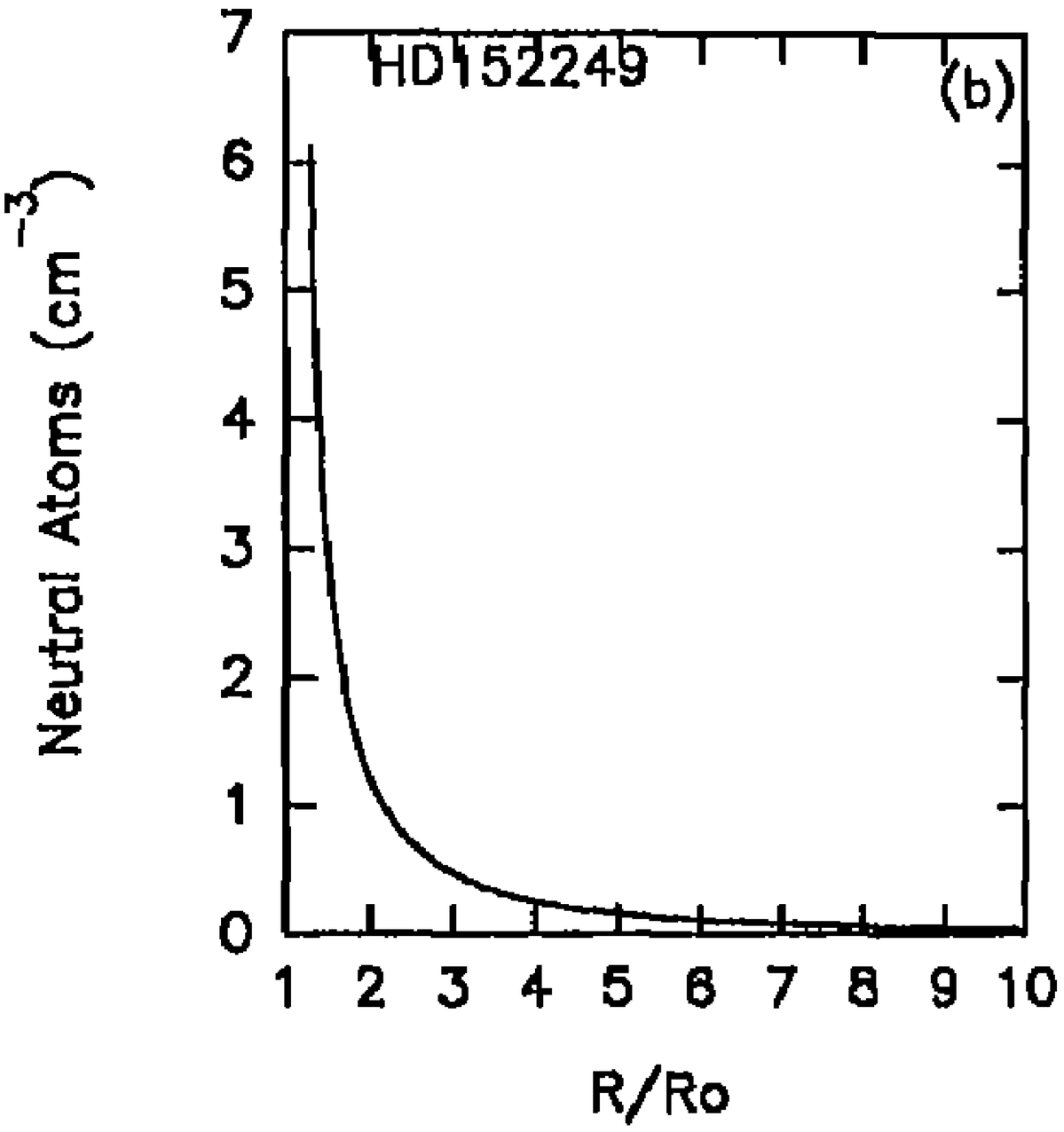

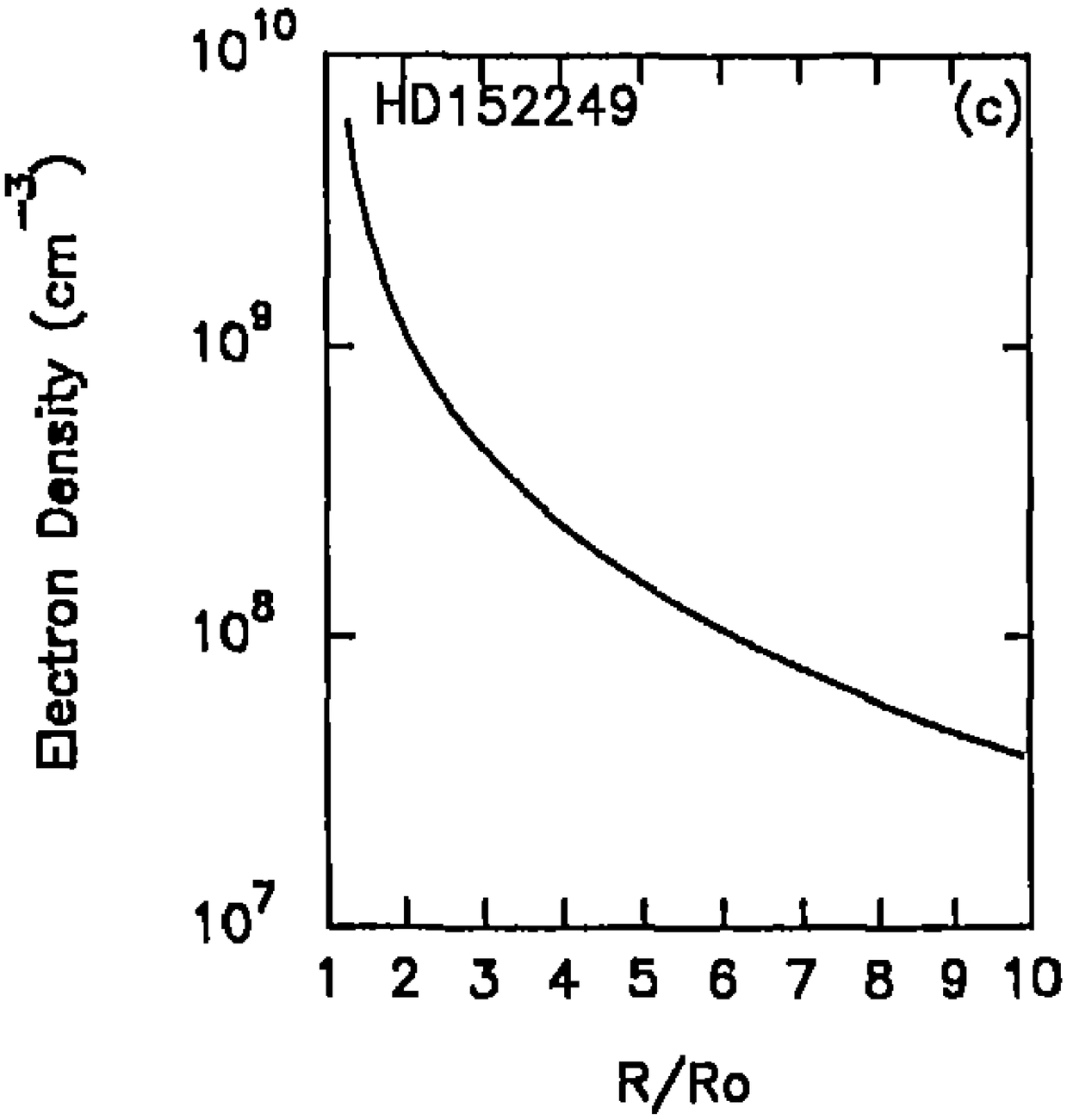

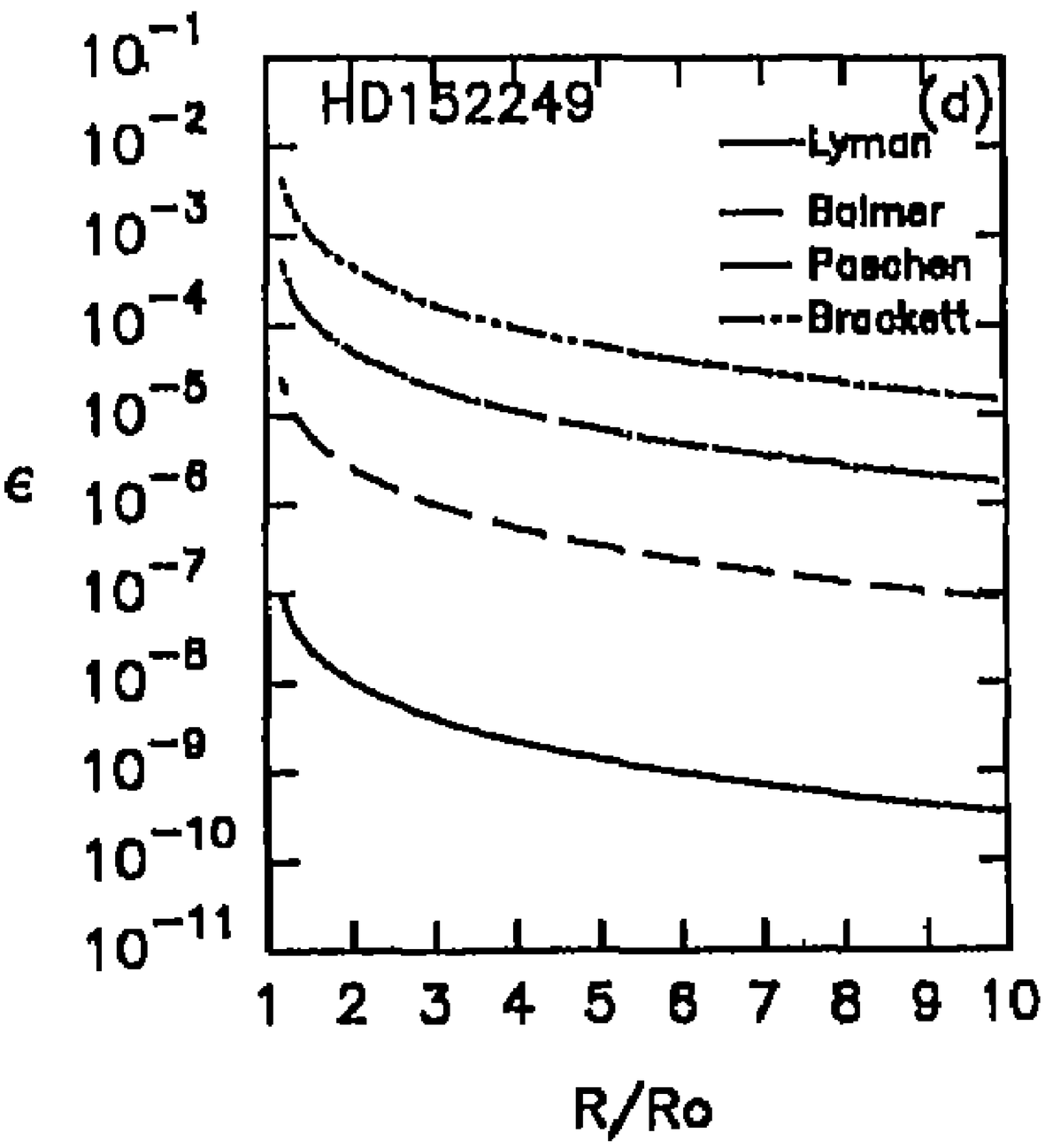

Figure 16 (a,b,c,d)

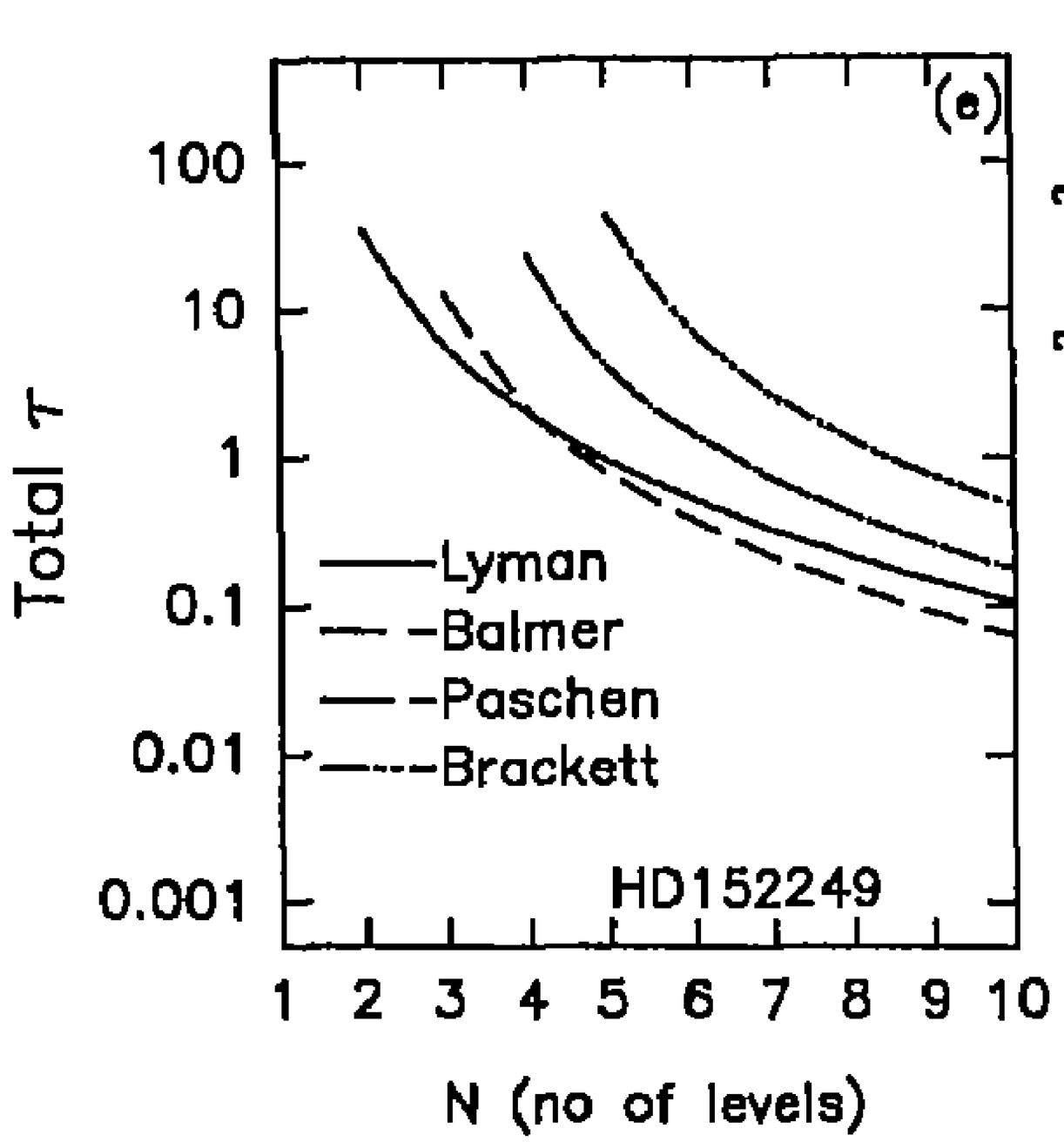

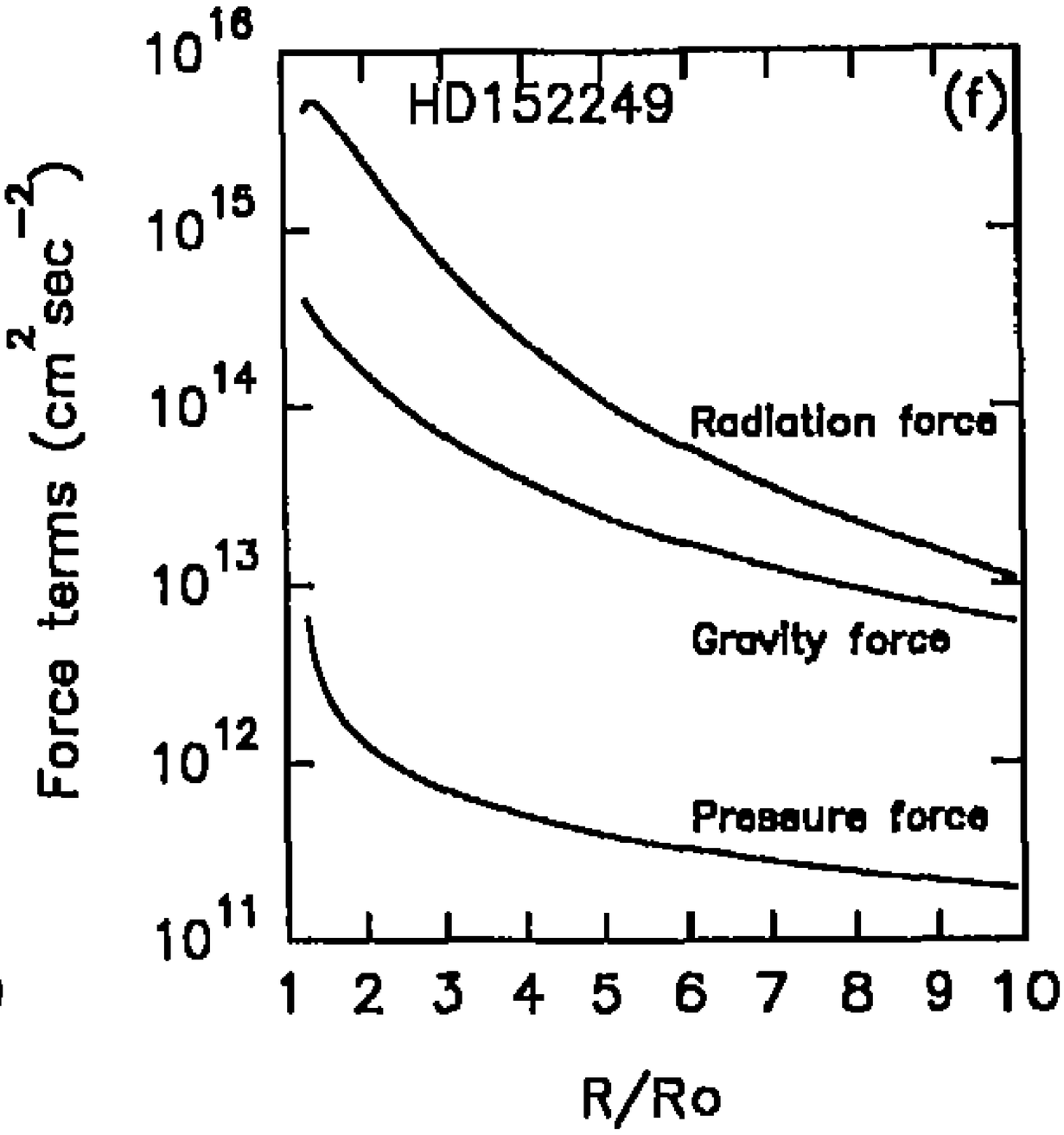

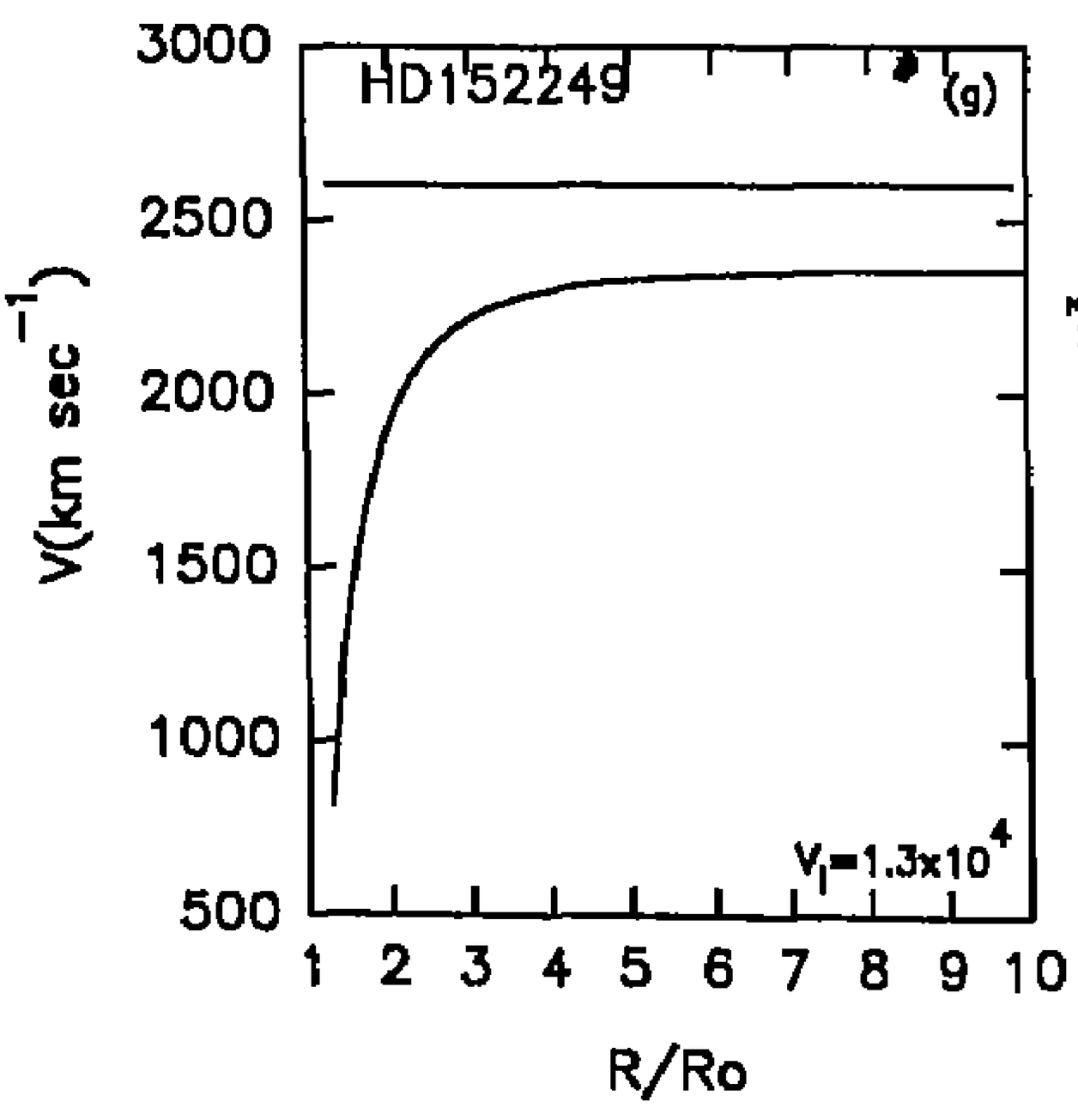

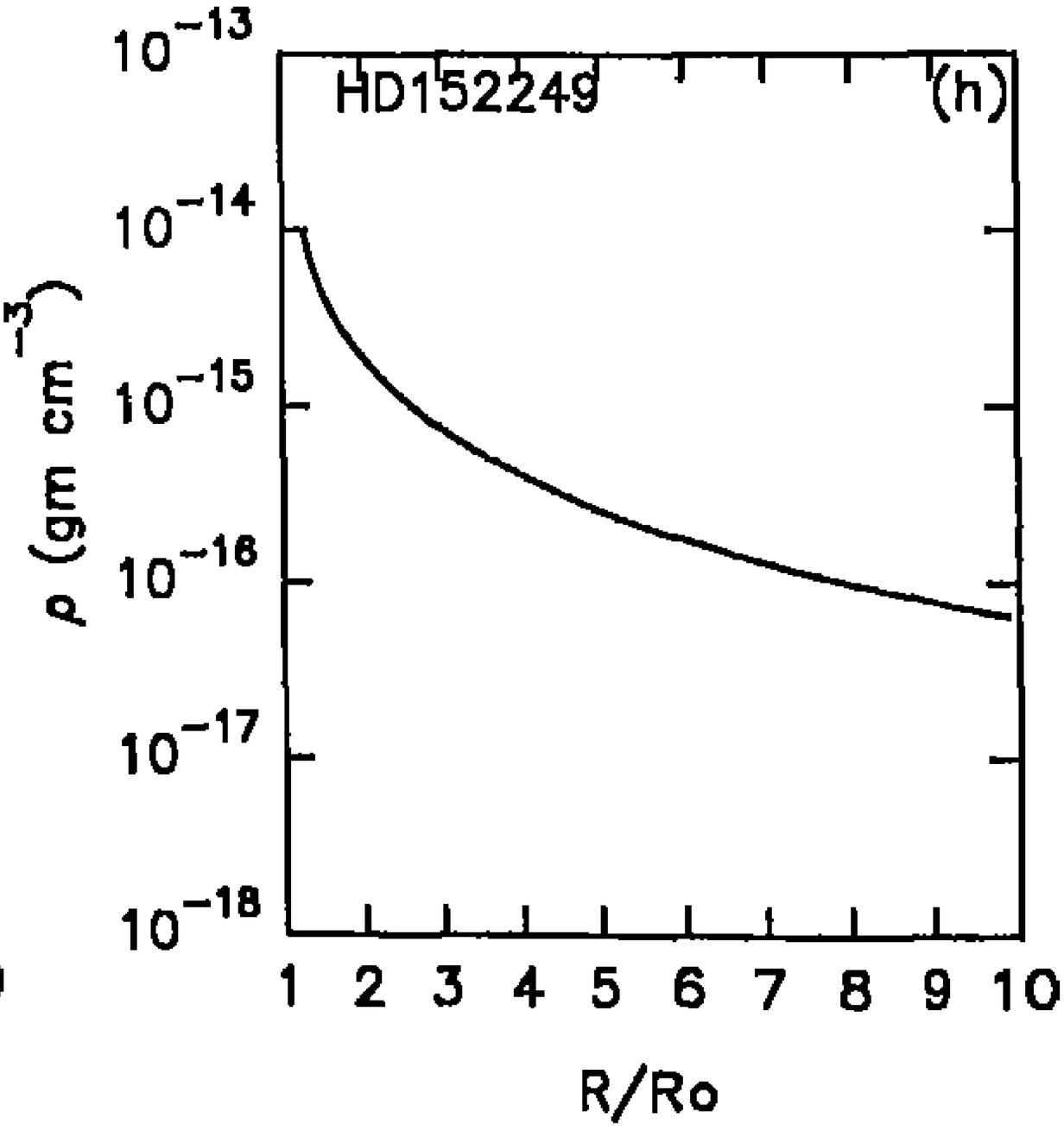

Figure 16 (e,f,g,h)

(e) τ (Lyman α) > τ (Balmer α)

τ (Lyman α) > τ (Paschen α)

τ (Lyman α) $\approx$ τ (Brackett α)

τ (Brackett 6) > τ (Lyman 9)

τ (Brackett 6) > τ (Paschen 7)

τ (Brackett 6) > τ (Balmer 8)

(f) Radiation force and gravity force tend to meet at $R/R_0 >> 10$.

(g) The v_∞ (computed) < v_∞ (observed) with $v_t = 1.3 \times 10^4$ cm s^{-1}.

(h) 10^{-17} gr cm $^{-3} < \rho < 10^{-14}$ gr cm^{-3}.

Figure 17

HD 157857, O7(f) (Blomme 1990a)

$T_{eff} = 36308$ K

M =4.42 $\times$ 10^{34} gr

R =9.17 $\times$ 10^{11} cm

$V_{mic} = 661$ km s^{-1}

$V_\infty = 3250$ km s ^{1}

$\dot{M}$ =4.95 $\times$ $10^{-6} M_\odot$/yr.

(a), (b), (c), (d) are similar to those of the earlier systems.

(e) τ (Lyman α) < τ (Brackett α)

τ (Lyman α) > (Balmer α)

τ (Lyman α) > (Paschen α)

τ (Lyman 9) $\approx$ τ (Balmer 8)

τ (Lyman 9) < τ (Paschen 7)

τ (Lyman 9) < τ (Brackett 6)

(f) Radiation force falls more rapidly and may equal the gravity force at $R/R_0 > 10$.

(g) v_∞ (calculated) $\approx$ v_∞ (observed or expected) $\approx$ 3250 km s^{-1}. 0.8 < β 0.9.

(h) 10^{-16} gr cm$^{-3} < \rho < 10^{-13}$ gr cm $^{-3}$.

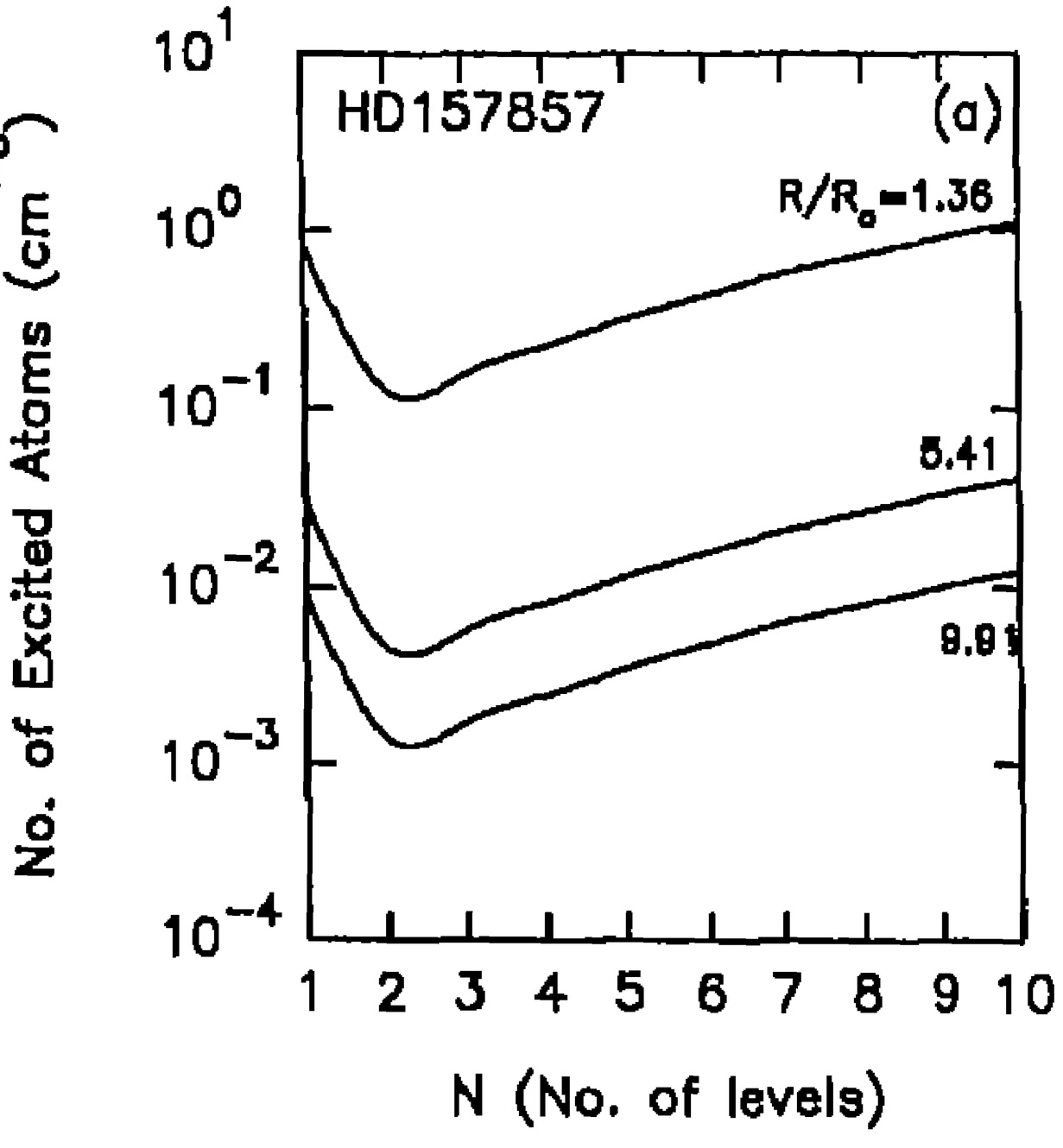

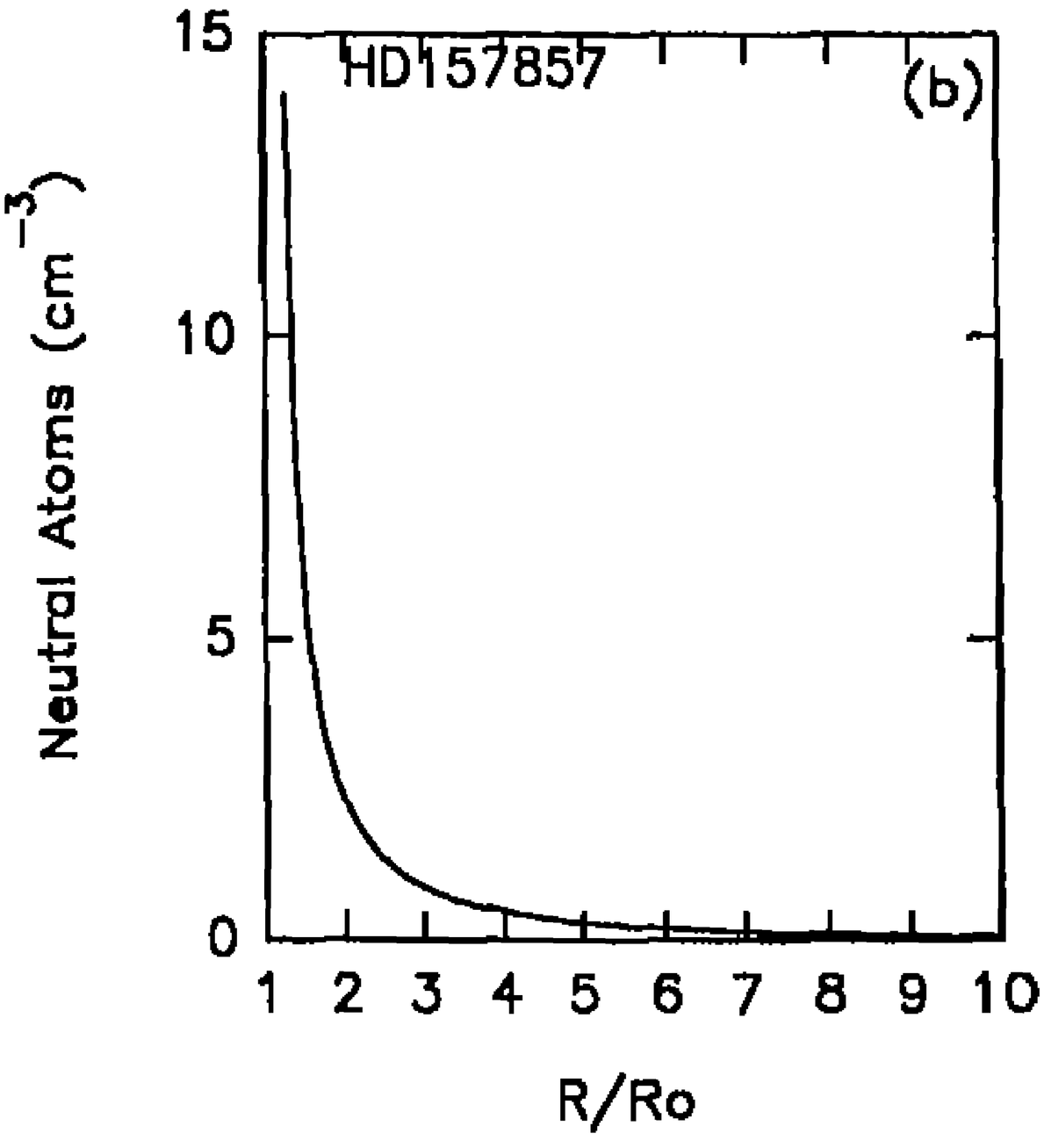

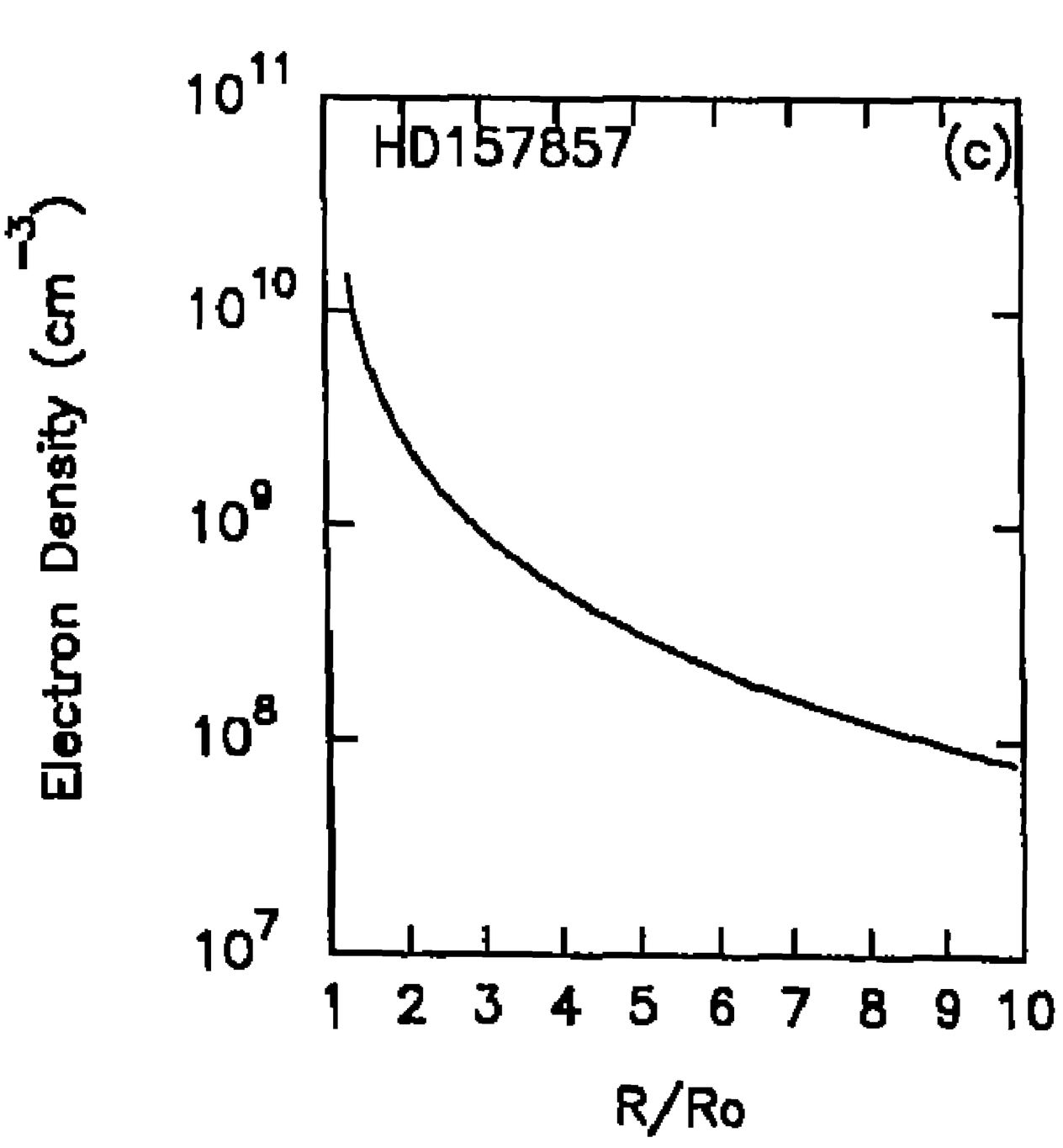

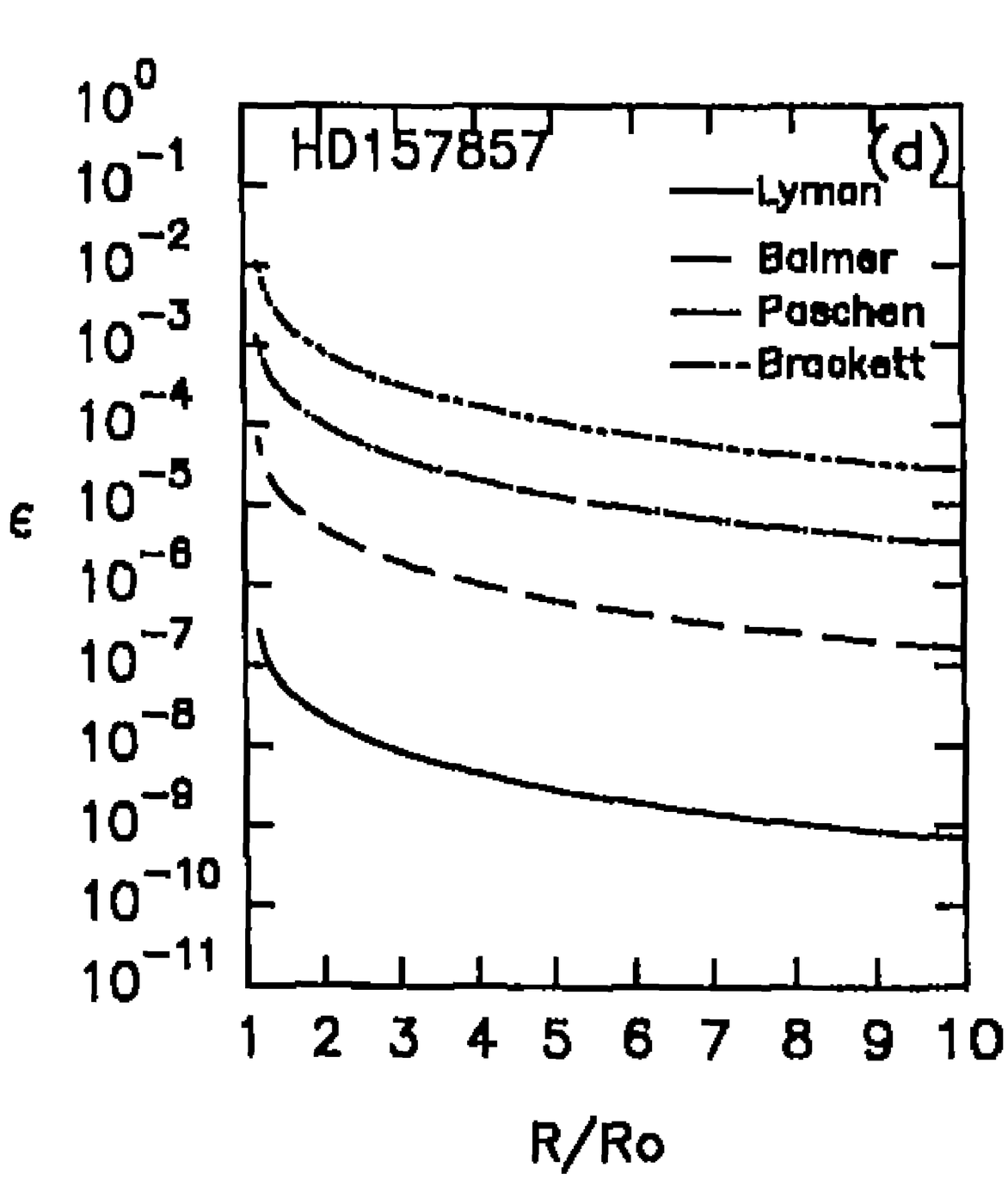

Figure 17 (a,b,c,d)

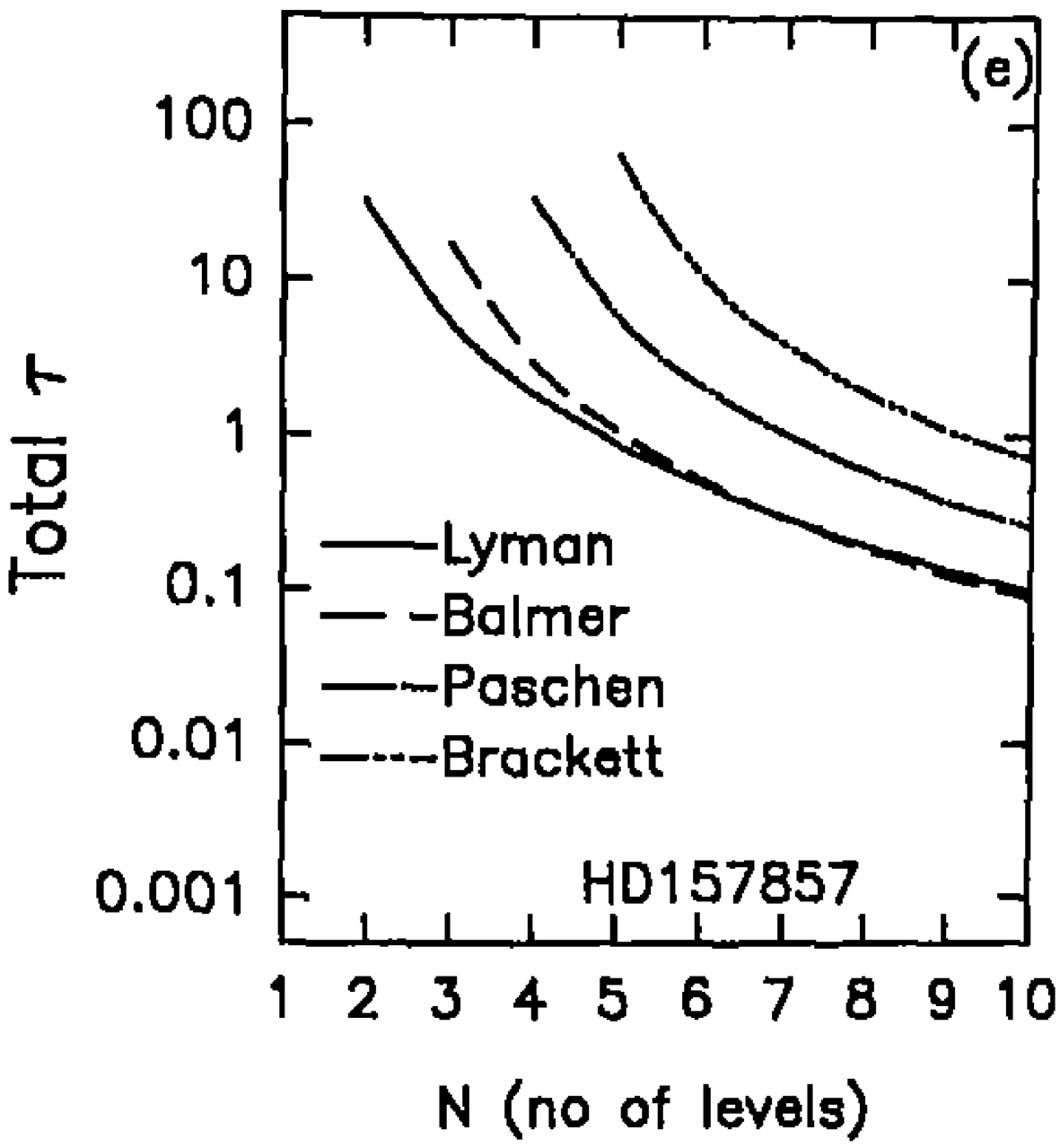

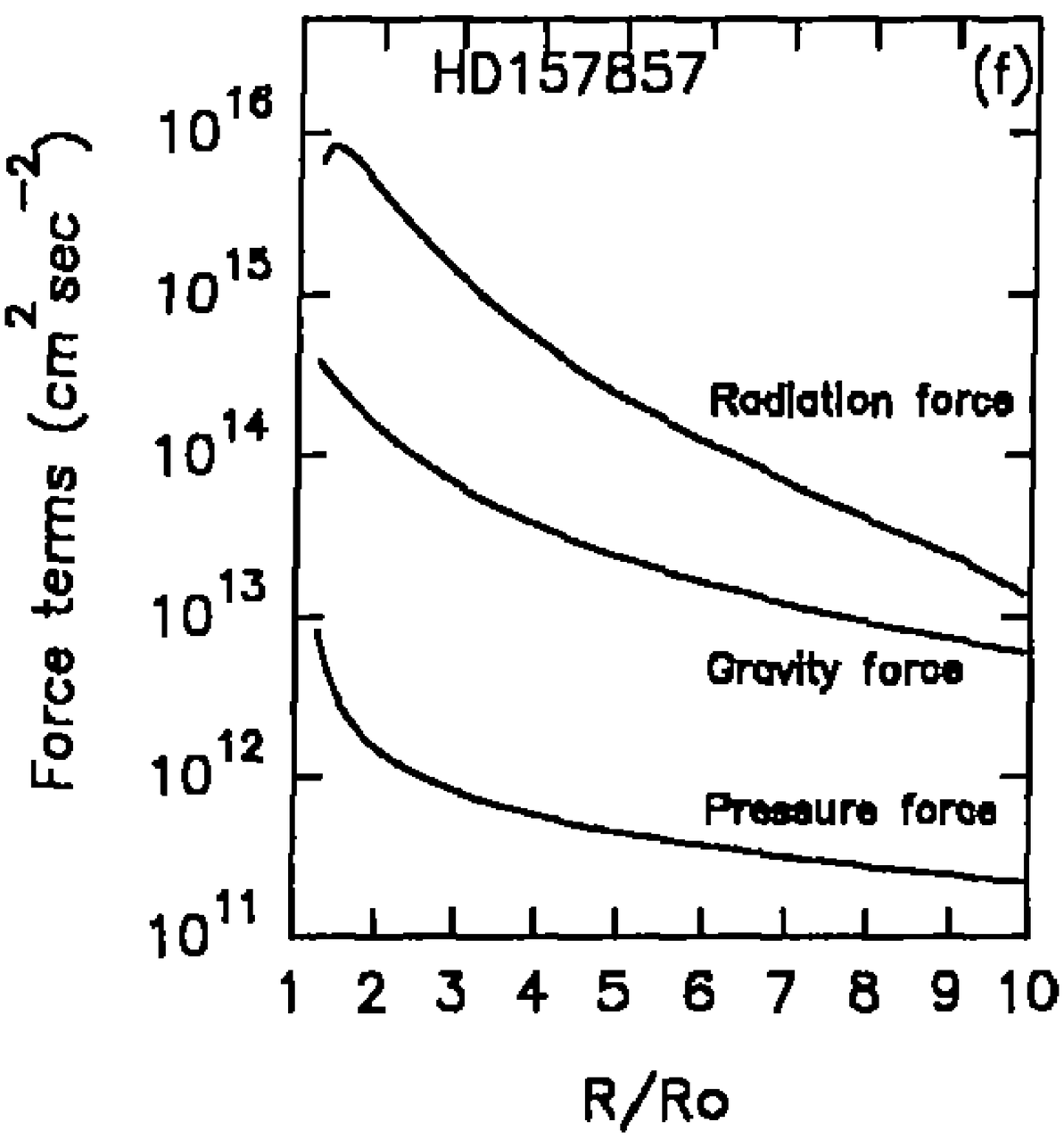

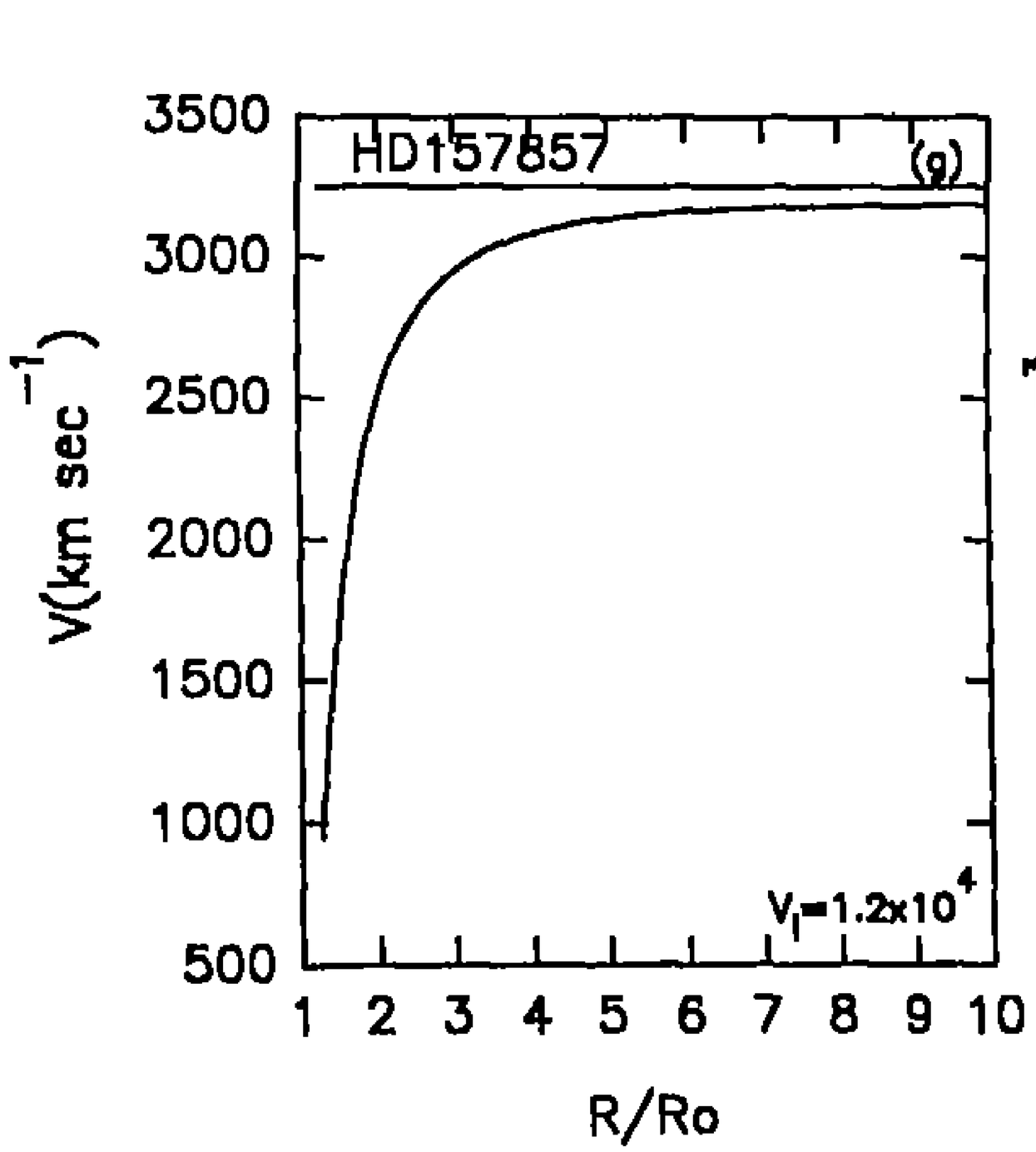

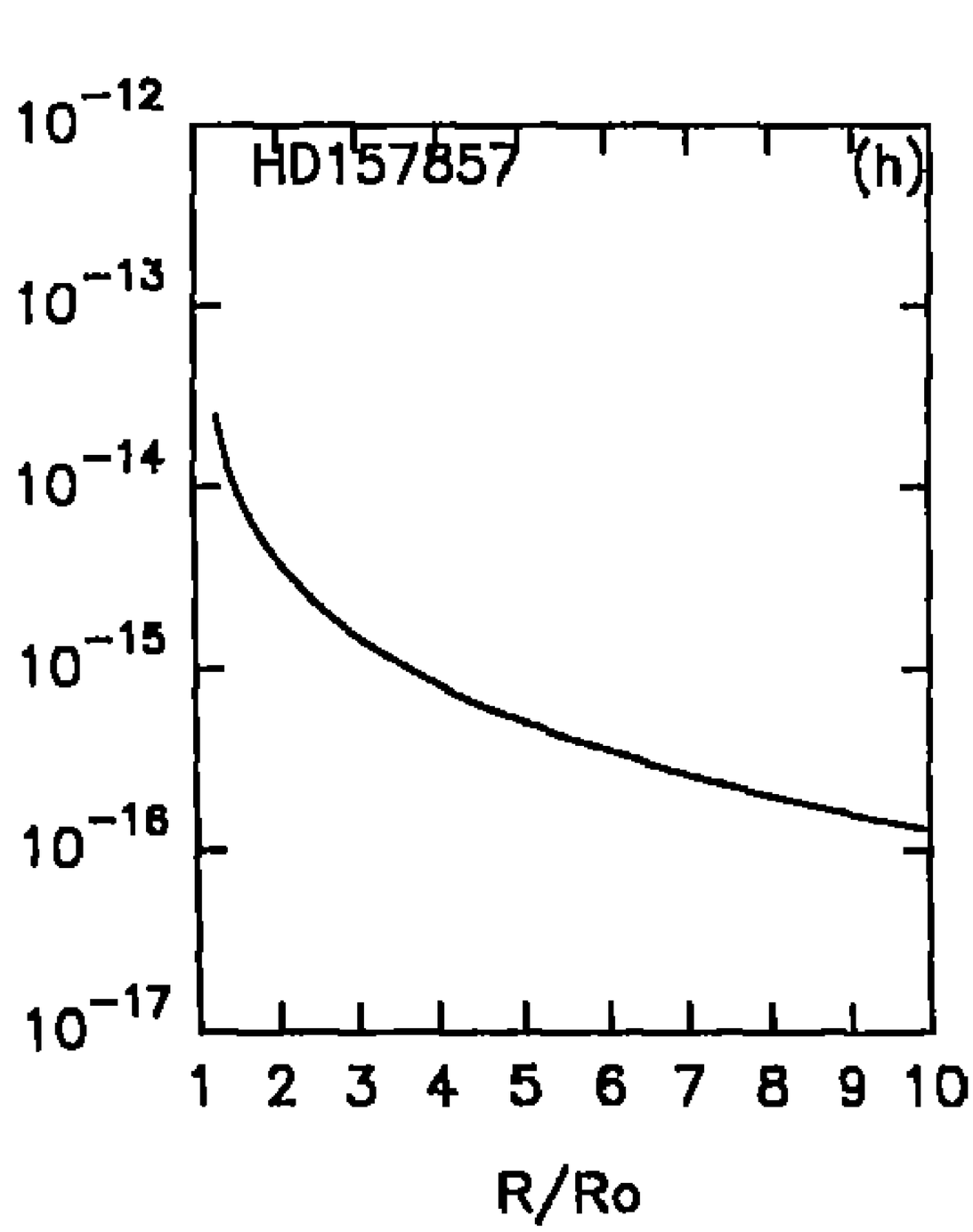

Figure 17 (e,f,g,h)

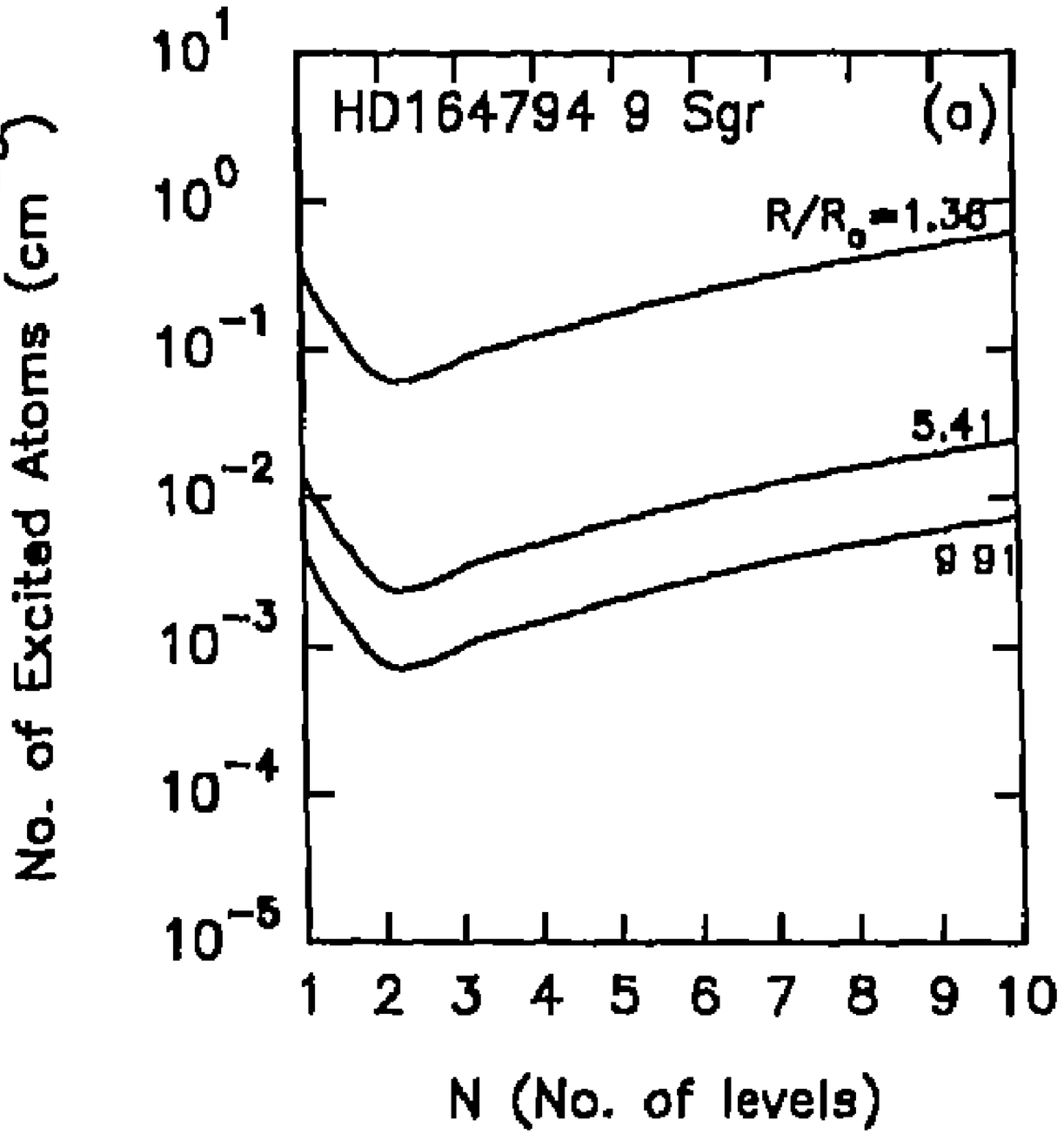

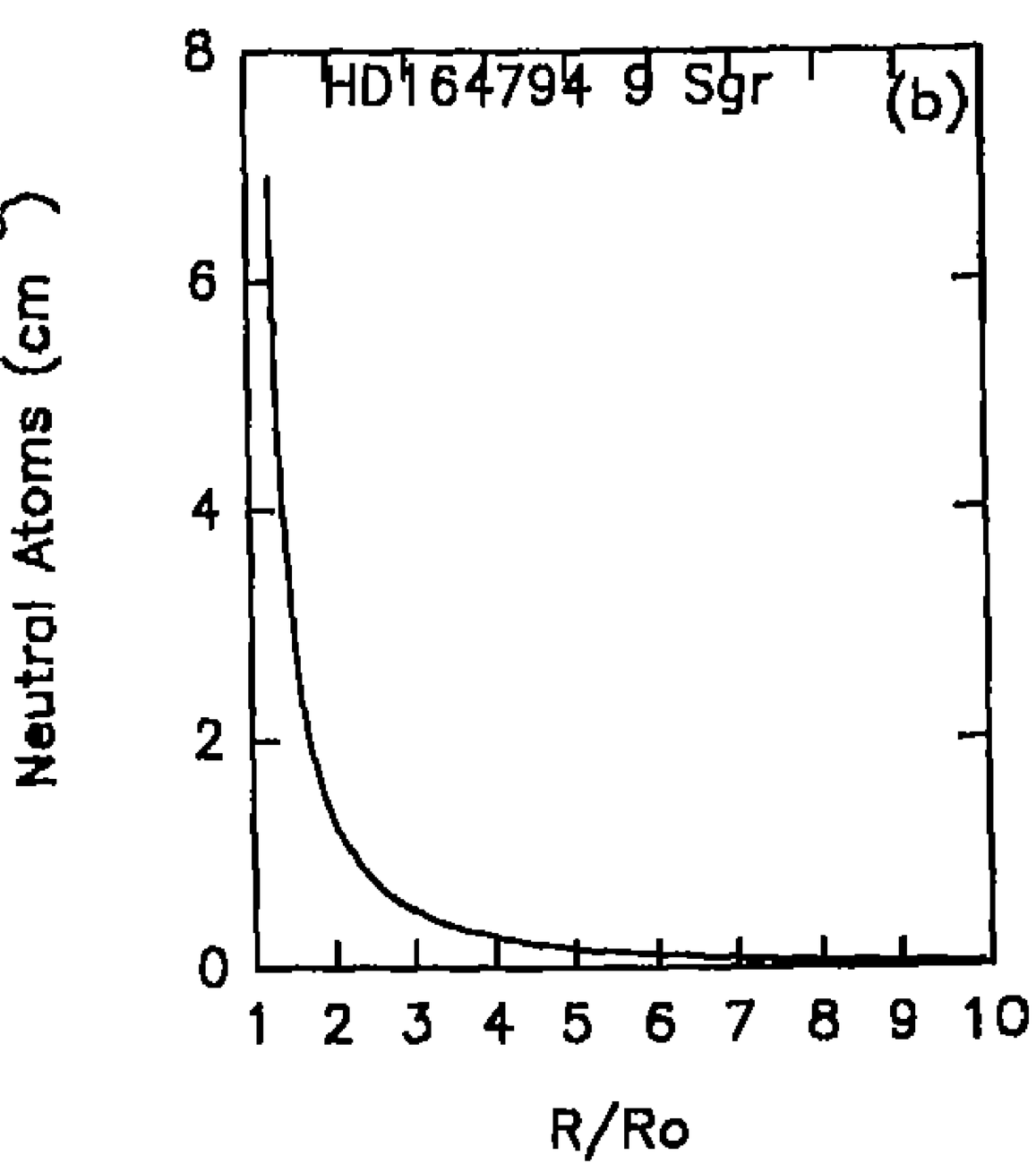

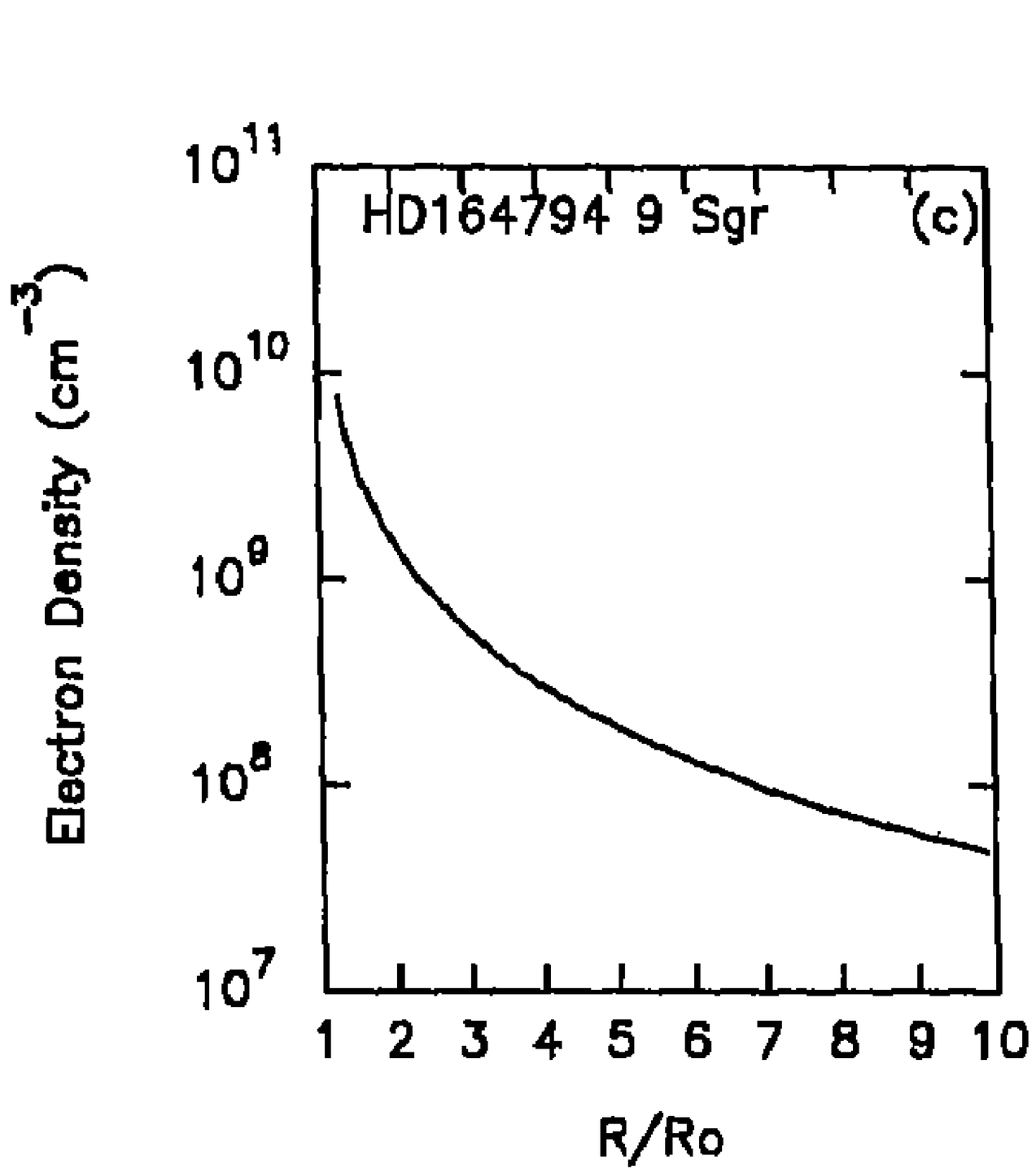

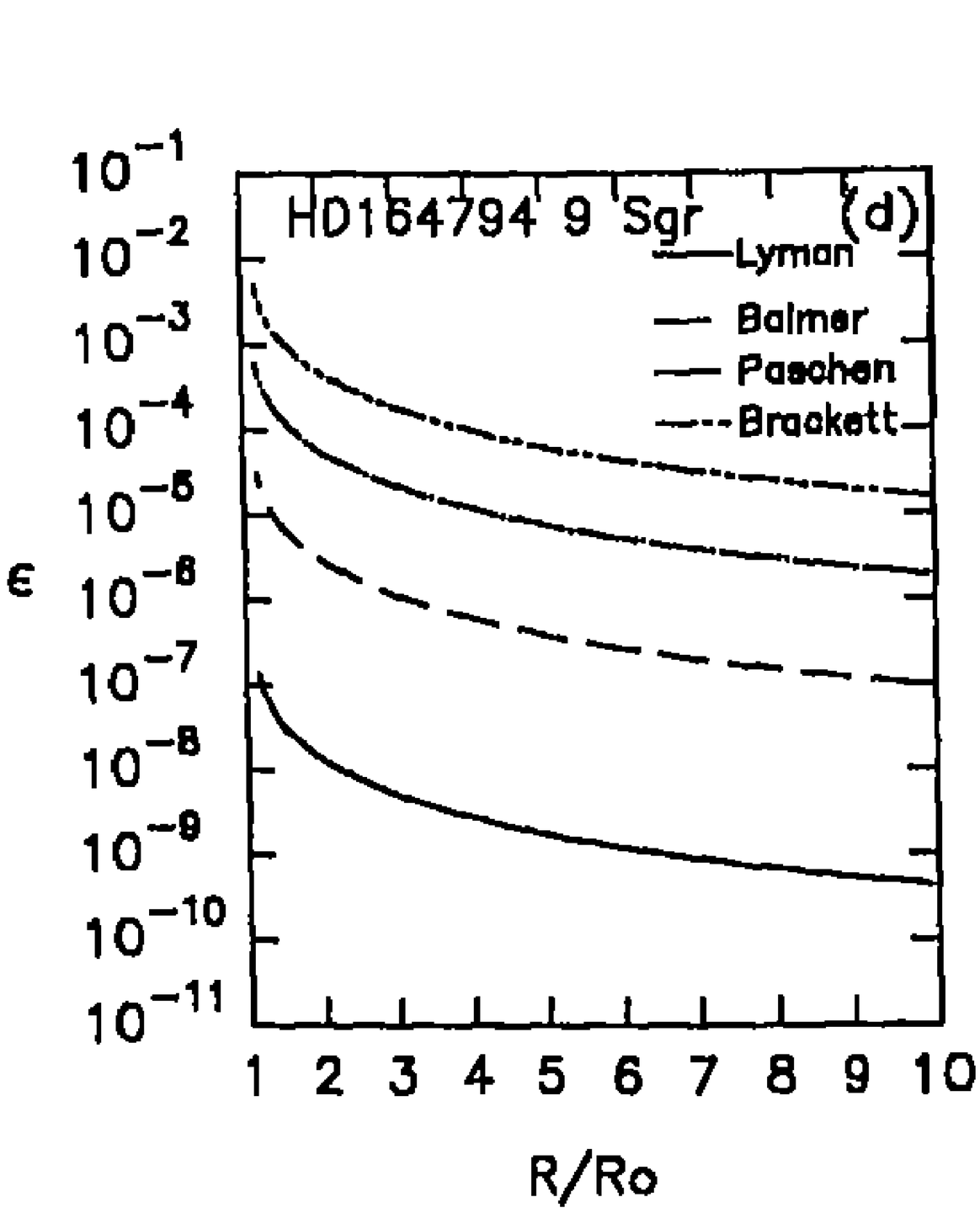

Figure 18 (a,b,c,d)

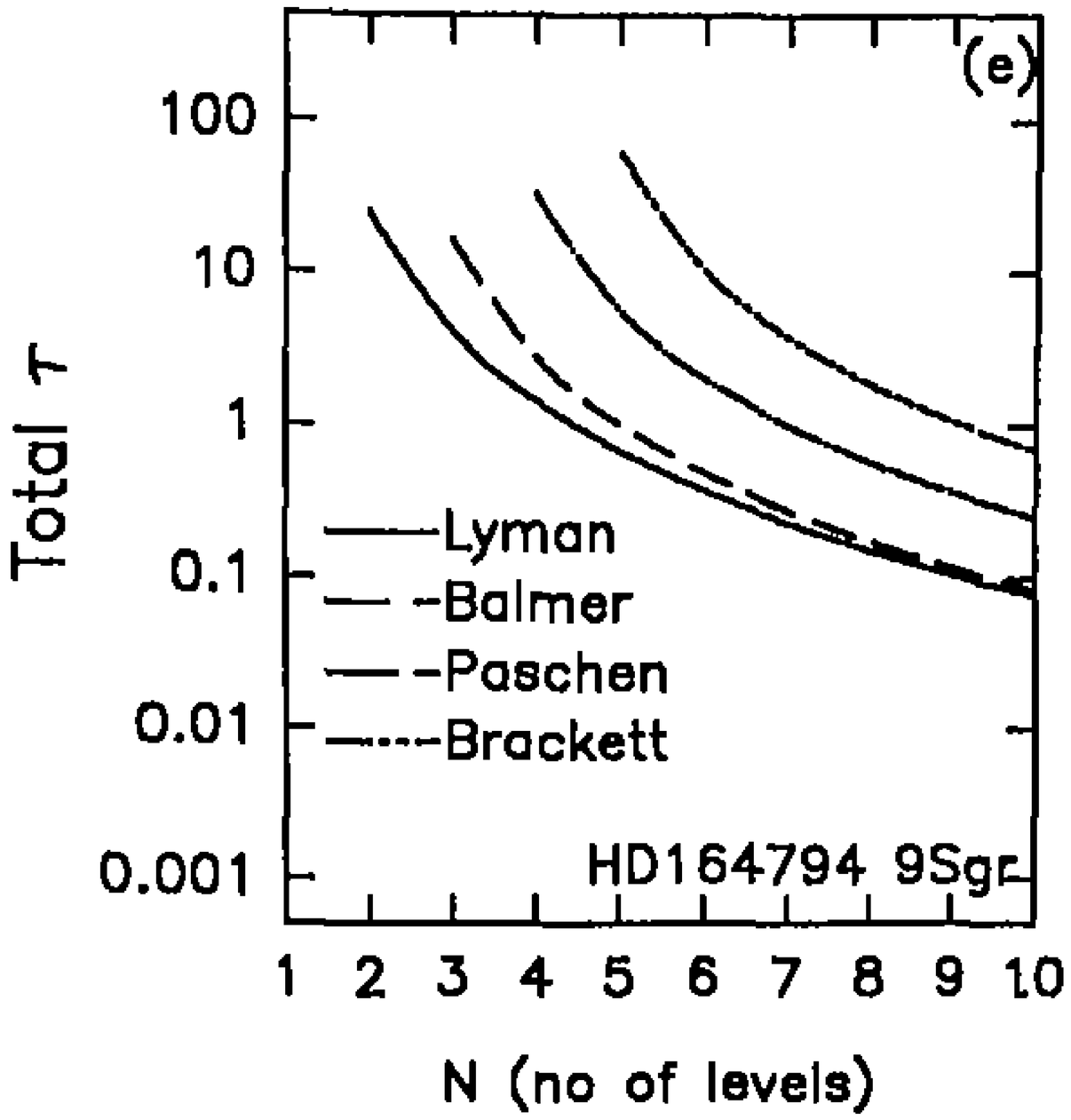

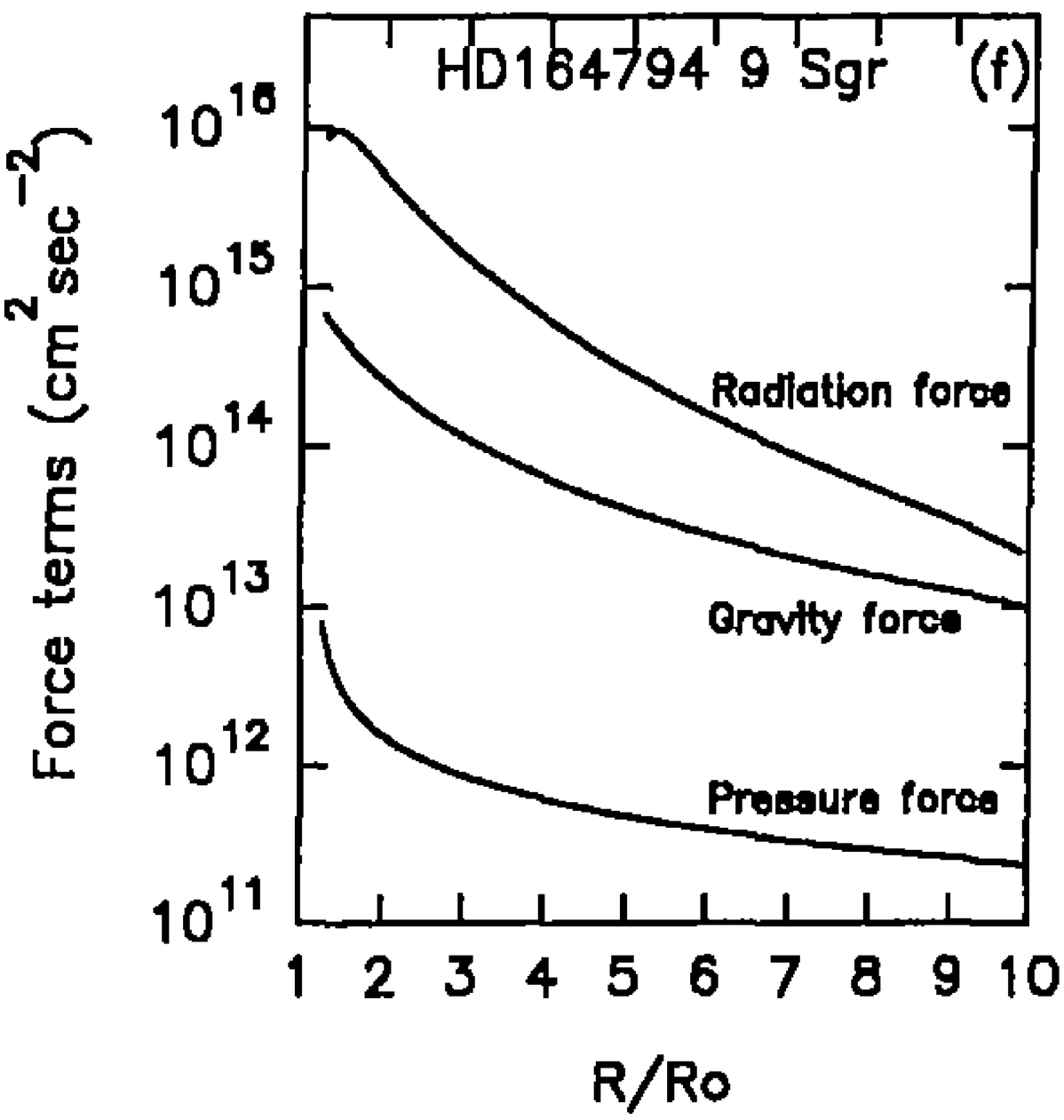

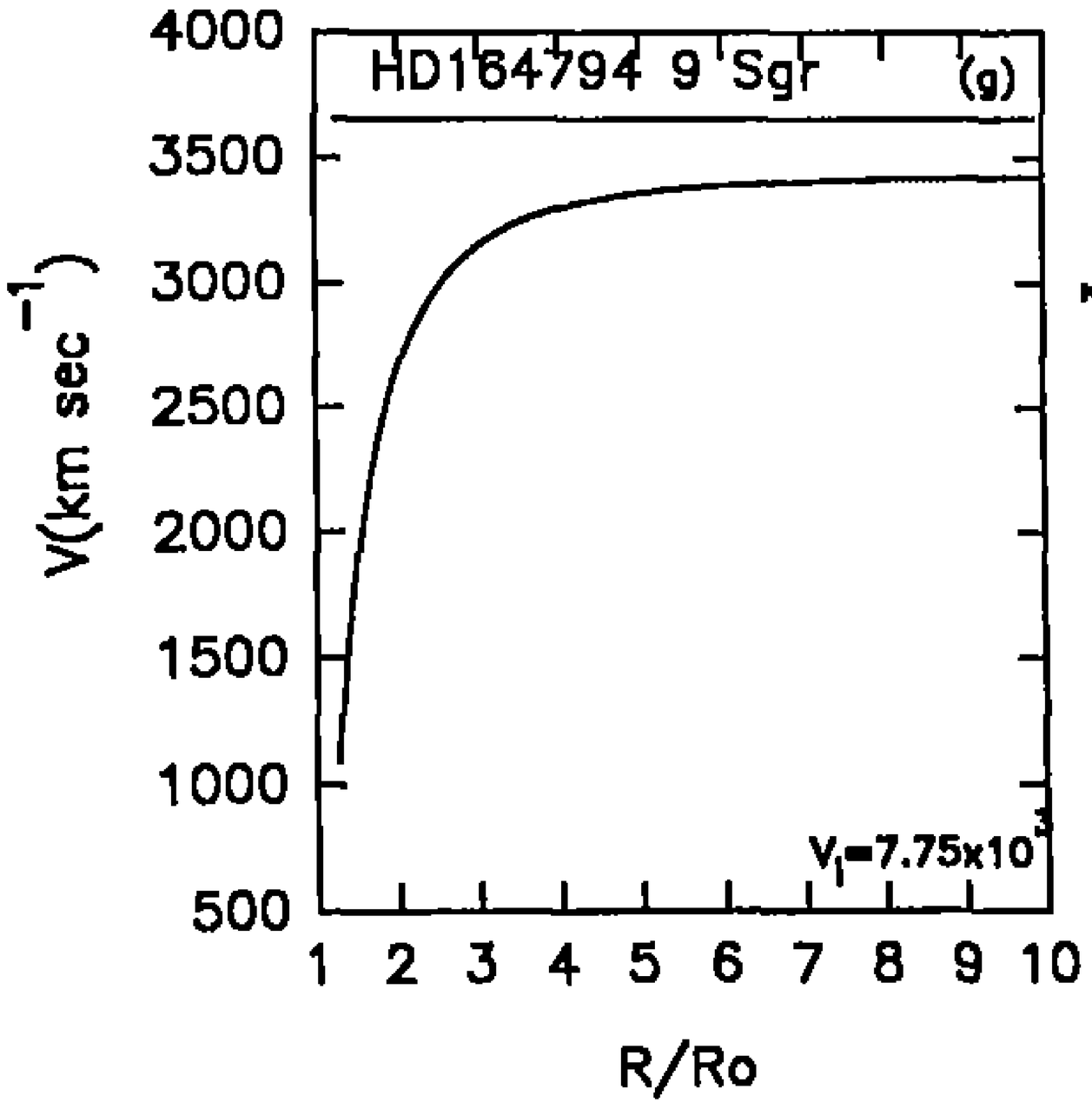

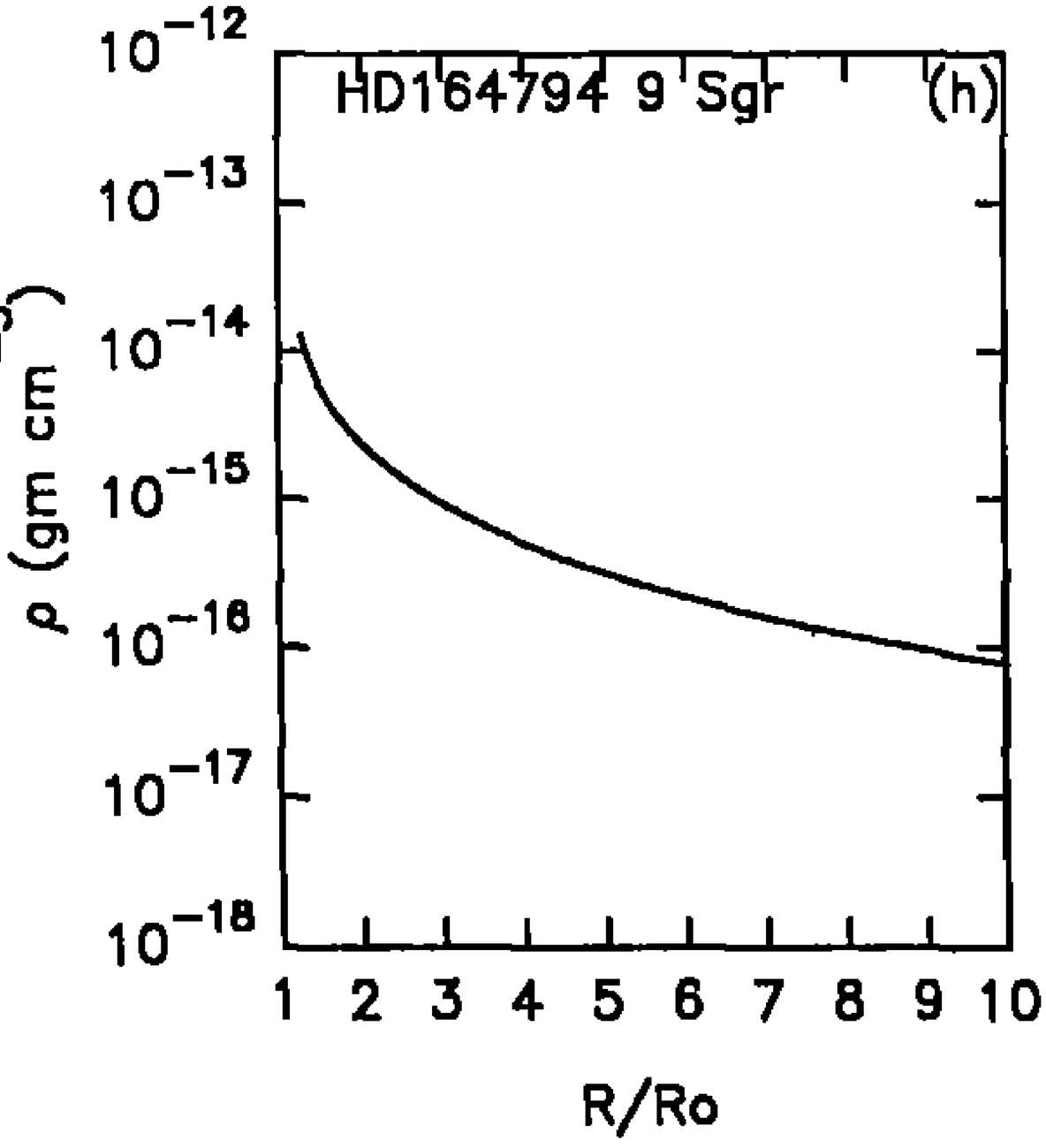

Figure 18 (e,f,g,h)

Figure 18

HD 164794 (9 Sgr) 04(f)

	Pauldrauch et al. (1986)	Abbott (1978)	Blomme (1990a)
T_{eff}	50,000 K	50118 K	38004 K
M	1.27×10^{35} gr	2×10^{35} gr	1.004×10^{35} gr
R	8.4×10^{11} cm	1.05×10^{12} cm	1.197×10^{12} cm
V_{esc}	1420 km s^{-1}	1200 km s^{-1}	876 km s^{-1}
V_∞	3440 km s^{-1}	$V_{edge} = 3440$ km s^{-1}	3650 km s^{-1}
$\dot{M}$	$4 \times 10^{-6} M_\odot/yr$		$2.92 \times 10^{-5} M_\odot$/yr

(a), (b), (c), (d) are similar to the earlier results.

(e) τ (Lyman α) > τ (Balmer α)

τ (Lyman α) > τ (Paschen)

τ (Lyman α) < τ (Brackett)

τ (Lyman 9) < τ (Balmer 8)

τ (Lyman 9) < τ (Paschen 7)

τ (Lyman 9) < τ (Brackett 6)

(f) radiation force falls rapidly and tends to be equal to gravity force beyond $R/R_0 >> 10$

(g) v_∞ (calculated) < v_∞ (observed) $\approx$ 3650 km s^{-1}.

(h) 10^{-16} gr cm^{-3} < ρ < 10^{-14} gr cm^{-3}.

Figure 19

HD 167263 (16 Sgr) O9 III

	Abbott (1978)	Blomme (1990a)
T_{eff}	30903 K	33884 K
M	6×10^{34} gr	7.7×10^{34} gr
R	1.19×10^{12} cm	1.337×10^{12} cm
V_{esc}	760 km s^{-1}	735 km s^{-1}
V_∞	$V_{edge} = 1780$ km s^{-1}	2450 km s^{-1}
$\dot{M}$		$3.1675 \times 10^{-6} M_\odot$/yr

These results are similar to those of HD 164794.

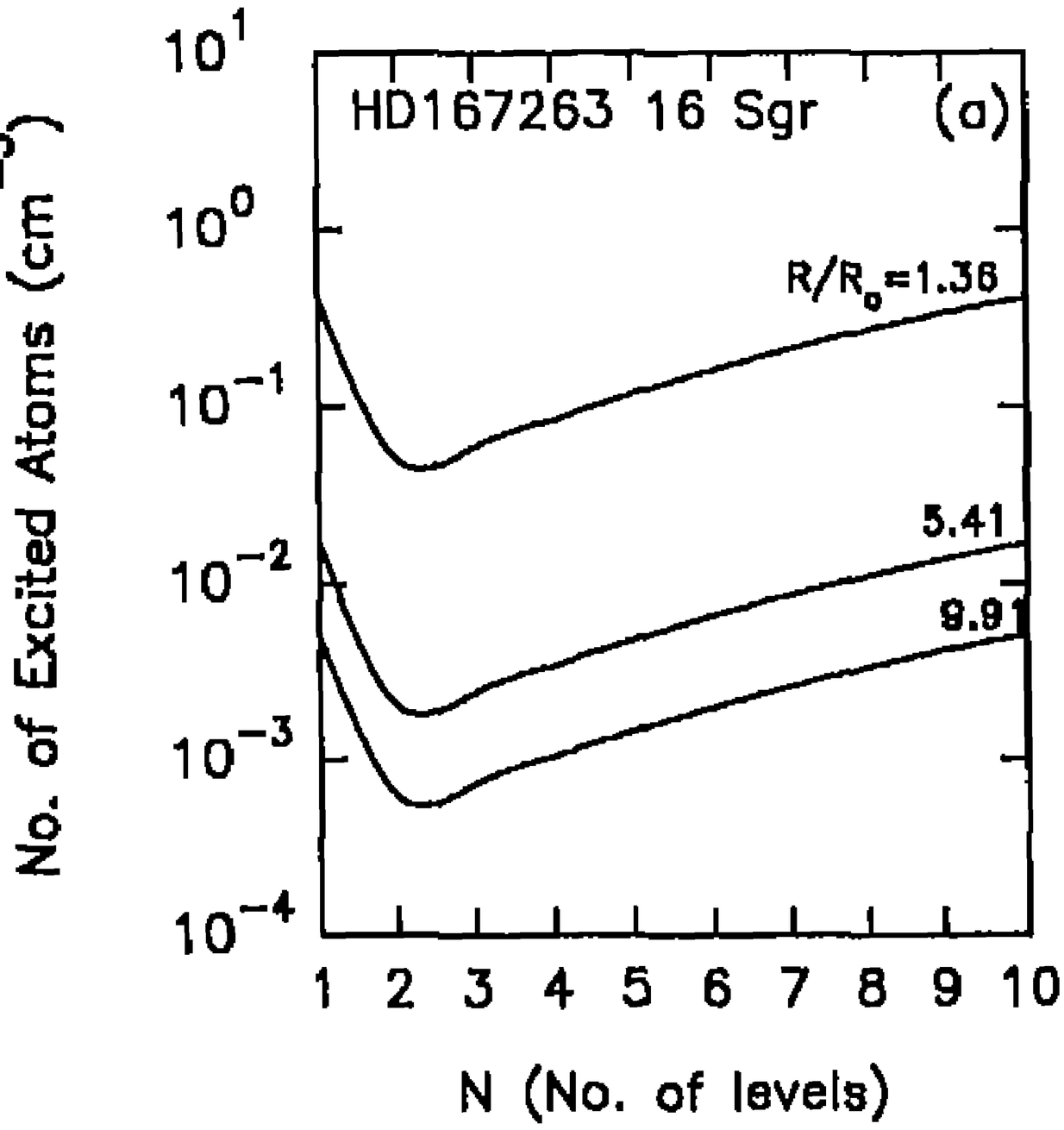

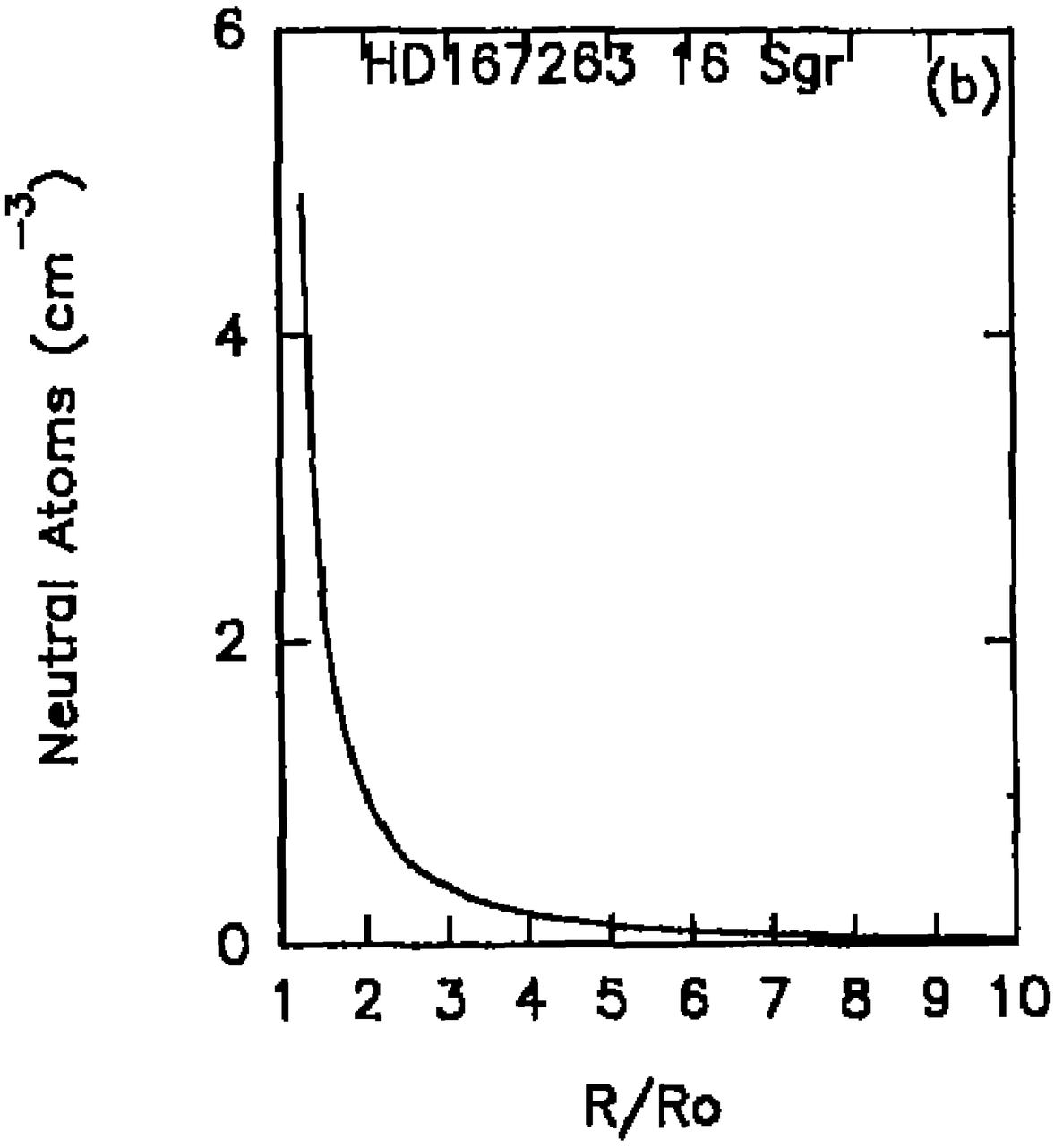

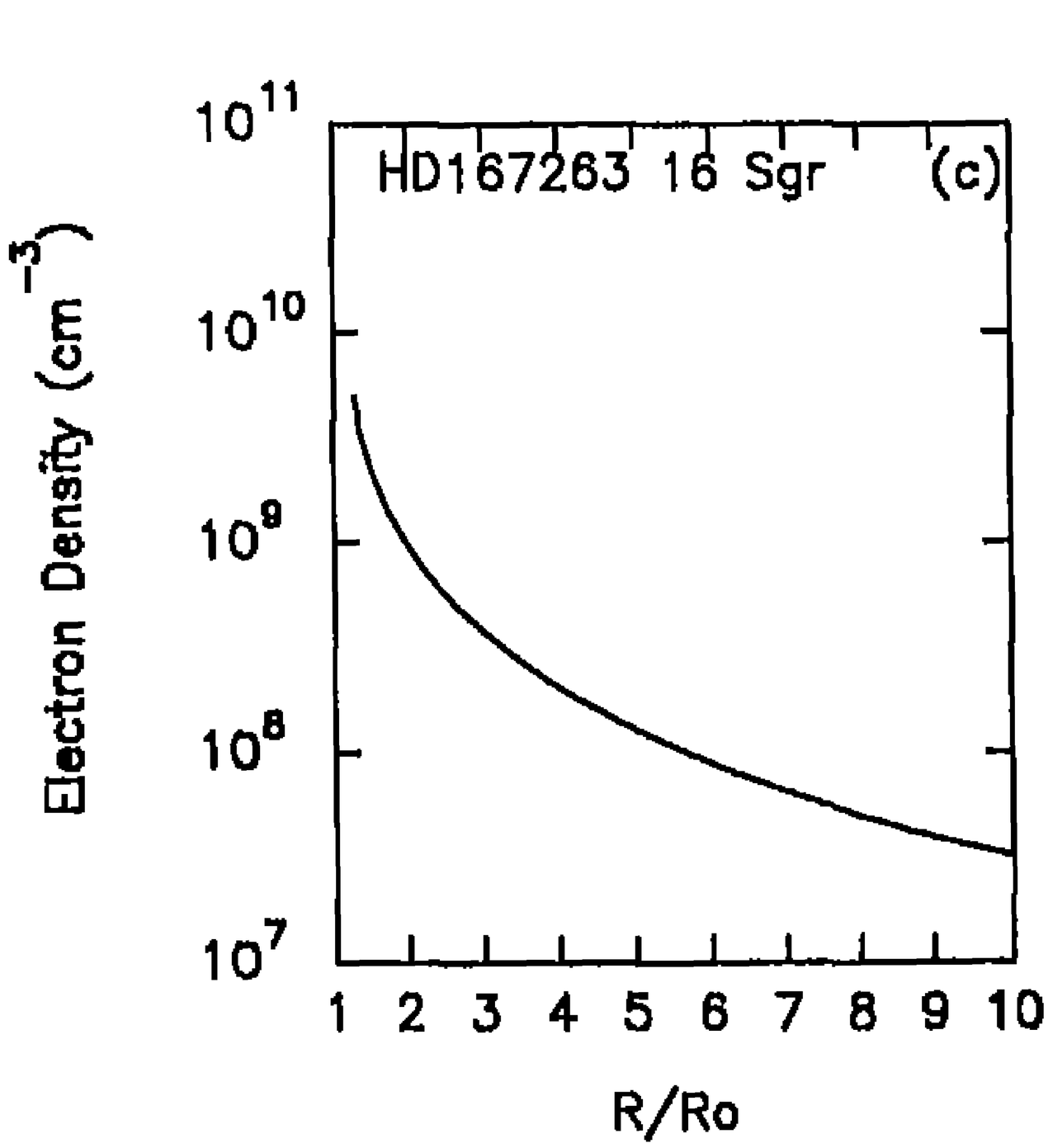

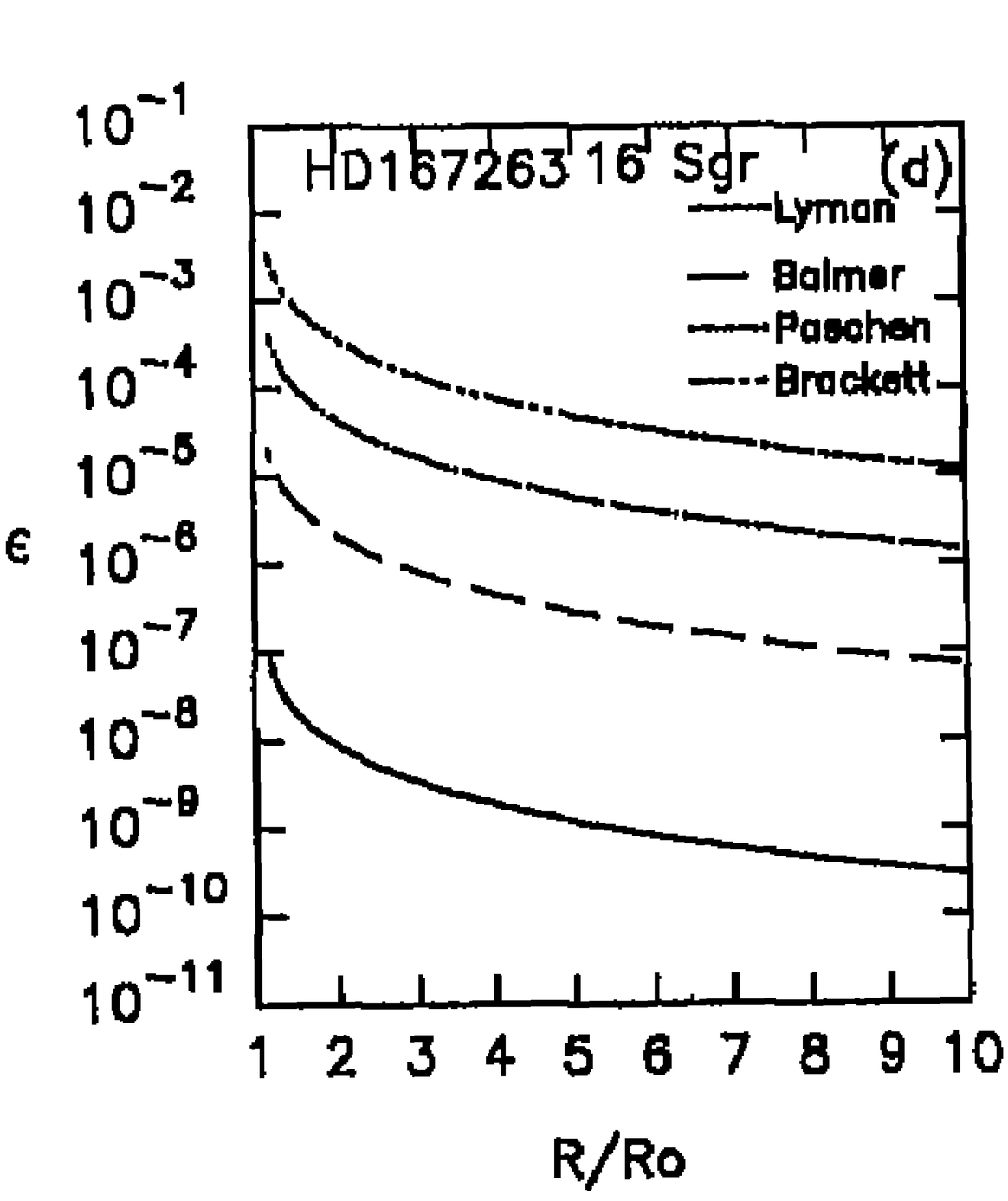

Figure 19 (a,b,c,d)

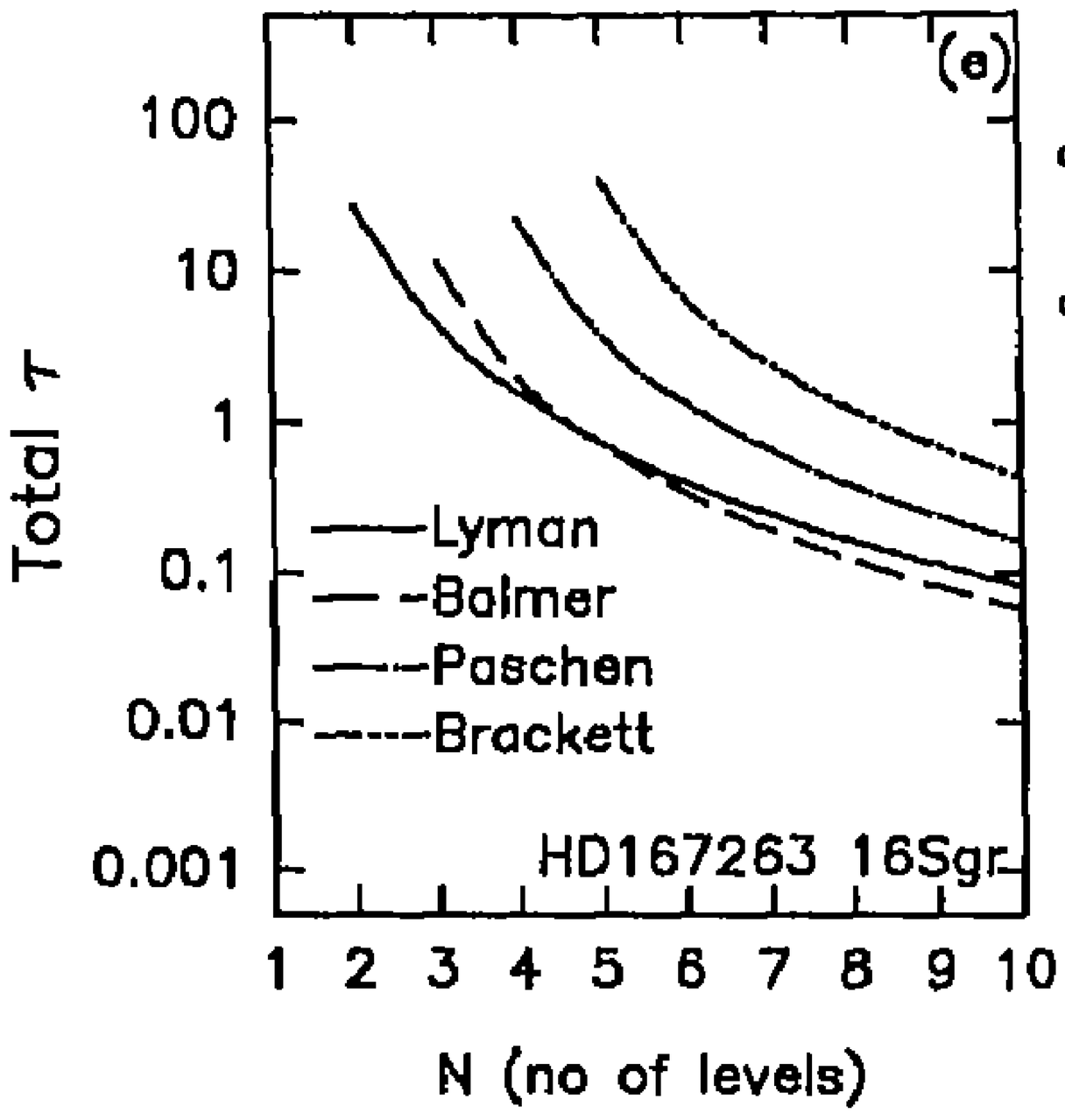

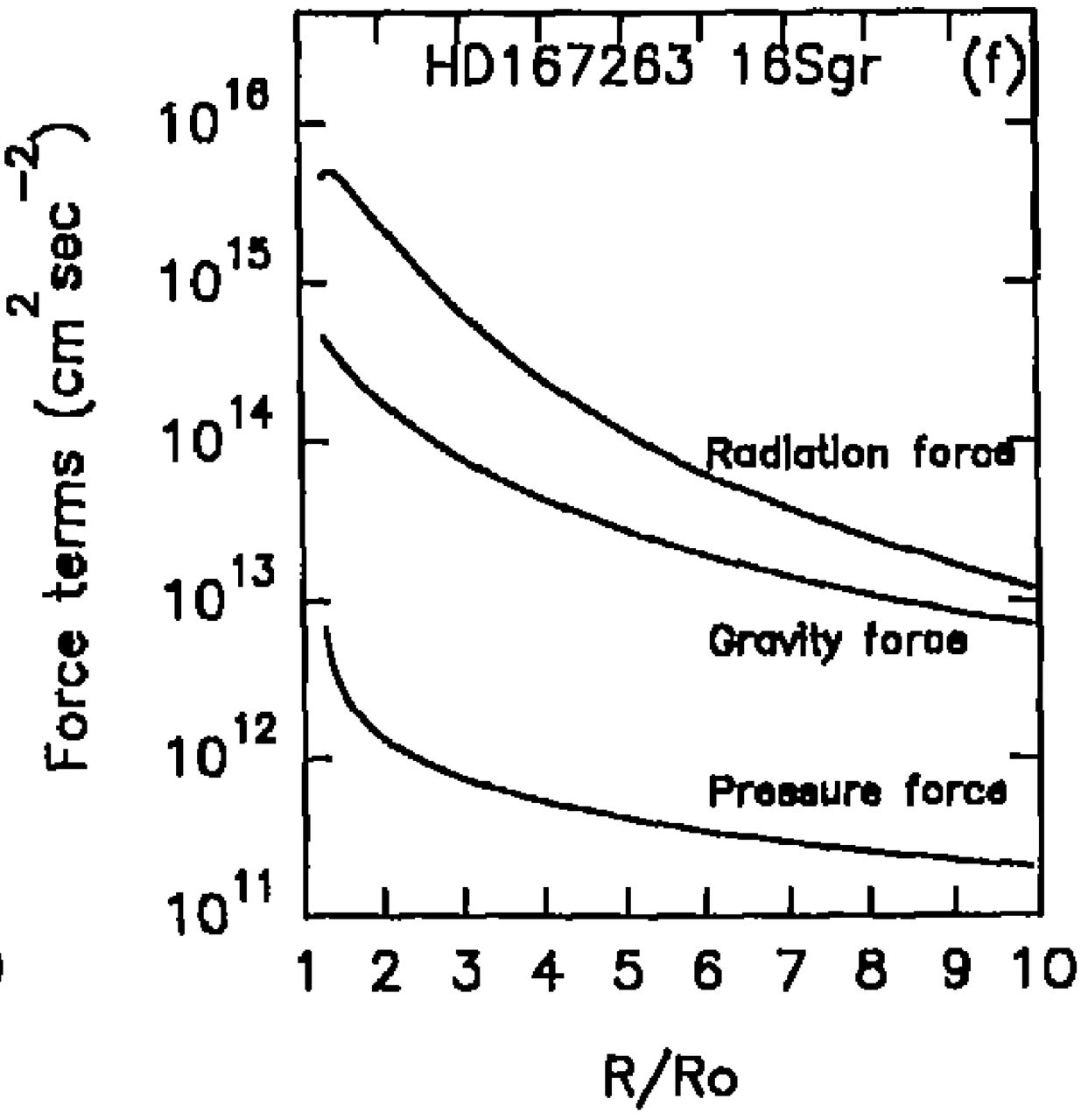

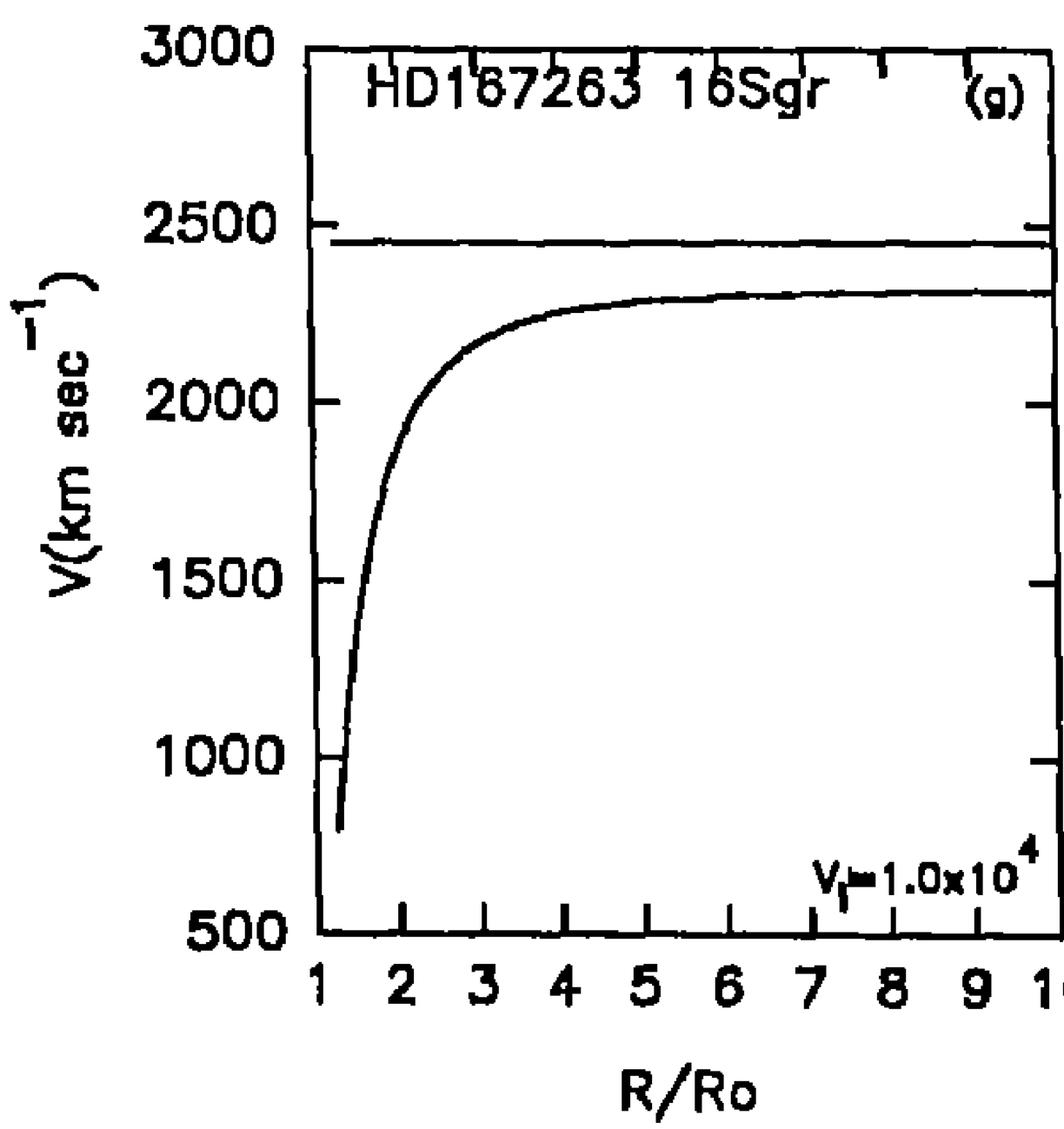

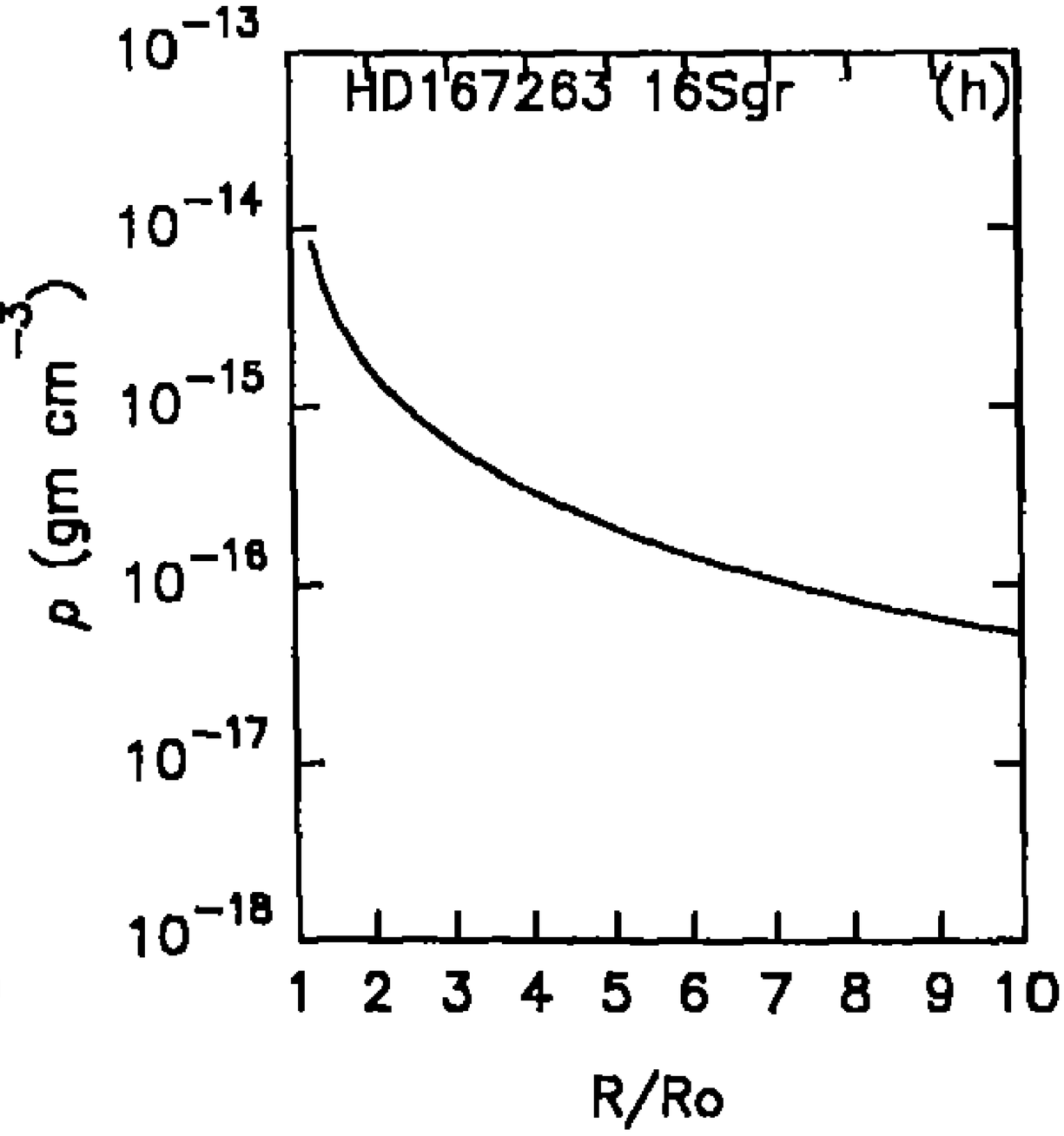

Figure 19 (e,f,g,h)

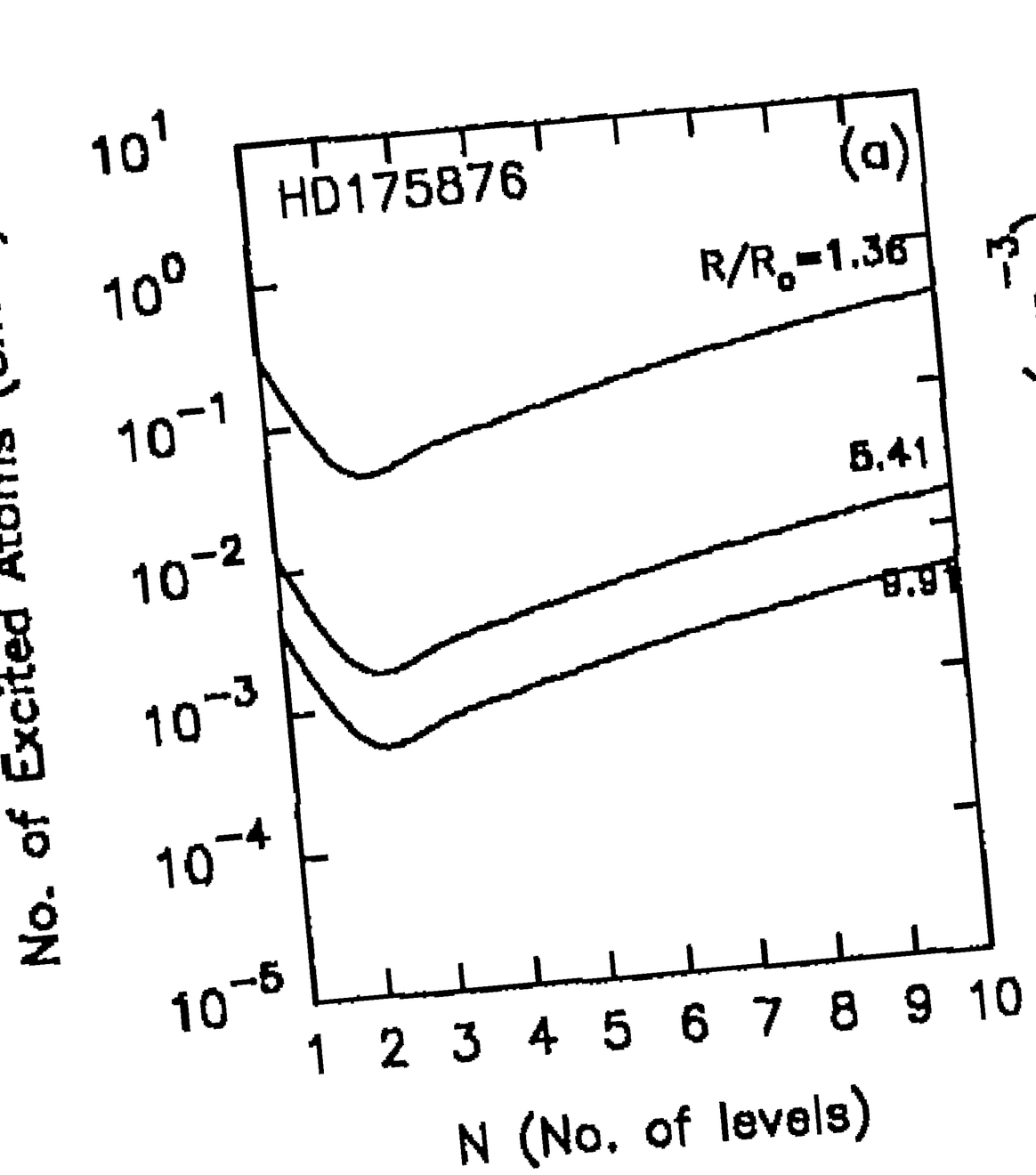

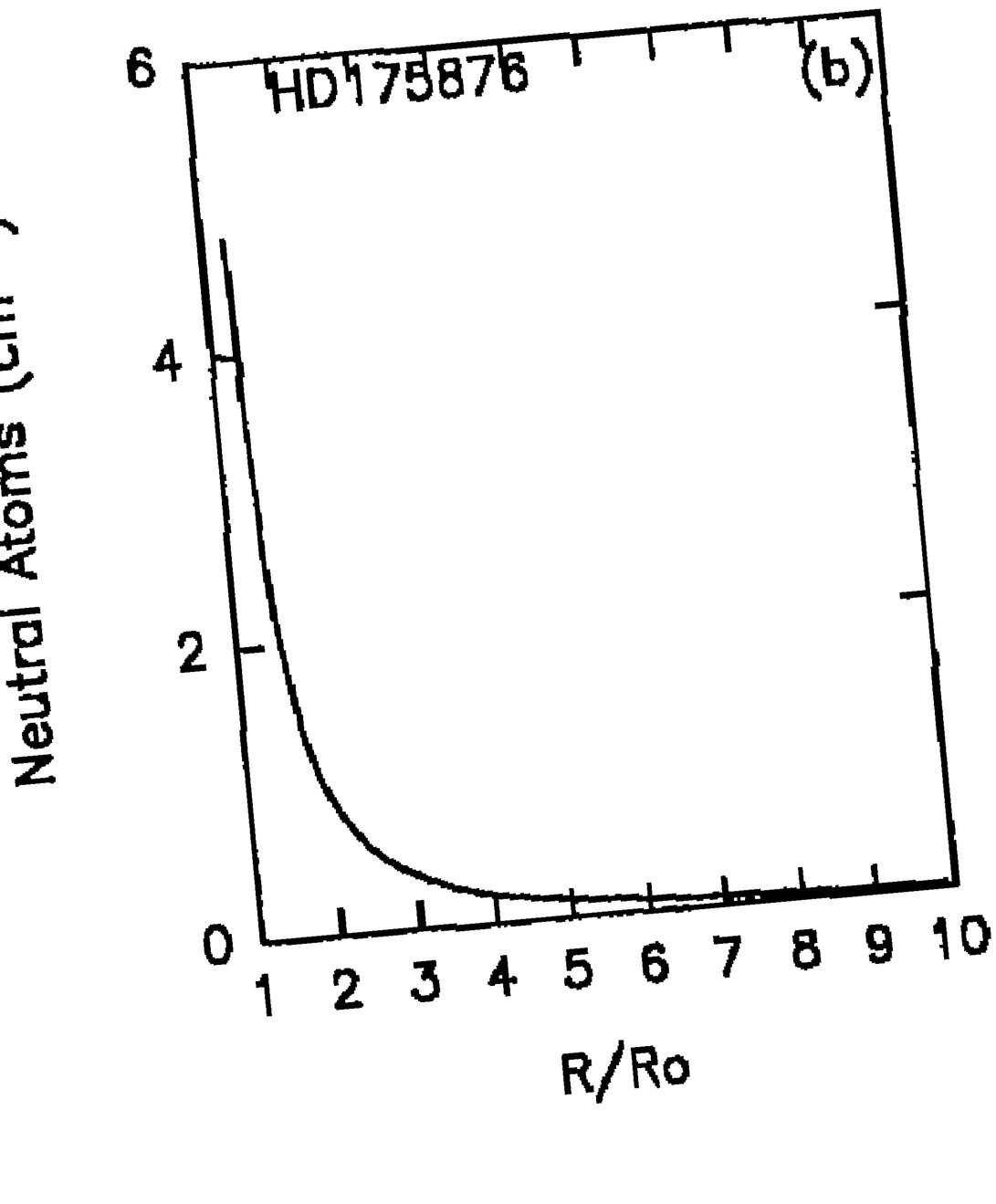

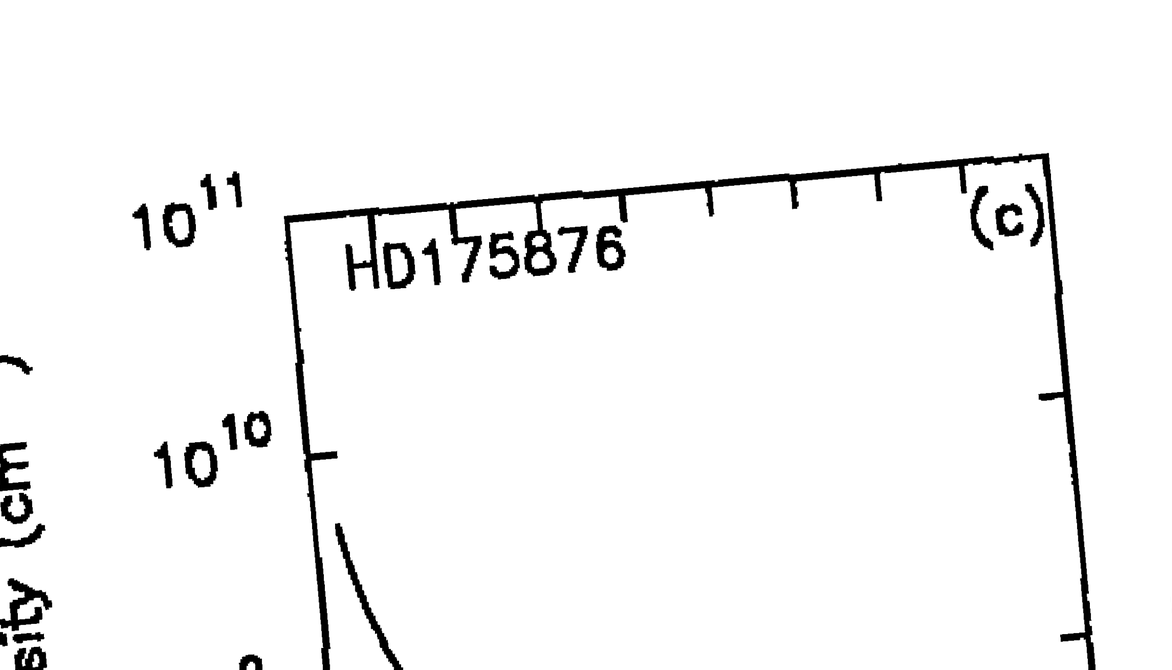

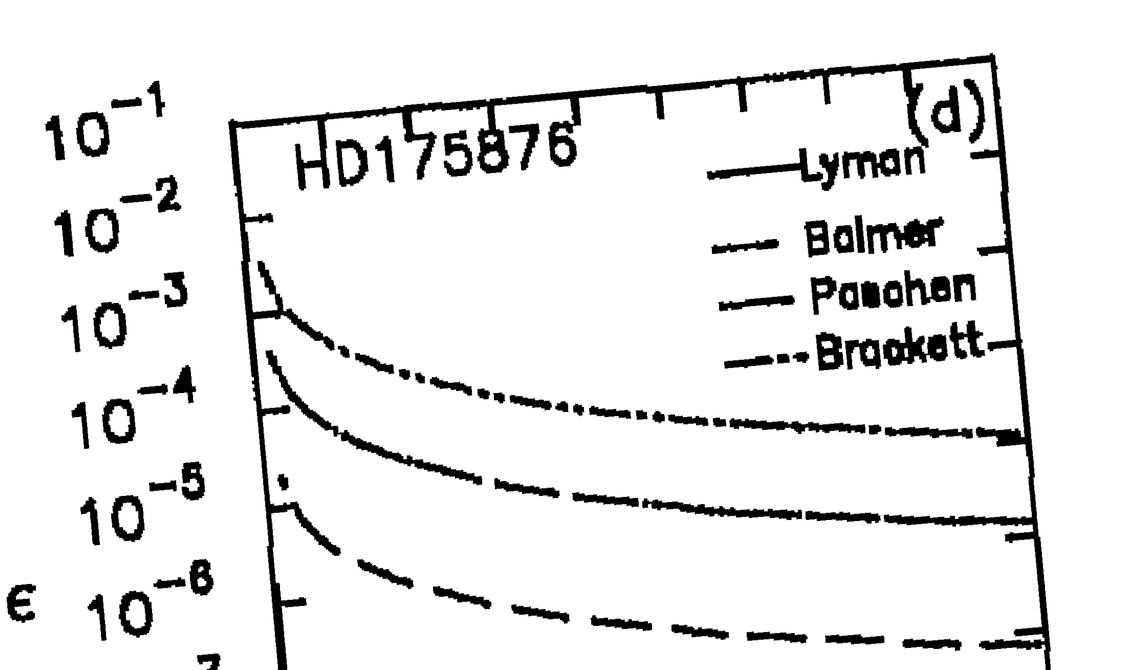

Figure 20 (a,b,c,d)

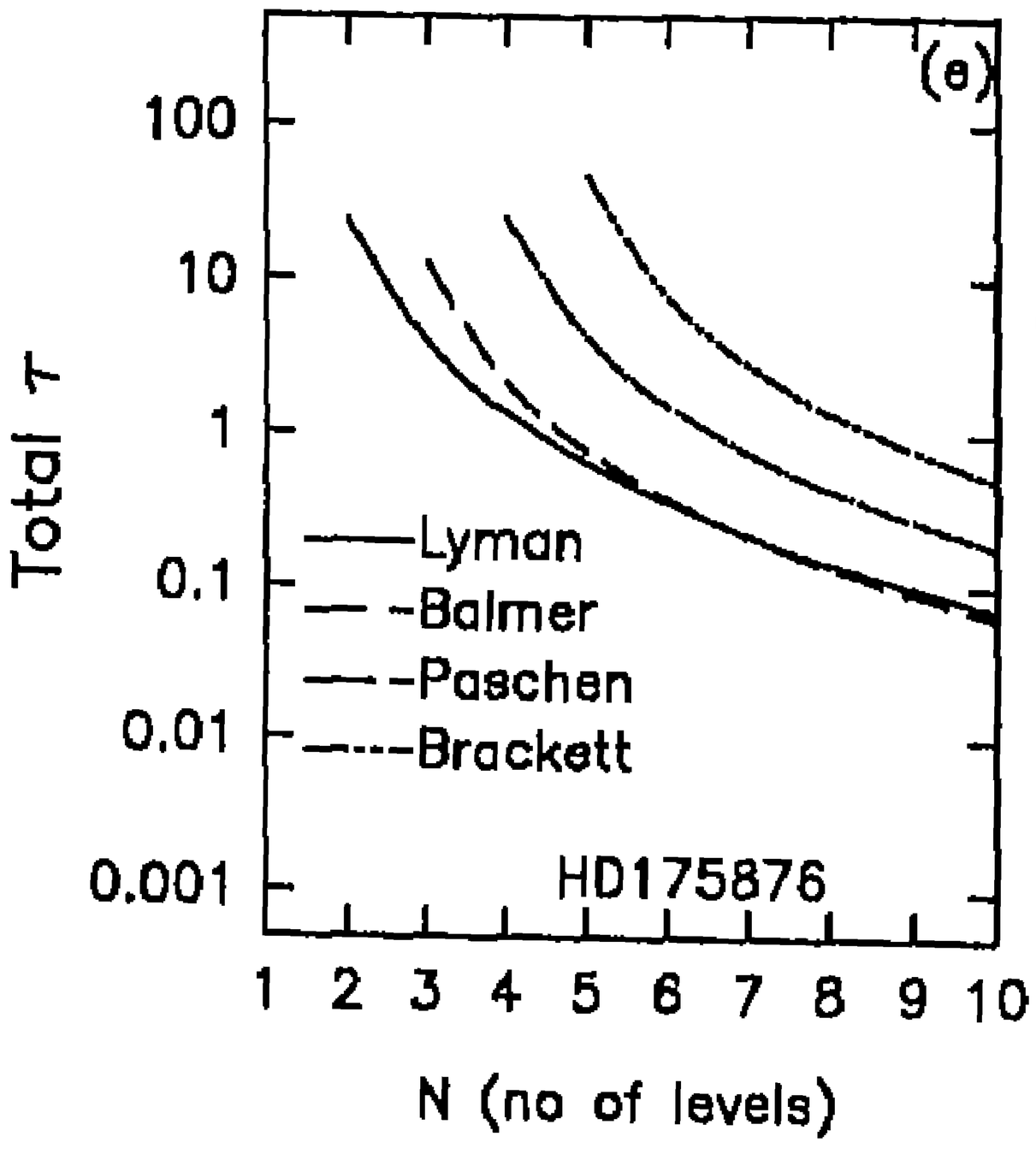

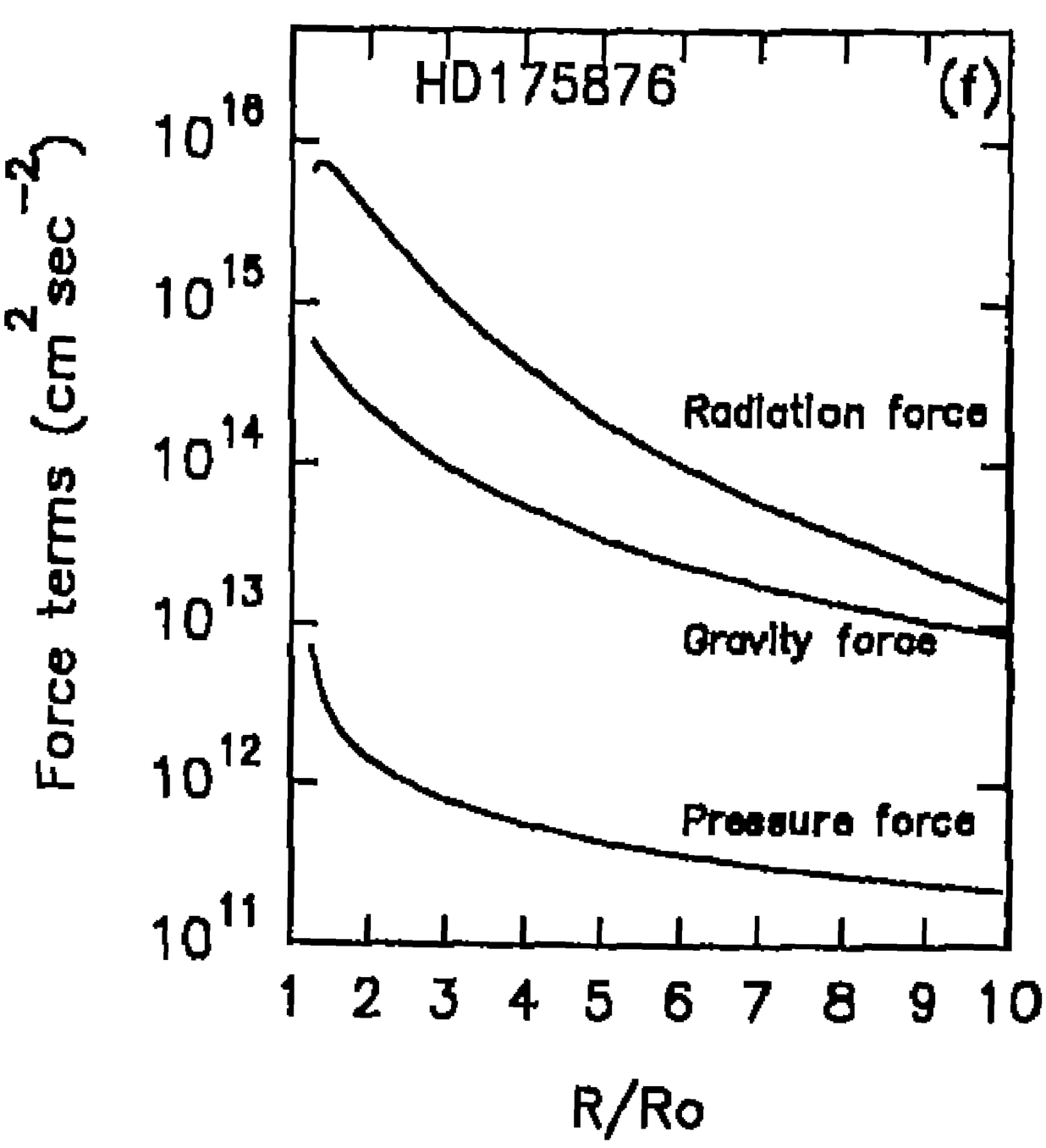

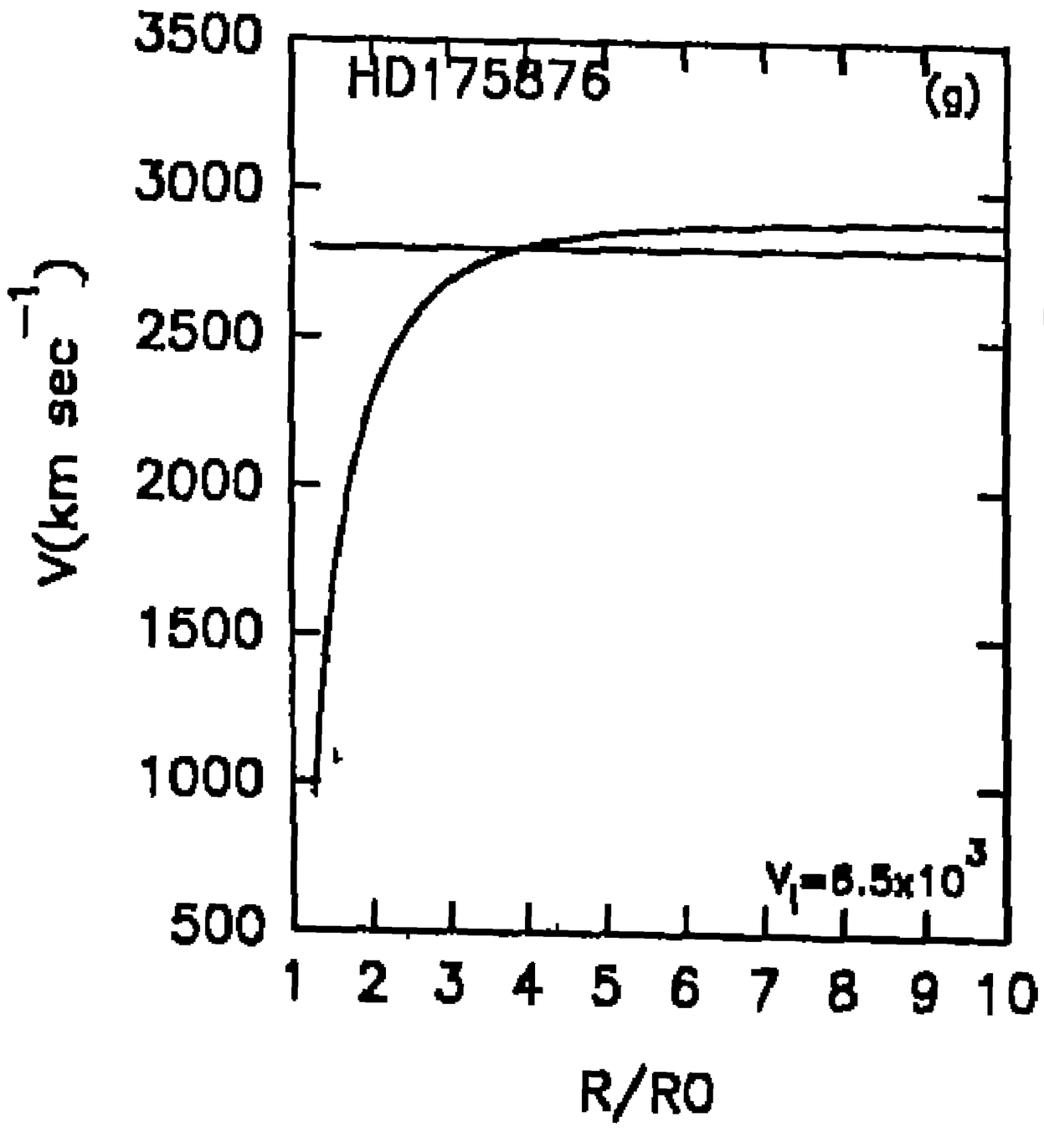

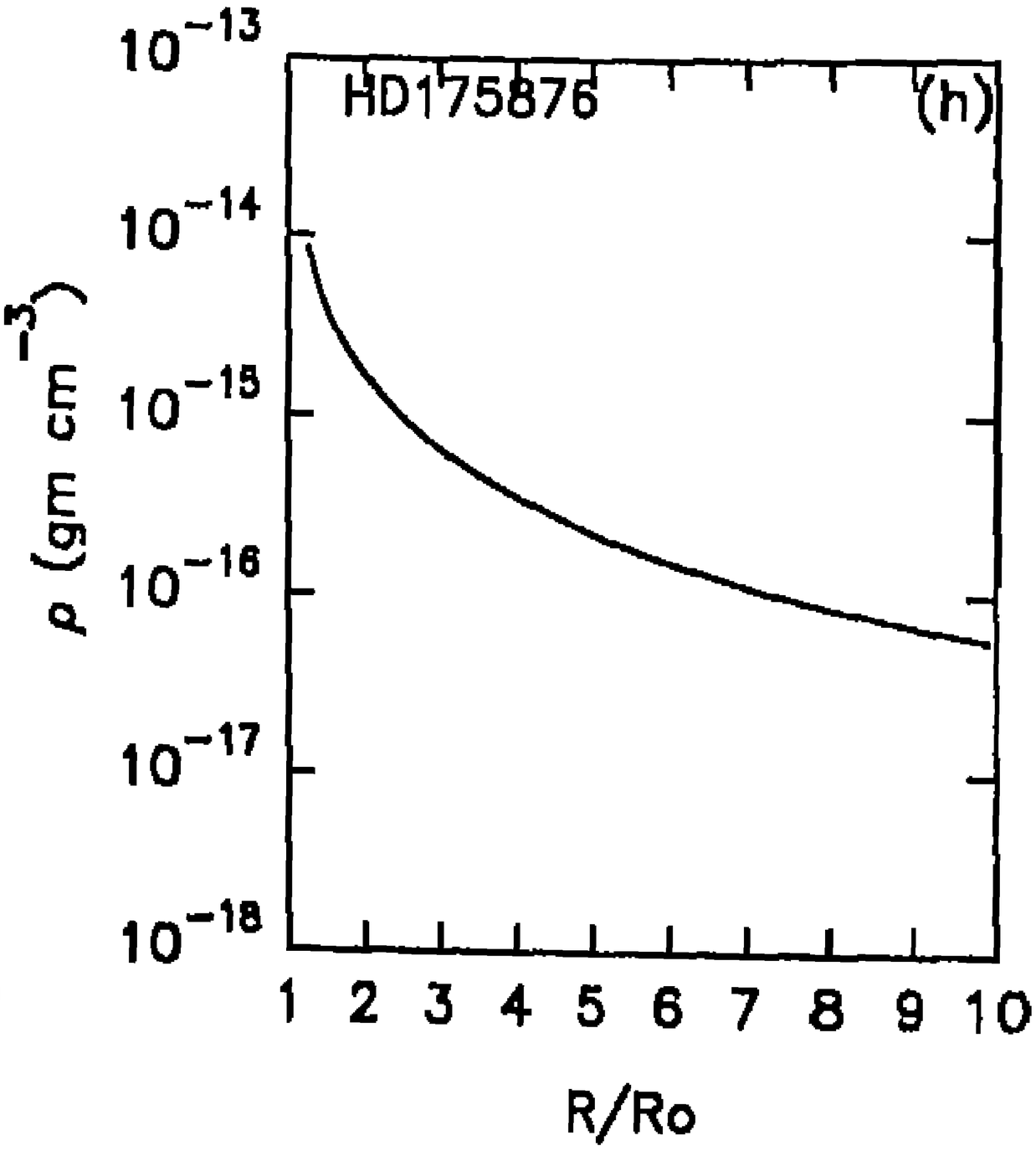

Figure 20 (e,f,g,h)

Figure 20

HD 175876, O7 (Blomme 1990a)

T_{eff} = 36308 K

M =7.76 × 10^{34} gr

R =1 078 × 10^{12} cm

V_{esc} = 848 km s^{-1}

V_{∞} = 2800 km s^{-1}

$\dot{M}$ =3.82 × $10^{-5} M_{\odot}$/yr

(a), (b), (c), (d), (e), (f), (h) are similar to the earlier results.

(g) The calculatel v_{∞} crosses the expected or observed v_{∞} ($\approx$ 2800 km s^{-1}) at R/R_0 = 4. $\beta \approx 0.85$.

Figure 21

HD 210839 (λ Cep) O6 ef

	Pauldrach et al (1986)	Abbott (1978)
T_{eff}	42000 K	37153 K
M	1.064 × 10^{36} gr	1.34 × 10^{36} gr
R	1.19 × 10^{12} cm	1.68 × 10^{12} cm
V_{esc}	1092 km s^{-1}	830 km s^{-1}
V_{∞}	2500 km s^{-1}	V_{edge} = 2560 km s^{-1}
$\dot{M}$	4 × $10^{-6} M_{\odot}$/yr	

(a), (b), (c), (d) as the mass loss rate is small, we get a low density of excited atoms, neutral atoms and electron density. The high temperature of 42000 K gives higher population densities at higher levels. Therefore we find the densities of excited atoms at n = 10 are more than the densities at n = 1.

(e) As a consequence of high density at n = 10 we get τ (Brackett) > τ (Lyman, Balmer, Paschen).

(f) Radiation force falls rapidly at $R/R_0 \approx 10$ and tends to become less than gravity force at $R/R_0 > 10$.

(g) The calculated v_{∞} crosses the expected v_{∞} ($\approx$ 2500 km s^{-1}) at about R/R_0 = 4
$\beta \approx 0.85$.

(h) 10^{-16} gr $cm^{-3} < \rho < 10^{-13}$ gr cm^{-3}

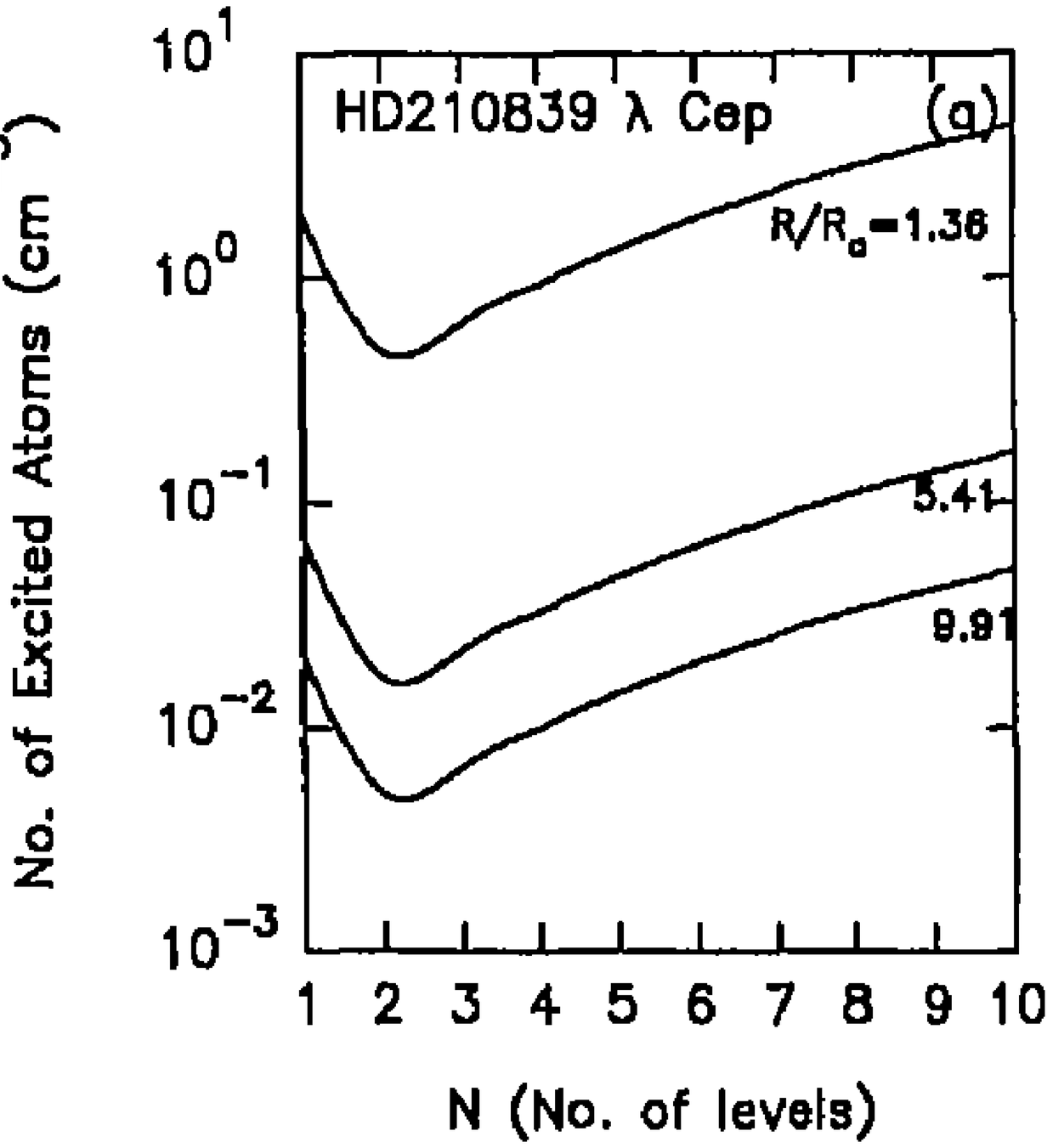

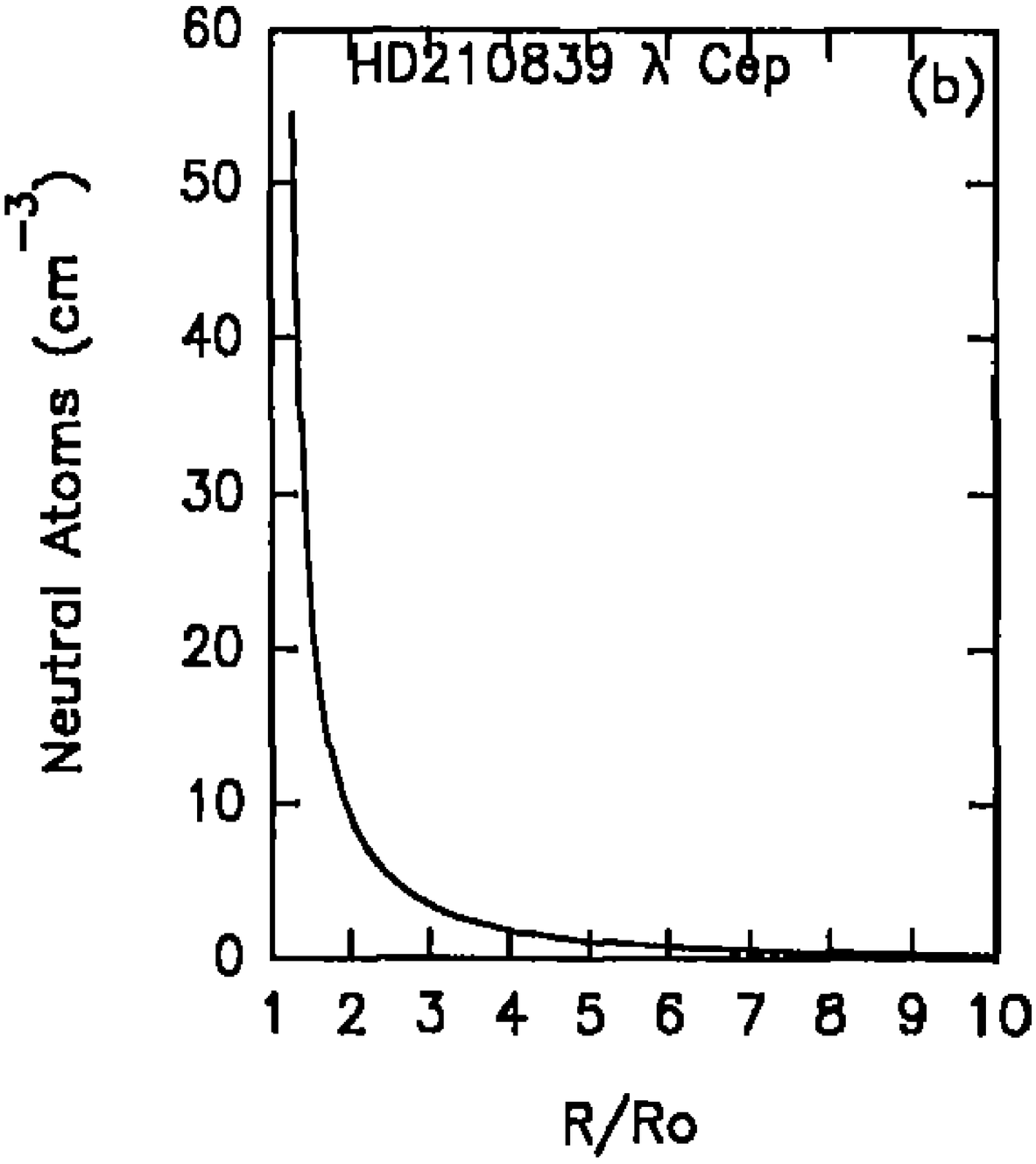

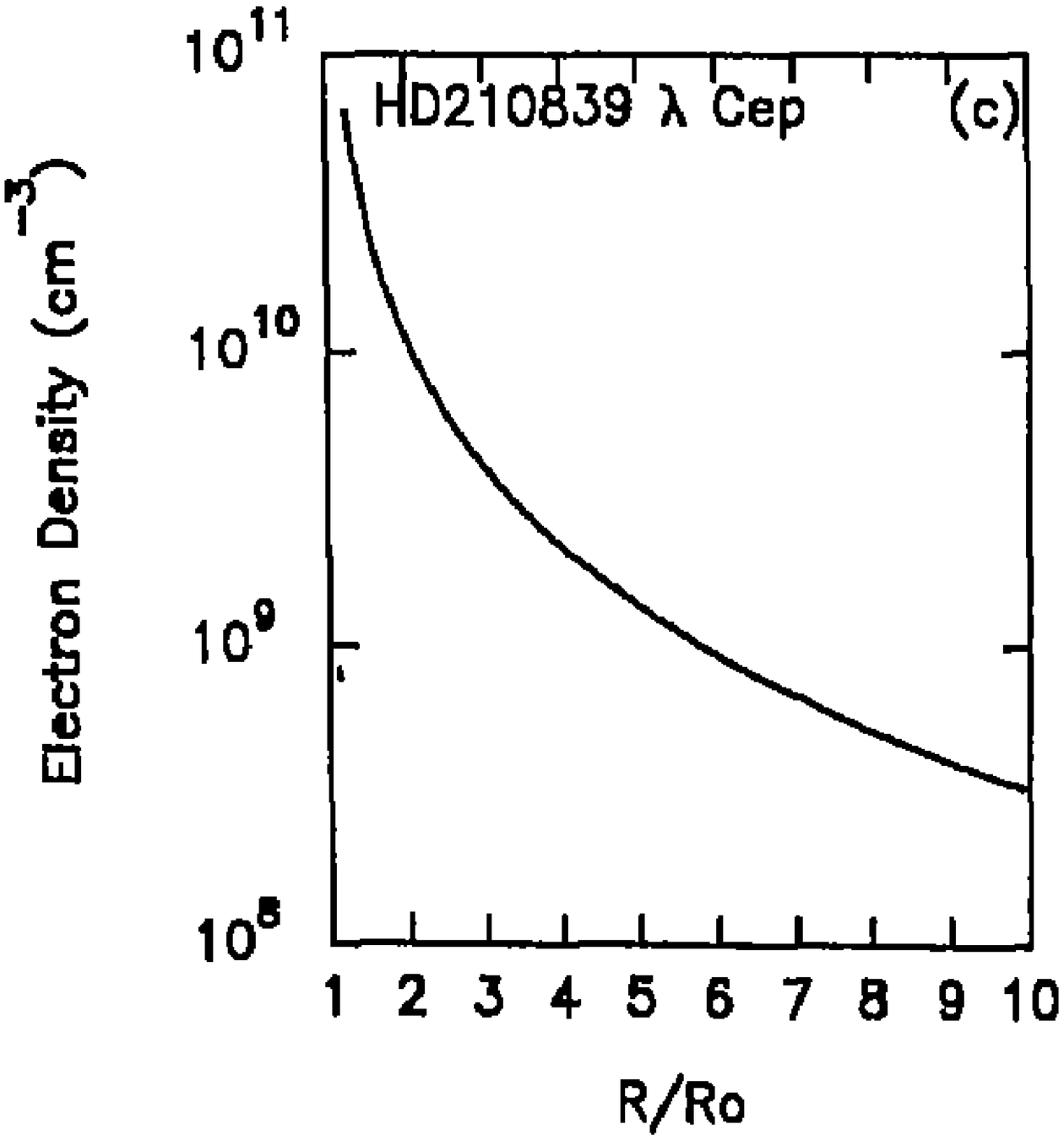

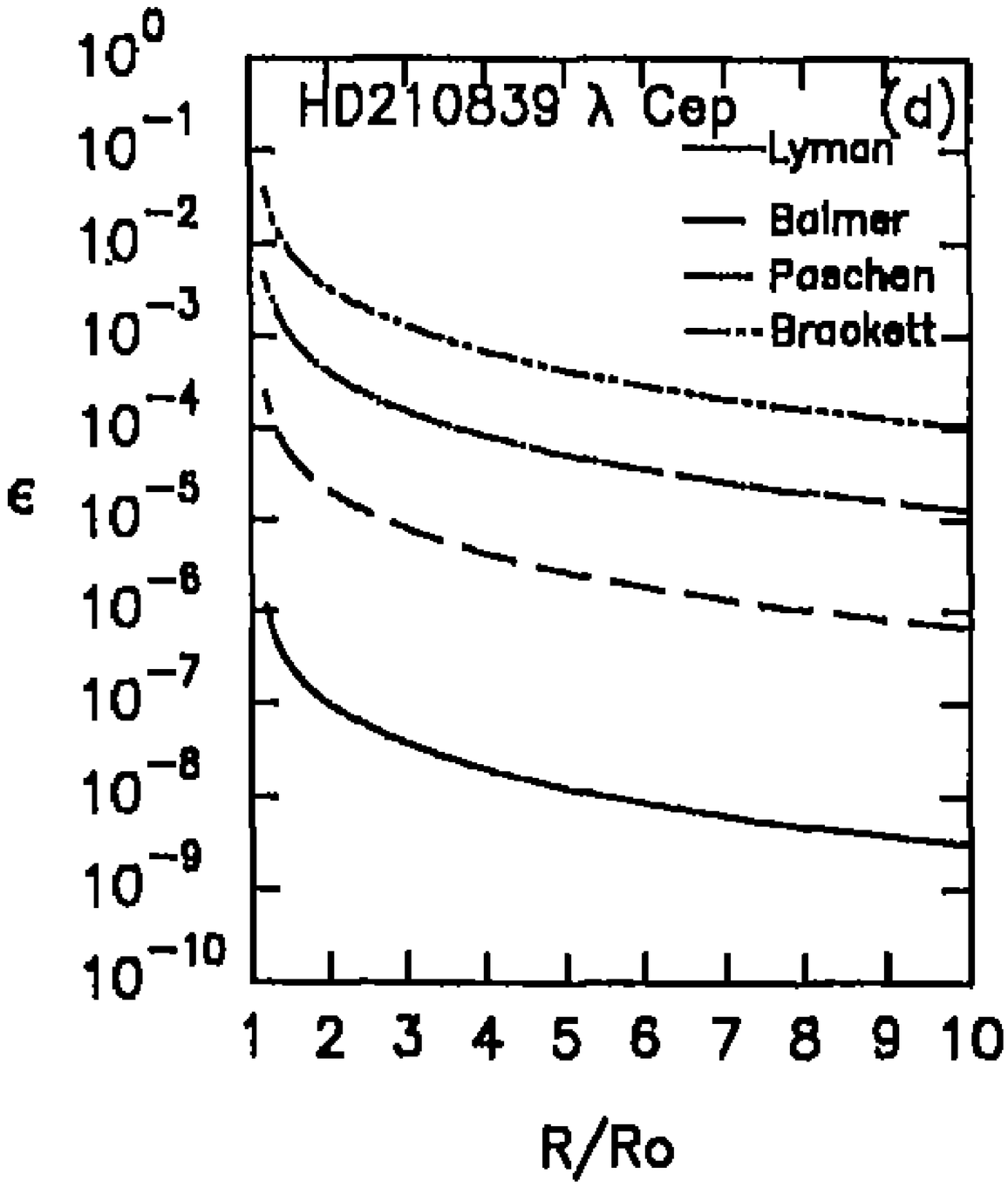

Figure 21 (a,b,c,d)

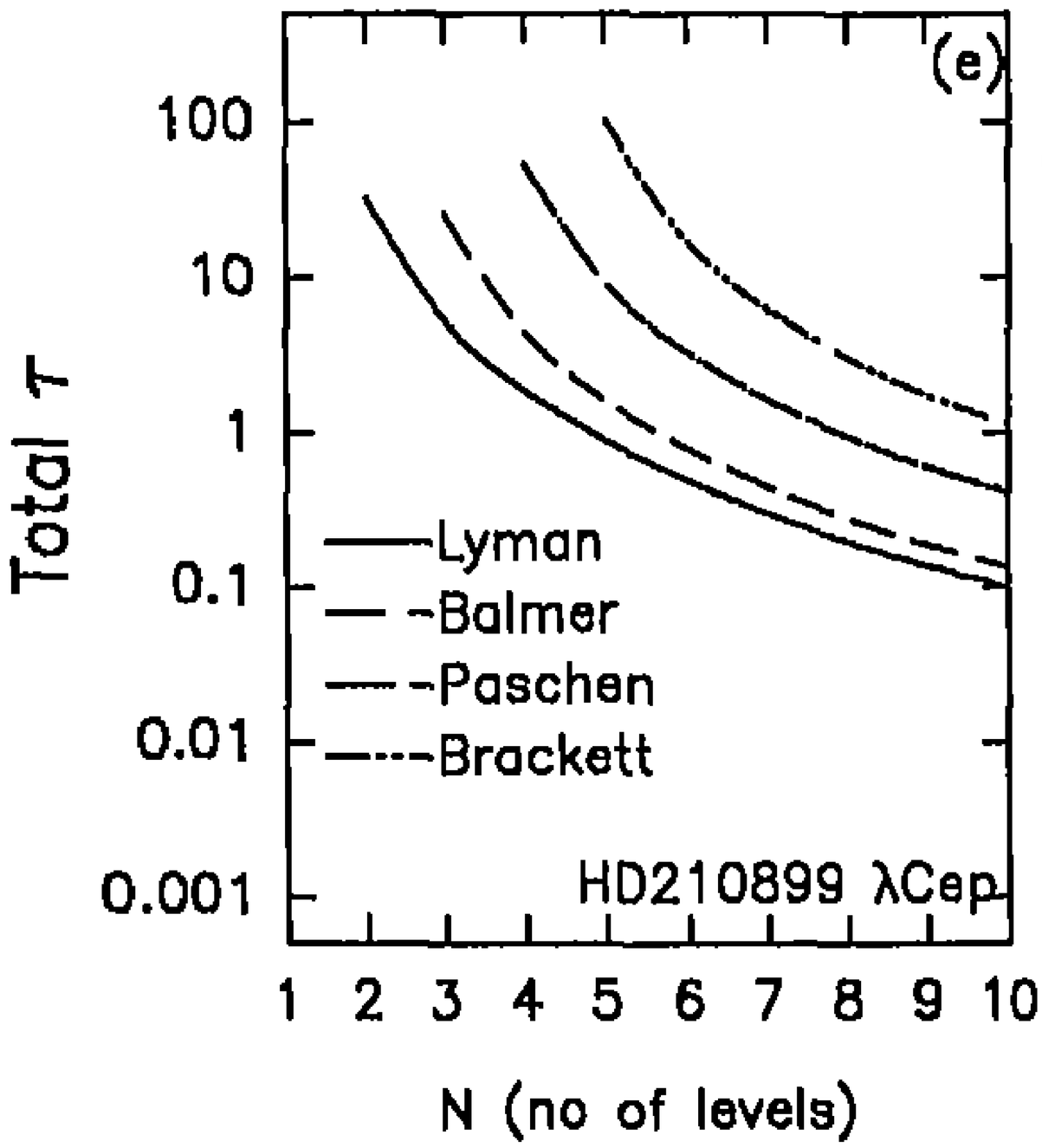

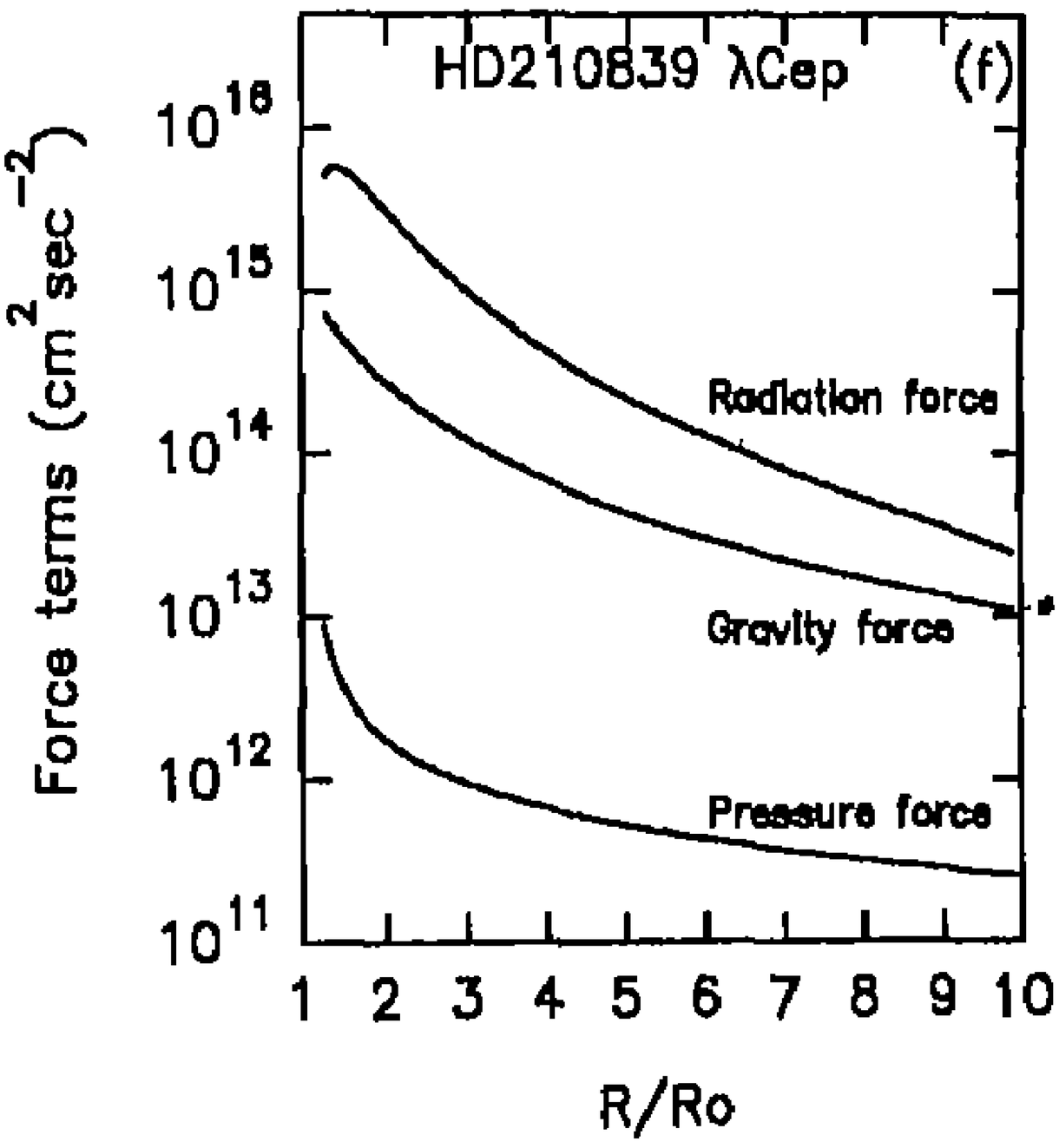

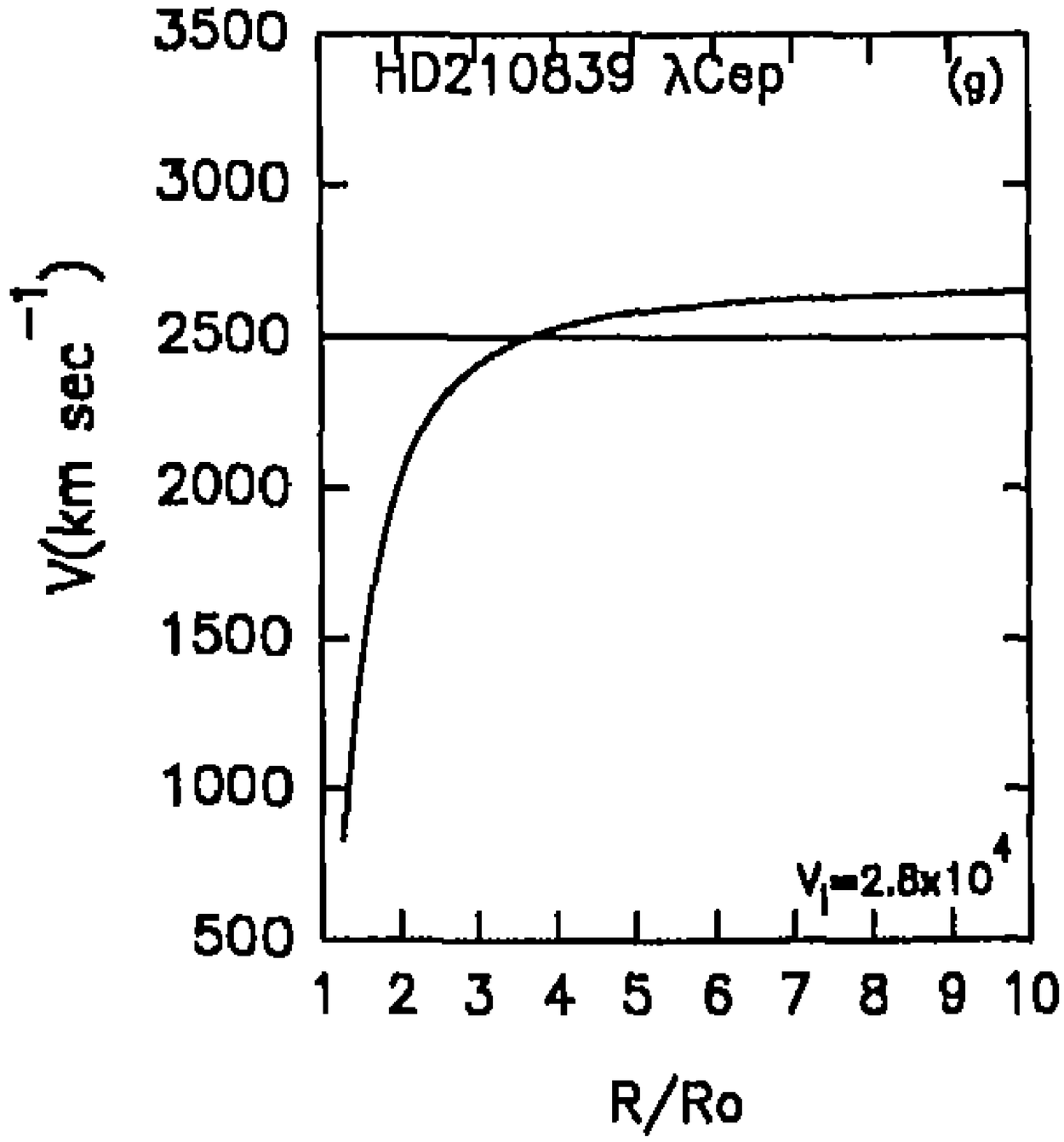

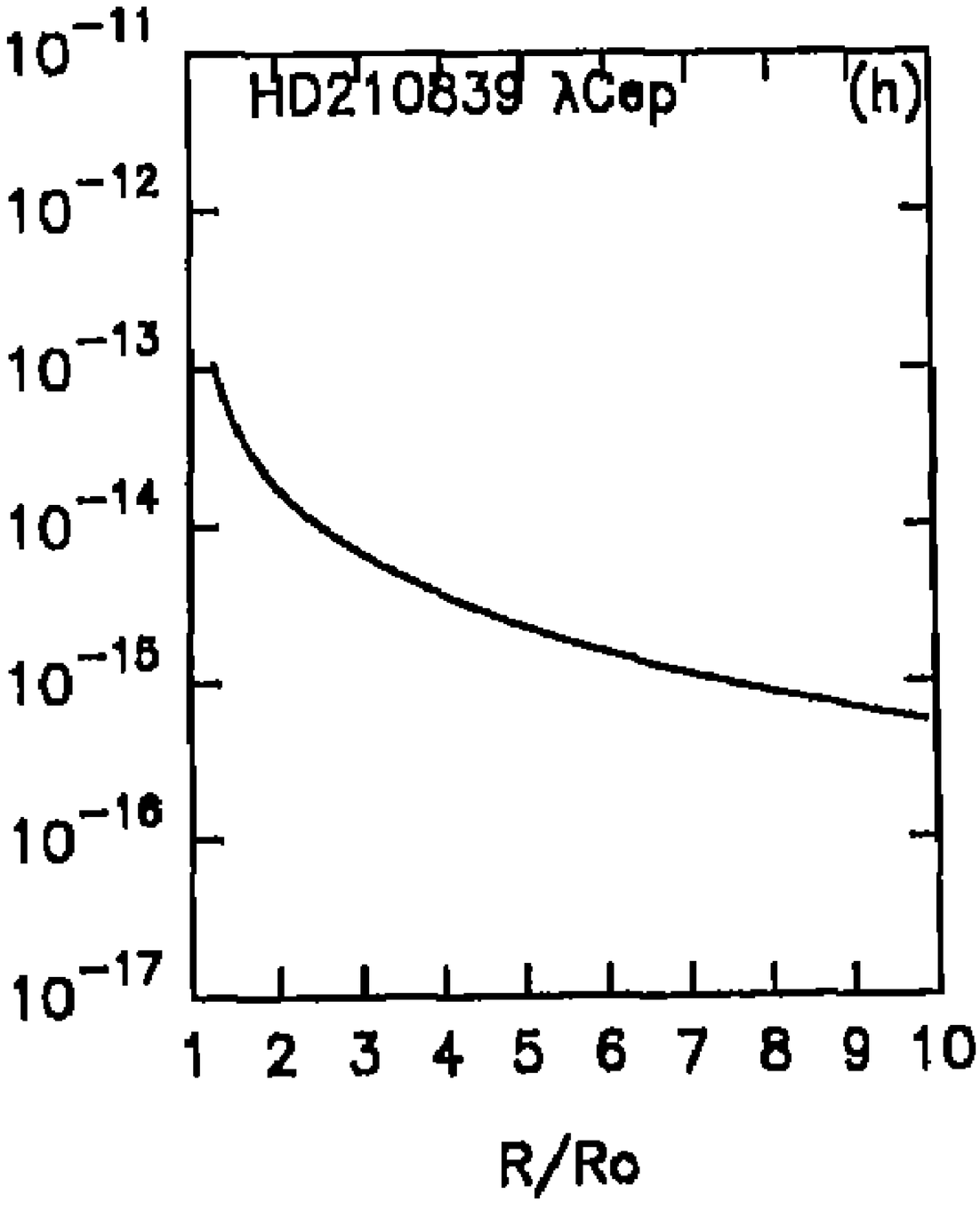

Figure 21 (e,f,g,h)

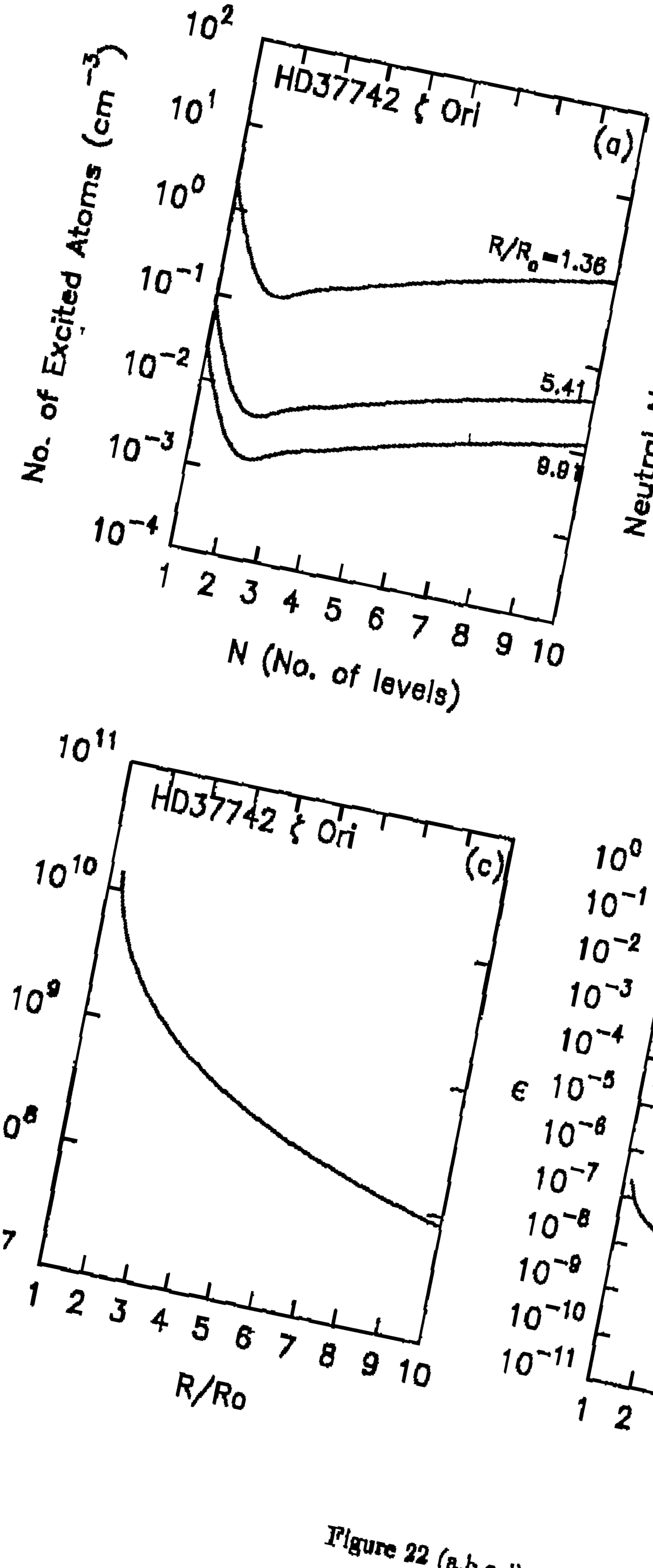

Figure 22 (a,b,c,d)

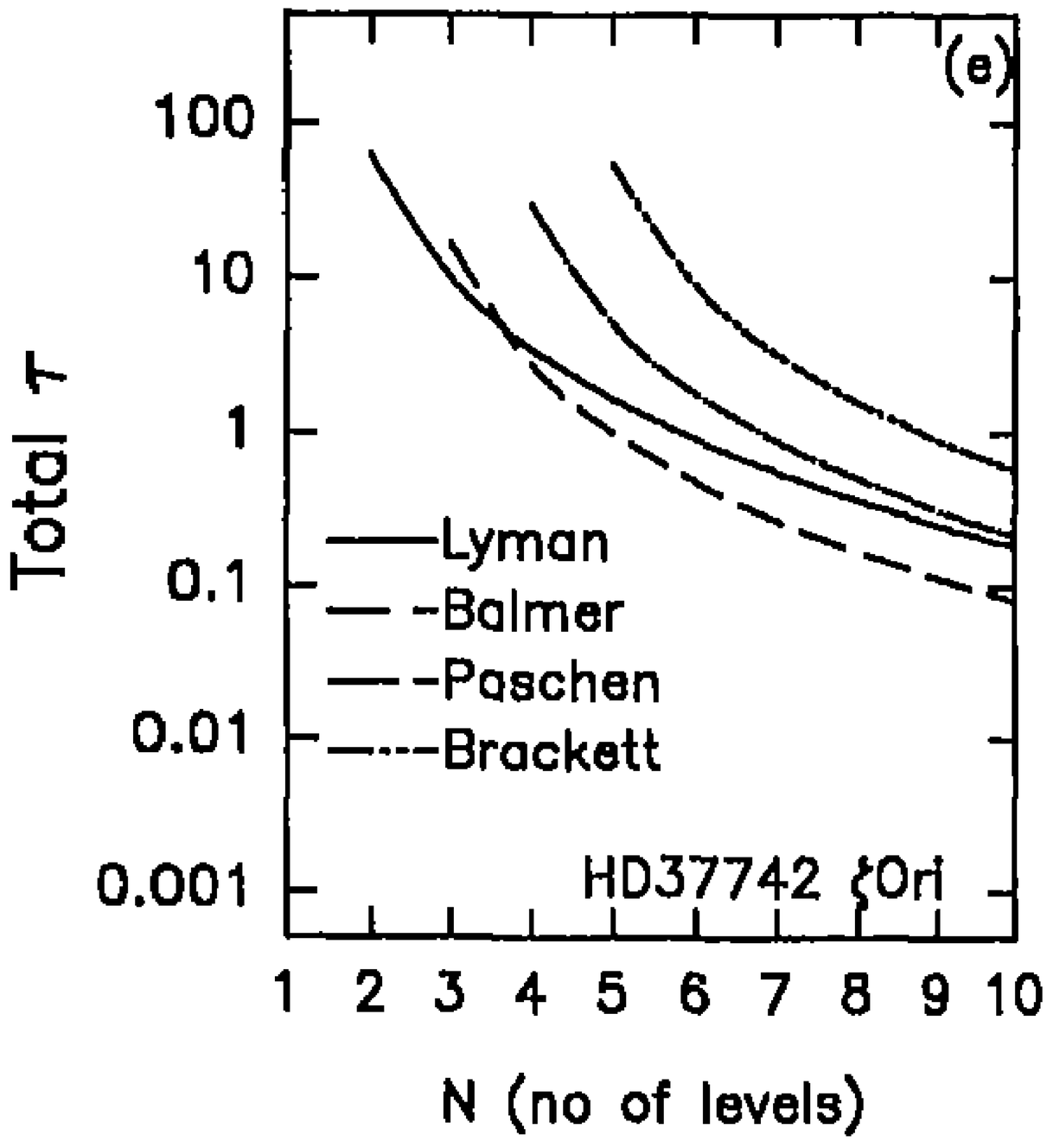

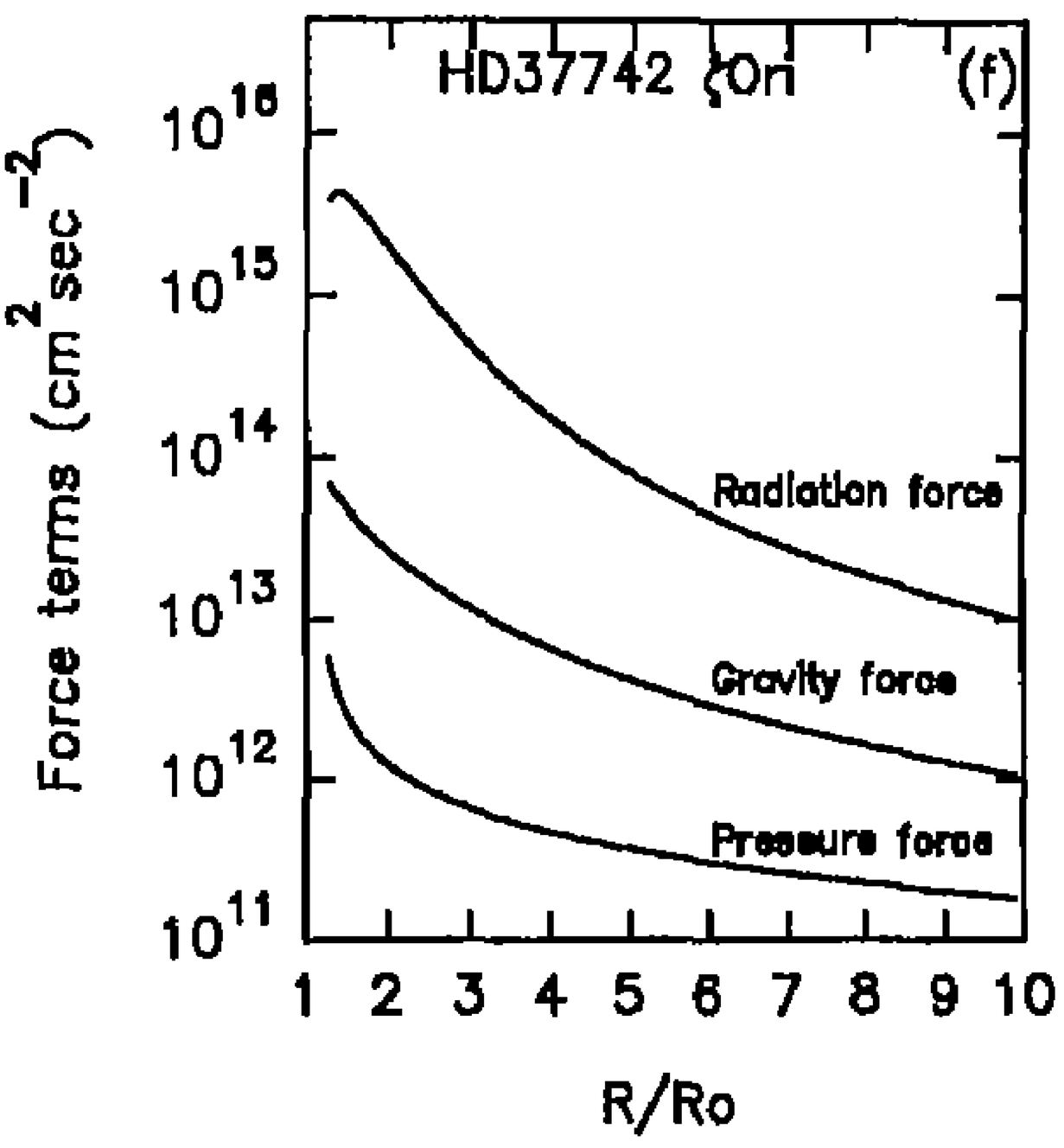

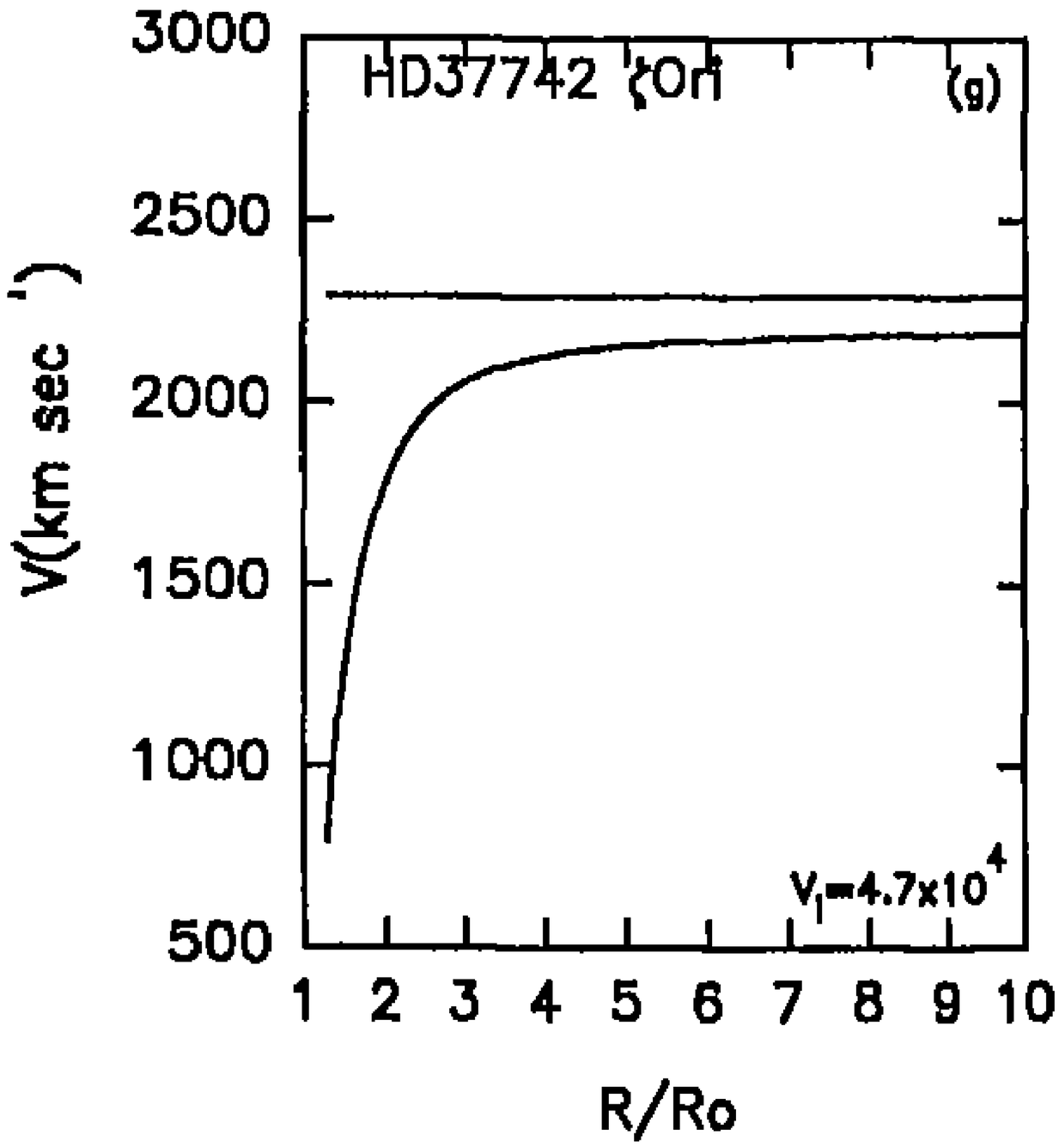

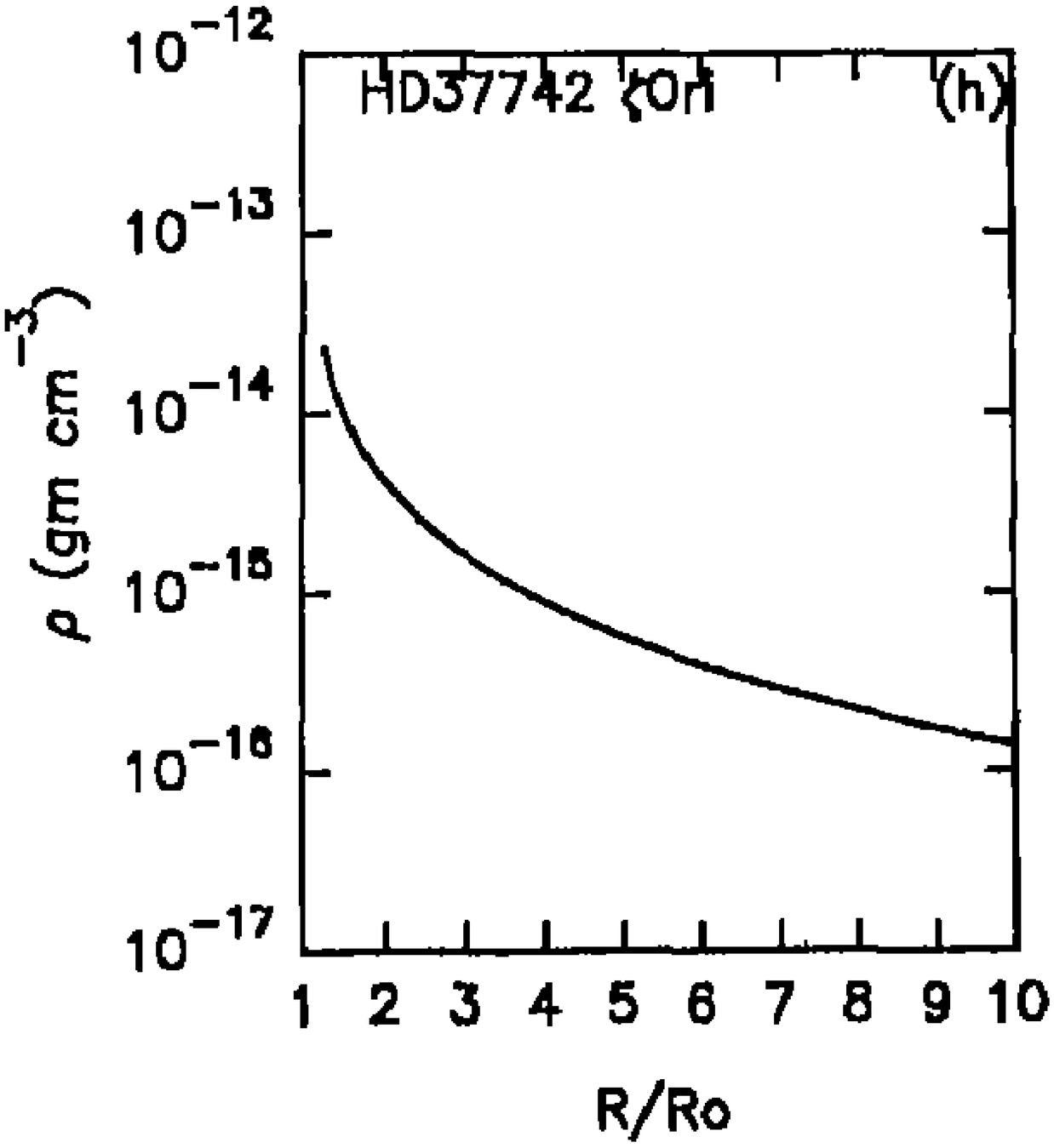

Figure 22 (e,f,g,h)

Figure 22

HD 37742 (ζ Ori) O9.5 I

	Pauldrach et al. (1986)	Abbott (1978)
T_{eff}	30,000 K	28840 K
M	1.74×10^{34} gr	6.8×10^{34} gr
R	2.03×10^{12} cm	1.68×10^{12} cm
V_{esc}	1069 km s^{-1}	630 km s^{-1}
V_∞	2290 km s^{-1}	2200 km s^{-1}
$\dot{M}$	$2.3 \times 10^{-6} M_\odot$/yr	

These results are similar to those of the previous systems.

Figure 23

HD 37128 (ε Ori) BO Ia

	Pauldrach et al. (1986)	Abbott (1978)
T_{eff}	28500 K	28840 K
M	1.788×10^{35} gr	9×10^{34} gr
R	2.59×10^{12} cm	2.31×10^{12} cm
V_{esc}	959 km s^{-1}	580 km s^{-1}
V_∞	2010 km s^{-1}	$V_{edge} = 2010$ km s^{-1}
$\dot{M}$	$3.1 \times 10^{-6} M_\odot$/yr	

In this system the data is taken from Pauldrach et al. (1986).

(a) and (b) There is a sudden fall in the neutral atom density at $R/R_0 = 2$. Very few neutral atoms left at $R/R_0 = 10$ This reflects in the density of the excited atoms and different levels at different radial points in the medium.

(c) Electron density changes between 10^{10} (cm^{-3}) to a few times 10^7 (cm^{-3}).

(d) ϵ (Lyman α) < ϵ (Balmer α) < ϵ (Paschen α) < ϵ (Brackett α).

(e) τ (Lyman α) > τ (Balmer α)

τ (Lyman α) > τ (Paschen α)

τ (Lyman α) > τ (Brackett α)

τ (Brackett 6) > τ (Lyman 9)

τ (Brackett 6) > τ (Balmer 8)

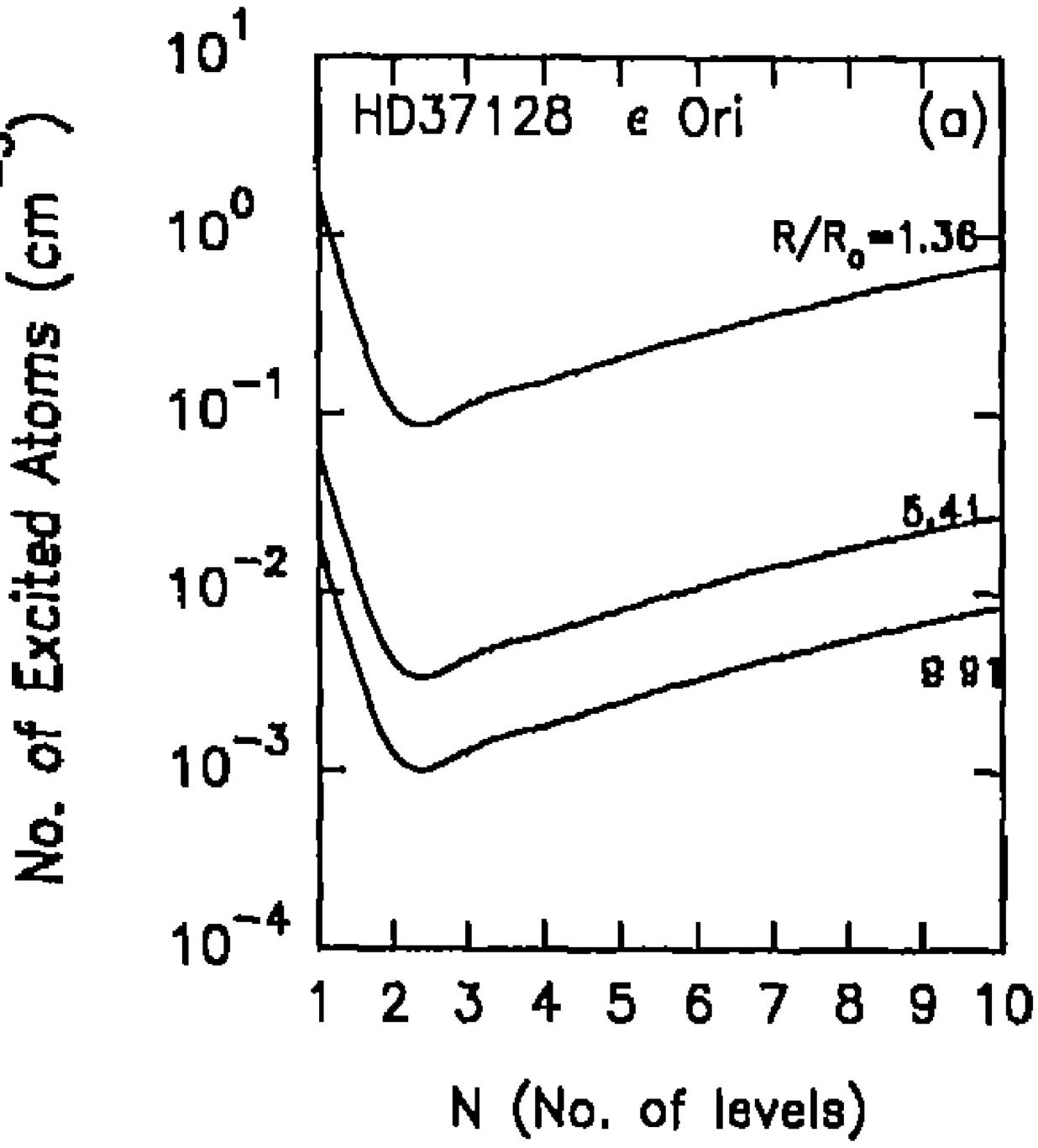

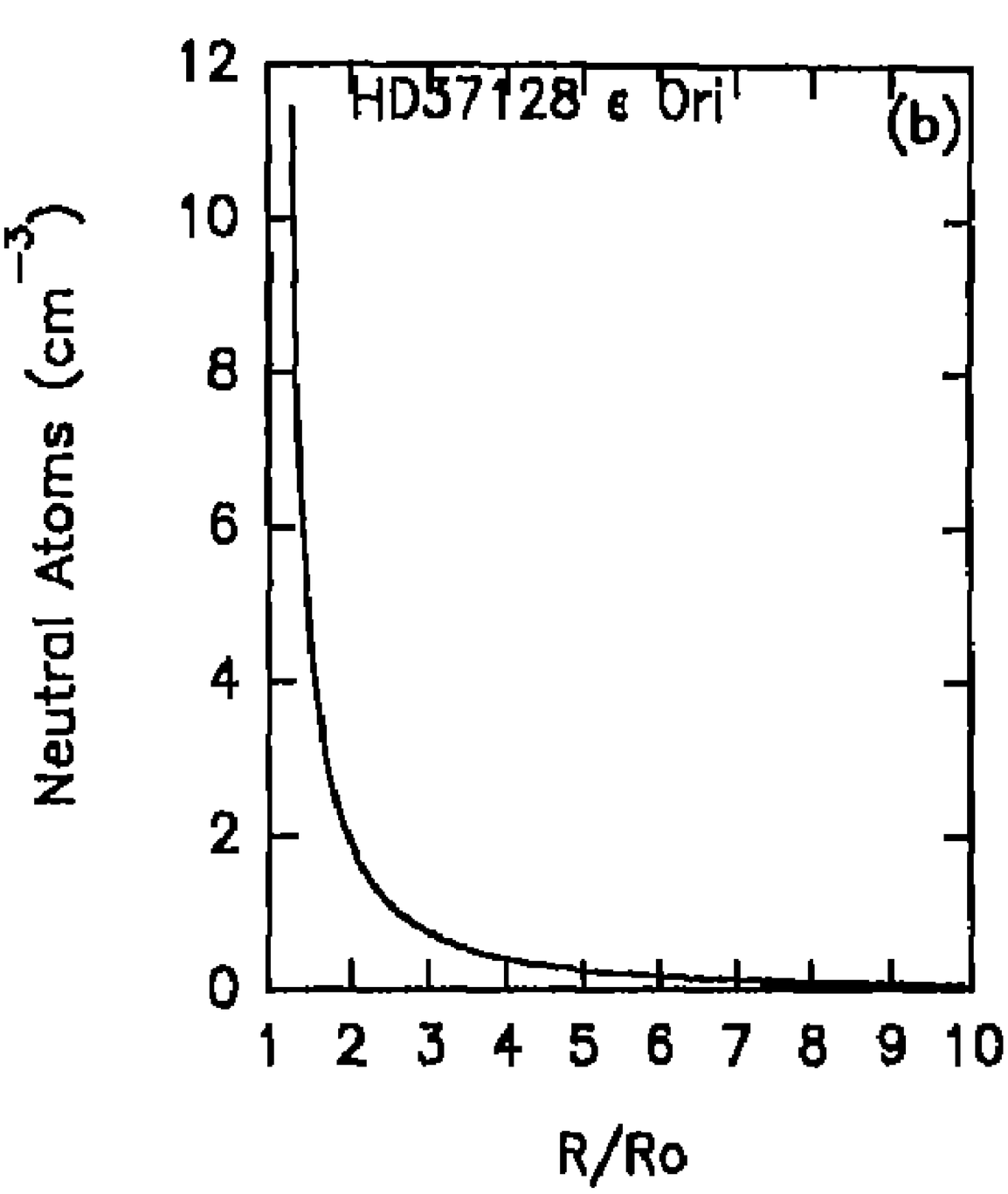

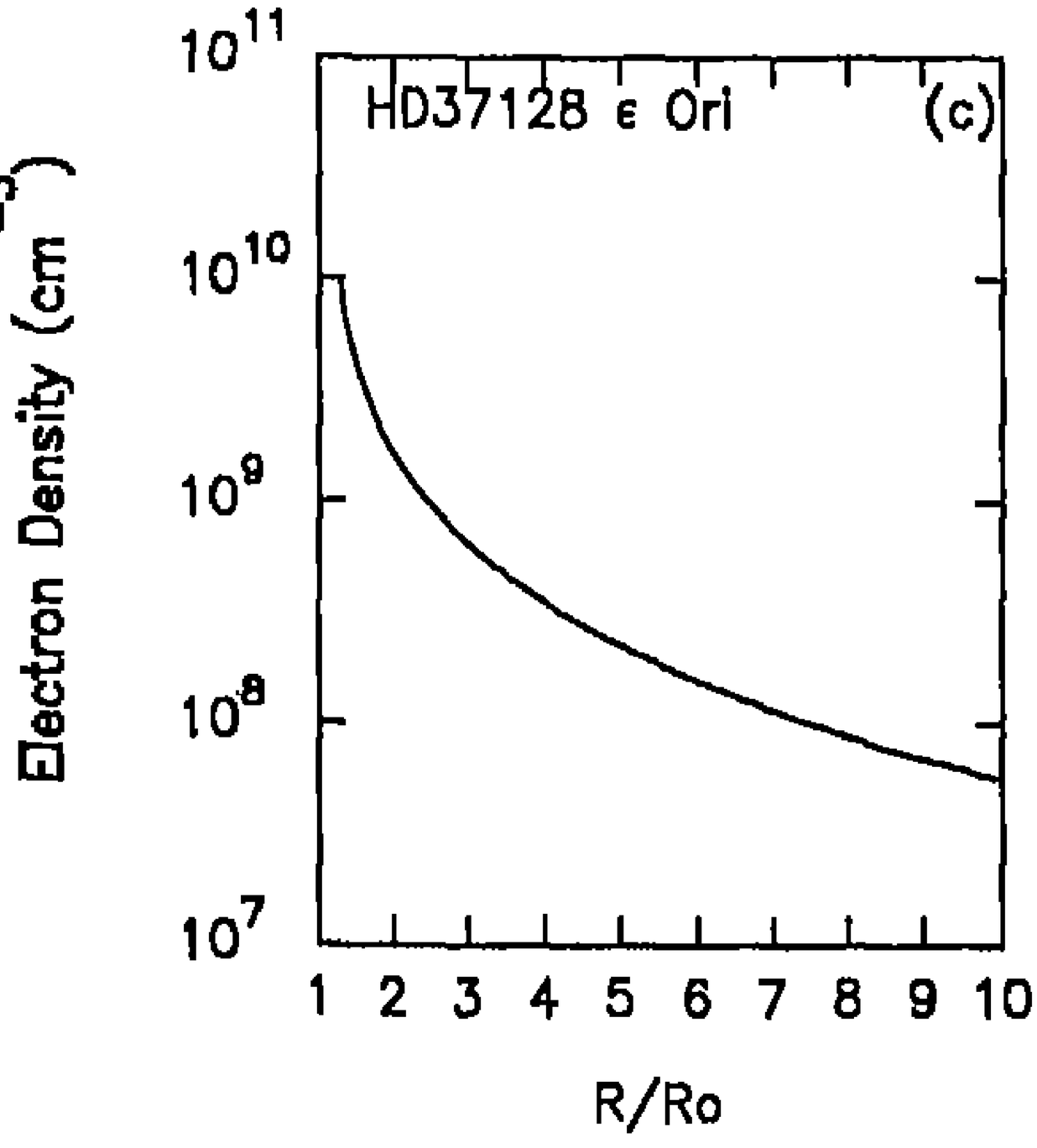

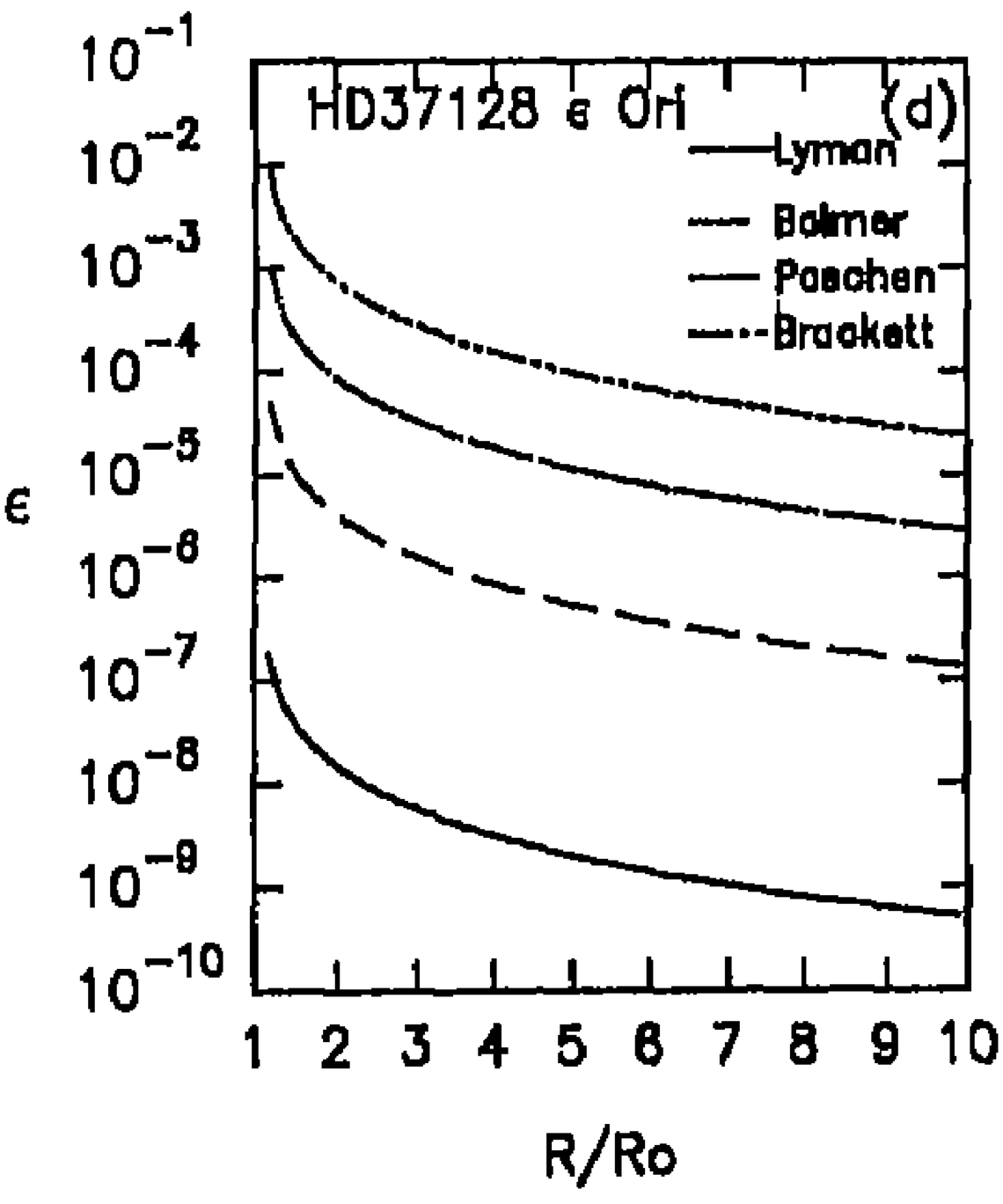

Figure 23 (a,b,c,d)

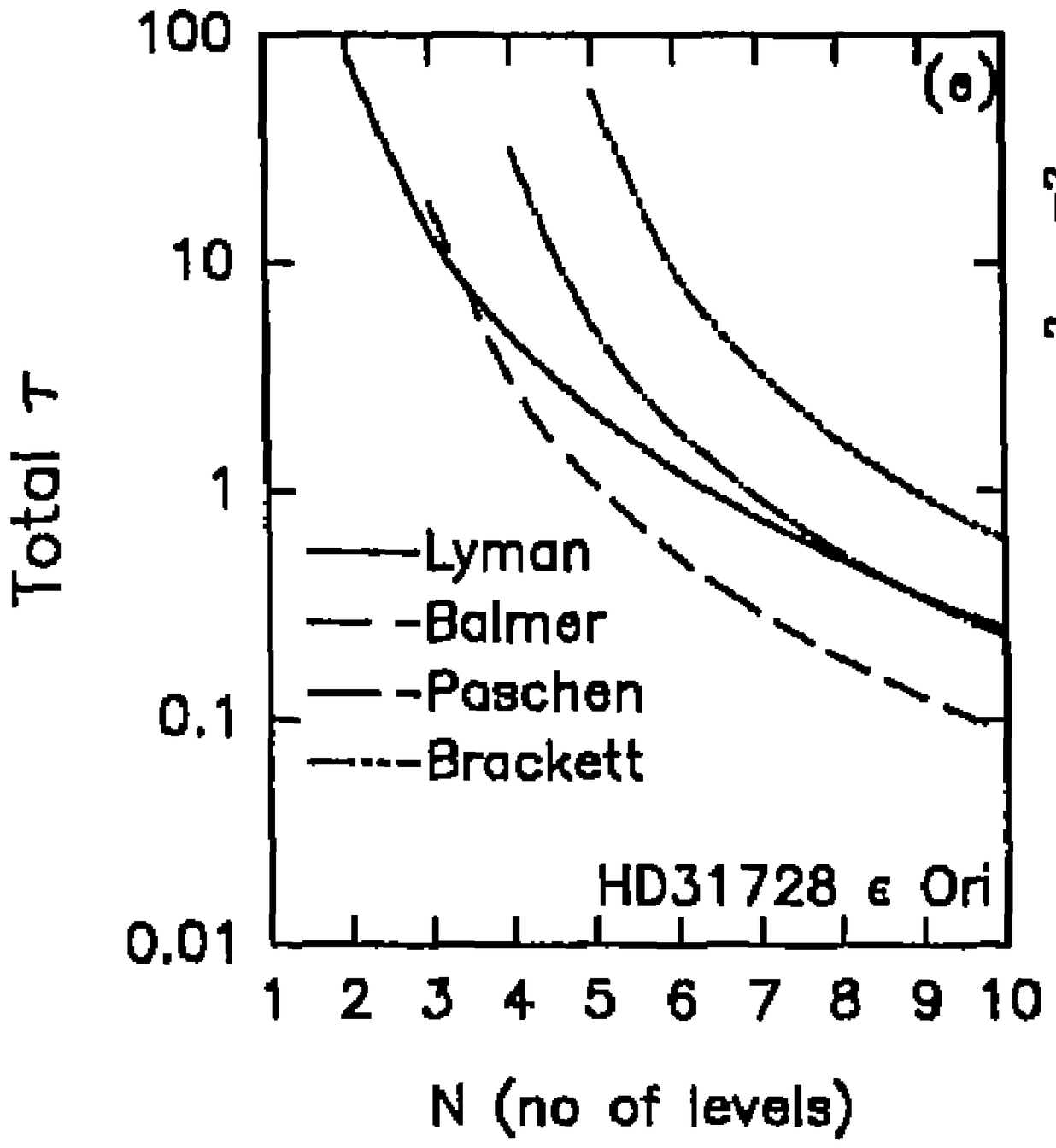

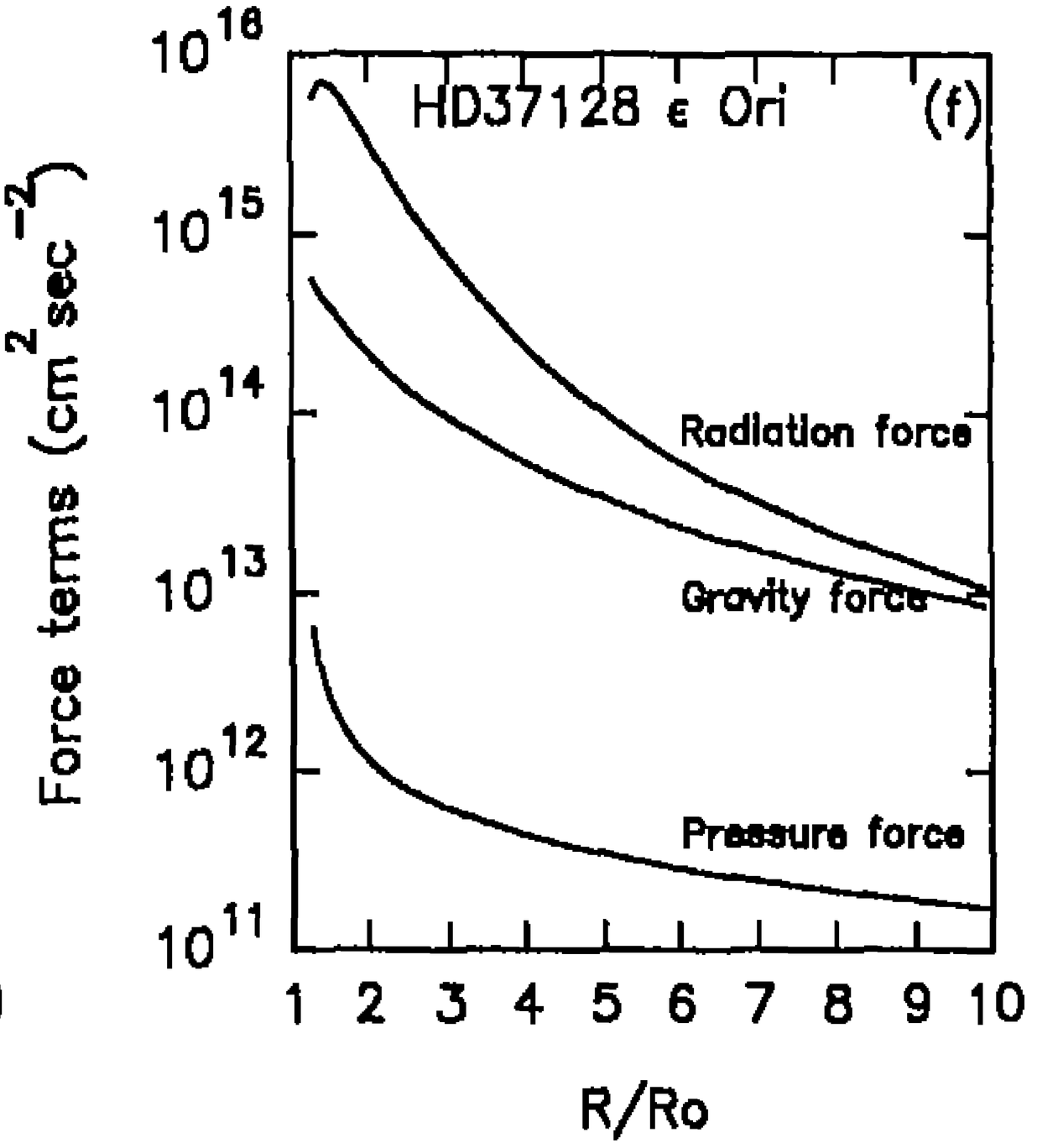

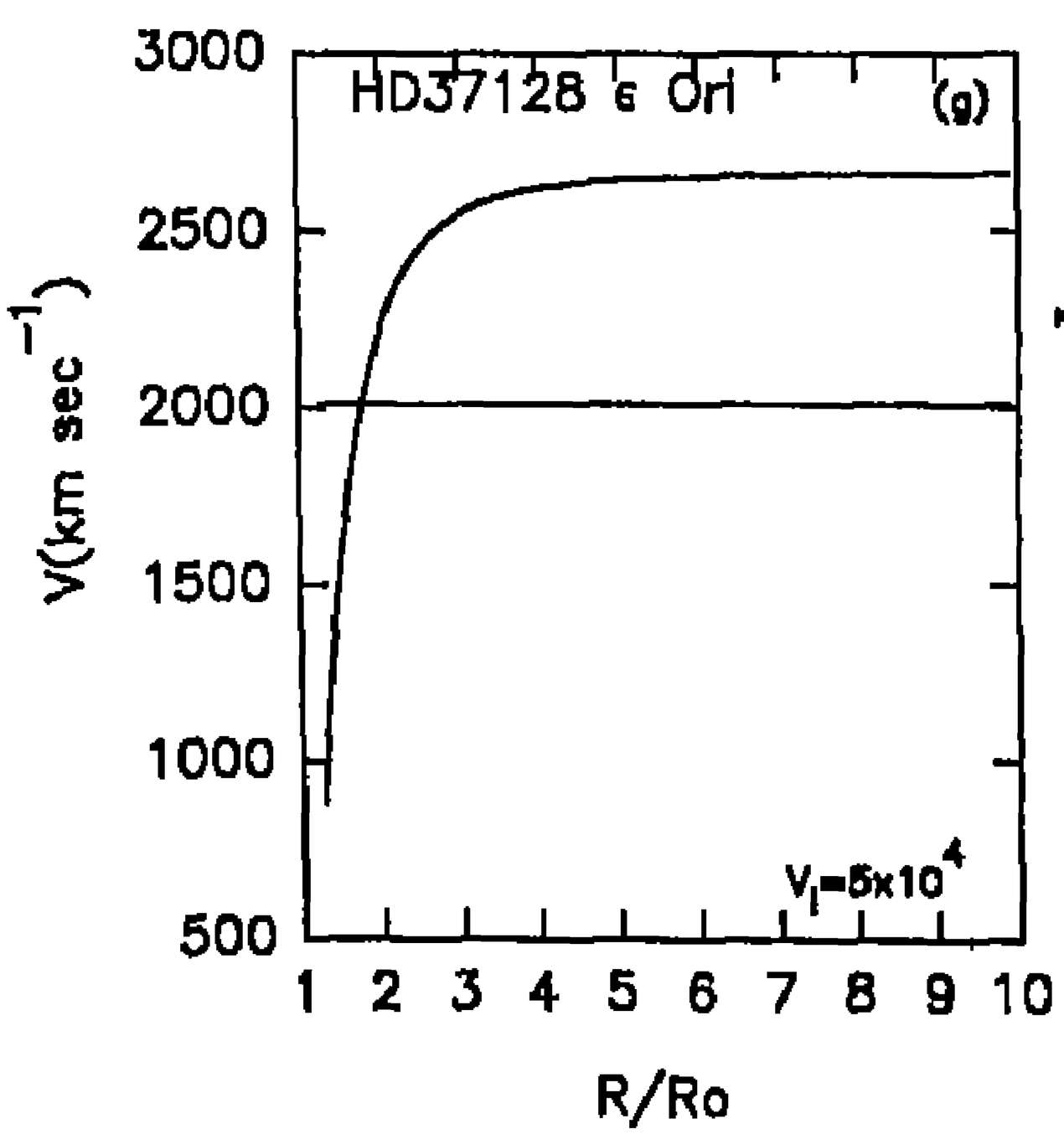

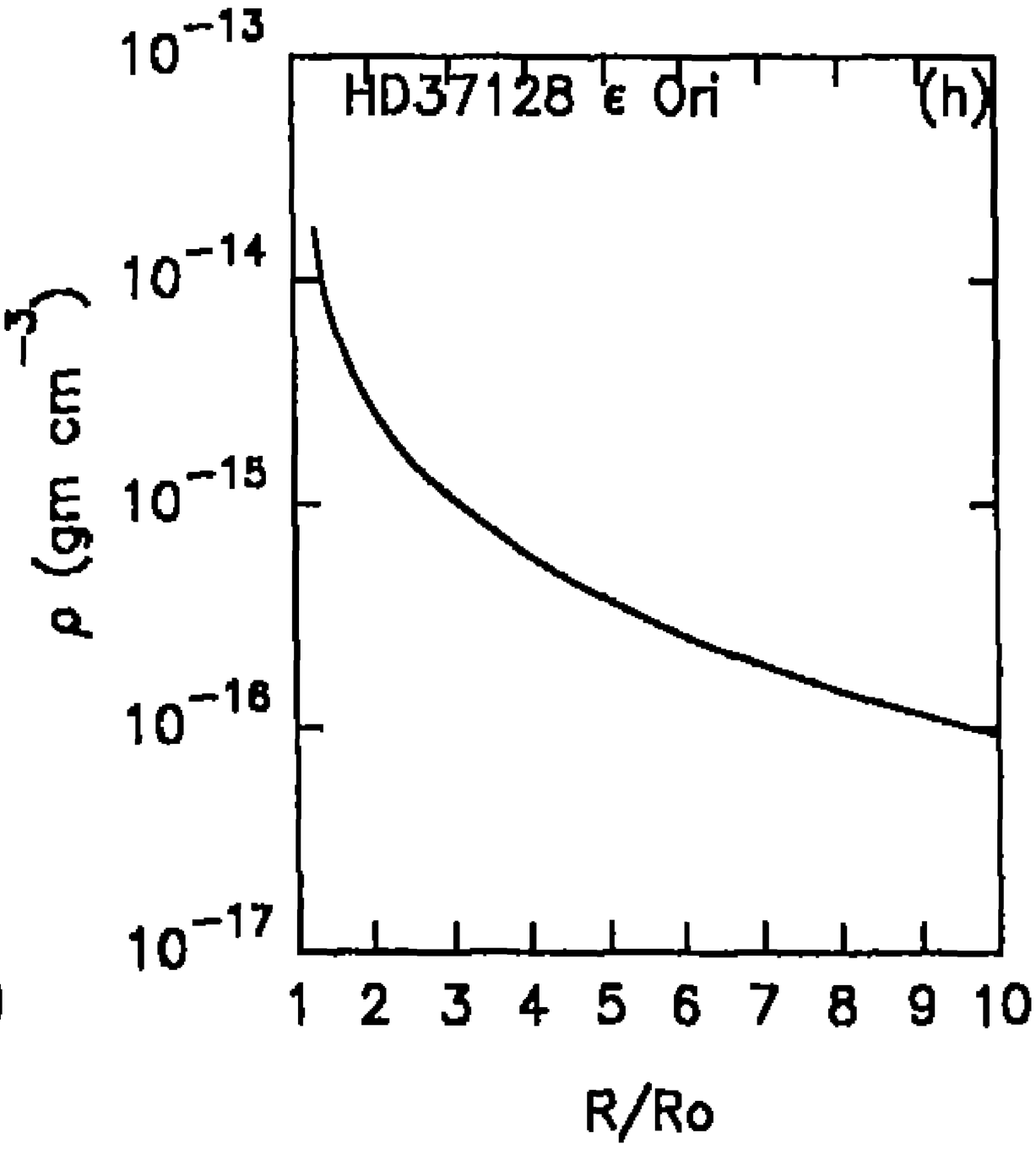

Figure 23 (e,f,g,h)

τ (Brackett 6) > τ (Paschen 7)

τ (Lyman 9) τ (Balmer 8)

τ (Brackett 6) > τ (Paschen 7)

(f) Radiation force is falling much faster than gravity force.

(g) The expected $v_\infty \sim 1010$ km s^{-1}, with $v_i = v_{i/sr}$ the converged v_∞ is too low. With $v_i = 1/2$ km s^{-1}, we obtain $v_\infty \sim 2500$ km s^{-1}.

(h) The density changes from few times 10^{-14} gr cm^{-3} to 10^{-16} gr cm^{-3}.

Figure 24

HD 193237 (P Cyg) B1 Ia

	Pauldrach et al. (1986)	Abbott (1978)
T_{eff}	18000 K	19052 K
M	3.1×10^{34} gr	1.12×10^{35} gr
R	4.76×10^{12} cm	6.44×10^{12} cm
V_{sr}	309 km s^{-1}	330 km s^{-1}
V_∞	400 km s^{-1}	$V_{edge} = 600$ km s^{-1}
$\dot{M}$	$2.5 \times 10^{-5} M_\odot$/yr	

(a), (b), (c), (d) The results are similar to those given above for other systems.

(e) τ (Lyman $\alpha, \beta, \gamma, \ldots 9$) > τ (Balmer $\alpha, \beta, \ldots 8$)

> τ (Paschen $\alpha, \beta, \ldots, 7$)

> τ (Brackett $\alpha, \beta, \ldots, 6$)

(f) The radiation force falls slowly and tends to be larger than gravity force even after $R/R_0 > 10$.

(g) The calculated v_∞ attains the observed $v_\infty (\approx 400$ km s$^{-1})$ at about $R/R_0 \approx 3$. The v_∞ appears to be increasing. This can be understood from Figure (f) in which the radiation force is always larger than gravity force and gravity force falls rather faster than radiation force. $\beta \approx 0.8$.

(h) 10^{-15} gr cm$^{-3} < \rho < 10^{-12}$ gr cm^{-3}.

Figure 25

HD 42088 06.5 V Pauldrach et al. (1986)

$T_{eff} = 40{,}000$ K

M =2.773×10^{34} gr

R =4.06×10^{11} cm

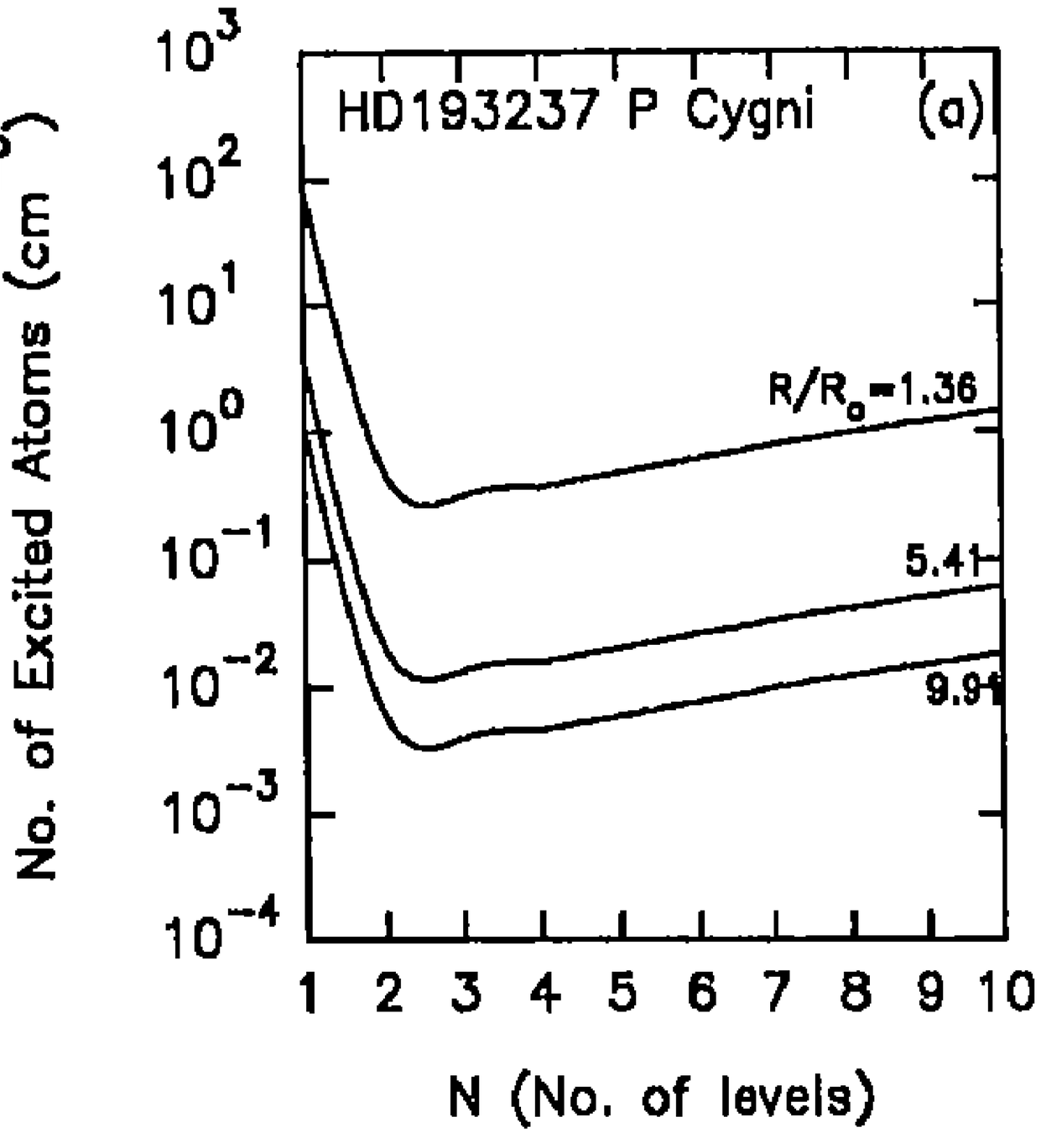

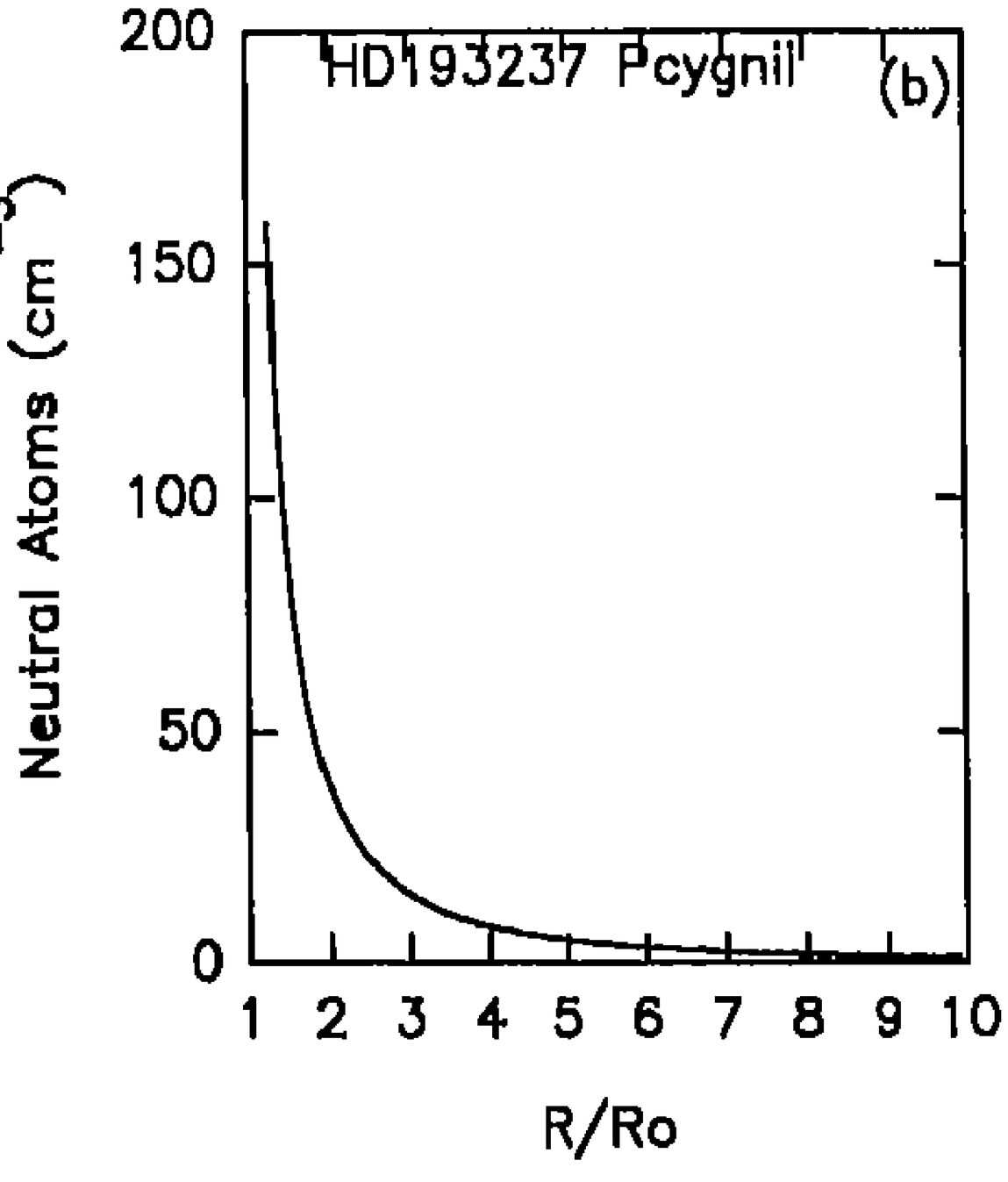

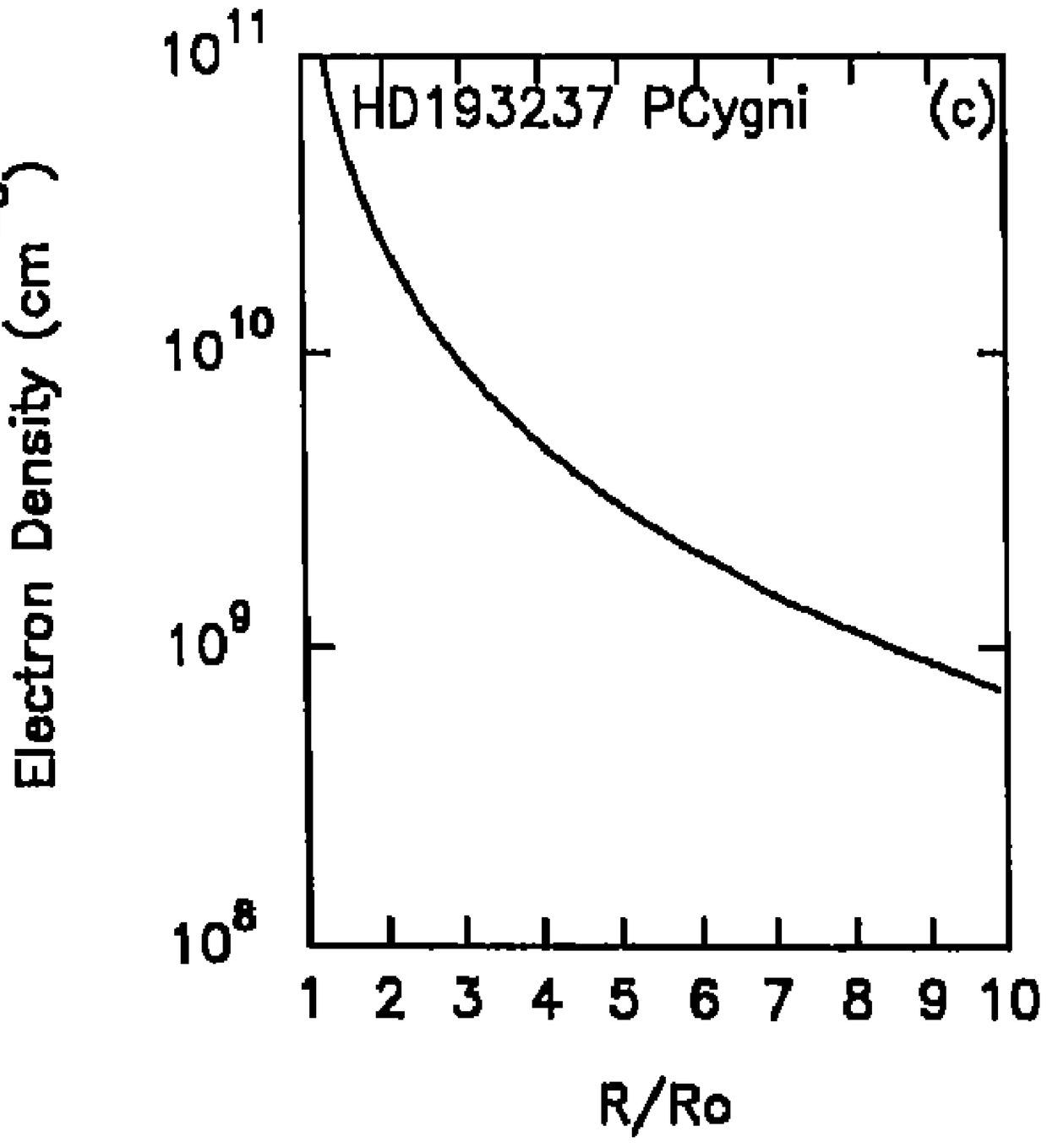

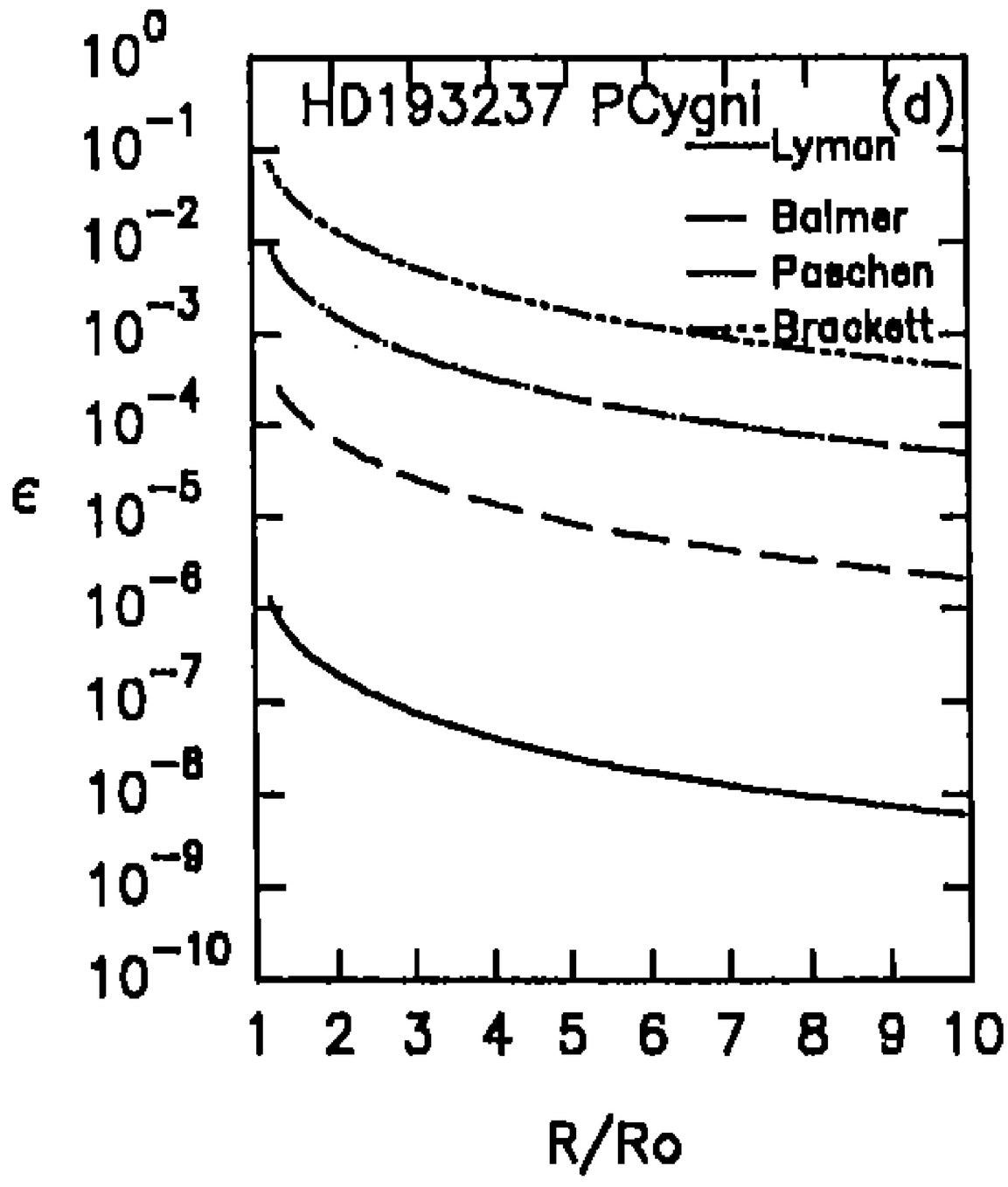

Figure 24 (a,b,c,d)

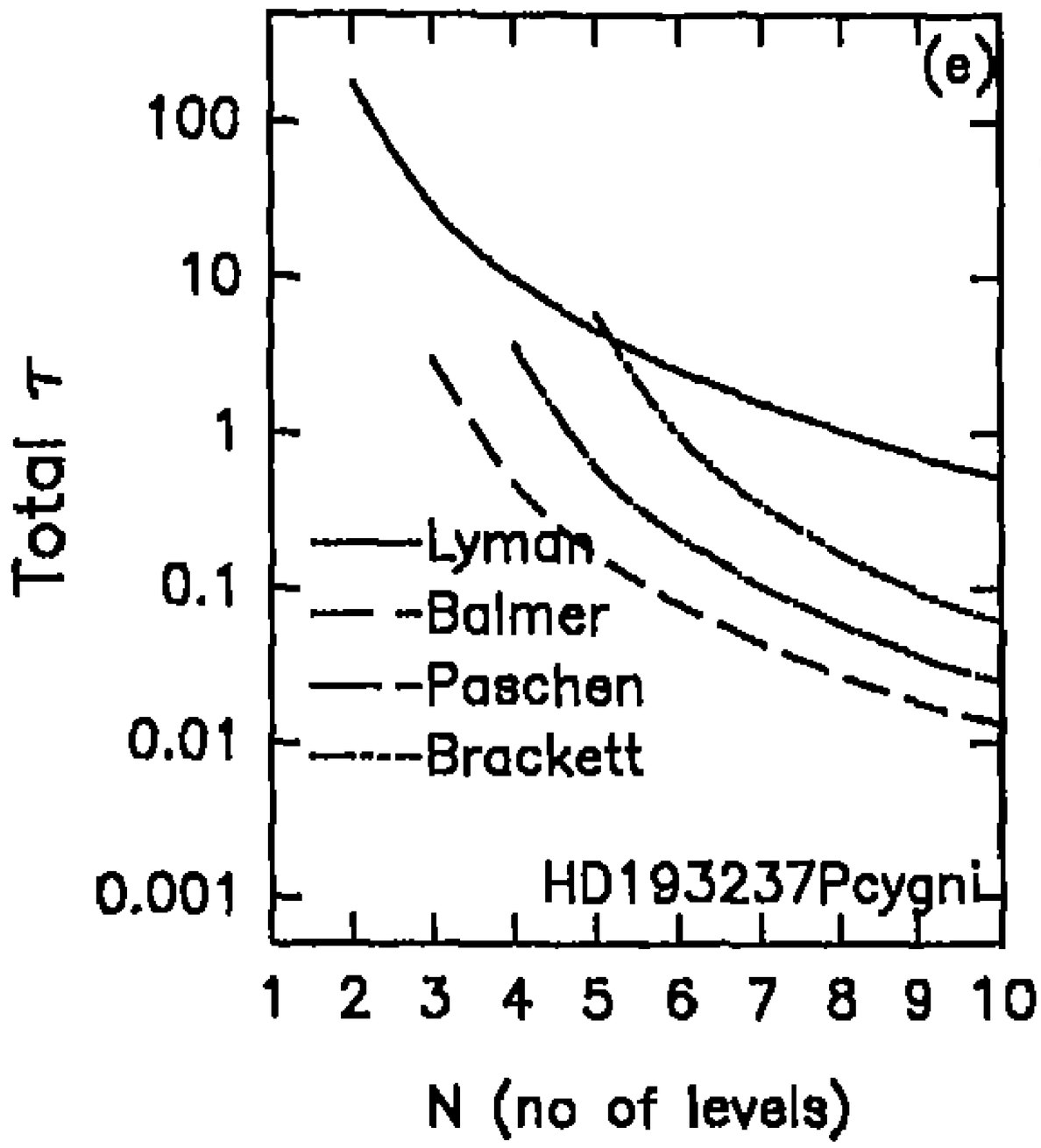

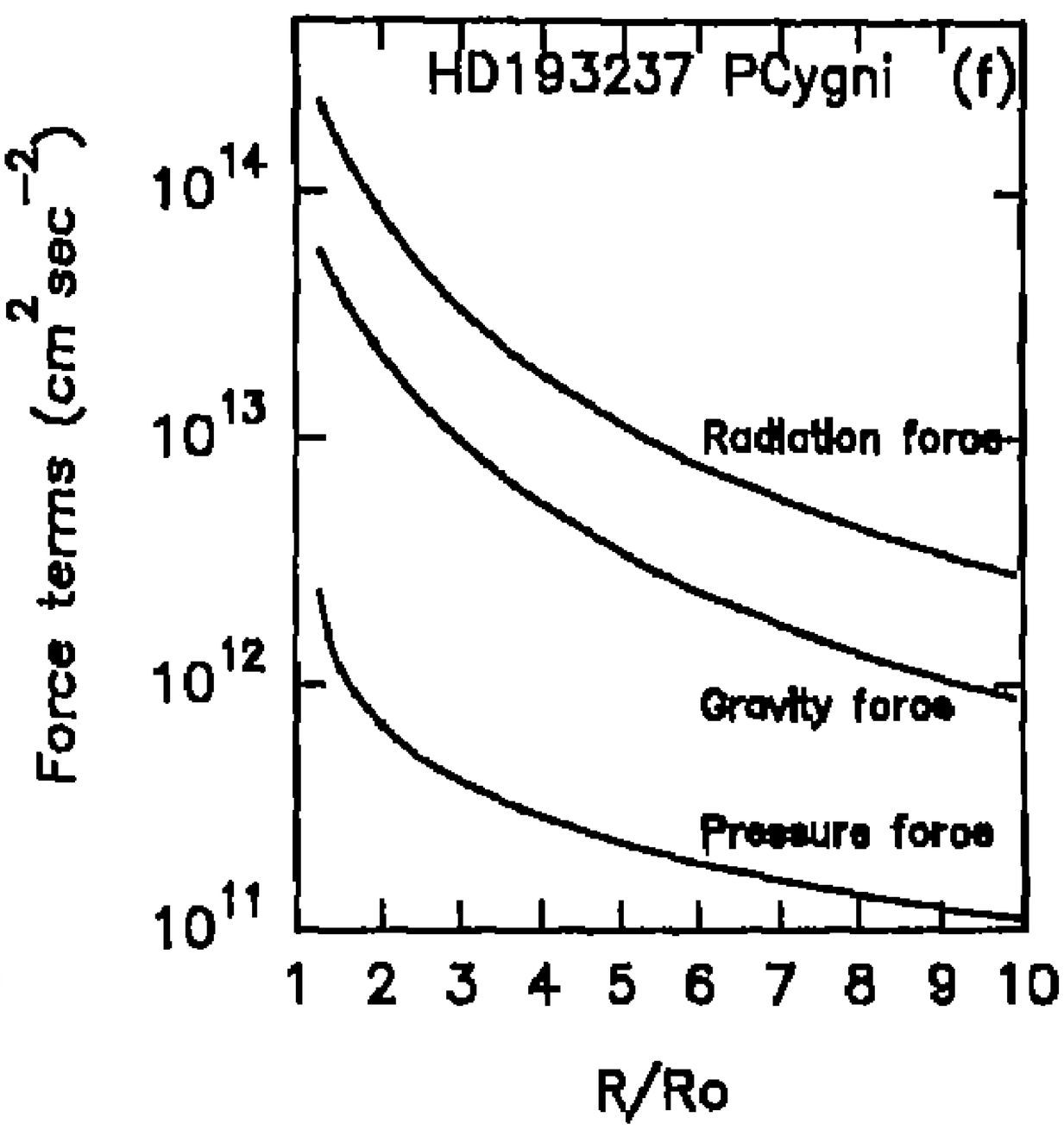

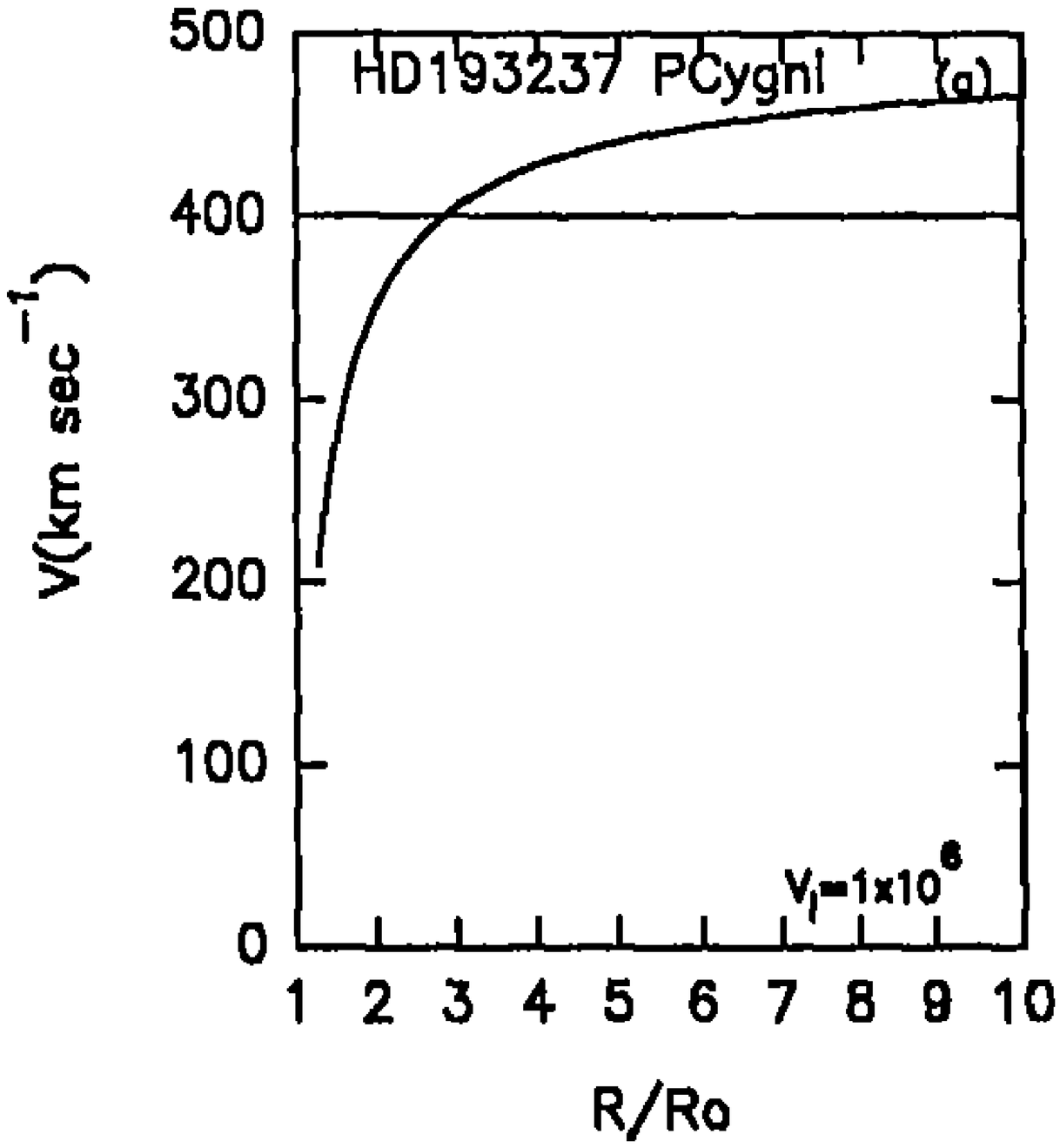

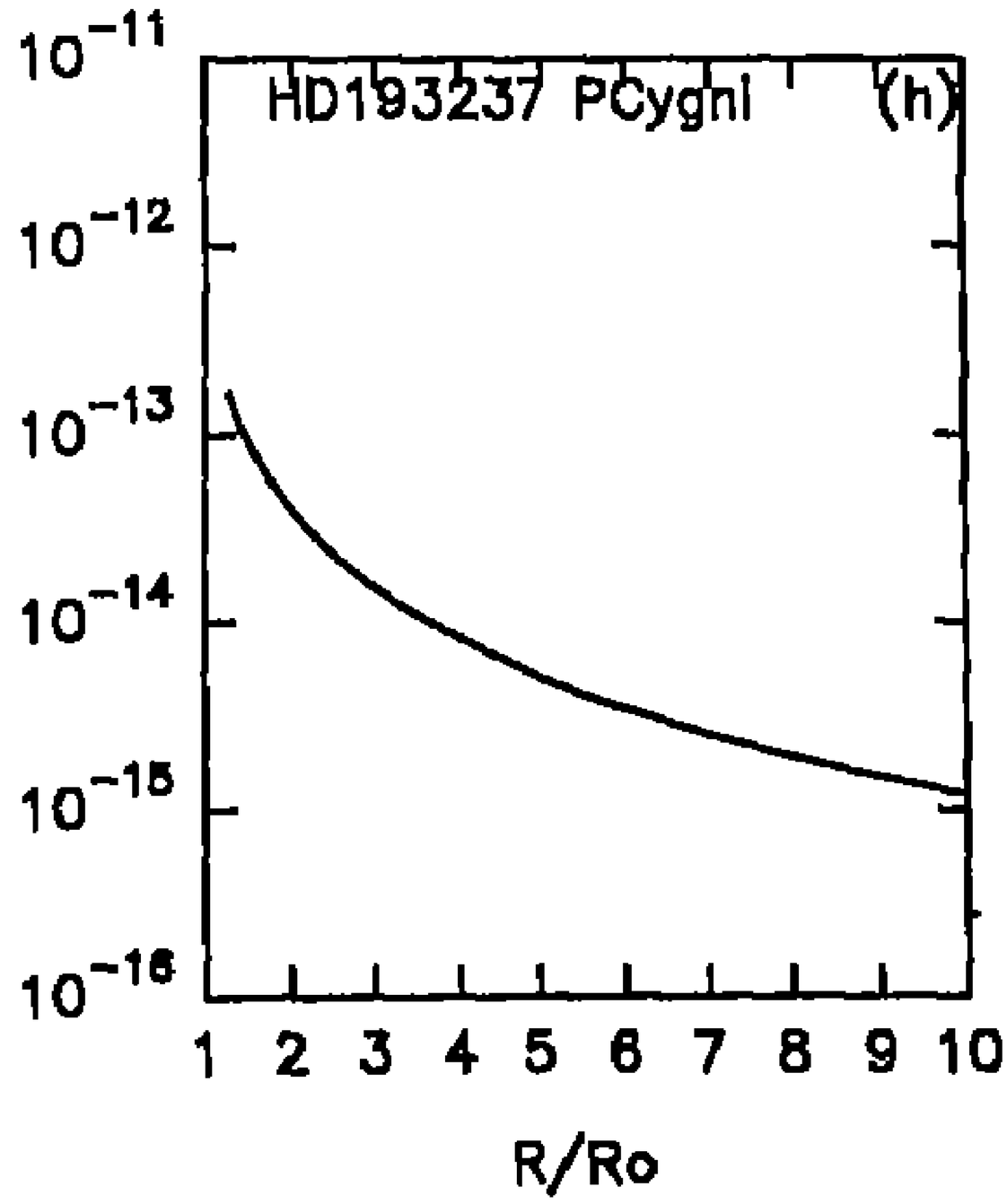

Figure 24 (e,f,g,h)

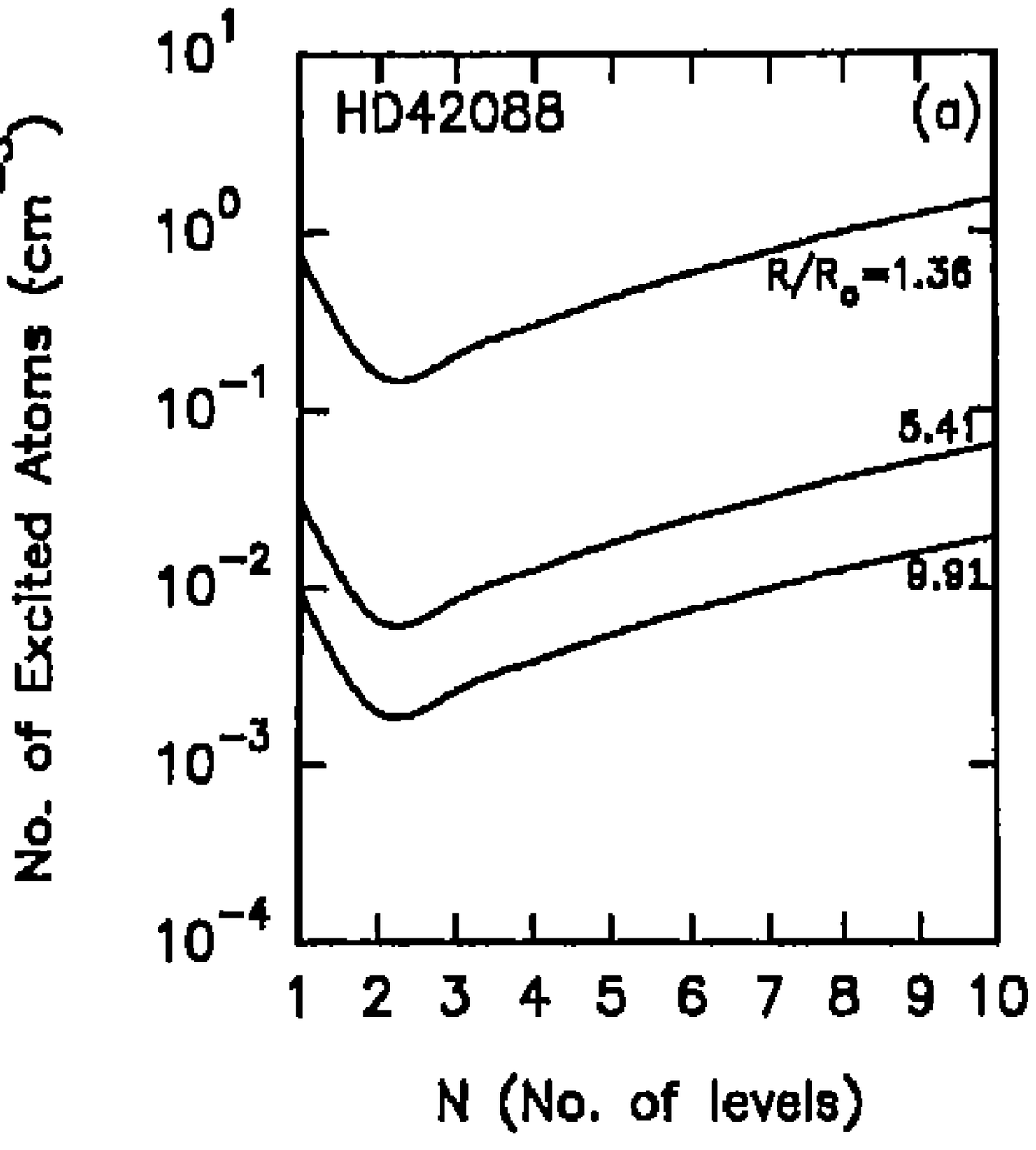

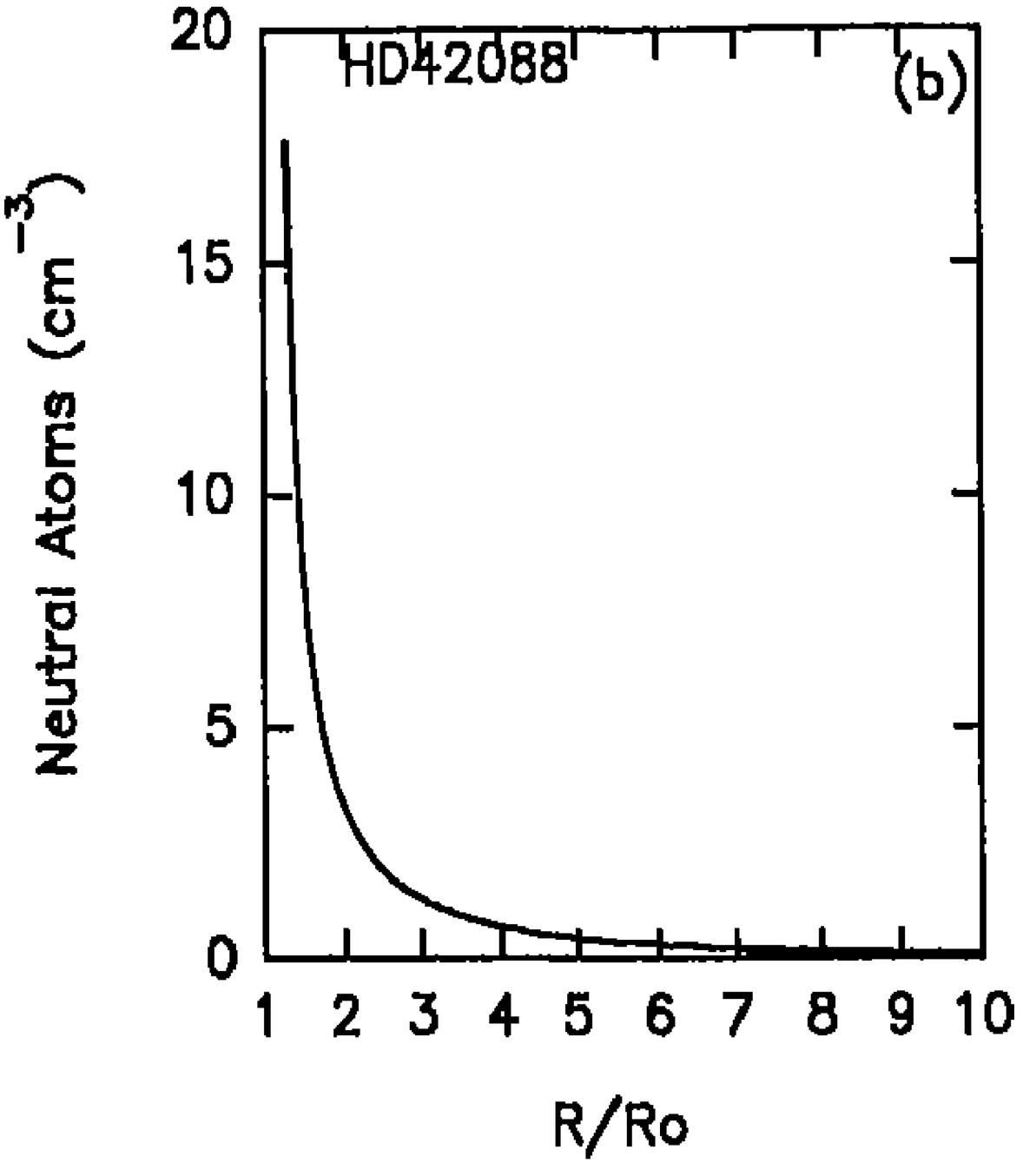

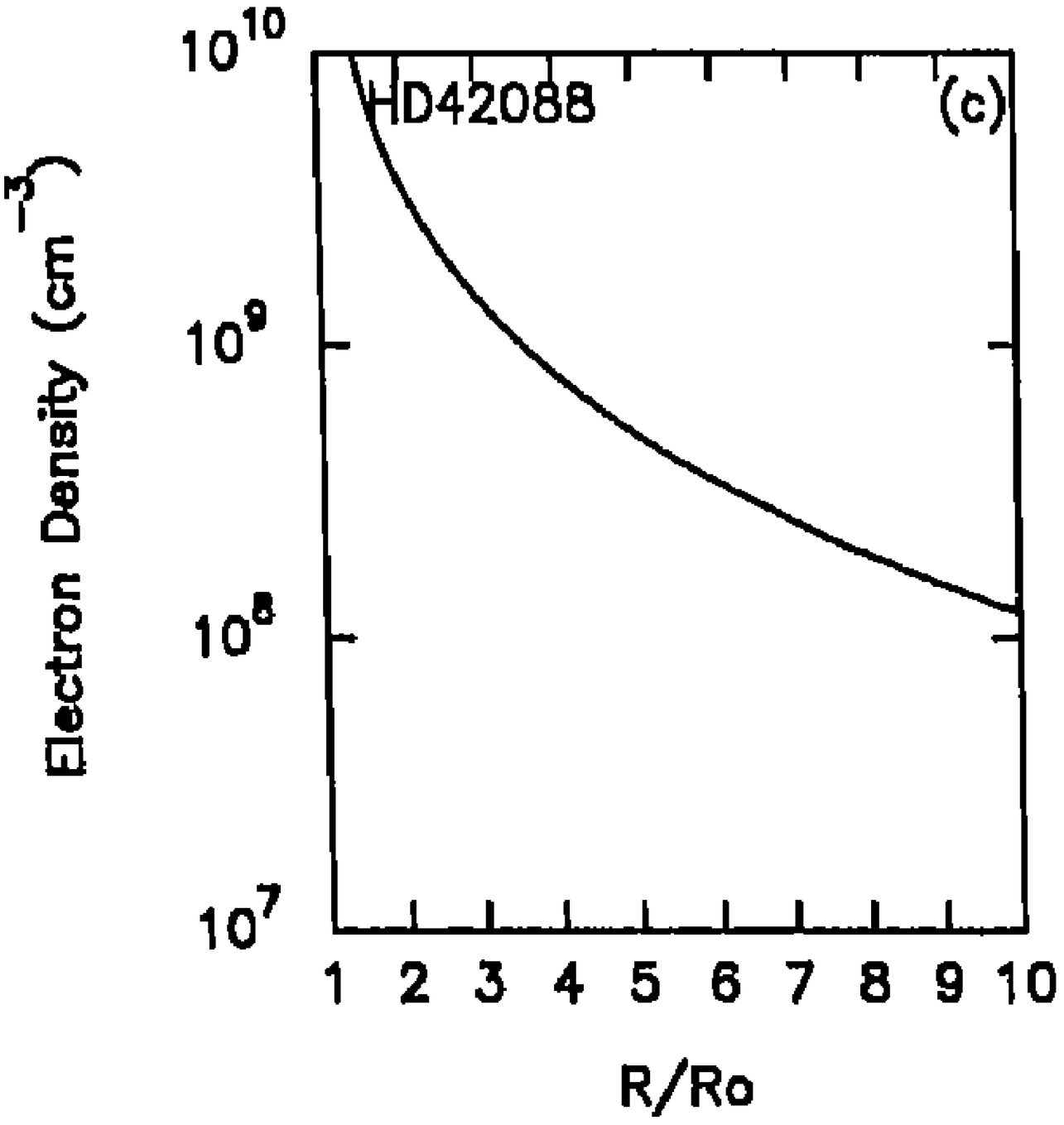

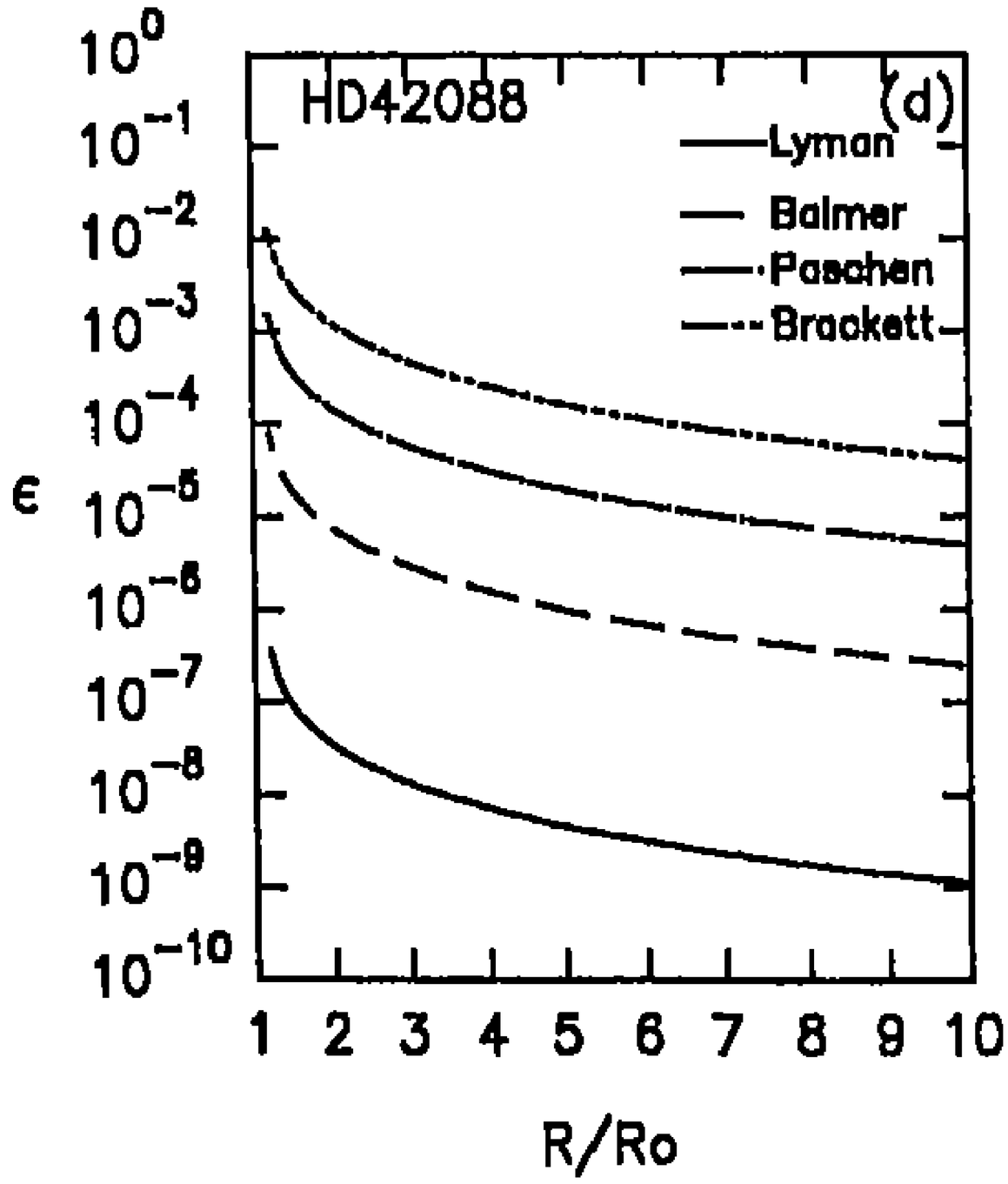

Figure 25 (a,b,c,d)

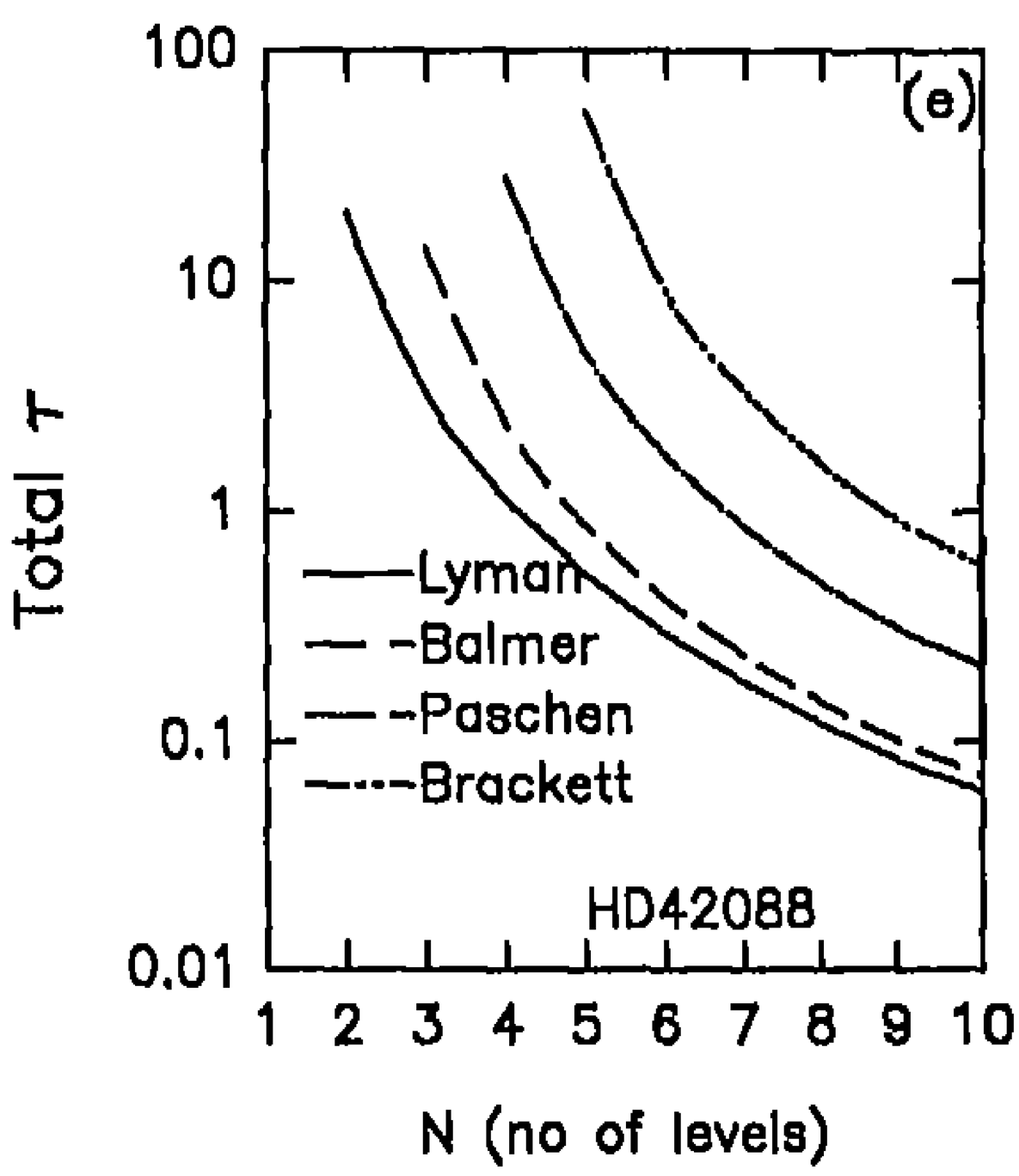

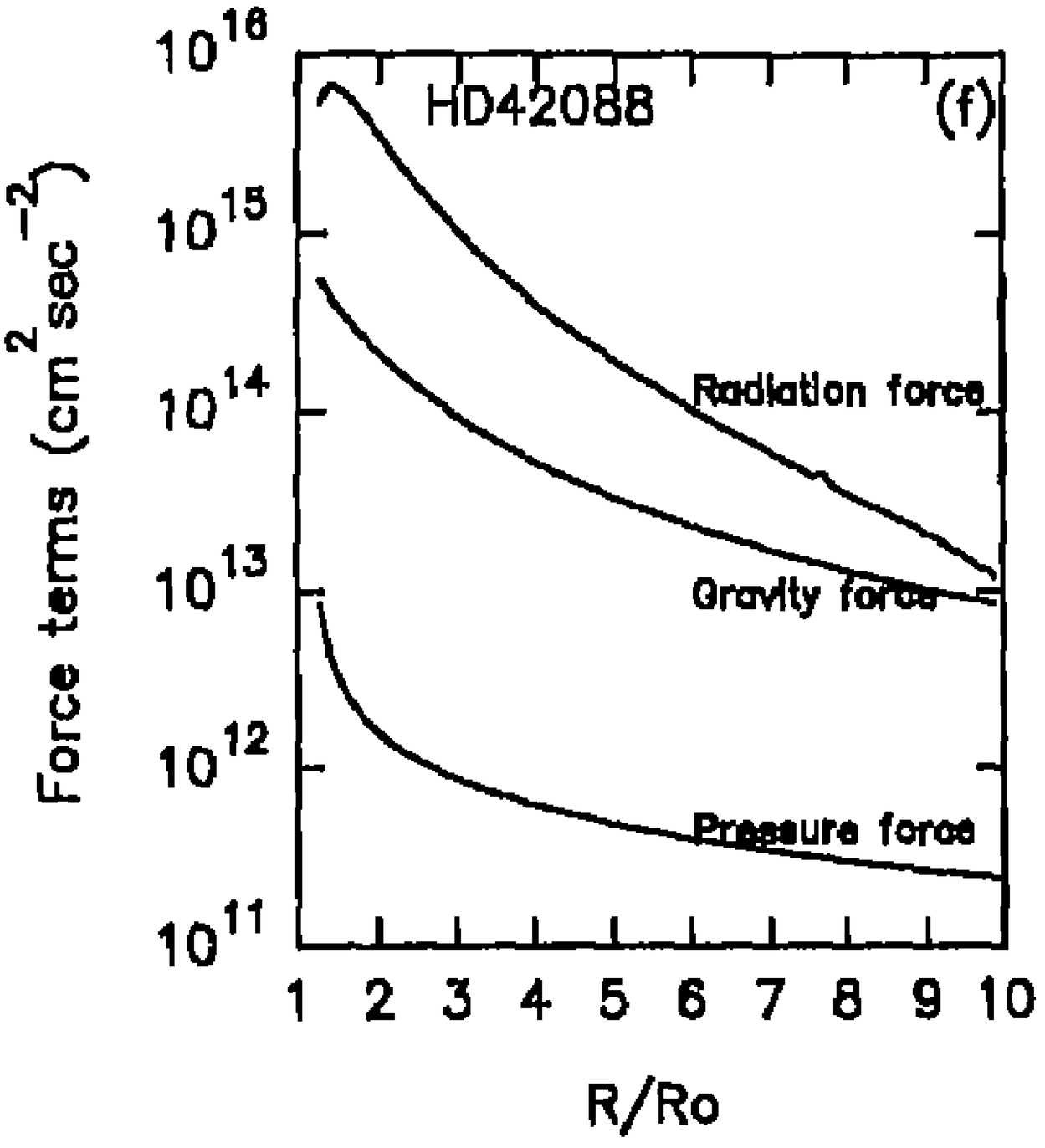

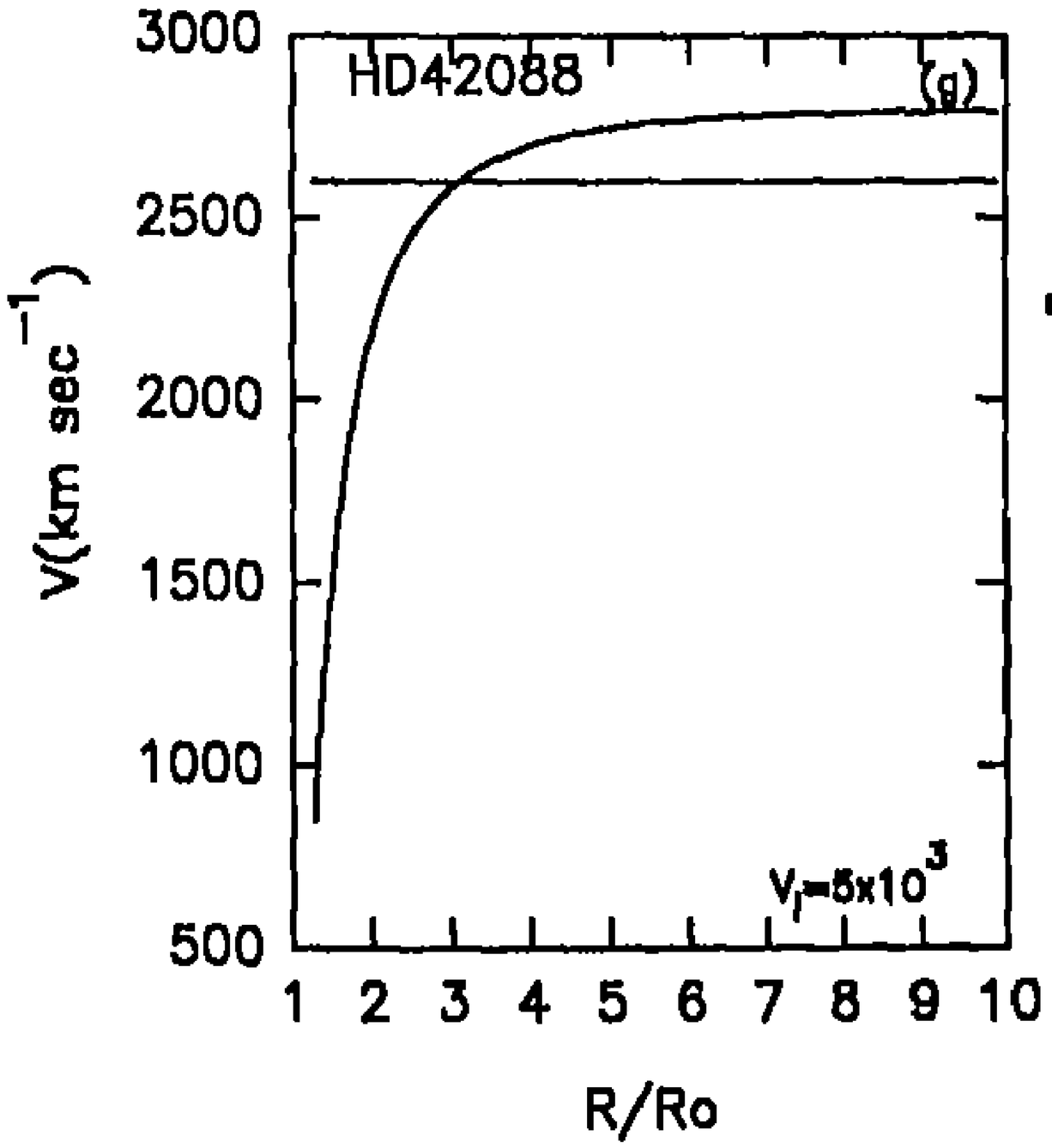

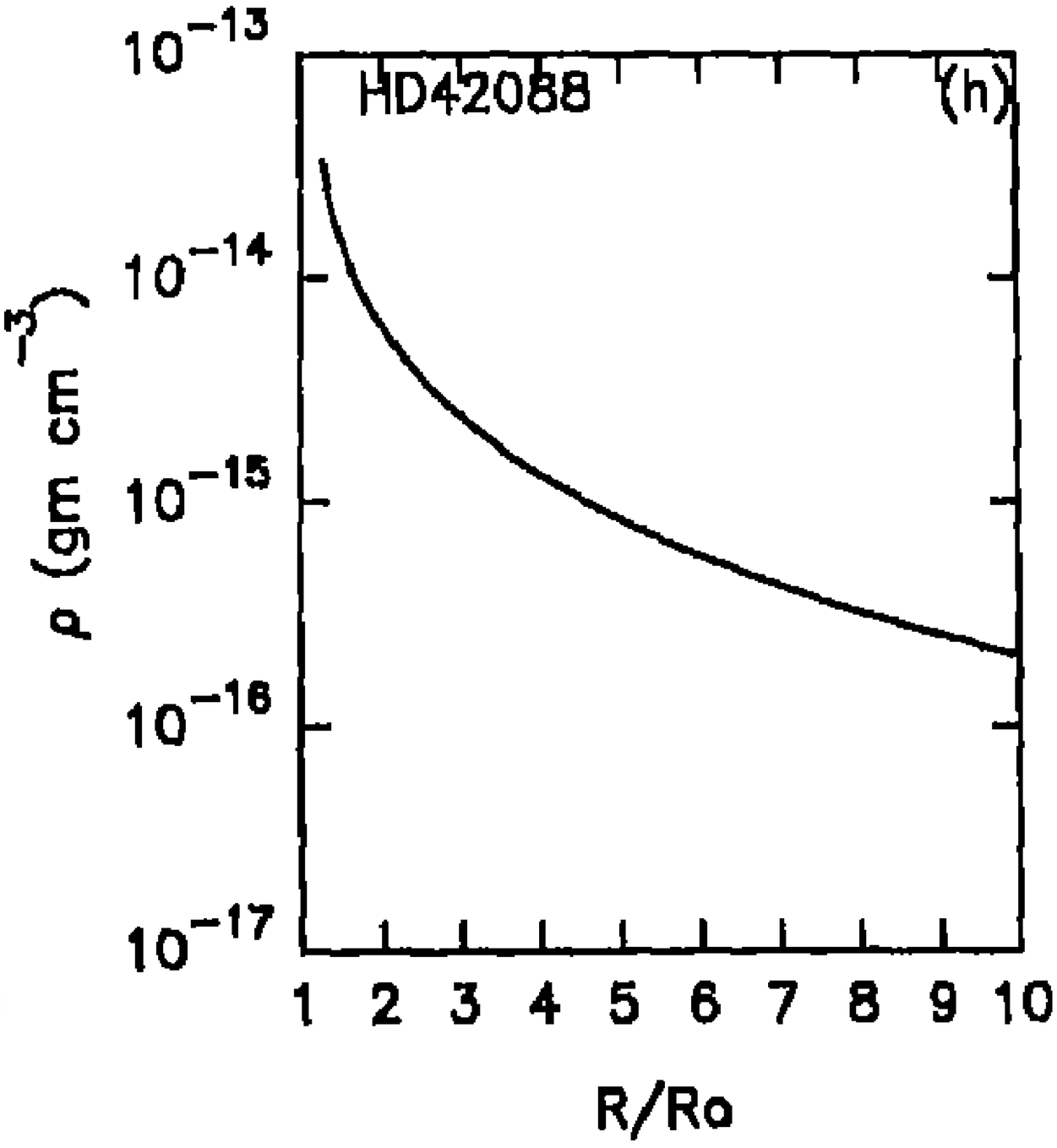

Figure 25 (e,f,g,h)

$V_{esc} = 954$ km s^{-1}

$V_{\infty} = 2600$ km s^{-1}

$\dot{M} = 1.3 \times 10^{-7} M_{\odot}$/yr

(a) As the temperature is high the higher levels of excitation are more populated than the lower levels.

(b), (c), (d) are similar to those of the earlier systems.

(e) τ (Lyman α) $> \tau$ (Balmer α)

$> \tau$ (Paschen α)

$< \tau$ (Brackett)

τ (Lyman 9) $< \tau$ (Balmer 8)

$< \tau$ (Paschen 7)

$< \tau$ (Brackett 6)

(f) Radiation force falls rapidly and tends to cross the gravity force after $R/R_0 > 10$.

(g) The calculated v_{∞} cross the obeserved v_{∞} at about $R/R_0 \approx 3$, then it continues to increase but slowly. $\beta \approx 0.0$.

(h) 10^{16} gr cm$^{-3} < \rho < 10^{-13}$ gr cm^{-3}.

3. Conclusions

The line radiation pressure is calculated taking into account the diffuse radiation in the lines of Lyman, Balmer, Paschen and Brackett upto 10 hydrogen levels. We are able to obtain the observed terminal velocities in few cases. The terminal velocities develop at about a radial distance of 3 to 5 stellar radii. The boundary conditions, especially the initial velocity to start the iteration is very uncertain. One needs to look into this problem seriously. We need to calculate the level population densities by employing statistical equilibrium equation for hydrogen, and see how much these results would differ from what we have obtained in this paper. A further improvement in this is that we need to include heavy ions of C, N, Si, Mg etc. Temperature structure is to be derived by adding the equation of energy to the present system of equations.

Acknowledgements

One of us (A.P.) would like to thank Dr. Ronny Blomme of Royal Observatory of Belgium for exchanging several ideas.

References

Abbott, D.C., 1978, Astrophysical J. **225**, 893.

Abbott, D.C., Beiging, J.H., Churchwell, E., Cassinelli, J.P., 1980, Astrophy.J. **238**, 196.

Abbott, D.C., Telesco, C.M., Wolff, S.C., 1984, Astrophys.J.**279**, 225.

Abbott, D.C., 1982, Astrophys.J. **259**, 282.

Abbott, D.C., 1986 ,Proceedings of 3rd Trieste workshop, Sac Peak.

Aller, L.H., 1963, Atmospheres of the Sun and Stars, Second ed. Ronald Press Company, New York.

Beals, C.S., 1929, Mon. Not. Roy. Astron. Soc. 40, 202.

Barlow, M.J , Cohen, M., 1977, Astrophys.J., 213, 737.

Bertout, C., Leither, C., Stahl,O., Wolf, B., 1985, Astron.Astrophys., 144, 87.

Blomme, R., 1990a, The Radiatively Driven Stellar Wind of Early Type Stars. Ph.D Thesis, Vrije Universitelt Brussel, Belgium.

Blomme, R., 1990b, Astron Astrophys., 229, 513.

Blomme, R., Vanbeveren, D., Van Rensbergen, W., 1991, Astron. Astrophys., 241, 479.

Blomme, R., Van Rensbergen, W., 1988, Astron. Astrophys., 207, 70.

Bohm-Vitense, E., 1989, Introduction to Stellar Astrophysics 2: Stellar Atmospheres, Cambridge University Press, Cambridge.

Conti, P.S., Leep, E M., 1974, Astrophys.J 193, 113

Castor, J.I., Abbott, D.C., Klein, R.I., 1975, Astrophys J. 195, 157.

Garmany, C.D., 1988, in "O stars and Wolf-Rayet Stars", eds. P.S.Conti, A.B.Underhill (NASA SP-497).

Illiner, W.A., Garrison, R.F , Schild, R.E., 1969, Astrophys.J., 157, 313

Johnson, H.L., Morgan, W W., 1953, Astrophys.J. 117, 313.

Jefferies, J., 1968, Spectral Line Formation, Waltham, Mass: Blaisdel.

Leroy, M., Lafon, J. - P.J., 1982, Astron.Astrophys., 106, 345.

Lamers, H.J.G.L.M., Waters, L.B.F.M., 1984, Astron.Astrophys. 136, 37.

Lucy, L.B., Soloman, P.M , 1970, Astrophys J.159, 879.

Mendoza, E.E., 1958, Astrophys.J. 128, 207.

Mihalas, D., 1978, Stellar Atmospheres, Second Ed. W.H.Freeman and Company, San Francisco.

Morton, D.C., 1967, Astrophys.J 147, 1017.

Pauldrach, A., 1987, Astron.Astrophys. 183, 295.

Pauldrach, A., Kudritzki, R.P., Puls, J., Butler,K., 1990, Astron.Astrophys. 228, 125.

Pauldrach, A., Puls, J., Kudritzki, R P., 1986, Astron. Astrophys., 164, 86.

Peraiah, A., 1980, Acta Astronomica, 30, 525.

Peraiah, A., 1991, Astrophysical J., 380, 212.

Underhill, A.B., Divan, L., Provot-Burnichon, M.-L., Doazan, V., 1979, Mon. Not. Roy. Astron. Soc. 189, 601.

Wever, S., 1981, Astrophys.J. 243, 954.

Wiese, W.L., Smith, M.W., Glennon, B.M., 1966, Atomic Transition probabilities, Vol.1, Hydrogen Through Neon. National Standard of Reference Data Series, National Bureau of standards 4 (Catagory 3 - Atomic and Molecular properties). Issued May 20, 1966.